

**HEARING LOSS IN EXPERIMENTAL  
BACTERIAL MENINGITIS**

by

**ANDREW JOHN WINTER**

A thesis submitted to the Faculty of Medicine and  
Dentistry for the degree of  
**DOCTOR OF PHILOSOPHY**

Department of Infection  
School of Medicine  
Faculty of Medicine and Dentistry  
The University of Birmingham  
July 1996

UNIVERSITY OF  
BIRMINGHAM

**University of Birmingham Research Archive**

**e-theses repository**

This unpublished thesis/dissertation is copyright of the author and/or third parties. The intellectual property rights of the author or third parties in respect of this work are as defined by The Copyright Designs and Patents Act 1988 or as modified by any successor legislation.

Any use made of information contained in this thesis/dissertation must be in accordance with that legislation and must be properly acknowledged. Further distribution or reproduction in any format is prohibited without the permission of the copyright holder.

## ABSTRACT

Experimental meningitis was induced in pigmented guinea pigs by subarachnoid inoculation of  $1 \times 10^9$  *Escherichia coli* K-12 or  $3 \times 10^7$  CFU *Streptococcus pneumoniae* serotype 2 D39 (NCTC 7466) or PLN-A,  $\Delta$ NA1 or  $\Delta$ HY1, defined isogenic derivatives of D39 deficient in pneumolysin, neuraminidase or hyaluronidase respectively. All animals developed a meningeal inflammatory response and a labyrinthitis. Hearing loss in pneumococcal meningitis was measured by recording the evoked auditory nerve compound action potential from the round window membrane. Animals infected with PLN-A sustained significantly less hearing loss than those infected with wild-type D39 (12 dB vs. 50 dB 12 h post inoculation;  $P < 0.0001$ ), Neuraminidase deficiency did not alter the course of the meningeal inflammatory response nor affect hearing loss. The  $\Delta$ HY1 mutant survived poorly in the cerebrospinal fluid and blood but still caused hearing loss. Both pneumococcal and *E. coli* meningitis induced specific ultrastructural lesions in the organ of Corti as judged by high-resolution scanning and transmission electron microscopy, and these lesions were most severe with pneumolysin-sufficient pneumococcal infection.

Microperfusion of  $5 \times 10^6$  CFU *S. pneumoniae* D39 directly into the scala tympani of guinea pigs also resulted in electrophysiological and ultrastructural damage to the organ of Corti that could be diminished by pretreatment with antibiotics.

The data confirm the cochlea as the site of meningogenic deafness. They suggest that pneumolysin expression is chiefly responsible for meningogenic deafness and that if pneumococci invade the inner ear during bacterial meningitis, cochlear deafness will rapidly ensue.

## ACKNOWLEDGEMENTS AND DEDICATION

I would like to thank Professor **AM** Geddes and Dr Spiro Comis for guidance and supervision at all stages, Dr John Stephen for his kind encouragement and lively discussions, Dr Mike Tarlow for help with obtaining a Sheldon fellowship and a travel grant and for commenting on drafts of this thesis, Dr Mike Osborne for his special role in interpreting the electron micrographs and discussions, and lab colleagues Sarah Marwick, Angela Roberts, Harriet McMillan-Browse, Olwynne Tarlow, Shelley Drew and Lyn Dover. Chief technician Trevor Hayward was largely responsible for developing the excellent photomicrographs. Many other aspects of this work would have been impossible without his invaluable and selfless assistance, especially his help in modifying the lab to allow category II containment work. Margaret Glover and Jenny Birch undertook much of the laborious preparation of the SEM specimens and TEM sections. Professor Coote kindly allowed me to work in the Department of Physiology, and Professor Morton helped obtain the necessary Home Office licences.

Dr Tim Mitchell, Professor Peter Andrew and their team (Andrew Wallis, Val Clarke and Janet Alexander) at the Department of Medical Microbiology and Immunology, University of Leicester, provided the strains of pneumococci and performed the quality control assays. Without their helpful and enthusiastic collaboration much of the work in this thesis would have been impossible.

The laboratory was funded by the Wellcome Trust and the Medical Research Council. A very generous bursary from Hoechst-Roussel enabled this work to be completed. A travel grant from the Salt Bequest helped towards the cost of presenting some of the data at the seventh International Congress for Infectious Diseases in Hong Kong in June 1996.

I would also like to thank those clinicians who, understanding my situation, offered me part time employment which enabled me to fund the final year particularly Drs Maggie Godley, Keith Radcliffe, Mohsen Shamhanesh and Mia Huengsborg.

To my friends and family who have supported me through some particularly difficult times in the last two years I am deeply grateful.

My grandparents Bill and Marjorie Roberts lost their first daughter Pamela from meningitis (probably pneumococcal) on 1 August 1940, before penicillin became generally available. Admitted to a fever hospital, her parents were not allowed to visit for the four days she survived. She was just seven years old. At the age of 90 my grandfather has followed this project on meningitis with great interest and enthusiasm. As a testament to the advances in medicine he has seen in his lifetime I would like to dedicate this thesis to him.

# TABLE OF CONTENTS

<b>1. INTRODUCTION</b> .....	<b>1</b>
1.1. Bacterial meningitis.....	1
1.1.1. Epidemiology and causative agents.....	1
1.1.2. Clinical presentation and treatment .....	3
<b>1.2. Streptococcus pneumoniae</b> .....	<b>4</b>
1.2.1. Introduction.....	4
1.2.2. Pneumococcal structure.....	4
1.2.3. Colonisation of the host.....	<b>5</b>
1.2.4. Capsule.....	6
1.2.5. Cell wall.....	9
1.2.6. Pneumolysin.....	10
1.2.7. Neuraminidase.....	16
1.2.8. Hyaluronidase.....	17
1.3. Auditory anatomy and physiology.....	19
1.3.1. Gross anatomy.....	19
1.3.2. The cochlear aqueduct.....	19
1.3.3. Ultrastructure of the organ of Corti.....	20
1.3.4. Sound transduction.....	23
1.3.5. Electrophysiological measurements.....	24
1.4. Experimental bacterial meningitis.....	32
1.4.1. Practical considerations.....	32
1.4.2. Pathogenesis of bacterial meningitis.....	34
1.4.3. Anti-inflammatory strategies.....	39
1.5. Deafness in clinical and experimental meningitis.....	42
1.5.1. Epidemiology.....	42
1.5.2. Mechanisms of post-meningitic hearing loss.....	45
1.5.3. The steroid controversy.....	48
1.6. Conclusions.....	51
<b>2. MATERIALS AND METHODS</b> .....	<b>53</b>
2.1 Common methods .....	53
2.1.1 Overall strategy.....	53
2.1.2 Use of animals.....	53
2.1.3 Anaesthesia and conditions.....	54
2.1.4. Bacterial preparation .....	<b>55</b>
2.1.5 Pneumococcal cell wall preparation.....	<b>58</b>
2.2. Meningitis model .....	60

2.2.1. Experimental design.....	60
2.2.2. Consideration of inoculum and antibiotic doses .....	63
2.2.3. Induction of meningitis.....	63
2.2.4. Hearing loss assessment .....	65
2.2.5. Rabbit meningitis.....	68
2.3. Cochlear perfusion.....	70
2.3.1. Experimental design .....	70
2.3.2. Preparation of the animal.....	70
2.3.3. Recording techniques.....	71
2.4 Electron microscopy and photo-micrography .....	72
2.4.1. Fixation.....	72
2.4.2. Scanning electron microscopy.....	72
2.4.3. Transmission electron microscopy.....	72
2.4.4. Image processing .....	73
2.5 Data analysis .....	73
<b>3. EXPERIMENTAL MENINGITIS.....</b>	<b>75</b>
3.1. <i>E. coli</i> K-12 meningitis.....	75
3.1.1. Overview .....	75
3.1.2. Bacteriological preparation and CSF bacterial counts.....	75
3.1.3. Inflammatory response .....	76
3.1.4. Electrophysiological data.....	77
3.1.5. Ultrastructural findings (organ of Corti).....	78
3.1.6. Ultrastructural findings (basilar membrane and bacteria).....	79
3.1.7. Effects of cefotaxime on the SEM appearance of <i>E. coli</i> .....	79
3.2. Pneumococcal meningitis: development of recording techniques.....	96
3.2.1. Bacteriological preparation and findings.....	96
3.2.2. Inflammatory response.....	97
3.2.3. Electrophysiological data and development of techniques.....	98
3.2.4. Ultrastructural findings.....	102
3.3. Experimental meningitis with wild type (D39) organisms.....	119
3.3.1. Introduction and exclusions.....	119
3.3.2. Bacteriological findings.....	119
3.3.3. Inflammatory response.....	120
3.3.4. Electrophysiological data.....	120
3.3.5. Ultrastructural findings.....	122
3.4. Experimental meningitis with pneumolysin-deficient organisms <b>(PLN-A)</b> .....	139
3.4.1. Introduction and exclusions.....	139
3.4.2. Bacteriological findings.....	139
3.4.3. Inflammatory response.....	140

3.4.4. Electrophysiological data.....	140
3.4.5. Ultrastructural findings.....	141
3.5. Experimental meningitis with neuraminidase-deficient organisms ( $\Delta$ NA1).....	154
3.5.1. Introduction and exclusions.....	154
3.5.2. Bacteriological findings.....	154
3.5.3. Inflammatory response.....	154
3.5.4. Electrophysiological data.....	155
3.5.5. Ultrastructural findings.....	156
3.6. Experimental meningitis with hyaluronidase-deficient organisms ( $\Delta$ HY1).....	168
3.6.1. Introduction and exclusions.....	168
3.6.2. Bacteriological findings.....	168
3.6.3. Inflammatory response.....	169
3.6.4. Electrophysiological data.....	169
3.6.5. Ultrastructural findings.....	170
3.7. Induction of meningitis by purified pneumococcal cell wall.....	177
3.7.1. Introduction.....	177
3.7.2. Inflammatory response.....	177
3.7.3. Electrophysiological data.....	177
3.7.4. Ultrastructural findings.....	177
3.8. Statistical analysis of the comparative experiments.....	180
3.8.1. Differences in inoculum, CSF bacterial counts and bacteremia.....	180
3.8.2. Differences in CSF inflammatory markers.....	181
3.8.3. Comparison of <b>CAP</b> loss at 12 h in the comparative study groups.....	182
3.8.4. Comparison of rates of CAP loss.....	183
3.8.5. Comparison of cochlear microphonics.....	184
3.9. Pneumococcal meningitis in the rabbit: a comparison of wild-type (D39) and pneumolysin-deficient (PLN-A) infection.....	195
3.9.1. Introduction and exclusions.....	195
3.9.2. Inflammatory response.....	195
3.9.3. Electrophysiological data.....	195
3.9.4. Ultrastructural findings.....	195

<b>4. COCHLEAR PERFUSION</b> .....	<b>203</b>
4.1. Introduction.....	203
4.1.1. Overview.....	203
4.1.2. Inocula.....	203
4.2. <i>E. coli</i> perfusion.....	204
4.2.1. Electrophysiological data.....	204
4.2.2. Ultrastructural findings.....	204
4.3. Pneumococcal perfusion alone.....	208
4.3.1. Experimental details and exclusions.....	208
4.3.2. In vitro growth.....	208
4.3.3. Electrophysiological data.....	208
4.3.4. Ultrastructural findings.....	209
4.4. Pneumococcal perfusion with antibiotic pretreatment.....	216
4.4.1. Experimental details and exclusions.....	216
4.4.2. Electrophysiological data.....	216
4.4.3. Ultrastructural findings.....	217
4.5. Pneumococcal perfusion with dexamethasone pretreatment.....	228
4.5.1. Experimental details.....	228
4.5.2. Results .....	228
<b>5. DISCUSSION</b> .....	<b>230</b>
5.1. Experimental meningitis model.....	230
5.1.1. Clinical relevance of this experimental meningitis model .....	230
5.1.2. Preparation and administration of the inoculum .....	231
5.1.3. Documenting the induction of meningitis.....	233
5.2. Cochlear damage in experimental meningitis and other conditions.....	234
5.2.1. Data from other experimental meningitis models.....	234
5.2.2. Ultrastructural lesions of the organ of Corti in experimental meningitis.....	239
5.2.3. Cochlear lesions in other conditions.....	244
5.3. The role of pneumococcal products in causing meningogenic deafness.....	245
5.3.1. Interpreting data in insertion-duplication mutagenesis studies: a caution.....	245
5.3.2. Pneumolysin.....	246
5.3.3. Neuraminidase .....	248
5.3.4. Hyaluronidase .....	249
5.3.5. Pneumococcal cell wall .....	249
5.4. Cochlear perfusion.....	250
5.4.1. Comparison with cochlear lesions in meningitis .....	250

5.4.2. Antibiotic effects.....	251
5.5. Mechanisms of cochlear damage and its prevention.....	252
5.5.1. Dissipation of the endocochlear potential and mixing of cochlear fluids.....	252
5.5.2. Loss of hair cells and damage to hair bundles: the putative role of nitric oxide.....	253
5.5.3. Excitotoxic and physical damage to the neural elements .....	254
<b>5.5.4. Other factors</b> .....	255
5.6. Conclusions.....	256
<b>Appendix A:</b> Composition of solutions used .....	258
<b>Appendix B:</b> Details of the construction of the isogenic mutants of <i>S.pneumoniae</i> D39 deficient in pneumolysin, neuraminidase or hyaluronidase.....	260
<b>Appendix C:</b> Assays for pneumolysin, neuraminidase and hyaluronidase.....	262
<b>Appendix D:</b> Raw data from comparative meningitis experiments.....	262
<b>REFERENCES:</b> .....	follow page 266

# LIST OF FIGURES

## Chapter 1

<b>Figure 1.1:</b> Diagram of the cochlea in cross-section.....	26
<b>Figure 1.2:</b> Relationship of the inner ear to the subarachnoid space .....	27
<b>Figure 1.3:</b> Three-dimensional impression of the organ of Corti.....	28
<b>Figure 1.4:</b> Diagram of the ultrastructure of an inner hair cell.....	29
<b>Figure 1.5:</b> Diagram of the ultrastructure of an outer hair cell.....	30
<b>Figure 1.6:</b> Electrophysiological recordings from the round window.....	31

## Chapter 2

<b>Figure 2.1:</b> Tone-evoked responses: equipment diagram .....	69
---	----

## Chapter 3

<b>Figure 3.1:</b> <i>E. coli</i> K-12 meningitis: CSF bacterial concentration.....	83
<b>Figure 3.2:</b> <i>E. coli</i> K-12 meningitis: CSF white cell count.....	84
<b>Figure 3.3:</b> <i>E. coli</i> K-12 meningitis: click-evoked brain-stem auditory responses.....	85
<b>Figure 3.4:</b> <i>E. coli</i> K-12 meningitis: Summary of hearing loss.....	86
<b>Figure 3.5:</b> Spectral analysis of unramped tone pips.....	105
<b>Figure 3.6:</b> Spectral analysis of 10 MIZ tone pip: ramped vs. unramped.....	106
<b>Figure 3.7:</b> Spectral analysis of 3 kHz tone pip: ramped vs. unramped.....	107
<b>Figure 3.8:</b> Pneumococcal meningitis (D39): typical tone-evoked brain stem Potentials.....	108
<b>Figure 3.9:</b> Pneumococcal meningitis (D39): example of hearing loss over time (BAEP).....	109
<b>Figure 3.10:</b> Tone-evoked brain stem Potentials: stimulus/responsecurve 3 h apart.....	110
<b>Figure 3.11:</b> Tone-evoked brain stem Potentials: stimulus/responsecurve.....	111
<b>Figure 3.12:</b> Tone-evoked compound action potential: stimulus/responsecurve.....	112

<b>Figure 3.13:</b> The definition of the compound action potential threshold in terms of a reference level.....	113
<b>Figure 3.14:</b> Control round window recording.....	<b>125</b>
<b>Figure 3.15:</b> D39 meningitis: hearing loss over time in a typical experiment.....	126
<b>Figure 3.16:</b> D39 meningitis: mean hearing loss over time.....	127
<b>Figure 3.17:</b> D39 meningitis: audiograms (3 h and 6 h) .....	128
<b>Figure 3.18:</b> D39 meningitis: audiograms (9 h and 12 h) .....	129
<b>Figure 3.19:</b> Serial CAP recordings from unaffected and affected ears.....	130
<b>Figure 3.20:</b> PLN-A meningitis: mean hearing loss over time.....	143
<b>Figure 3.21:</b> PLN-A meningitis: audiograms (3 h and 6 h).....	144
<b>Figure 3.22:</b> PLN-A meningitis: audiograms (9 h and 12 h).....	145
<b>Figure 3.23:</b> $\Delta$ NA1 meningitis: mean hearing loss over time.....	158
<b>Figure 3.24:</b> ANA1 meningitis: audiograms (3 h and 6 h) .....	159
<b>Figure 3.25:</b> ANA1 meningitis: audiograms (9 h and 12 h) .....	160
<b>Figure 3.26:</b> $\Delta$ HY1 meningitis: mean hearing loss over time.....	172
<b>Figure 3.27:</b> $\Delta$ HY1 meningitis: audiograms (3 h and 6 h) .....	173
<b>Figure 3.28:</b> $\Delta$ HY1 meningitis: audiograms (9 h and 12 h) .....	174
<b>Figure 3.29:</b> In vitro growth curves of <i>S.pneumoniae</i> D39, $\Delta$ NA1 and $\Delta$ HY1.....	185
<b>Figure 3.30:</b> Pneumococcal meningitis: inoculum given.....	186
<b>Figure 3.31:</b> Pneumococcal meningitis: CSF bacterial count.....	187
<b>Figure 3.32:</b> Pneumococcal meningitis: CSF white cell count.....	<b>188</b>
<b>Figure 3.33:</b> Pneumococcal meningitis: CSF protein concentration.....	189
<b>Figure 3.34:</b> Pneumococcal meningitis: blood bacterial count.....	190
<b>Figure 3.35:</b> Pneumococcal meningitis: scatter plot of 10 <b>kHz</b> hearing loss.....	191
<b>Figure 3.36:</b> Pneumococcal meningitis: scatter plot of 3 <b>kHz</b> hearing loss.....	192
<b>Figure 3.37:</b> Pneumococcal meningitis: scatter plot of <b>CM</b> loss.....	193
<b>Figure 3.38:</b> Pneumococcal meningitis: scatter plot of CAP vs. <b>CM</b> .....	194
<b>Figure 3.39:</b> Rabbit pneumococcal meningitis: scatter plot of hearing loss.....	202

## Chapter 4

<b>Figure 4.1:</b> Growth of <i>S.pneumoniae</i> D39 in artificial perilymph.....	211
<b>Figure 4.2:</b> Cochlear perfusion: scatter plot of change in compound action potential.....	220
<b>Figure 4.3:</b> Cochlear perfusion: scatter plot of change in cochlear microphonic.....	221
<b>Figure 4.4:</b> Effect of cefotaxime on pneumococcal-induced hearing loss.....	222
<b>Figure 4.5:</b> Effect of amoxicillin on pneumococcal-induced hearing loss.....	223

## Appendix

<b>Figure:</b> Schematic diagram of insertion-duplicationmutagenesis .....	261
--	-----

## LIST OF PLATES

### Chapter 3: Experimental meningitis

<b>Plate 3.1–3.7:</b>	<i>E. coli</i> K-12: organ of Corti (guinea pig) .....	87–90
<b>Plate 3.8–3.10:</b>	<i>E. coli</i> K-12: undersurface of basilar membrane .....	.90–91
<b>Plate 3.11–3.18:</b>	Effect of cefotaxime on morphology of <i>E. coli</i> .....	.92–95
<b>Plate 3.19–3.24:</b>	<i>S.pneumoniae</i> D39: organ of Corti (guinea pig) .....	114–116
<b>Plate 3.25–3.26:</b>	<i>S.pneumoniae</i> D39: undersurface of basilar membrane.....	117
<b>Plate 3.27:</b>	Cross section of <i>S.pneumoniae</i> (TEM) .....	118
<b>Plate 3.28–3.40:</b>	<i>S.pneumoniae</i> D39: organ of Corti (guinea pig) .....	131–138
<b>Plate 3.41–3.52:</b>	<i>S.pneumoniae</i> PLN-A: organ of Corti (guinea pig) .....	146–153
<b>Plate 3.53–3.61:</b>	<i>S.pneumoniae</i> $\Delta$ NA1: organ of Corti (guinea pig) .....	161–167
<b>Plate 3.62–3.65:</b>	<i>S.pneumoniae</i> $\Delta$ HY1: organ of Corti (guinea pig).....	175–176
<b>Plate 3.66–3.67:</b>	Basilar membrane after pneumococcal cell wall challenge .....	179
<b>Plate 3.68–3.71:</b>	<i>S.pneumoniae</i> D39: organ of Corti (rabbit).....	198–199
<b>Plate 3.72–3.75:</b>	<i>S.pneumoniae</i> PLN-A: organ of Corti (rabbit) .....	.200–201

### Chapter 4: Cochlear perfusion

<b>Plate 4.1–4.4:</b>	<i>E. coli</i> K-12: organ of Corti .....	206–207
<b>Plate 4.5–4.12:</b>	<i>S.pneumoniae</i> D39 (no pretreatment): organ of Corti .....	212–215
<b>Plate 4.13–4.14:</b>	<i>S.pneumoniae</i> D39 (cefotaxime pretreatment): organ of Corti .....	224
<b>Plate 4.15–4.16:</b>	<i>S.pneumoniae</i> D39: (amoxicillin pretreatment): organ of Corti.....	225
<b>Plate 4.17–4.20:</b>	Effect of amoxicillin on morphology of <i>S.pneumoniae</i> D39 .....	226–227
<b>Plate 4.21–4.22:</b>	<i>S.pneumoniae</i> D39 (dexamethasone pretreatment).....	229

# LIST OF TABLES

## Chapter 1

<b>Table 1.1:</b> Possible pneumococcal virulence factors. ....	8
<b>Table 1.2:</b> Activities of purified pneumolysin possibly related to pathogenesis of infection.....	13
<b>Table 1.3:</b> A classification of hearing loss .....	42
<b>Table 1.4:</b> Final audiological outcome in 142 children with meningitis (taken from Wald <i>et al</i> 1995).....	50

## Chapter 2

<b>Table 2.1:</b> Derivatives of <i>S. pneumoniae</i> D39 used. ....	57
<b>Table 2.2:</b> Batches of <i>S. pneumoniae</i> used. ....	59
<b>Table 2.3:</b> Numbering of guinea pig experiments.....	61

## Chapter 3

<b>Table 3.1:</b> Untreated <i>E. coli</i> K-12 meningitis: CSF and hearing loss data. Summary of morphological findings.....	81
<b>Table 3.2:</b> Cefotaxime-treated <i>E. coli</i> K-12 meningitis: CSF and hearing loss data. Summary of morphological findings.....	82
<b>Table 3.3:</b> Effect of ramp time on frequency specificity of tone pips. ....	99
<b>Table 3.4:</b> Evaluation of pneumococcal meningitis: CSF and blood data.....	103
<b>Table 3.5:</b> Evaluation of pneumococcal meningitis: hearing loss and ultrastructural data.....	104
<b>Table 3.6:</b> D39 (wild-type) meningitis experiments included in comparative study. ....	124
<b>Table 3.7:</b> PLN-A (pneumolysin-deficient) meningitis experiments included in comparative study.....	142
<b>Table 3.8:</b> ANA1 (neuraminidase-deficient) meningitis experiments included in comparative study.....	157
<b>Table 3.9:</b> $\Delta$ HY1 (hyaluronidase-deficient) meningitis experiments included in comparative study.....	171
<b>Table 3.10:</b> Details of experiments with pneumococcal cell wall material.....	178
<b>Table 3.11:</b> CSF viable counts in comparative study.....	180
<b>Table 3.12:</b> Blood viable counts in comparative study.....	181

<b>Table 3.13:</b> CSF inflammatory response in comparative study.....	181
<b>Table 3.14:</b> CAP loss in comparative study.....	182
<b>Table 3.15:</b> Rate of CAP loss in comparative study.....	183
<b>Table 3.16:</b> Cochlear microphonic loss in comparative study.....	<b>184</b>
<b>Table 3.17:</b> Details of rabbit meningitis experiments.....	197

#### **Chapter 4**

<b>Table 4.1:</b> Cochlear perfusion with <i>E. coli</i> K-12: electrophysiological data .....	<b>205</b>
<b>Table 4.1:</b> Cochlear perfusion of <i>S. pneumoniae</i> D39: electrophysiological data.....	210
<b>Table 4.2:</b> Cochlear perfusion of <i>S. pneumoniae</i> D39 with cefotaxime pretreatment: electrophysiological data.....	218
<b>Table 4.3:</b> Cochlear perfusion of <i>S. pneumoniae</i> D39 with amoxicillin pretreatment: electrophysiological data.....	219
<b>Table 4.4:</b> Cochlear perfusion of <i>S. pneumoniae</i> D39 with dexamethasone pretreatment: electrophysiological data.....	228

## ABBREVIATIONS

95%CI	95% Confidence interval
AMOX	Amoxicillin
APL	Artificial perilymph
CFU	Colony forming units
CSF	Cerebrospinal fluid
CTX	Cefotaxime
ERY	Erythromycin
Hib	<i>Haemophilus influenzae</i> type B
<i>HY</i>	Hyaluronidase
IHC	Inner hair cell
IL-1 (-6,-8)	Interleukin-1 (-6,-8)
LD50	Lethal dose for 50% of test group
<i>MUAN</i>	2'-(4-methylumbelliferyl)- $\alpha$ -D-N-acetylneuraminic acid
NA	Neuraminidase
NO	Nitric oxide
OHC	Outer hair cell
p.i.	Post inoculation
PAF	Platelet activating factor
PBS	Phosphate-buffered saline
PCW	Pneumococcal cell wall
PLY	Pneumolysin
SEM	Scanning electron microscopy
TEM	Transmission electron microscopy
<b><i>TNF<math>\alpha</math></i></b>	Tumour necrosis factor alpha

# 1. INTRODUCTION

## 1.1. Bacterial meningitis.

Acute bacterial meningitis is a common and much-feared disease with a significant mortality. In spite of dramatic improvements in antibiotic therapy and supportive care over the last **fifty** years, not everyone who survives bacterial meningitis can expect to make a full recovery. Around 10% of survivors will have some kind of neurological deficit, ranging from sensorineural deafness to hemiplegia or worse. Patients in developing countries fare especially badly, and pneumococcal meningitis in particular carries a grim prognosis.

This thesis is chiefly concerned with pneumococcal meningitis and the deafness which it causes. Data from a newly developed model of hearing loss in experimental meningitis in the guinea pig are presented. The findings show that experimental meningitis damages the physiological function and ultrastructure of the inner ear. Evidence for the importance of pneumococcal toxin pneumolysin in this process will be discussed. Some of the first in vivo data obtained from experimental infections with pneumococci deficient in neuraminidase or hyaluronidase will also be presented.

This introduction will review:

- clinical aspects of bacterial meningitis;
- the pathogenesis of pneumococcal disease;
- the structure and function of the inner ear;
- the pathogenesis of meningitis with reference to experimental infection models;
- evidence from clinical and experimental studies of deafness in meningitis.

The final section discusses shortcomings in the current paradigm used to explain why deafness occurs in meningitis and outlines the experimental data to be presented in subsequent chapters.

### 1.1.1. Epidemiology and causative agents.

The annual mean incidence of bacterial meningitis in the **USA** was between 1.9 per 100,000 and 4.0 per 100,000 in a recent survey (Wenger *et al* 1990) and is probably similar in the UK. In developing countries, attack rates may be ten times higher (Bryan *et al* 1990). Three organisms are responsible for the majority of cases of bacterial meningitis: *Neisseria meningitidis*, *Streptococcus pneumoniae* and *Haemophilus influenzae* with case fatality

rates in the USA in the early 1980s of 10.3%, 26.3% and 6.0% respectively (Schlech *et al* 1985). All are exclusive human pathogens and are commonly carried in the nasopharynx of healthy people (Austrian, 1986). *Streptococcus pneumoniae* will be considered in detail in section 1.2; we will briefly consider here the other major pathogens.

*Haemophilus influenzae* is a small (0.3–0.5 x 1–2 µm) non-motile non-sporing fastidious Gram-negative cocco-bacillus. Haemophili are facultative anaerobes which grow best in enriched media. Almost all clinically significant disease is caused by the encapsulated *Haemophilus influenzae* type B (Hib). Penicillin resistance is common. Until the recent introduction of the Hib conjugate vaccine in most developed countries, Hib was the commonest cause of bacterial meningitis in children under five and was an important cause of invasive bacteremia in infants. The incidence declines in older children, who acquire specific neutralising antibody. Because of the rapid fall in the incidence of invasive Hib infection, clinical studies of meningitis conducted at a time of high Hib prevalence must be interpreted carefully today. There has been a suggestion that the incidence of pneumococcal infection has increased to fill the niche left by eradication of Hib (Baer *et al* 1995). Globally, invasive Hib infections remain an extremely serious problem because Hib conjugate vaccination has not been made available to the deprived children in the developing world that need it most (Dagan 1996).

*Neisseria meningitidis* (meningococcus) is a delicate non-sporing non-motile Gram negative oval diplococcus (0.8 µm in diameter) which also requires enriched media (such as Mueller-Hinton medium) for isolation. There are eight main serogroups which vary in their pathogenicity and geographical distribution. Group B serotypes are mainly responsible for outbreaks in the UK, but groups A and C are common in the sub-Saharan epidemics. Invasive meningococcal disease can progress at frightening speed and can kill within 12 h of initial symptoms. There is an important distinction between meningococcal meningitis, in which the infection is limited to the cerebrospinal fluid (CSF) space, and the severe systemic illness of meningococcal septicaemia. Meningococci are exquisitely sensitive to penicillin and there is as yet little problem with resistance.

*Escherichia coli* is a common cause of neonatal meningitis. Eighty per cent of isolates bear the K1 capsular subtype (Mulder *et al* 1984). *E. coli* are Gram-negative, motile, non-sporing bacilli (0.5 x 1–2 µm). Colonies grown on Macconkey medium are smooth, glossy and tinged rose-pink due to lactose fermentation. Three kinds of surface antigens are demonstrable: the O (somatic), K (capsular) and H (flagellar) antigens. Between serogroups there is great diversity in antibiotic sensitivity, virulence and production of enterotoxins.

Other causes of acute bacterial meningitis include *Citrobacter* spp and Group B *Streptococci* (GBS) in neonates, and *Listeria monocytogenes*, *Pseudomonas* and *Staphylococcus* in adults. *Mycobacterium tuberculosis* can present as an acute meningitis but will not be further considered here.

### **1.1.2. Clinical presentation and treatment**

The initial symptoms of bacterial meningitis resemble the onset of 'flu. Babies may refuse feeds, vomit, become difficult to wake and feverish. Adults and children commonly develop headache, neck stiffness and drowsiness. They may be unable to tolerate bright lights (photophobia) and become confused. In meningococcal septicaemia, a purplish blotchy rash can develop. A recent retrospective survey of 305 cases of bacterial meningitis occurring in the UK during 1989 and 1990 showed that two-thirds of patients had been unwell for at least 12 h prior to admission. Less than 18% of patients had received antibiotic therapy before admission as is currently recommended (British Society for the Study of Infection 1995). Signs found on examination include fever, neck stiffness, impaired consciousness or coma, and a purpuric rash (usually but not invariably associated with meningococcal disease). The occurrence of seizures and coma are poor prognostic factors. The most important investigation is examination of the cerebrospinal fluid (CSF) by Gram stain, culture and cell count. A definitive diagnosis rests on CSF culture or detection of pneumococcal antigen. Contrary to popular belief organisms can be isolated from the majority of cases given antibiotics before admission. Classically the CSF in acute bacterial meningitis is turbid, with a predominant neutrophil leukocytosis in excess of 5-10 cells/ $\mu\text{l}$ , sometimes over 10,000 cells/ $\mu\text{l}$ , a raised CSF protein concentration ( $>0.5\text{ g/l}$ ) and a reduced CSF:plasma glucose ratio ( $<2/3$ ). However, in 18% of the cases in the BSSI series the CSF was clear even though it contained viable organisms. Blood cultures are positive in around 60% of cases.

Treatment of acute bacterial meningitis requires hospital admission, prompt intravenous antimicrobial therapy and good supportive care. The choice of antibiotic is dictated by local epidemiology and resistance patterns. In the UK, the combination of benzylpenicillin and chloramphenicol remains popular (British Society for the Study of Infection, 1995). Penicillin-resistant pneumococci (PRSP) probably originated in Spain and are now distributed widely around the world, being a particular problem in the USA and South Africa (Klugman, 1994b). In these areas, first line therapy consists of a third-generation cephalosporin such as cefotaxime. Because PRSP often exhibit intermediate resistance to third-generation cephalosporins (Klugman, 1994a), some authors now recommend adding vancomycin to the initial blind therapy in such areas (McCracken, Jr., 1996). The prevalence

of PRSP isolates in England and Wales rose from 1.5% in 1990 to 3.9% in 1995 (Johnson, 1996), indicating a serious problem ahead.

## **1.2. Streptococcus pneumoniae.**

### **1.2.1. Introduction.**

*Streptococcus pneumoniae* (the pneumococcus) is an important human pathogen. It is a major cause of community-acquired pneumonia, otitis media, meningitis, and bacteremia, particularly attacking people at extremes of age, those with underlying disease such as HIV infection, and hyposplenic individuals. Common predisposing factors for pneumococcal meningitis include pneumonia, sinusitis, middle ear pathology and CSF leak following head injury. In the UK during the period 1982-1992 there were 22 567 reports of pneumococcal bacteraemia and 3500 reports of pneumococcal meningitis, representing about 18% of the total meningitis reports received by the Public Health Laboratory Service (PHLS). The annual mean incidence of pneumococcal meningitis in the UK during the period 1989-92 was 8.7 episodes per 100,000 population (Askenasy *et al* 1995). In the US the reported incidence is about 1.1 per 100,000 population but rises to 30 per 100,000 in infants under 5 months of age (Schlech, 1985). Globally, *S. pneumoniae* causes over 1 million deaths a year in children under the age of 5 years (Obaro, 1996). Pneumococcal meningitis occurs in epidemics across sub-Saharan Africa and is the most common form of meningitis in some areas (Dagan, 1996).

Study of the pneumococcus has yielded much information, including the discovery of DNA as the transforming factor and the recognition of capsular polysaccharide as an immunogen, leading to the manufacture of the first bacterial polysaccharide vaccine (Avery and Dubos, 1931; Austrian, 1981; Tuomanen *et al* 1995; Watson *et al* 1993).

### **1.2.2. Pneumococcal structure.**

Pneumococci are Gram-positive cocci about 1  $\mu\text{m}$  in diameter which grow in pairs or short chains. They are non-motile and non sporing. Three layers make up the surface: the plasma membrane, the cell wall, and the polysaccharide capsule. The capsule is some 200-400 nm thick and conceals the underlying layers during exponential growth. Differences in capsular structure provide immunological diversity and form the basis for serotyping organisms. The cell wall has a triple-layered peptidoglycan backbone consisting of alternating N-acetylglucosamine and N-acetylmuramic acid residues cross-linked through peptide chains. It is a dynamic macromolecule with components being continuously inserted into and

released from the structure (Tuomanen *et al* 1995). Cell wall polysaccharide, a complex teichoic acid, is linked to the peptidoglycan backbone by N-acetylmuramic acid. A specific enzyme, autolysin (N-acetylmuramic acid-L-alanine amidase), cleaves this linkage. The Forssmann antigen, which is an inhibitor of autolysin, is a lipoteichoic acid embedded in the plasma membrane. Cells in the stationary phase of growth liberate Forssmann antigen, so deregulating local autolysin and inducing cell lysis. Both peptidoglycan and teichoic acid are powerful stimulators of the immune response (Tuomanen *et al* 1985a). Little is known about the function of the various surface proteins that have recently been identified (Tuomanen *et al* 1995). Pneumococcal surface protein A (PspA) is an antigenically variable surface protein which is firmly anchored in the cell wall and appears to be essential for full virulence. It might act by inhibiting complement activation (AlonsoDeVelasco *et al* 1995). Other surface proteins are probably involved in pneumococcal adherence to epithelial cells (Paton *et al* 1993a) and degradation of complement component C3 (Angel *et al* 1994).

Pneumococci are aerobic and facultatively anaerobic and grow well in most laboratory media such as Todd Hewitt medium, or Brain Heart Infusion broth. In broth culture, pneumococci tend to autolyse once stationary phase is reached. Colonies of encapsulated organisms on blood agar are small, smooth and transparent and surrounded by a greenish area of  $\alpha$ -haemolysis. Unencapsulated pneumococci form rough colonies. The presence of capsule can be confirmed with the Quellung test which is serotype specific (Frasch, 1995). At least three interchangeable variants can be defined on colonial morphology: opaque, semi-transparent and transparent.

### **1.2.3. Colonisation of the host.**

Pneumococci generally reside in the human nasopharynx and probably the entire human population is colonised at some time (Austrian, 1986). Some of these people go on to develop invasive disease. This seems to be associated with recent colonisation and is more likely with certain serotypes (Boulnois, 1992). The main route of infection is by aerosol inhalation of pneumococci which colonise the upper and then the lower respiratory tract. The lower respiratory tract is protected by several non-specific mechanisms, such as the cough reflex, mucociliary transport and IgA secretions, and by the presence of resident alveolar macrophages. Pneumococci secrete an IgA1-specific protease, which would inhibit mucosal immunity provided by IgA. Colonisation and invasion is aided by a specific interaction with disaccharide molecules such as N-acetyl glucosamine  $\beta$ 1-3 galactose (GlcNAc $\beta$ 1-3Gal) found on oral epithelial cells. Pneumococcal phase variation contributes to the colonisation **as** the transparent phenotype binds up to  $10^6$  times more efficiently to GlcNAc $\beta$ 1-3Gal than the opaque phenotype (Cundell *et al* 1995). Resting pneumocytes express two classes of

receptors to which pneumococci of any phase can bind: **N-acetyl-D-galactosamine** linked  $\beta$ 1–3 or  $\beta$  1 4 to galactose (GalNAc $\beta$ 1–3Gal or GalNAc $\beta$ 1-4Gal). Transparent-phase pneumococci also bind to a platelet-activating factor (*PAF*) receptor expressed on activated pneumocytes (Cundell *et al* 1995), which may explain increased susceptibility to pneumococcal disease after respiratory viral infections. It has also been suggested that neuraminidase derived from pneumococci or during co-infection with the influenza virus exposes target receptors on the host cells by cleaving sialic acid from glycolipids (Krivan *et al* 1988). In isolated organ cultures of human respiratory epithelium, pneumococci are found to adhere only to mucus and to damaged ciliated mucosa, where they attach to the gaps between cells (Rayner *et al* 1995).

Once established in the alveoli, intra-alveolar replication gives rise to the classic lobar pneumonia. A bacteraemia can ensue, either by invasion from the pneumonic lung or perhaps directly by invasion from the upper respiratory tract. Pneumococci are cleared from the blood stream by the liver and spleen. **An** acute phase protein, C-reactive protein (CRP), binds to pneumococcal cell wall **and** activates the classical complement pathway, so acting **as** a primitive antibody. Pneumococci probably reach the meninges by haematogenous spread but the exact mechanisms of entry into the subarachnoid space remain a mystery. **As** discussed below, various pneumococcal components elicit a vigorous local immune response. Host tissue damage results both from an excessive local immune reaction and from pneumococcal products which are directly cytotoxic.

#### **1.2.4. Capsule.**

The possession of a polysaccharide capsule is essential for invasive pneumococcal disease to occur. At least 84 capsular types are recognised (Collee *et al* 1989). The capsule acts to resist opsonophagocytosis (Wood, Jr. and Smith, 1949). Encapsulated strains are some  $10^5$  times more virulent than unencapsulated strains in experimental models in vivo and all strains isolated from clinically invasive disease are encapsulated (Avery and Dubos, 1931; Austrian, 1981). Capsule is not however necessary for pneumococcal replication in the CSF space (Tuomanen *et al* 1985b). Although capsule is an essential virulence factor, capsular polysaccharides are in general poor stimulators of the inflammatory reaction which is held to be responsible for so much autologous tissue damage. In spite of this, purified capsular polysaccharides can stimulate production and secretion of tumour necrosis factor-alpha (**TNF $\alpha$** ) by murine macrophages (Simpson *et al* 1994). Certain serotypes are frequently isolated from cases but rarely found in carriers, suggesting these serotypes are more virulent for invasive disease. Variation of the capsule itself is at least partly responsible for the difference in virulence between serotypes. For example, replacing the capsule of a highly

virulent type 5 strain with type 3 capsule by genetic manipulation renders the otherwise isogenic derivative avirulent for mouse bacteremia. But switching the capsule of a relatively apathogenic type 6B strain to the same type 3 capsule enhances virulence (Kelly *et al* 1994). These data demonstrate that there is a complex interaction between capsular type and other virulence mechanisms such as differences in exposure of the cell wall components. There is also serotype variation in the activation of the alternate complement pathway, one of the immune system's first line defences (Fine, 1975).

The current 23-valent polysaccharide vaccine contains types 1, 2, 3, 4, 6B, 7F, 8, 9N, 9V, 10A, 11A, 12F, 14, 15B, 17F, 18C, 19F, 19A, 20, 22F, 23F and 33F. The prevalence of invasive pneumococcal serotypes varies geographically and with age, so the expected level of protection afforded by the vaccine varies between patient groups. In the UK at least, of 750 pneumococcal blood isolates and 130 CSF isolates serotyped in the UK by the PHLS in 1993, over 95% belonged to serotypes present in the 23-valent vaccine (George, 1995). In spite of this apparently good coverage capsular polysaccharides are poorly immunogenic in those most at risk of infection (Lee and Wang, 1994). Thus over recent years attention has focused on other pneumococcal constituents which may induce inflammation or enhance virulence. This work aims firstly to improve upon current immunisation techniques by finding more immunogenic targets for at-risk populations and provide cross-serotype immunity (Alexander *et al* 1994; Lock *et al* 1992). Conjugate vaccines help promote a T-helper cell response, and so induce better immunity in young infants. Polysaccharide-protein conjugate vaccines containing a biologically inactive toxoid such as a derivative of the pneumococcal protein pneumolysin are showing great promise (Lee and Wang, 1994; Mitchell *et al* 1992). Unfortunately for the majority of those at risk, conjugate vaccines undergoing trials at present omit serotypes 1, 5 and 7 which are common causes of invasive pneumococcal disease in children in developing countries (Dagan, 1996). Study of such accessory virulence factors also helps to elucidate the mechanism of pneumococcal disease. Table 1.1 (derived from AlonsoDeVelasco, 1995) lists some characteristics of the major proposed pneumococcal virulence factors.

Virulence factor	Proposed mechanism of virulence	Selected References
Capsule	Resists phagocytosis Poorly immunogenic Fails to activate alternative complement pathway	Wood, Jr. and Smith, 1949 Avery and Dubos, 1931 Fine, 1975
Cell wall products	Induces inflammation and Chemotaxis  Attaches to endothelial cells and is cytotoxic Directly cytotoxic for astrocytes	Tuomanen <i>et al</i> 1985a Tanaka <i>et al</i> 1994 Heumann <i>et al</i> 1994 Geelen <i>et al</i> 1993  Kim <i>et al</i> 1995
Pneumolysin	see table 1.2	
Neuraminidase	Exposes cell surface receptors for pneumococcal adherence Damage to glycolipids, glycoproteins and oligosaccharides Promotes neutrophil adherence	Krivan <i>et al</i> 1988  Paton <i>et al</i> 1993a  Marin <i>et al</i> 1995
Hyaluronidase	Bacterial dissemination and breaching the blood brain barrier Survival in the blood stream and CSF ?Nutritional	Kostyukova <i>et al</i> 1995  Hill <i>et al</i> 1996 (this thesis)
Autolysin	Release of pneumolysin and cell wall material during spontaneous lysis	Lock <i>et al</i> 1992 Berry <i>et al</i> 1992 Canvin <i>et al</i> 1995
Hydrogen peroxide	Cytotoxic for alveolar epithelial cells	Duane <i>et al</i> 1993
PspA	Inhibits complement activation	AlonsoDeVelasco <i>et al</i> 1995
IgA1 protease	Inhibits mucosal defence	Kornfield and Plaut, 1981
C3 degrading proteinase	Resists opsonophagocytosis	Angel <i>et al</i> 1994
Adhesins	Binding to epithelial cells	Paton <i>et al</i> 1993a
Oxidative response inhibitor	Prevents neutrophil killing due to reactive oxygen intermediates	Perry <i>et al</i> 1994

**Table 1.1:** Possible pneumococcal virulence factors.

### 1.2.5. Cell wall.

Tuomanen and colleagues (1995) emphasise the role of cell wall products in the pathogenesis of pneumococcal infection. Pneumococcal cell wall (PCW) material liberated during exponential growth in the alveolar space binds to epithelial and endothelial cells (Geelen *et al* 1993). PCW causes contiguous endothelial cells to separate from each other, resulting in tissue oedema and probably aiding pneumococcal invasion. Activation of the procoagulant cascade causes fibrin deposition. Liberated PCW also binds to leukocyte CD14 receptors, eliciting the production of cytokines, particularly interleukin-1 (IL-1) in vitro. However, Heumann *et al* (1994) found that in the presence of 10% pooled plasma, various intact Gram-positive cell walls could also induce **TNF- $\alpha$**  and interleukin-6 (IL-6) expression by monocytes. In vivo, therefore, all three of these proinflammatory cytokines are likely to be expressed. Leukocytes are recruited both by the selectin-integrin (CD18) pathway commonly activated by many infections, and in the lung by a CD18-independent but PAF-dependent pathway unique to pneumococcal infection. Leukocyte recruitment into the subarachnoid space in response to challenge with pneumococci (but not with *Haemophilus influenzae*) is reduced by a specific PAF-receptor antagonist (Cabellos *et al* 1992). Local activation of complement amplifies the immune response. As leukocytes begin to control the infection by phagocytosing organisms, the dying bacteria release more PCW and soluble factors such as pneumolysin, which serve to increase autologous tissue damage. Rapid destruction of bacteria by cell wall active antibiotics will, according to this model, cause a transient rise in local inflammation due to the excess PCW released. Pneumococcal cell wall products at a similar concentration to that which provokes meningeal inflammation in vivo induce **TNF $\alpha$**  and nitric oxide production by cultured rat glial cells. This is inhibited by dexamethasone (Freyer *et al* 1996). Heat-killed pneumococci and PCW are cytotoxic for both human microglia and astrocytes in cell culture, but there is no evidence that pneumococcal cell products are directly toxic for neuronal cell lines (Kim *et al* 1995). Different components of PCW have different activities in vivo. Meningeal inflammation provoked by the teichoic acid component of PCW peaks at 5 h whereas that due to the peptidoglycan component peaks at 24 h (Tuomanen *et al* 1985a).

Although the role of cell wall in inducing inflammation is undisputed, Boulnois (1992) and Paton (1993) have emphasised the role of pneumococcal proteins in pathogenesis. Pneumolysin, neuraminidase, and hyaluronidase are of particular relevance to this thesis and will be considered below in more detail.

### 1.2.6. Pneumolysin.

The production of a haemolysin by the pneumococcus was first reported by Libman (1905), and the factor responsible was purified to homogeneity by Shumway *et al* (1971). The gene has been isolated, cloned and expressed in *E. coli* by two independent groups (Paton *et al* 1986; Walker *et al* 1987).

#### *Structure and function of pneumolysin*

Pneumolysin consists of single 53 kD polypeptide chain. It is one of a family of cholesterol-binding cytolysins (previously known as thiol-activated cytolysins) produced by Gram-positive organisms which share certain characteristics, including similar molecular weight, reversible loss of activity upon oxidation of crude preparation or exposure to cholesterol, and immunological cross-reactivity (Mitchell *et al* 1992). The most important difference between pneumolysin and other similar toxins is that pneumolysin is located in the cytoplasm, and the predicted amino acid sequence lacks a typical N-terminal signal peptide (Walker *et al* 1987). Cytolysins bind to cholesterol in plasma membranes, oligomerise, and form large (40-50 nm) transmembrane pores which cause cell lysis. Pneumolysin possesses a structural motif of an 11 amino acid sequence surrounding a single cysteine residue which is common to other pore-forming toxins. This is thought to form an amphiphilic helix spanning the cell membrane. Evidence from site directed and random mutagenesis studies have shown that mutations within this motif can abolish haemolytic activity. The altered proteins resulting from such mutagenesis studies are referred to as pneumolysoids or simply toxoids. Thiol-activation is in fact only necessary for the crude preparations of the toxin as oxidation does not affect the haemolytic activity of the purified protein. Consistent with this, the single cysteine residue itself is not necessary for full haemolytic activity as this property was not affected by a Cys-428→Ala substitution (Saunders *et al* 1989). The greatest reduction in haemolytic activity achieved by a single substitution is for Trp-433→Phe (a 99% fall) (Hill *et al* 1994) but the combination of Trp-433→Phe and Cys-428→Gly reduces haemolytic activity to 0.0001% of wild type (Berry *et al* 1995). A His-367→Arg substitution prevents the toxin forming oligomers in the cell membrane and also reduces haemolytic activity by 99% (Mitchell *et al* 1992).

Cell binding appears to be mediated by the C-terminus of the peptide, with deletion of as few as six terminal residues decreasing cell binding by 98% (Owen *et al* 1994). The ability of pneumolysin to activate complement is critically dependent upon yet another part of the molecule, being abolished by a Asp-385→Asn substitution, which reduces but does not completely abolish binding to Fc (Mitchell *et al* 1991). Blocking studies with monoclonal antibodies confirm that haemolytic activity is independent of cell binding and complement

activation. Two of these monoclonals also cross-react with the clostridial toxin, perfringolysin O (deLosToyos *et al* 1996).

The exact structure of the pore-forming mechanism remains unclear but recent ultrastructural studies by Morgan *et al* (1994, 1995) confirm that oligomerisation occurs and that the four domains of pneumolysin pack into a square planar arrangement. In lipid bilayers, pneumolysin forms multiple-sized channels with varying cation:anion selectivity. The small, more cation-selective channels become voltage sensitive in the presence of divalent cations (Korchev *et al* 1992).

### ***Role in pathogenesis***

Evidence for the role of pneumolysin in pathogenesis has come from three main areas of research:

- Study of the direct cytotoxic and immunomodulatory activity of the toxin itself using native or recombinant protein;
- Modification of the course of pneumococcal infection in animals previously immunised with pneumolysin or toxoided pneumolysin;
- Comparison of the course of experimental infection induced by wild type pneumococcal infection with that due to isogenic mutants deficient in pneumolysin or expressing toxoided pneumolysin.

### ***Activities of pneumolysin***

Pneumolysin has a wide range of cytotoxic and immunomodulatory effects, some of which are detailed in table 1.2 (see also Paton 1996). The potential contribution of pneumolysin to the pathogenesis of infection is large. Toxicity has usually been assessed using cultured cell lines. There are data available about the in vivo toxicity of purified pneumolysin in rat lung, guinea pig inner ear and rabbit cornea. Toxoided pneumolysin has also been tested in all of these systems (although the data for intracochlear perfusion is unpublished). In a model of rabbit meningitis, recombinant pneumolysin (0.1 µg to 1 µg) administered by cisternal injection induces a CSF leukocytosis (maximal at 4 h) and a rise in CSF concentrations of **TNF $\alpha$**  (maximal at 2 h), lactate and protein (Friedland *et al* 1995). This inflammatory response is unaffected by a substitution (Asp-385→Asn) which renders the toxoid unable to activate complement. However, a toxoid deficient in haemolytic activity (Trp-433→Phe) induces less meningeal inflammation. Both of these toxoids also exhibit less ability than intact pneumolysin to induce pneurnonic change when administered into rat lung (Feldman *et al* 1991). A non-haemolytic toxoid (Trp-433→Phe) still causes ultrastructural

damage to the organ of Corti characteristic of pneumolysin when perfused into scala tympani of guinea pigs (SD Comis, *MP* Osborne and A Cohen, unpublished findings).

Protection by *immunity to pneumolysin*.

Immunisation of BALB/c mice with highly purified native pneumolysin (Paton *et al* 1983) or a toxoided derivative (**Cys-428→Gly**) (Paton *et al* 1993b) provides significant protection from intraperitoneal challenge with virulent serotype 2 *S. pneumoniae* strain D39. More interestingly, concurrent immunisation with autolysin does not enhance survival. Immunity to autolysin alone does not alter the course of infection with a pneumolysin-deficient strain (PLN-A) although it does provide partial protection from wild type infection. This suggests that the main contribution of autolysin *in vivo* is to release pneumolysin. Immunity against pneumolysin should provide protection across serotypes. Immunisation of mice with the pneumolysoid (**Trp-433→Phe**) provides partial or complete protection against at least nine different pneumococcal serotypes except for one clinical isolate (strain GB05; serotype 3) when administered intranasally (Alexander *et al* 1994). In general, pneumolysoid immunisation is more effective in countering intranasal challenge than preventing bacteraemia after intraperitoneal challenge.

Activity	Reference
<b>Cytotoxicity:</b>	
Cytolytic for RBCs at high concentrations( $\mu\text{g/ml}$ )	Boulnois, 1992
Inhibits ciliary beating in human nasal turbinate organ culture (1-50 $\mu\text{g/ml}$ )	Steinfort <i>et al</i> 1989
Toxic to cultured bovine pulmonary artery endothelial cells	Rubins <i>et al</i> 1992
Toxic to cultured pulmonary alveolar epithelial cells (30 ng/ml). Increases alveolar permeability in isolated perfused rat lung (200 ng/ml)	Rubins <i>et al</i> 1993
<b>Immunomodulatory functions:</b>	
Irreversibly inhibits human lymphocyte proliferation and antibody production in vitro (10 ng/ml)	Ferrante <i>et al</i> 1984
Activates complement (1-10 $\mu\text{g/ml}$ )	Paton <i>et al</i> 1984
Binds Fc fragment of antibody (1-10 $\mu\text{g/ml}$ )	Mitchell <i>et al</i> 1991
Inhibits respiratory burst of neutrophils	Perry <i>et al</i> 1993
Induces IL-1 $\beta$ and <b>TNF<math>\alpha</math></b> in human mononuclear phagocytes (1 ng/ml)	Houldsworth <i>et al</i> 1994
Activates PLA2 in cultured pulmonary endothelial cells (10 ng/ml to 1 $\mu\text{g/ml}$ )	Rubins <i>et al</i> 1994
<b>In vivo effects:</b>	
Induces salient features of pneumonia in rat lung	Feldman <i>et al</i> 1991
Intracisternal injection induces a CSF leukocytosis and TNF response in rabbits	Friedland <i>et al</i> 1995
Intracochlear perfusion causes electrophysiological and ultrastructural damage to the organ of Corti of guinea pigs (1-10 $\mu\text{g/ml}$ )	Comis <i>et al</i> 1993

Approximate concentration of pneumolysin needed is given where clear from the literature. Typical specific activity for recombinant pneumolysin is about  $5 \times 10^5$  haemolytic units per mg protein. Thus 1  $\mu\text{g/ml}$  = ca. 500 HU/ml

**Table 1.2:** Activities of purified pneumolysin possibly related to pathogenesis of infection

### *Investigations with pneumolysin-deficient organisms.*

The different course of an experimental infection induced by pneumococci deficient in pneumolysin compared to that induced by wild-type infection might provide significant clues about the actual functions of pneumolysin *in vivo*. The isolation of the pneumolysin gene (*pin*) allowed the construction by insertion-duplication mutagenesis of defined isogenic mutant strains deficient in pneumolysin or containing modified pneumolysin. One of the key difficulties encountered was that encapsulated pneumococci proved difficult to transform with the vector DNA, so a two-stage process proved necessary (see appendix A) (Berry *et al* 1989). The resulting pneumolysin-deficient mutant, PLN-A, has been studied in several different infection models including that described in the current work.

In the first description, Berry *et al* (1989) reported that the LD<sub>50</sub> of PLN-A for intraperitoneal injection in the mouse is about 100 times higher than the LD<sub>50</sub> of the parent strain D39. Similar results were obtained in the unusual species of Quackenbrush mice when the work was repeated with another defined pneumolysin-deficient strain of a serotype 3 pneumococcus (Berry *et al* 1992). The absence of pneumolysin therefore modifies the infection but does not prevent death. Benton *et al* (1995) looked more carefully at the kinetics of *in vivo* growth after intraperitoneal inoculation of D39 or PLN-A in CBA/N mice. Animals inoculated with wild-type D39 sustain an exponential bacteraemia (doubling time ca. 1.4 h) which continues until death ensues. Those inoculated with PLN-A initially develop a similar exponential bacteraemia which then plateaus at around 10<sup>6</sup> CFU/ml. Co-infection with D39 restores the ability of PLN-A to grow exponentially beyond the plateau level, suggesting strongly that pneumolysin production is required for exponential growth to occur in the bloodstream. Pre-infection with PLN-A prevents D39 from growing beyond the plateau level, perhaps because of the induction of tolerant immunity.

What about the earlier steps of infection? PLN-A when inoculated intranasally in mice induces a less severe pneumonia and a delayed bacteraemia compared to wild type infection, even though cell wall products are released. But an autolysin-negative mutant (AL<sub>-2</sub>) causes neither pneumonia nor bacteraemia (Canvin *et al* 1995). This suggests there may be an interaction between the cellular products released by autolysin, perhaps between cell wall and pneumolysin or an as yet unidentified toxin. When PLN-A is applied to an isolated human nasal turbinate preparation, the onset of a decline in ciliary beat frequency is significantly delayed compared to wild type. Only with wild-type organisms is there significant damage to the cell surfaces, with blebbing of the ciliated cell surface and breakdown of the intercellular tight junctions (Rayner *et al* 1995). One of the possible mechanisms of action of pneumolysin therefore is to promote breakdown of the respiratory epithelium and augment invasion. This is of great relevance to the findings in the inner ear

to be described later. In isolated rat lung, Rubin *et al* (1995) reported that PLN-A induces less injury to the capillary barrier and is unable to replicate as well as wild type. The addition of exogenous pneumolysin corrects these defects.

The contribution of the various activities of pneumolysin to pathogenesis has been assessed by manufacturing isogenic mutants which express toxoided pneumolysin genes. In a mouse bacteraemia model, median survival is prolonged by intraperitoneal challenge with either of two pneumococcal mutants which express toxoids deficient in haemolytic activity (**His-367→Arg**, and **Trp-433→Phe** plus **Cys-428→Gly**). Mice infected with a complement-activation deficient mutant (**Asp-385→Asn**) have the same median survival as mice infected with the parent strain (Berry *et al* 1995). Both types of mutant have impaired virulence for mouse pneumonia, although pneumolysin-related haemolytic activity accounts for much of the acute lung injury and early intra-alveolar replication, while pneumolysin-related complement activation augments bacteraemia (Rubins *et al* 1996).

Not all the experimental data support a significant role for pneumolysin. Friedland *et al* (1995) induced meningitis in rabbits by intracisternal inoculation of 3x10<sup>3</sup> CFU log-phase D39 or PLN-A. There were no differences in the course of CSF leukocytosis or CSF concentrations of **TNF $\alpha$** , lactate and protein. Both organisms grew exponentially at the same rate with no lag phase (a phenomenon sometimes observed with other pneumococcal strains and also with the pneumolysin-deficient mutant produced by Johnson in this model (Tuomanen *et al* 1985b; Johnson *et al* 1992 and Prof A Tomasz, personal communication). From this the authors concluded that pneumolysin has no pathogenic role once pneumococci have entered the CSF space. However, they did not examine the brains histologically or seek other evidence of differences in end-organ damage. In a chinchilla otitis media model, a pneumolysin-negative derivative (P-1) of a type 3 pneumococcus induces an identical infection to a wild type strain, with a similar inflammatory cell response in the middle ear fluid and no differences in the concentrations of IL-1 $\beta$ , IL-6 and IL-8 (Sato *et al* 1996). These were not isogenic strains, so other unsuspected differences may explain the lack of activity of pneumolysin.

In conclusion, it seems that pneumolysin expression augments intra-alveolar replication, provides one of the mechanisms by which pneumococci may invade capillary blood, and causes specific damage to mucosa and the organ of Corti. Once in the bloodstream, pneumolysin is necessary for continued exponential growth. The role of pneumolysin once pneumococci penetrate the CSF space or the middle ear is less clear but pneumolysin seems not to augment the inflammatory stimulus, at least during the exponential growth phase. In both the blood stream and CSF space, the haemolytic activity of pneumolysin seems to be more important than its ability to activate complement. Even if the concentration of

cytokines and leukocytes in the CSF is not altered by the absence of pneumolysin, there may still be important differences in end-organ damage.

### 1.2.7. Neuraminidase.

Neuraminidase cleaves terminal sialic acid residues (e.g. N-acetylneuraminic acid; **NANA**) from mucin, glycoproteins, glycolipids and oligosaccharides on cell surfaces and in body fluids. Of relevance to this thesis, the glycocalyx of the epithelial cell surfaces bordering the endolymphatic space in the inner ear has a high sialic acid content (Vanbenthem *et al* 1992). All clinical pneumococcal isolates express neuraminidase (Kelly *et al* 1967), although the quantity varies according to strain (Dr T Mitchell, personal communication). Neuraminidase activity can be enhanced in vitro by adding N-acetylmannosamine to the culture medium (Kelly *et al* 1966) and can be lost from organisms subcultured only on artificial media. Pneumococcal neuraminidase proved difficult to purify and many different molecular weights have been reported. Lock (1988b) purified neuraminidase with a molecular weight of 86 **kD** to electrophoretic purity. A polyclonal antibody to this molecule reacted with a larger species in crude pneumococcal extract (*MW* 107 **kD**), which was eventually purified intact, suggesting that proteolytic degradation during purification was responsible for the reports of multiple isoenzymes. One putative gene was cloned by Berry *et al* (1988) (clone pJCP301) and a second gene (*nad*) was cloned and expressed by Camara *et al* (1991). These genes are unrelated and have been shown to be present in all pneumococcal strains tested. *NanA* mRNA is definitely expressed during in-vitro growth (Camara *et al* 1994) and the gene product has a predicted *MW* of 144 **kD**.

The pneumococcal neuraminidase(s) are classified with the “large” bacterial neuraminidases (>60 **kD**) which share a common feature of an “aspartic box” sequence. There remains some confusion over the specificity of certain bacterial neuraminidases due to lack of specificity of older bioassays. For example, a purified Group B streptococcal enzyme previously thought to be a neuraminidase has in fact turned out to be a hyaluronidase (Savic and Ferretti, 1994). The *MUAN* cleavage assay (see appendix C) used in the work to be presented is however a specific assay. The cellular location of neuraminidase is also debated. Some evidence suggests that it is cytoplasmic (Lock *et al* 1988b) but certain features of the *nad* gene suggests that it encodes for a surface protein and this appeared to be confirmed by immunogold labelling (Camara *et al* 1994).

The potential role of neuraminidase in pneumococcal adhesion to respiratory epithelium has been discussed (Krivan *et al* 1988). The evidence that neuraminidase may be directly involved in tissue damage in meningitis is conflicting and somewhat circumstantial. In support of a role is a clinical study which demonstrated a correlation between a poor

outcome from pneumococcal meningitis and the level of free NANA in the CSF (O'Toole *et al* 1971). Free NANA was found only in pneumococcal meningitis, and none of the isolates of *H. influenzae* or *N. meningitidis* expressed neuraminidase activity. Kelly and Grieff (1970) challenged weanling mice with sonicated extracts of pneumococci grown in medium enriched with N-acetylmannosamine. Mice challenged by intracerebral or intraperitoneal injection developed neurological signs and died. However, such a crude extract may have been contaminated with cell wall, or even pneumolysin. There have been few reports published about the effects of purified pneumococcal neuraminidase on cultured cells or in vivo preparations. Mice immunized with purified neuraminidase are partially protected against pneumococcal infection (Lock *et al* 1988a). Intravenous injection of purified pneumococcal neuraminidase in rats promotes binding of circulating leukocytes to the kidney (Marin *et al* 1995) and neutrophils exposed to neuraminidase show increased adherence to endothelial cells (Dwarakanath *et al* 1995).

In evidence against a role for neuraminidase in virulence, O'Toole *et al* (1975) induced meningitis in dogs by intrathecal injection of viable pneumococci or crude pneumococcal extract. Infection with viable organisms induces a rise in free NANA in the CSF. But challenge with the neuraminidase preparation causes no ill effects in the animals, although the NANA content of cortical brain subcellular organelles is reduced by some 30%. Kelly and Grieff (1966) reported that lethality of pneumococcal strains in mice does not relate to neuraminidase activity.

Because of the conflicting evidence about the role of neuraminidase, the construction of neuraminidase-negative isogenic mutants represents a significant step forward. The results to be presented in this thesis are among the first data from the use of these mutants in an infection model.

### **1.2.8. Hyaluronidase.**

In common with other streptococci almost all strains of *Streptococcus pneumoniae* produce hyaluronidase, an enzyme which cleaves hyaluronic acid, a major constituent of the extracellular matrix (Paton *et al* 1993a). Very little is actually known about the role of hyaluronidases in virulence. It is assumed that breakdown of connective tissue contributes to bacterial spread and invasion. A pneumococcal hyaluronidase gene has recently been isolated (Berry *et al* 1994; Hill *et al* 1996). Other mucosal and wound pathogens also express hyaluronidases but the gene sequences appear to be unrelated (Canard *et al* 1994; Hynes *et al* 1995).

The only clinical evidence for the importance of hyaluronidase in bacterial meningitis comes from a study of pneumococcal meningitis conducted in St Petersburg. Hyaluronidase was expressed by all of 39 strains isolated ~~from~~ the CSF but by only 11% of capsulated strains carried in the upper respiratory tract (Kostyukova et al 1995). It was not expressed by non-encapsulated strains. Mice challenged intranasally with strains expressing high levels of hyaluronidase developed meningitis more readily.

There have as yet been no reported studies of the toxicity of purified recombinant hyaluronidase in vivo or for cultured cells, and there are no data about protection from pneumococcal infection after immunisation. A hyaluronidase-negative isogenic mutant has recently been constructed (Hill et al 1996) and some of the first experimental infection data obtained with this organism are presented in this thesis.

### 1.3. Auditory anatomy and physiology.

#### 1.3.1. Gross anatomy.

The auditory apparatus consists of the pinna and external auditory meatus of the outer ear, an air-filled middle ear containing an ossicular chain, and the inner ear. The middle ear is divided from the outer ear by the tympanic membrane and communicates with the inner ear at the oval and round windows. The ossicles consist of the *malleus*, *incus*, and *stapes*. These serve to transmit sound vibrations from the tympanic membrane to the oval window. The inner ear is encased in the temporal bone in humans and consists of the cochlea, the vestibule and the semicircular canals. The bony cochlea is a snail-shell shaped spiral which coils for just over 2 turns in humans and up to 5 turns in guinea pigs. It is divided into three compartments (fig 1.1, page 26). The *scala vestibuli* and the *scala tympani* communicate at the apex of the cochlea at the *helicotrema*. They are filled with *perilymph*, a fluid of a similar composition to cerebrospinal fluid ( $K^+$  7 mM,  $Na^+$  140 mM,  $Cl^-$  120 mM). The guinea pig cochlea contains about 8  $\mu$ l of perilymph. The scala vestibuli is bordered by the oval window and communicates with the vestibular space. The scala tympani is bordered by the round window and communicates with the subarachnoid space via the cochlear aqueduct (see below). The *basilar membrane* stretches from the inner osseous spiral lamina (or *modiolus*) to the outer wall of the cochlea. The *scala media* is divided from the scala tympani by the basilar membrane and from the scala vestibuli by *Reissner's membrane*. The sensory organ of the ear, the *organ of Corti*, rests on the basilar membrane. The scala media is filled with *endolymph*, an extracellular fluid rich in potassium with a composition more akin to intracellular fluid ( $K^+$  150 mM,  $Na^+$  1 mM,  $Cl^-$  130 mM). Spiralling around the outer rim of the scala media is found the *stria vascularis*, a site of intense ATPase activity. This regulates the composition of endolymph and maintains the electrical potential of the scala media some +80 mV above that of the scala tympani.

#### 1.3.2. The cochlear aqueduct.

Figure 1.2 shows diagrammatically how the scala tympani and perilymphatic space communicate with the subarachnoid space via the cochlear aqueduct. The cochlear aqueduct is present in all mammals. It extends from the wall of the scala tympani in the basal turn and emerges medial to the jugular fossa. Within the aqueduct is the periotic duct, a potential space filled with a reticular meshwork of connective tissue, reticular cells and macrophages (Donaldson *et al* 1992; Duckert, 1974). It is thought that the duct facilitates exchange between CSF and perilymphatic fluid while the meshwork of tissue and macrophages acts as a damper to sudden pressure changes in the CSF and defends the inner

ear from microbial invasion (Blank *et al* 1994). Recent electron microscopic studies have confirmed that there is no physical barrier to fluid flow along the duct (Toriya *et al* 1991).

There has been a great deal of debate about the functional patency of the cochlear aqueduct in humans and lower mammals. The cochlear aqueduct of the guinea pig appears to be widely patent, some 240  $\mu\text{m}$  in diameter and about 2.5 mm long (Moscovitch *et al* 1973; Duckert, 1974). In the guinea pig there is no doubt that CSF flows into the perilymph. Salt *et al* (1994) calculated the flow rate into an unopened cochlea to be about 2 nl/min, or sufficient to replace the entire perilymph in just under 3 days. Such a communication is not essential for inner ear function as no ill effects are observed if the cochlear aqueduct is blocked for several months (Kimura *et al* 1974). If the cochlea is opened (fistulized) much as for the cochlear perfusion experiments to be described in chapter 4 then the flow rate can rise to 500 nl/min, sufficient to replace the entire perilymph in around 10 minutes (Moscovitch *et al* 1973). Flow can be almost abolished by blocking the cochlear aqueduct (Sait *et al* 1991) or opening the cisterna magna to reduce the hydrostatic pressure of the CSF (Salt and Stopp, 1979). Particulate tracers easily pass from the CSF into the perilymph in the guinea pig (Duvall and Quick, 1969). Blocking the cochlear aqueduct prevents particles penetrating the inner ear (Sando *et al* 1971).

Histopathological data from human post-mortem studies largely suggest that the cochlear aqueduct is patent. Palva (1970) found the cochlear aqueduct of six neonates to have a mean length of 3.5 mm, compared to 6.5 mm in adults, and a minimum diameter of 150  $\mu\text{m}$ . In a study of adults, the cochlear aqueduct was blocked in only 3 of 82 post mortem specimens, with a mean length of 12.9 mm and minimum width of 140  $\mu\text{m}$  (Rask-Anderson *et al* 1977). The aqueduct is wider in infants than adults but is still longer and narrower than in experimental animals. It is obviously difficult to study flow rates of CSF into perilymph to assess whether the cochlear aqueduct is functionally as well as anatomically patent in humans.

Other communications routes between the CSF space and the inner ear include the internal auditory canal with its perineural and perivascular spaces, and the canal housing the inferior cochlear vein.

### 1.3.3. Ultrastructure of the organ of Corti.

#### *Overview*

The spiral organ of Corti consists of a series of epithelial structures placed upon the upper surface of the basilar membrane (fig 1.3). The *internal* and *external rods* (or *pillars*) of Corti form an triangular arch enclosing the tunnel of Corti. On the medial side of the inner

rods lie a single row of *inner hair cells* and on the lateral side of the outer rods lie three to four rows of *outer hair cells* along with their supporting cells. The organ is covered by the *tectorial membrane*, a jelly-like structure which stretches out from the spiral lamina.

### ***Inner hair cells (IHCs).***

These are ovoid cells about 35  $\mu\text{m}$  long and 10  $\mu\text{m}$  in diameter with a central nucleus (see fig 1.4). They form a single rank along the whole length of the organ of Corti. Inner hair cells rest directly on the basilar membrane and **at** their free end are surrounded by *inner phalangeal cells*. On the medial side, there are slender *border cells* and these are succeeded in turn by the cuboidal epithelium lining the inner spiral sulcus. At the apical surface of the IHC there is a cuticular thickening, the *cuticular plate*, into which the rootlets of the stereocilia insert. A small area of the apical surface has no cuticular covering. Each cell has between 60 to 100 stereocilia arranged in 3 to 4 rows, with the shortest hairs closest to the modiolus. The stereocilia are packed with actin filaments in a paracrystalline array and are bound together by lateral links so that the row functions as a single unit. Fine tip links hold the tips of the shorter stereocilia in towards the longer stereocilia of the adjacent row (Osborne *et al* 1984). A thick layer of negatively-charged glyocalyx overlies the sensory cells (but not the supporting cells) and probably serves to keep the stereocilia separate. Stereocilia of the IHCs are not thought to contact the tectorial membrane directly (Lim, 1986).

### ***Outer hair cells (OHCs)***

These are narrow, cylindrical cells about 25 to 40  $\mu\text{m}$  long and 7  $\mu\text{m}$  in diameter with a basal nucleus (see fig. 1.5). Three to five rows of OHCs are distributed radially around the organ of Corti. Outer hair cells rest in cup-like depressions of the *external phalangeal cells of Dieters* which lie on the basilar membrane. Processes from the Dieters' cells reach up and surround the apical surface of the OHCs. The apical surface of the outer hair cells, together with the tight junctions between OHCs and the neighbouring phalangeal processes and supporting cells, form a common *reticular lamina* across which there is an electrochemical gradient between perilymph and endolymph. Therefore while the stereocilia and the apical cell surface membrane are bathed in endolymph, the rest of the cell body is bathed in perilymph.

Outer hair cell stereocilia are arranged in a clear V or W shape, opening towards the modiolus with the tallest hairs outermost. It is likely that the tallest hairs meet the tectorial membrane (Lim, 1986). Stereocilia are anchored into a thick cuticular plate. The non-cuticular part of the apical surface of the OHC sometimes shows remnants of a kinocilium (*basal Corpuscle*). Later the effects of bacterial invasion on this particular area of structural

weakness will be documented. Mitochondria are situated both beneath the apical surface and basally. With abundant contractile elements and predominant efferent innervation, it seems that the OHC enables the cochlea to act as an 'active receptor' by modifying the local mechanical interaction between the tectorial membrane and associated stereocilia.

### ***Innervation***

Most of the data regarding innervation of the mammalian cochlea has been obtained from studies of rodents, guinea pigs and cats but is probably true for humans. Eybalin (1993) and Lim (1986) have provided succinct reviews. About 95% of the total neuronal population of the spiral ganglion are large myelinated ***type I afferent primary auditory neurons*** which are connected exclusively to the **IHCs** and project to the homolateral ventral subdivision of the cochlear nucleus. Each **IHC** receives innervation from up to 30 separate radial afferent dendrites. Afferent nerve units can be divided on the basis of spontaneous discharge into two populations with a high (>18 spike/s) or low-to-medium (0-18 spikes/s) firing rate. High spontaneous rate units formed by the thicker type I radial dendrites have a much lower auditory threshold. Some ***lateral efferent dendrites*** projecting mostly from the lateral superior olive form ***en passant*** synapses with the terminal portion of the radial dendrites. ***Glutamate*** is probably the principal IHC neurotransmitter. Evidence for this is derived from biochemical assays of different parts of the cochlea, electrophysiological findings when the cochlea is perfused with various glutamatergic agonists and antagonists, and immunolocalisation studies (Eybalin, 1993, p3 17). Glutamate and its agonists decrease the auditory nerve compound action potential (***CAP'***) by inducing an excitotoxic block. Glutamate antagonists also decrease the ***CAP*** and block radial afferents. The presence of N-methyl-D-aspartate (NMDA) receptors in the cochlea has been disputed until recently (Puel *et al* 1991). **NMDA** antagonists reduce the ***CAP'*** amplitude with loud stimuli, but have little effect with quiet stimuli. On the other hand, nanomolar quantities of kainate perfused into the perilymphatic space irreversibly abolish the ***CAP*** without affecting the CM, and cause dramatic dendritic swelling, suggesting an important role for non-NMDA excitatory amino acid receptors. Glutamate antagonists also protect against some of the effects of agonist- and ischemia-induced excitotoxicity, and this will be of great relevance later when the mechanisms of damage to the organ of Corti during bacterial meningitis are considered. A ***glutamate-glutamine cycle*** has been proposed, whereby excess extracellular glutamate is taken up by local glial cells in the osseous spiral lamina and converted to glutamine by the action of glutamine synthetase. Inner hair cells take up this glutamine to generate glutamate.

The predominant innervation of the outer hair cells comes from contralateral myelinated ***medial*** and ***lateral efferent neurons***. About 5% of the spiral ganglion neurons consist of small unmyelinated ***type II afferent auditory neurons***, which project from the basal poles of

OHCs to the homolateral cochlear nucleus. Each dendrite contacts up to 100 different OHCs.

#### **1.3.4. Sound transduction.**

Acoustic vibrations are transmitted from the tympanic membrane via the ossicular chain. If airborne vibrations were to act directly upon the oval window some 98% of the acoustic energy would be reflected. The ossicular chain acts as an impedance transformer, improving the efficiency of transfer of sound energy to about 67% (Buser and Imbert, 1992, p146). Vibrations at the oval window set up a standing wave in the basilar membrane. The stiffness of the basilar membrane varies from base to apex. Therefore sounds of different frequencies produce travelling waves that peak at different places along the cochlea. In this way the basilar membrane acts as a spatial separator. Low frequencies are detected at the apex of the cochlea, while higher frequencies are detected in the basal turn. The tuning mechanism is reinforced by the active involvement of the OHCs. The displacement of the basilar membrane causes a tangential slippage between the tectorial membrane and the reticular lamina. This deflects the hair bundles of the OHCs (the tips of the tallest stereocilia being in contact with the tectorial membrane), so depolarizing the cell. Contractions of the OHC modify the local displacement of the basilar membrane, refining the tonotopic tuning. The stereocilia of the IHC in this area are then deflected due to shearing forces between the stereocilia and the fluid immediately surrounding them.

The transduction of vibrations into electrical current by the mammalian cochlea is astonishingly sensitive and capable of resolving remarkably high frequencies. This is due to the unique properties of sensory “hair cells”. Hair cells have evolved to detect prolonged vibrations of low energy compared to background noise (Hudspeth, 1985). The currently accepted model for mechano-electrical transduction is as follows. Displacement of the stereocilia at right angles to the axis of the bundle stretches and compresses the fine tip-links which join the tip of the shorter stereocilia to the flank of the taller stereocilia in the adjacent row (Osborne and Comis, 1990). This opens a non-selective cation channel, admitting  $K^+$  which is in high concentration in the fluid bathing the stereocilia, and so depolarizing the cell. Voltage-sensitive  $Ca^{2+}$  channels open to augment the depolarisation, but the influx of  $Ca^{2+}$  in turn triggers the efflux of  $K^+$  from the basolateral aspect of the cell. Random motion of the hair cell stereocilia due to Brownian motion of the surrounding molecules generates a certain amount of noise, but when the stereocilia are deflected by displacement of the basilar membrane the channels spend proportionately longer in the open phase. Because there is no second messenger and the channels alternate between open and closed states continuously, the response time is extremely rapid. Channels begin to carry

current within a few microseconds of a stimulus. The sensitivity of a typical mammalian cochlear hair cell is as great as 0.4 mV per nm displacement of the hair bundle tip (Buser and Imbert, 1992; p233). Each hair cell also appears to have a characteristic resonant frequency which further contributes to tonal discrimination.

### **1.3.5. Electrophysiological measurements.**

#### *Definition of sound pressure level*

Equipment for audiological measurements must be calibrated so that experiments are comparable. For much of the work to be described in this thesis relative rather than absolute changes are measured. Comparison of sound intensities is normally done by a ratio scale. A *sound pressure level* ( $L_p$ ) is designated according to the logarithm of its ratio to a reference magnitude of sound pressure  $p_0$ . Usually a reference sound pressure level of 20  $\mu\text{Pa}$  is taken, as this represents the typical human auditory threshold at 1 **kHz**. This is equivalent to 1  $\text{pW/m}^2$  in SI units. The ratio has units of Bels, or for convenience, decibels:

$$L(\text{dB}) = 20 \log_{10} (p/p_0)$$

Sound propagates at 340  $\text{m/s}$  in air at **15°C** at sea level. Allowance must be made for this when calculating the latency of a measurement. For example, it would take 0.3 ms for a sound stimulus to travel 10 cm from a transducer to the tympanic membrane.

#### *Compound action potential (CAP).*

The auditory nerve compound action potential (CAF) is built up from nearly simultaneous contributions of a population of primary auditory neurons (Kiang *et al* 1976). It is easily excited by a transient click or brief tone pulse. A typical **CAP** recorded from the round window membrane in response to a 10 kHz tone pip is shown in fig 1.6. It consists of an initial positive peak ( $P_0$ ), a negative peak ( $N_1$ ) with a latency of about 1 ms, and a subsequent positive peak ( $P_1$ ). Further peaks ( $N_2$  and  $N_3$ ) occur about 1 and 2 ms later respectively. The  $P_0$  wave is thought to represent the summed far field current of the excitatory postsynaptic Potentials in radial dendrites (Eybalin, 1993; p 323). The  $N_1$  peak is particularly due to receptors at the base of the cochlea and has been shown to reflect activity at the level of the auditory nerve (Kiang *et al* 1976). The CAP is frequency dependent when evoked by tonal stimuli at low to moderate sound intensities (Cody *et al* 1980; van Heusden and Smoorenburg, 1981; Eggermont, 1976). Audiograms obtained with CAP recording correlate with behavioural audiograms (Eggermont, 1976). CAP thresholds are some 0-20 dB less sensitive than single-fibre thresholds.

### ***Cochlear microphonics (CM).***

The *cochlear microphonics* (CM) potential is easily recorded from the round window membrane. It originates from the massed activity of receptor cells which lie as a transversally arranged dipole across the high resistance reticular lamina. The potential exactly follows the amplitude of the stimulus (just like a microphone), has almost no latency and does not adapt. It can be recorded for some time after the death of an animal, well after the CAP can no longer be elicited. The log of the CM amplitude is linearly related to the stimulus intensity (in decibels) over a wide range of 90 dB and there is very little distortion in the CM even at saturation. Potentials from OHCs contribute the bulk of the CM. Kanamycin, which destroys 90% of the OHCs while sparing the IHCs, causes a 90% fall in CM potential (Buser and Imbert, 1992).

When recorded from the round window, the CM potential only properly reflects cochlear function within a few millimetres of the round window (16 kHz and above) because contributions from the lower frequency zones are obscured by contributions from the nearer CM generators (van Heusden and Smoorenburg, 1981).

### ***Brain stem auditory evoked Potentials (BAEP).***

Recording of CAP or CM involves invasive approaches to the cochlea. Far-field Potentials in response to an auditory stimulus can be recorded from scalp electrodes and by signal averaging various waves can be detected that relate to auditory activity. Even under good conditions at least 256 and more usually 1024 stimuli are necessary to extract the signal from background noise. In spite of these limitations this technique is of great use clinically because it is non-invasive.

The different components are identified by the different latencies (Jewett and Williston, 1971). The short latency components arise from the brain-stem with a latencies of between 1.5 ms and 10 ms. At least five successive peaks are usually recognizable (see figure 3.3). A detailed derivation of the waves based on simultaneous recordings from the scalp surface and the brainstem can be found in Maller *et al* (1986) . The first peak of the brain-stem response is probably a far-field recording of the CAP and is usually of low amplitude. Wave III appears to be the most robust wave for analysis. It is probably generated by the cochlear nucleus. Thresholds obtained by BAEP recording are within 10 dB of those obtained by CAP recording under ideal conditions and demonstrate similar frequency selectivity (Brown and Abbas, 1987).

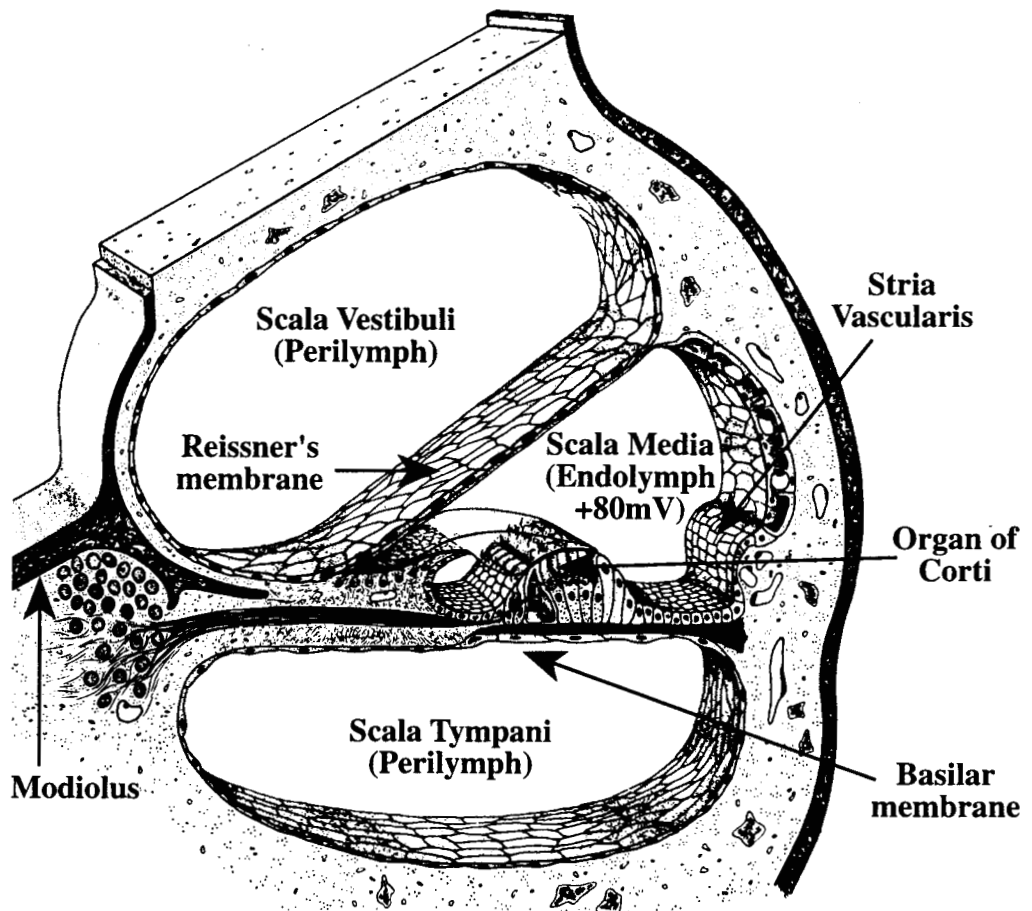


**Figure 1.1:** Diagram of the cochlea in cross-section.

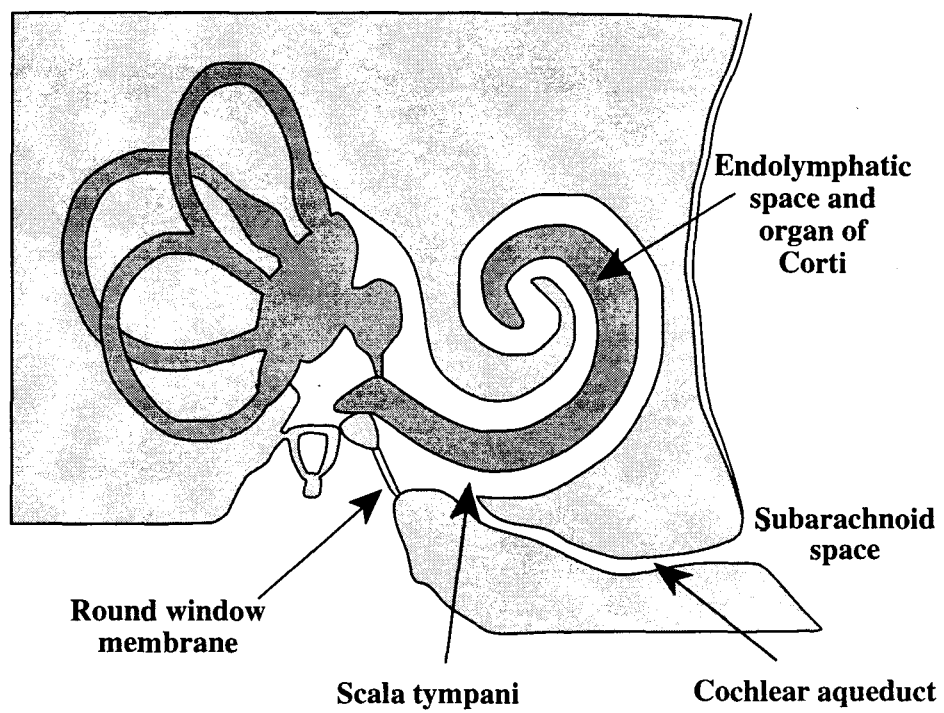


**Figure 1.2:** Relationship of the inner ear to the subarachnoid space (After Bhatt *et al* 1993).

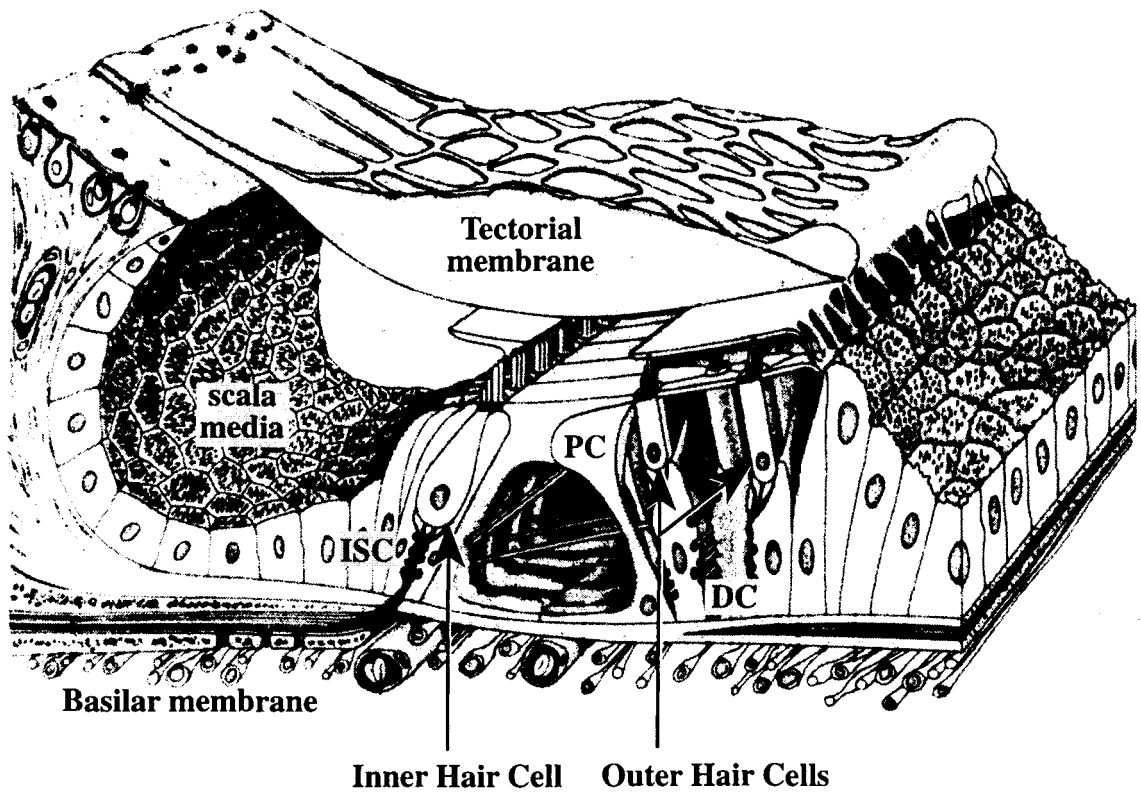


**Figure 1.3:** Three-dimensional impression of the organ of Corti. ISC: inner supporting cells; DC: Dieter's cells; PC: pillars (rods) of Corti. (from Lim (1986))

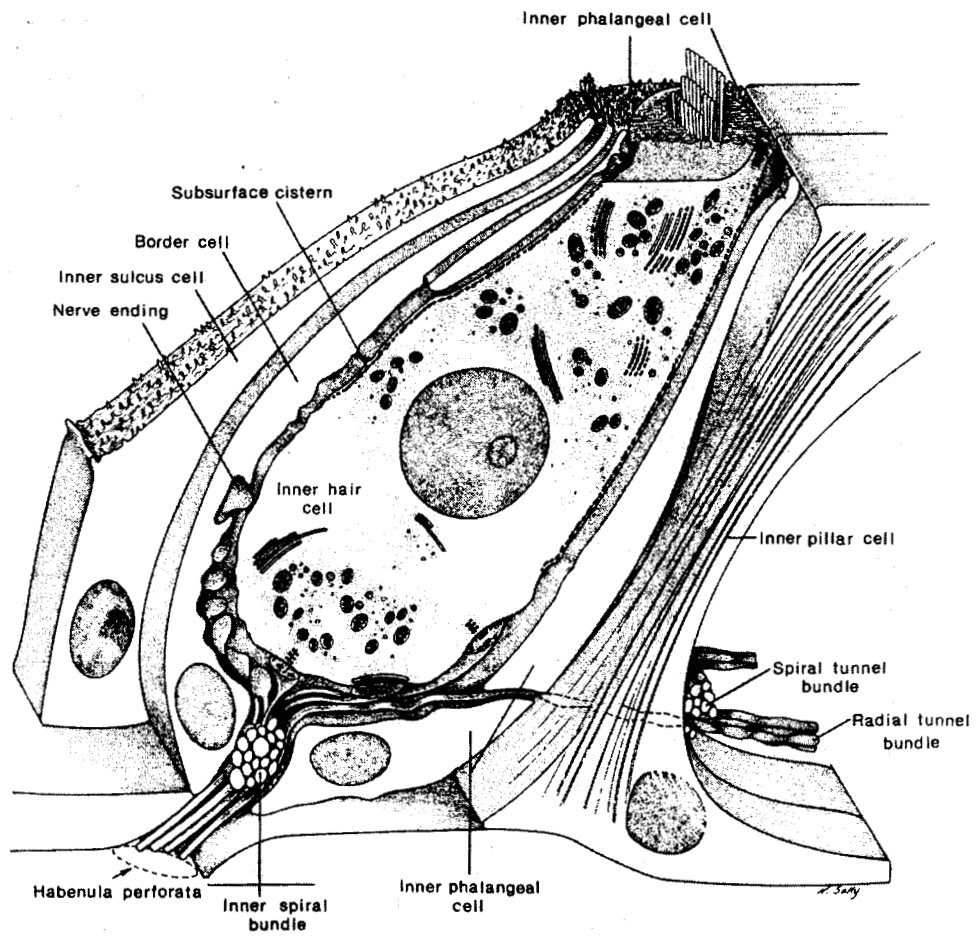


**Figure 1.4:** Diagram of the ultrastructure of an inner hair cell.  
From Lim (1986)

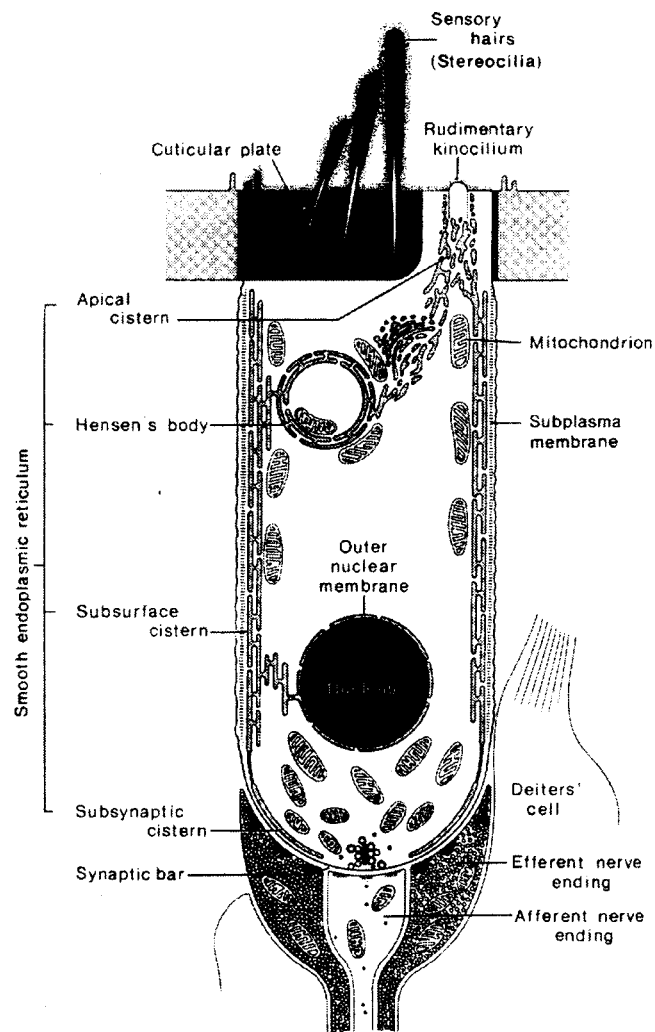
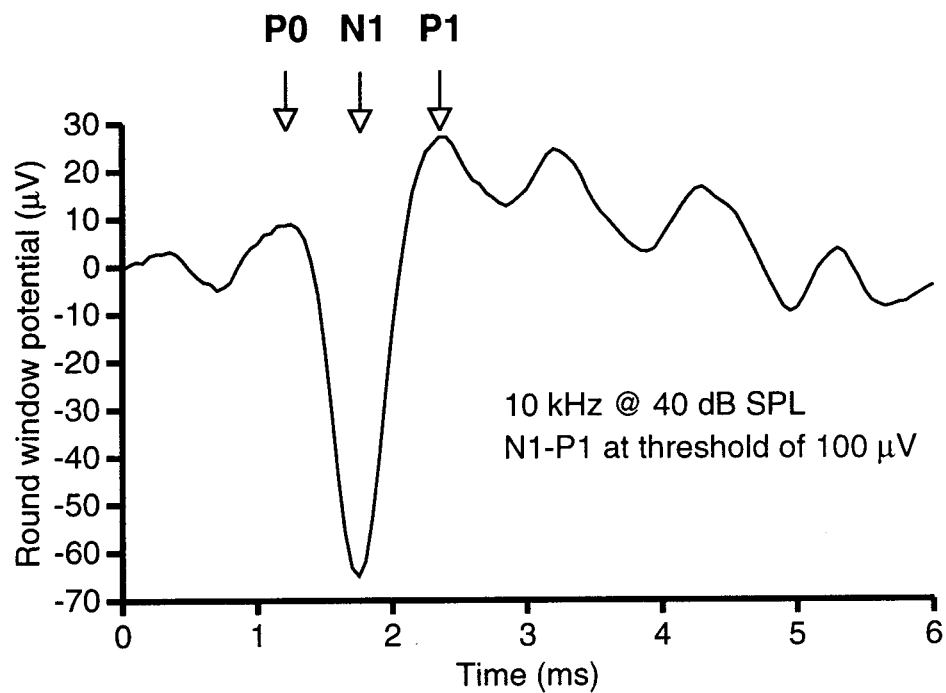


**Figure 1.5:** Diagram of the ultrastructure of an outer hair cell.  
From Lim (1986)

## Compound action potential



## Cochlear microphonic potential

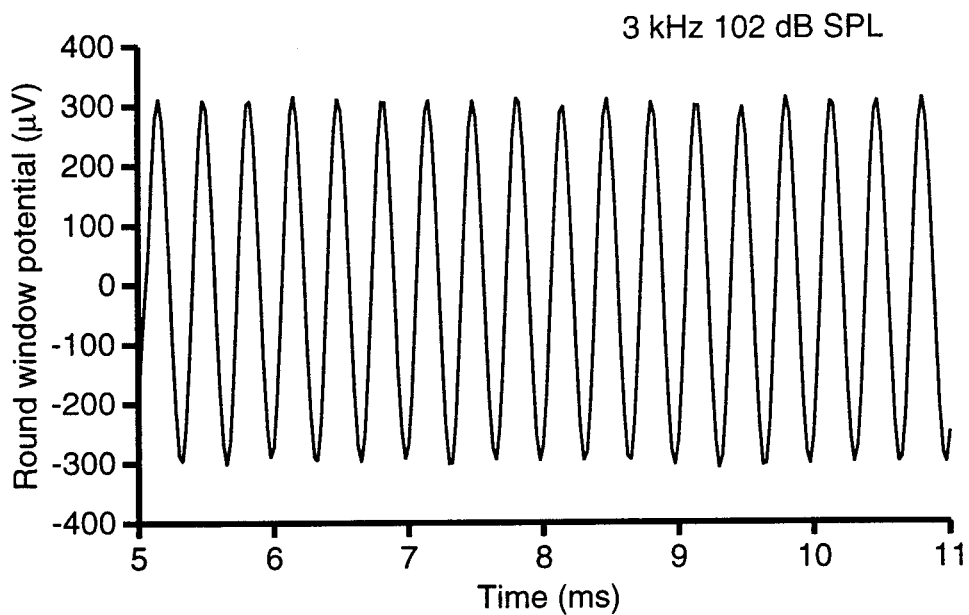


Figure 1.6: Electrophysiological recordings from the round window.

## 1.4. Experimental bacterial meningitis.

Harter and Petersdorf (1960) described the following criteria which remain ideal aims for any model of experimental meningitis. Compared with human infection, the experimental infection must:

- Have the same portal of entry and route of dissemination by the infecting organism;
- Show equivalent differences in virulence between serotypes;
- Show similar histopathological lesions;
- Have a predictable and reproducible course;
- Be simple to perform.

Clearly no one experimental model can satisfy all of these criteria. Nevertheless, experimental infections in animals have contributed greatly to understanding of the pathophysiology of meningitis, particularly with respect to the mediation of inflammation in the subarachnoid space. Several recently published comprehensive reviews summarize this work (Tunkel *et al* 1990a; Quagliarello and Scheld, 1992; Tunkel *et al* 1990b; Tunkel and Scheld, 1993a; Tunkel and Scheld, 1993b; Spellerberg and Tuomanen, 1994).

### 1.4.1. Practical considerations.

#### *Systemic versus local inoculation*

It is worth pointing out at the outset that there are no good models for CSF invasion by the common pathogens. Only neonatal rats and mice reliably develop meningitis when inoculated peripherally with invasive organisms. Neonatal animals yield tiny quantities of CSF and are difficult to work with. Unfortunately, only a fraction of adult animals of any species develops meningitis after systemic inoculation of viable organisms (in the same way, of course, that not all bacteraemic patients go on to develop meningitis). The chance of inducing meningitis can be increased by giving the inoculum in combination with an adjuvant such as mucin or iron dextran. Because of the high wastage of animals if organisms are injected systemically, experimental meningitis **is** usually induced by directly injecting viable organisms (prepared by a wide variety of different culture techniques), bacterial components or inflammatory mediators into the subarachnoid space (usually the *cisterna magna*). This bypasses the initial stages of invasion and is therefore somewhat removed from the normal course of infection. In spite of this, much useful information has been obtained from such an approach.

### ***Endpoints***

A large body of work rests on the analysis of CSF. CSF leukocyte count and protein concentration are usually used as measures of meningeal inflammation. However, a number of other biological variables have been measured in experimental meningitis according to the particular interest of the research group. These include:

- Mortality (judged by the LD50);
- CSF concentrations of leukocytes, viable bacteria, immunoglobulin, endotoxin (assessed by limulus lysate bioassay), and inflammatory mediators such as cytokines measured by bioassay or immunochemically by ELISA (Tuomanen *et al* 1985b; McCracken, Jr. and Sakata, 1985)
- Blood brain barrier structure investigated by transmission electron microscopy (Quagliarello *et al* 1991a) and its function quantitated using intravenous 125I-labelled albumin as a tracer (Kim *et al* 1992b; Townsend and Scheld, 1994);
- Cerebral blood flow measured by laser Doppler flowmetry; direct monitoring of intracranial pressure; brain oedema calculated by drying the brain after death and subtracting dry weight from wet weight (Pfister *et al* 1990; Tauber *et al* 1993);
- Microvascular changes monitored with confocal laser scanning microscopy via a “pial window” (Lorenzl *et al* 1993);
- In-vivo microdialysis of brain tissue to measure concentrations of excitatory amino acids (Perry *et al* 1993) or pH (Andersen *et al* 1989);
- Histopathological analysis of brain tissues with quantitation of neural damage (Leib *et al* 1996) or immunostaining for inflammatory mediators of interest (Tauber *et al* 1992a);
- Histopathological or ultrastructural analysis of the inner ear with or without measurement of hearing loss (Osborne *et al* 1995; Winter *et al* 1996; Rodriguez *et al* 1991; Kay, 1991; Wiedermann *et al* 1986);
- Behavioural changes judged by standard rat psychology tests to demonstrate that meningitis impairs future learning ability (Konkol *et al* 1987).

### ***Choice of species***

Dacey and Sande (1974) first described the most widely used model of experimental meningitis which is in the rabbit. Serial CSF samples can be taken by repeated sterile cisternal puncture with transient sedation or anaesthesia. Intracisternal inoculation of *S pneumoniae* (Tauber *et al* 1984), *E. coli* (Friedland *et al* 1993), *N. meningitidis* (Tuomanen *et al* 1989), *Haemophilus influenzae* (Mustafa *et al* 1989b) endotoxin, bacterial cell wall

products (Tuomanen *et al* 1985a), and proinflammatory cytokines (Saukkonen *et al* 1990) all induce meningeal inflammation. Because of the quantity of CSF available, rabbits are the main species used to investigate the effects of meningitis on CSF constituents and to assess the efficacy of new antibiotics against meningitis. Experiments with rabbit models have shed little light on the mechanisms of meningeal invasion but have greatly increased knowledge about local mediators of inflammation and potential disease modifiers. Recently, the cost of rabbits has become a major disadvantage both locally and in the USA (Prof. Tomasz, personal communication).

Studies of experimental rat meningitis have particularly investigated blood brain barrier functions and the detailed histopathology of brain tissue. As rats are used widely in neuroscience, there are data available about local production of cytokines, cytokine receptors, prostaglandins, the febrile response, and neuroimmunoendocrine interactions. The study of neonatal rat models helped define the route of meningeal invasion of *Haemophilus influenzae* type B (Hib) (Moxon and Ostrow, 1977).

Meningococcal infection has mainly been studied in neonatal mice (Salit and Tomalty, 1986). Adult mice have been used to model cryptococcal meningitis (Ailendoerfer *et al* 1991) and toxoplasma encephalitis (Hunter *et al* 1992).

Experimental meningitis has also been induced in guinea pigs (*S.pneumoniae*, Blank *et al* 1994; *Streptococcus suis*, Kay, 1991), pigs (*Streptococcus suis*, Williams and Blakemore, 1990b), dogs (*S.pneumoniae*, Scheld *et al* 1979), cats (*Klebsiella*, *S.pneumoniae*, Hochwald *et al* 1984), primates (*Haemophilus influenzae*, Scheifele *et al* 1980) and calves (*E. coli* endotoxin, Nakajima *et al* 1991).

#### **1.4.2. Pathogenesis of bacterial meningitis**

##### ***Invasion***

Pathogenic bacteria colonise and invade the nasopharyngeal mucosa and local lymph nodes, aided by a variety of factors discussed in section 1.2. Meningitis almost certainly results from haematogenous spread of organisms (Moxon and Ostrow, 1977). Circulating bacteria probably gain access to the CSF through the highly vascular choroid plexus (Daum *et al* 1978), perhaps aided by specific receptors (Kim *et al* 1992a) or concealed within circulating monocytes (the so-called 'Trojan horse' hypothesis) (Williams and Blakemore, 1990a). Normal cerebrospinal fluid contains little complement or specific antibody (Zwahlen *et al* 1982). Invading bacteria exploit this immune 'window' as phagocyte function is impaired in the absence of opsonization. Bacterial growth rate in the CSF is not enhanced in rabbits rendered neutropaenic before inoculation, suggesting that (at least initially) neutrophils are

unable to control the infection in the CSF (Ernst *et al* 1983). Organisms multiplying in the CSF space can secondarily invade the blood stream. This can occur early and before the peak of the CSF leukocyte response (Scheld *et al* 1979).

### *The cytokine response*

As part of the local inflammatory response, a host of toxic intermediates is liberated. Complement components and arachidonic acid metabolites (Ernst *et al* 1984; Kadurugamuwa *et al* 1989), pro-inflammatory cytokines (*TNF $\alpha$* , interleukin (IL)-1 $\beta$ , IL-6, IL-8, PAF (Frei *et al* 1993)), excitatory amino acids such as glutamate (Perry *et al* 1993; Guerra-Romero *et al* 1993), reactive oxygen intermediates (Pfister *et al* 1992d), and nitric oxide (Koedel *et al* 1995; Boje, 1995) have all been detected but their relative importance in bacterial meningitis remains uncertain. Some of the brain damage in meningitis may well be mediated by cytotoxic effects of these mediators. For example, IL-1 and *TNF $\alpha$*  in combination are cytotoxic for cultured human foetal neurons. This damage is reduced both by blockade of NO synthase and independently by N-methyl-D-aspartate (NMDA)-antagonists (Chao *et al* 1995). Similar results are obtained if co-cultures of microglial cells and cerebellar granule neurons are challenged with cytokines or lipopolysaccharide (Boje and Arora, 1992). The current understanding of the complex mechanisms which account for cytokine-mediated neurotoxicity in bacterial meningitis has been reviewed in a recent workshop summary (Pfister *et al* 1994).

The lipopolysaccharide component of Gram-negative bacteria, endotoxin, has long been recognised as an important mediator of inflammation, and indeed clinical studies have shown that poor outcome after Gram-negative meningitis is correlated with the concentration of free endotoxin in the CSF (Mustafa *et al* 1989a; Mertsola *et al* 1991). Endotoxin can activate complement by the alternate pathway and triggers the release of *TNF $\alpha$* , IL-1 and IL-6 from leukocytes and other cells (Ulich *et al* 1989; Ulich *et al* 1990; Ulich *et al* 1992; Spangelo *et al* 1990). These and other cytokines such as macrophage inflammatory proteins 1 and 2 (MIP-1, MIP-2) and IL-8 can induce an inflammatory response in the CSF when inoculated intracisternally in rabbits (Ramilo *et al* 1990; Saukkonen *et al* 1990). It is probable therefore that bacterial products stimulate release of pro-inflammatory cytokines which are then the chief inducers of meningeal inflammation. As discussed in section 1.2.4 Gram-positive cell wall components trigger inflammation in Gram-positive infection in a way analogous to endotoxin (Tuomanen *et al* 1995; Cundell *et al* 1995). Interestingly, indomethacin prevents the cytokine expression triggered by pneumococci but has no effect on that induced by endotoxin, suggesting that arachidonic acid metabolites help mediate cytokine induction in pneumococcal infection (Simpson *et al* 1994).

The predominant action of endotoxin appears to be to promote a leukocytosis in CSF, whereas other components of the Gram-negative cell wall appear to promote damage to the blood brain barrier (Burroughs *et al* 1992). Endotoxin induces a localised CSF inflammatory response when administered a variety of animals (Nakajima *et al* 1991), and causes specific damage to the organ of Corti and tectorial membrane when microperfused into scala tympani of the guinea pig (Tarlow *et al* 1991; Comis *et al* 1991). Endotoxin impairs the function of cultured astrocytes (Koller *et al* 1994) and isolated outer hair cells (Dulon *et al* 1990) but is not known to be directly cytolytic (in contrast to pneumolysin, for example).

Lytic antibiotics have the potential to release large amounts of bacterial cell products over a short time, and this phenomenon has certainly been observed in experimental meningitis (Tauber *et al* 1987). In a rabbit *Escherichia coli* meningitis model, a single intravenous dose of cefotaxime, cefpirome, meropenem, chloramphenicol, or gentamicin provokes a 2- to 10-fold increase in cerebrospinal fluid concentrations of free endotoxin within 2 h of starting treatment. By contrast, free endotoxin concentrations increase almost 100-fold in untreated animals 4 h later as bacteria continued to multiply. Antibiotic therapy in *E. coli* meningitis, irrespective of the agent used, may result in an increase in free endotoxin but the amount of endotoxin liberated is considerably smaller than that shed by untreated bacteria (Friedland *et al* 1993). There is some evidence that under carefully controlled conditions in experimental meningitis, administration of an antibiotic bolus can transiently enhance the concentrations of inflammatory mediators in the CSF such as **TNF $\alpha$**  (Mustafa *et al* 1989b; Friedland *et al* 1995). This so-called antibiotic-induced inflammatory burst has been blamed for exacerbating brain damage in meningitis. However, it occurs only if the antibiotic bolus is given as the organisms enter log-phase growth (Pfister *et al* 1994) (and Prof. Tomasz, unpublished findings). Any earlier and the infection is aborted; any later and the inflammatory cascade is already well advanced and antibiotic treatment adds little to it. The clinical relevance of such an antibiotic-induced inflammatory burst in meningitis therefore remains controversial.

### ***The role of leukocytes***

There is conflicting evidence about the role of leukocytes in causing damage to host tissues in bacterial meningitis. Survival time in dogs with pneumococcal meningitis is increased if the animals are rendered leukopaenic before inoculation (Petersdorf and Luttrell, 1962). However, raised intracranial pressure and brain oedema are not diminished in neutropaenic rabbits with pneumococcal meningitis (Tauber *et al* 1988).

Evidence available suggests that the C5a component of complement is chiefly responsible for the initial phase of Chemotaxis in the CSF. Chemotactic ability in CSF from rabbits with pneumococcal meningitis appears some 2 h before the onset of leukocytosis and can be blocked by preincubating the neutrophils with rabbit C5a (Ernst *et al* 1984). Intracisternal injection of C5a into rabbits provokes a polymorph leukocytosis in the CSF within one hour, faster than any other putative inflammatory mediator (Kadurugamuwa *et al* 1989). Rabbits treated with cobra-venom factor to deplete complement and then inoculated intracisternally with viable pneumococci die earlier than normal animals. In complement-depleted animals CSF leukocytosis is of similar magnitude but slightly delayed whereas it is almost abolished by cyclooxygenase inhibitors (Tuomanen *et al* 1986). Therefore arachidonic acid metabolites are responsible for the bulk of leukocyte invasion, but opsonization is essential for leukocyte function.

The primary site of leukocyte extravasation in meningitis appears to be the pial post-capillary venules. Leukocyte adherence to the vascular endothelium can be seen as little as one hour after induction of pneumococcal meningitis (Lorenzl *et al* 1993). The mechanisms of leukocyte adherence can be inferred from work conducted on isolated endothelial cells (Beilke, 1989). Selectins, including the endothelial cell adhesion molecules ELAM-1 (E-selectin) and P-selectin (CD62) and leukocyte L-selectin, mediate initial adherence. P-selectin is stored in endothelial granules and platelets, and is rapidly mobilized after stimulation. ELAM-1 is transiently expressed on endothelial cells 2-8 hours after exposure to endotoxin, **TNF $\alpha$**  or IL1 $\beta$  (Bevilacqua *et al* 1989). Both specifically recognise myeloid cells and are preferentially expressed in postcapillary venules. Before firmly binding to the endothelial surface, leukocytes "roll" slowly along the venular endothelial lining. This dynamic and reversible step can be inhibited by fucoidin, a polysaccharide which binds to leukocyte L-selectin. Fucoidin almost completely inhibits the influx of leukocytes into the subarachnoid space in response to intrathecal administration of heat-killed pneumococci in rabbits (Granert *et al* 1994; Tuomanen, 1994). There are no data about the ability of fucoidin to minimise brain oedema or neuronal damage in experimental meningitis induced by viable organisms

The next step in adherence and extravasation is mediated by the second major group of adhesion molecules which belong to the immunoglobulin supergene family. **TNF $\alpha$** , IL1 $\beta$  and **IFN $\gamma$**  trigger endothelial cells to express surface ICAM-1 (CD54). This binds firmly to the leukocyte glycoprotein complex  $\beta$ 2-integrin (CD11/CD18). Endothelial **IL-8** activates neutrophils, upregulates  $\beta$ 2-integrin and reduces leukocyte adhesion to ELAM, so promoting diapedesis across the endothelium. Another inducible endothelial ligand, VCAM, primarily recruits lymphocytes and monocytes by binding to their VLA-4/ $\beta$ <sub>1</sub>-integrin

complex. It is probably less important early in bacterial meningitis, but may contribute towards more chronic infiltrate and resolution. Interestingly, the CNS parenchyma itself is remarkably resistant to leukocytic invasion. Injection of various pro-inflammatory cytokines directly into the hippocampus of the rat induces a brisk leukocytosis in the CSF but does not cause a localised abscess (Andersson *et al* 1992).

Specific inhibition of leukocyte adherence with an anti-CD18 monoclonal antibody (**IB4**) reduces CSF leukocytosis, mortality and histological brain damage in rabbits with pneumococcal meningitis (Tuomanen *et al* 1989). **IB4** is less effective at preventing endotoxin-induced meningeal inflammation, but acts synergistically with dexamethasone to greatly reduce meningeal inflammation in experimental *H. influenzae* type B meningitis without affecting bacterial clearance from the subarachnoid space (Saez-Llorens *et al* 1991).

### ***Blood-brain barrier, brain oedema and cerebral perfusion***

Brain oedema in bacterial meningitis is clearly caused by a number of factors. Raised blood-brain barrier (BBB) permeability causes vasogenic oedema as protein and fluid leak out (Quagliarello *et al* 1991a). This particularly affects the subcortical white matter. Arachnoid villi become plugged with neutrophils, increasing CSF outflow resistance and producing interstitial oedema as CSF fails to be reabsorbed. Toxic inflammatory intermediates induce a cytotoxic oedema by altering the permeability of cell membranes and damaging cell metabolism and homeostasis.

The anatomical site of the BBB is the cerebral capillary endothelium, which has a number of unique properties. Systemic capillaries are fenestrated to allow passage of macromolecules. In contrast, cerebral capillary endothelial cells are fused together with continuous intact intercellular tight junctions (*zonulae occludentes*). Pinocytic vesicles are very rare (Reese and Karnovsky, 1967). Sheets of cultured rat cerebral endothelial cells maintain a very high trans-endothelial electrical resistance (some 100 M $\Omega$ /cm<sup>2</sup>). This can be disrupted by cytokines (**TNF $\alpha$** , IL-1 $\beta$  and IL-6) but not in the presence of indomethacin, suggesting that prostaglandin activation in endothelial cells may contribute to breakdown of the BBB in bacterial meningitis (Devries *et al* 1996). Intracisternal administration of *H. influenzae* type B, *E. coli* K1, or type III *S.pneumoniae* in the rat all cause a uniform time-dependent injury to the cerebral capillary endothelium. Four hours after inoculation, there is an increase in pinocytic vesicle formation. This is followed by progressive breakdown and separation of up to 20% of the *zonulae occludentes* accompanied by a rise in BBB permeability (Quagliarello *et al* 1986). The precise site of the albumin leak across the injured BBB has been localized to open intercellular junctions in pial venules (Quagliarello *et al* 1991a).

Intracisternal injection of just nanogram amounts of IL1 $\beta$  or picogram amounts of Hib LOS can cause BBB injury in the rat (Quagliarello *et al* 1991b; Wispelwey *et al* 1988). There is reasonable evidence that leukocyte products contribute to brain oedema in bacterial meningitis. Brain oedema induced by intracranial injection of cytokines is completely abolished by the anti-CD18 antibody IB4 (Saukkonen *et al* 1990). Intracisternal injection of Hib LOS has no effect on BBB permeability in leukopaenic rats (Wispeley *et al* 1988).

In the early stages of meningitis cerebral blood flow rises, probably as a result of dysregulation of the pial arterioles which pass through the inflamed subarachnoid space (McKnight *et al* 1992). Nitric oxide is likely to be involved in this process. Heat-killed pneumococci induce the production of nitric oxide by cultured rat cerebral endothelial cells (Haberl *et al* 1994). Intravenous administration of N-nitro-L-arginine (L-NA) or N-G-nitro-L-arginine methyl ester (L-NAME) (nitric oxide synthase inhibitors) reduce the early changes in cerebral blood flow and prevent brain oedema and pial arteriolar dilation in experimental pneumococcal meningitis in rats (Haberl *et al* 1994; Koedel *et al* 1995). However, mortality increases in animals treated with NO synthase inhibitors. Another mechanism of injury may be due to the action of oxygen free radicals. In early experimental pneumococcal meningitis in rats, Superoxide dismutase (a free radical scavenger) or the antioxidant desferrioxamine both attenuate brain oedema, CSF leukocytosis, and the rise in intracranial pressure and regional cerebral blood flow (Pfister *et al* 1992d; Koedel *et al* 1995).

Later in the course of the illness, autoregulation fails and cerebral blood flow varies passively with mean arterial blood pressure (Tureen *et al* 1990). Cerebral perfusion is compromised by the rise in intracranial pressure combined with the systemic hypotension common in septicaemic illness. Large vessel abnormalities documented on angiography in patients with focal neurological deficits include sagittal sinus thrombosis, occlusion of branches of the middle cerebral artery, and narrowing of the internal carotid artery (Pfister *et al* 1992a).

In conclusion, the combination of inflammatory mediators, bacterial products (Tauber *et al* 1992b; Kim *et al* 1995), brain oedema, altered cerebral blood flow and vasculitis, and brain hypoxia in varying degrees result in parenchymal brain damage in bacterial meningitis.

### **1.4.3. Anti-inflammatory strategies.**

The assumption that much of the damage in meningitis could be mediated by an excessive host inflammatory response has led to a great deal of work to identify agents which might modulate this. Only dexamethasone is routinely used in such a way clinically (see section

1.5.3). Dexamethasone inhibits pro-inflammatory cytokine production by monocytes in response to endotoxin (van Furth *et al* 1994) and by glial cells in response to pneumococcal cell wall (Chao *et al* 1992). It inhibits induction of nitric oxide synthase in glial cells (Freyer *et al* 1996) and vascular endothelium (Rees *et al* 1990). In a variety of meningitis models, adjuvant treatment with dexamethasone reduces a variety of indicators of meningeal inflammation, particularly when administered just before the first antibiotic dose (Syrogiannopoulos *et al* 1987; Mustafa *et al* 1989b; Saez-Llorens *et al* 1991).

Pentoxifylline suppresses endotoxin-induced **TNF $\alpha$**  gene transcription in vitro and in a rabbit model diminishes the meningeal inflammatory response to both Hib LOS and IL1 $\beta$  (Saez-Llorens *et al* 1990). Pentoxifylline is less effective in this model than dexamethasone, which blocks human monocyte production of IL1 $\beta$  in addition to **TNF $\alpha$**  (van Furth *et al* 1994).

Thalidomide also diminishes **TNF $\alpha$**  production and can be used clinically to treat graft-versus-host disease. In experimental rabbit meningitis induced by pneumococcal cell wall material, thalidomide reduces the concentration of **TNF $\alpha$**  and leukocytes in the CSF. However, it has little impact on meningeal inflammation induced by *Haemophilus influenzae* cell lysate (Burroughs *et al* 1995).

Non-steroidal cyclo-oxygenase inhibitors such as indomethacin and oxindac reduce morbidity and death in pneumococcal meningitis in rabbits (Tuomanen *et al* 1987). They also reduce the burst of meningeal inflammation induced by ampicillin treatment and greatly diminish brain oedema in this model (Tureen *et al* 1991). There are conflicting data about the ability of indomethacin to reduce CSF leukocytosis in experimental meningitis (Tuomanen *et al* 1987; Tureen *et al* 1991).

Anti-endotoxin molecules were beneficial in experimental Gram-negative infections, but clinical trials were disappointing because it proved difficult to select patients with septic shock due to Gram-negative infection rather than other causes (Ziegler *et al* 1991). However a clinical trial of **HA-IA** (a humanised anti-endotoxin monoclonal) in childhood meningococcal septicaemia with shock is due for publication soon. There has been some enthusiasm for the idea that anti-cytokine treatment could be used to modify the host response to meningitis (Kornelisse *et al* 1995). However because of the many different ways in which bacterial products trigger inflammation, such a strategy would seem doomed to fail. Recent evidence from a rabbit model showed that neither soluble TNF receptor or IL-1 receptor antagonist alone could prevent *Haemophilus influenzae* lipooligosaccharide (Hib LOS) from inducing a meningeal inflammatory response (Paris *et al* 1995). Even if it proved effective, such adjuvant treatment would be exorbitantly costly if used clinically.

A problem common to all anti-inflammatory strategies is that they assume that modulating meningeal inflammation will also reduce the chance of hearing **loss**. Data to be presented later suggest that at least some meningogenic deafness is mediated directly by bacterial products. **An** additional objection is that by the time a patient presents with meningitis, the meningeal inflammatory cascade is already well advanced and agents acting early in this cascade are unlikely to have a great impact. More promise might lie in cytoprotective agents that could modify the putative final common mechanisms mediated by glutamate, nitric oxide and reactive oxygen intermediates that underlie neuronal damage (Leib *et al* 1996).

## 1.5. Deafness in clinical and experimental meningitis,

### 1.5.1. Epidemiology.

Almost all cases of acquired sensorineural deafness in the UK are secondary to meningitis, accounting for about 6% of all childhood deafness or approximately 60–70 children per year in the UK (Fortnum, 1992). Table 1.3 (after Dodge *et al*, 1984) compares the level of hearing loss as defined by audiometric testing with the expected disability.

<b>dB loss</b>	<b>Hearing class</b>	<b>Functional definition</b>
<30	Normal	Within normal limits
30–55	Mild loss	Difficulty with conversation beyond 3-4 feet
55–70	Moderate loss	Hearing aids and special training essential
70–90	Severe loss	Difficulty hearing speech with hearing aid. Educated as deaf person
>90	Profound loss	Deaf. Hearing aid of little benefit

**Table 1.3.** A classification of hearing loss .

Before the advent of antibiotics almost everyone who contracted pneumococcal meningitis died of the disease and there were few worries about late neurological sequelae. Once effective antibiotic treatment became available for pneumococcal disease it became evident that many sufferers were left severely handicapped by neurological damage. Trolle (1950) was one of the first to draw attention to the long-term audiological deficits that sometimes occurred after meningitis. In a review of studies of meningococcal meningitis published between 1905 and 1948 the overall incidence of defective hearing was around 16% (range **2.5%** to 50%). The use of quinine as a therapy although itself ototoxic may have confounded these figures. Case reports in the 1960s and 1970s contained several theories about the causes of sensorineural hearing loss but little hard evidence (Liebman *et al* 1969; Roesor *et al* 1975). Good epidemiological studies were aided by the advent of audiological evaluation in the form of brain-stem evoked response testing and a systematic approach to follow-up. Fortnum (1992) has recently provided an authoritative review which included a meta analysis of well-conducted clinical studies published between 1977 and 1992. In 1175 unselected cases in 8 reports, the overall incidence of any permanent sensorineural hearing

loss was **9.6%** (range **6.3–11.7%**) (Ozdamar *et al* 1983; Vienny *et al* 1984; Dodge *et al* 1984; Guiscafre *et al* 1984; Salwen *et al* 1987; Dawson *et al* 1988; Lebel *et al* 1988; Odio *et al* 1991). Profound bilateral or total hearing loss occurred in **1-4%** of cases. In **66** cases of pneumococcal meningitis, the incidence was **31.8%** (range **21–50%**), whereas after **398** cases of meningococcal meningitis estimated overall hearing loss was **7.5%** (range **5–10%**).

There are several issues which cloud the interpretation of such studies. Retrospective studies are prone to bias, particularly in over-reporting the incidence of neurological sequelae due to pneumococcal disease since it is possible that these patients will have been followed up more closely. Two large prospective trials provide conflicting data about the importance of bacterial aetiology in meningogenic hearing loss. Dodge *et al* (1984) found that patients with pneumococcal meningitis had a higher incidence of sensorineural hearing loss than those with meningitis due to other aetiologies (**31%** vs. **6%** for Hib and **10.5%** for *N meningitidis*). In a more recent prospective study, seven of **20 (35%)** children with pneumococcal disease sustained hearing loss, compared to eight of **39 (20%)** with Hib meningitis and two of **13 (15%)** with meningococcal disease (Wald *et al* 1995). These differences did not achieve statistical significance. Prospective studies also present problems because endpoints (which range from any degree of deafness to severe bilateral loss only) have sometimes been chosen to emphasise "significant" results (e.g. Schaad *et al* 1995 and Kanra *et al* 1995) and it is rarely made explicit whether the endpoints were chosen in advance. One study enrolled for evoked response testing only those thought to be at "high risk" of developing complications (Kaplan *et al* 1984). The antibiotic management of meningitis has changed over the last ten years with the advent of penicillin resistance. For example, it has become clear that treatment with cefuroxime is less effective and has a greater incidence of neurological sequelae than treatment with a third-generation cephalosporin (Lebel *et al* 1989). Finally, immunisation against *Haemophilus influenzae* type B has already greatly reduced the incidence of Hib meningitis in some countries and thereby increased the proportion of cases due to the pneumococcus (Baer *et al* 1995; Schaad *et al* 1995). Therefore clinical data from the pre-immunisation era may not be helpful in predicting the future incidence of post-meningitic deafness.

There are also geographical differences in the incidence of post-meningitic deafness. In studies from countries with a poor health care infrastructure, meningitis patients usually present late, often after visits to local practitioners. An Egyptian study reported that two-thirds of patients with meningitis (both adults and children) were admitted comatose (Girgis *et al* 1989). On the Pacific island of Vanuatu some **32%** of meningitis cases sustained neurological sequelae, about half of these being severely disabled (Carroll and Carroll, 1994). The situation is similar in the Sudan where **11%** of cases had a profound, persistent

hearing loss (Salih *et al* 1991). In the UK by contrast, a recent study found that only three of 123 (2.5%) children admitted with bacterial meningitis sustained long-term hearing loss (Richardson *et al* 1995). This is a lower incidence than reported from the USA perhaps because the UK's well-developed primary care system and public-health education of parents in the light of recent meningitis "scares" mean that patients present earlier.

Recent evidence has shown that hearing loss in patients with bacterial meningitis occurs early in the course of illness and is in many cases transient (Wilken *et al* 1995; Kaplan *et al* 1984; Richardson *et al* 1995; Vienny *et al* 1984; Guiscafre *et al* 1984). Recovery of audiometrically-confirmed hearing loss was first reported in the 1960s and 1970s (Liebman *et al* 1969; Roesor *et al* 1975). In their major US study, Dodge *et al* (1984) found no cases of recovery among 19 of 185 children with a sensorineural hearing deficit, but did demonstrate recovery in several patients with a conductive-type loss. However, initial audiometric testing was not performed until at least ten days after admission. Vienny *et al* (1984) addressed the question of early hearing loss directly by assessing 51 children presenting with meningitis within 48 h of admission with auditory evoked brain-stem response testing. Eleven patients (22%) developed transiently abnormal evoked responses while a further 5 (10%) went on to have permanent hearing impairment. These findings were confirmed by a recent well-conducted prospective multi-centre study from the US in which auditory brain-stem evoked responses were elicited within 24 h of admission on 173 children with meningitis aged between 8 weeks and 12 years (Wald *et al* 1995). Among 22 children (13%) with bilateral moderate or severe hearing loss at presentation, 13 had recovered normal hearing in at least one ear six months later. Nine of the 10 children with persistent bilateral deafness had been deaf at the first assessment. Richardson *et al* (1995) prospectively assessed the hearing of 123 children presenting with meningitis to hospitals in the south-west region of the UK. Otoacoustic emissions were recorded within 6 h of admission. Of the 13 children with hearing impairment at presentation, 9 had recovered hearing within 48 h. The use of this newly developed technique provides the first direct clinical evidence that early hearing loss is due to cochlear damage rather than disturbance of brain stem function or auditory nerve damage. There now seems to be general agreement that little further auditory impairment occurs more than 48 h after admission. It is also encouraging that many cases of cochlear hearing loss appear to be transient. Early case detection and prompt treatment before hearing loss progresses should reduce the chance of permanent sensorineural hearing loss. It might also be possible to design specific interventions to increase the chance of recovery if many patients are admitted with potentially recoverable hearing. A better understanding of the pathogenic mechanisms of cochlear damage in meningitis is therefore crucial.

## 1.5.2 Mechanisms of post-meningitic hearing loss.

### *Clinical studies*

Several findings suggest that hearing loss occurring after meningitis is due primarily to cochlear damage rather than to auditory nerve neuritis or brain damage at higher levels:

- Cochlear implantation is successful in many cases of meningogenic deafness (Johnson *et al* 1995);
- Hearing loss is frequently unilateral, occurs very early in the course of illness, and is often not accompanied by other brain damage (Dodge *et al* 1984; Fortnum, 1992; Vienny *et al* 1984; Wald *et al* 1995);
- Post mortem studies demonstrate suppurative labyrinthitis (Perlman and Lindsay, 1939);
- CT studies of the temporal bone show a high proportion of cochlear abnormalities (Johnson *et al* 1995);
- Otoacoustic emissions are reduced in children with meningogenic hearing loss (Richardson *et al* 1995).

There was little doubt in the pre-antibiotic era that post-meningitic deafness was due to a neurolabyrinthitis (Trolle, 1950). Trolle's review lists several post-mortem studies published between 1886 and 1940. The main limitation of such post-mortem studies is that they can only include cases with severe disease who may not be entirely representative. The preparation of temporal bones for histological analysis is also extremely difficult to do well and autolytic changes are inevitable. Trolle listed the potential causes of post-meningitic deafness thus:

- Infiltration of the eighth cranial nerve and secondary degeneration of the neural structures of the cochlea;
- Purulent labyrinthitis;
- Septic embolism of the internal auditory artery.
- *Hydrops labyrinthi* (secondary to a toxic or serous labyrinthitis)
- Otitis media (accessory role only in some cases);
- Disturbance of brain stem and higher auditory centres.

The sole alteration needed today would be to add that bacterial products are directly ototoxic (Comis *et al* 1993; Dulon *et al* 1990) (and evidence cited in this thesis). Leichenger (1937) also reported a case of meningococcaemia who survived but suffered hearing loss and suggested that the deafness was due to the effects of an exotoxin on the

inner ear. Of course, this list does not explain the actual mechanisms of hearing loss; that is, how labyrinthitis itself can affect the structure and function of the auditory apparatus. Some theories of this will be outlined in chapter 5.

Perlmann and Linsey (1939) investigated histopathological changes in the temporal bones of 30 patients who died from meningitis. In the first stage of labyrinthitis, polymorphs were found around the facial and acoustic nerves. In later stages, pus cells were seen invading along the cochlear aqueduct and filling the scala tympani. Eavey (1985) demonstrated retrograde invasion of the inner ear in four of eight fatal cases of pneumococcal meningitis. No studies have shown a direct route of extension from middle ear sepsis to the inner ear. The two major routes for the transmission of infection between the meninges and the labyrinth are agreed to be the cochlear aqueduct and the eighth cranial nerve (Igarishi and Schucknecht, 1962). Igarishi (1974) emphasised that bacteria could also invade the endolymphatic space via the blood stream, and described the destruction of the stria vascularis by bacterial thrombi in pneumococcal meningitis. It has been suggested that serous labyrinthitis induced by spread of "toxic" factors from the CSF may cause reversible deafness while true purulent labyrinthitis causes permanent inner ear damage (Liebman *et al* 1969; Fortnum, 1992). There is in fact little histopathological evidence to support such a contention. In less severe (i.e. non-fatal) cases, radiological studies of the temporal bone performed prior to cochlear implantation are frequently abnormal. In one study, 70% of patients with post-meningitic deafness had either cochlear stenosis or cochlear ossification demonstrable on high-resolution thin-section CT scanning (Johnson *et al* 1995). It is beyond reasonable doubt therefore that the vast majority of cases of post-meningitic deafness result from damage to the inner ear.

### ***Experimental meningitis***

Four other groups besides the Meningitis Research Group in Birmingham have published data related to meningogenic deafness in animal models. This body of work will be discussed in greater detail in the discussion (Chapter 5), but there follows a brief overview.

Sheldon Kaplan's group at Texas Childrens' Hospital have induced meningitis in infant rats by systemic inoculation of *H. influenzae* type b or (with less success) pneumococci. They demonstrated the development of labyrinthitis (detected with light microscopy), but did not measure hearing loss (Wiedermann *et al* 1986; Rodriguez *et al* 1991). The development of labyrinthitis was not related to the potential of the strain of Hib to induce deafness clinically. Sensitive immunofluorescent techniques were used to demonstrate Hib invasion of the cochlea. Labyrinthitis was not observed when rats were given ampicillin treatment one day after inoculation (Kaplan *et al* 1989). Blank *et al* (1994) reported that meningitis induced by

intrathecal inoculation of pneumococci in the guinea pig causes a labyrinthitis. Hearing loss was not assessed in this study either. Kay (1993) showed that inoculation of *Streptococcus suis* by intraperitoneal, intracranial or intrabullar routes in the guinea pig could induce a suppurative labyrinthitis. Hearing loss was assessed rather inadequately by click evoked auditory brain-stem response testing of animals surviving to the end point. Elaine Tuomanen's group at the Rockefeller have preferred to use the traditional Dacey and Sande rabbit pneumococcal meningitis model assessing hearing with of click- and tone-evoked auditory brain stem Potentials to give a frequency-specific assessment of hearing loss (Bhatt *et al* 1991; Bhatt *et al* 1993). Rabbits begin to lose hearing 12 h after intracisternal inoculation of *S. pneumoniae* ( $10^5$  CFU). This correlates with the onset of a leukocytosis in the CSF. Suppurative labyrinthitis occurs but the organ of Corti appears to be undamaged at a light-microscopic level. More recently, the effect of antibiotic treatment on the course of hearing loss has been studied in this model. Hearing assessments were performed up to 4 days after the induction of meningitis. Cefotaxime treatment improves auditory outcome but adjuvant dexamethasone treatment has no additional benefit (Bhatt *et al* 1995).

Ultrastructural damage of the organ of Corti during experimental *E coli* or Hib meningitis was reported in detail by Osborne *et al* (1995) from the University of Birmingham. Hearing loss was assessed by click-evoked auditory brain stem response testing. Specific ultrastructural lesions are detected once hearing loss exceeds 20 dB.

Whether meningitis is induced by systemic inoculation or by intracranial injection inflammation of the perilymphatic space is common whereas inflammation of the endolymphatic space is rare. This is consistent with inflammation spreading from the CSF space rather than by haematogenous dissemination. All reports agree about the importance of the cochlear aqueduct in allowing the spread of infection and, in one study, in defending the inner ear from such invasion (Yanagita *et al* 1984). *No* study has reported hearing loss at the cochlear level, but the ultrastructural damage observed is consistent with cochlear damage being the main cause of meningogenic hearing loss. These findings are certainly consistent with the postmortem studies and clinical investigations discussed above.

### ***Evidence from cochlear perfusion studies***

Four studies all conducted in Birmingham have reported the deleterious effects of the bacterial products endotoxin and pneumolysin on the electrophysiological function and ultrastructure of the organ of Corti when micropertused into the scala tympani of the guinea pig (Comis *et al* 1991; Tarlow *et al* 1991; Comis *et al* 1993; Amaee *et al* 1995). The relevance of these findings to the damage observed in experimental meningitis and putative mechanisms of meningogenic deafness will be discussed in Chapter 5.

### 1.5.3. The steroid controversy.

A great deal of controversy exists about the benefits of giving dexamethasone as adjuvant therapy to patients with meningitis. Glucocorticoids have many biological activities that might ameliorate the neurological damage caused by bacterial meningitis. These include anti-inflammatory effects such as reducing the liberation of cytokines in response to various inflammatory stimuli in vitro and in vivo (Velasco *et al* 1991; van Furth *et al* 1994; Mustafa *et al* 1989b; Ulich *et al* 1990; Mustafa *et al* 1990), as well as reducing brain oedema, intracranial pressure and blood-brain barrier permeability in experimental meningitis (Koedel *et al* 1994). Other agents which have been shown to modulate inflammation in the CSF space include indomethacin (Tuomanen *et al* 1987; Tureen *et al* 1991), pentoxifylline (Saez-Llorens *et al* 1990) and anti-CD-18 antibodies (Cabellos *et al* 1992) as discussed in section 1.4.3. Several assumptions have been used to support the use of such agents to reduce the incidence of neurological sequelae:

- The bulk of the neurological damage which ensues is caused by an excessive host inflammatory response.
- The underlying pathophysiology is broadly similar in meningitis due to *Haemophilus influenzae*, *Neisseria meningitidis* and *Streptococcus pneumoniae*.
- Modern lytic antibiotics provoke a *significant* and damaging rise in local inflammation compared to bacteriostatic agents.

Based on such theoretical considerations, a number of clinical trials were conducted in the late 1980s to assess the impact of dexamethasone treatment on the incidence of various neurological sequelae, including sensorineural deafness (Lebel *et al* 1988; Girgis *et al* 1989; Odio *et al* 1991). No significant benefit was seen unless the incidence of sequelae was raised because of sub-optimal antibiotic treatment or supportive care; two of the studies were conducted in under-resourced countries where patients presented very late in the course of disease. However, because of the theoretical arguments and the beneficial trends seen in such studies, adjuvant dexamethasone therapy was endorsed by the Committee on Infectious Diseases of the American Academy of Paediatrics in 1991 (although they suggested that the decision should be “individualised”) and the Meningitis Working Party of the British Paediatric Immunology and Infectious Disease Group in 1992. Recommendations suggested administering dexamethasone (0.4–0.6 mg/kg/day) for 4 days starting about 15 min before the first antibiotic dose. A large prospective trial studying 115 children admitted with bacterial meningitis in Switzerland appeared to show that dexamethasone reduces the incidence of any neurological complications (Schaad *et al* 1993). But there were no significant differences between groups in the incidence of severe

neurological sequelae or bilateral moderate to severe hearing loss, endpoints of perhaps greater importance. A meta-analysis of this and other recent studies conducted in developed nations where optimal treatment was given also suggested a significant benefit for adjuvant dexamethasone treatment (0.4 mg/kg/day) in bacterial meningitis, with a relative risk of developing any neurological or audiological sequelae without dexamethasone of **2.29 (95% CI 1.2 to 4.3)** (Schaad *et al* 1995). A study from Greece demonstrated that **2** days of dexamethasone treatment was just as effective as **4** days, with an overall incidence of any neurological or audiological sequelae of **1.8%** or **3.8%** respectively (Syrogiannopoulos *et al* 1994).

Many of the cases of meningitis in these studies were due to *H. influenzae* type b and it remains controversial whether these findings are applicable to the spectrum of disease encountered now Hib immunisation is widespread. More specifically, none of the studies have recruited sufficient numbers to assess the impact of dexamethasone in pneumococcal disease. A retrospective analysis from Dallas covering the years **1984** to **1990** purported to show a benefit for dexamethasone treatment but there were differences in the composition of groups and some children received an inferior antibiotic (cefuroxime). A prospective study from Turkey utilising behavioural audiometry showed no significant benefit from dexamethasone treatment (0.6 mg/kg/day) in **56** cases of pneumococcal meningitis at **6** week follow up, but with some judicious data dredging found a just-significant benefit at **3** month follow up (**P=0.04**) (Kanra *et al* 1995).

The conclusions of the most recent and best conducted prospective study of the use of dexamethasone in childhood bacterial meningitis are decidedly more guarded. Wald and colleagues (1995) in the study of **173** children referred to above (page **44**) found that dexamethasone (0.6 mg/kg/day for **4** days) reduced bilateral hearing loss in meningitis due to *H. influenzae* type b but was of no benefit in reducing other neurological sequelae or in meningitis due to other pathogens. The outcomes for the various aetiologies are given in table **1.4**.

The most likely explanation for the differences observed in these subgroups is that there were insufficient subjects, even in such a large, multi-centre trial. The initial power calculations suggested **300** subjects were needed, but the advent of Hib immunisation curtailed recruitment. This does not bode well for other trials of adjuvant therapy. The major criticism of this trial is that dexamethasone was administered up to **4** hours after the first antibiotic dose (which at least reflects typical practice if antibiotics are administered in primary care). It is most important that none of the children found to be deaf at the time of

first assessment (within 24 h) recovered hearing; that is dexamethasone failed to reverse cochlear damage.

<b>Aetiology</b>	<b>Dexamethasone</b> (bilateral deafness)	<b>Placebo</b> (bilateral deafness)	<b>P</b> (two-tailed by Fisher's exact test)
<i>H. influenzae</i> type b	0/43 (0%)	5/39 (13%)	0.02
<i>S. pneumoniae</i>	3/13 (23%)	2/20 (10%)	0.36
<i>A? meningitidis</i>	0/11 (0%)	0/13 (0%)	–
<b>TOTAL</b>	<b>3/67 (4.4%)</b>	<b>7/72 (9.4%)</b>	<b>0.33</b>

**Table 1.4:** Final audiological outcome in 142 children with meningitis  
(taken from Wald *et al* 1995)

Steroid therapy is not without adverse effects. Gastrointestinal bleeding (which is usually occult) and a higher incidence of secondary fever are not particularly worrying. Of more concern is that dexamethasone treatment reduces penetration of vancomycin into the CSF and delays CSF sterilization in experimental meningitis induced with penicillin-resistant pneumococci in the rabbit (Paris *et al* 1994). In areas where vancomycin is used as a first line agent, the use of dexamethasone does not appear sensible. In addition, many cases of meningitis are in fact viral in aetiology and there is no firm data that steroid treatment is without harm in this situation (Kaplan, in Schaad *et al*, 1995)

In conclusion, then, the *theoretical* benefits expected with adjuvant dexamethasone therapy have been more difficult to demonstrate in well-conducted clinical trials. This has not stopped various authors promoting steroid therapy quite vigorously, often relying heavily on data from experimental meningitis and arguing from hypotheses (rather than firm evidence) about the pathogenesis of infection (Quagliarello and Scheld, 1992; Tunkel and Scheld, 1993b). The most important findings from recent prospective trials have been the low incidence of severe neurological sequelae in developed countries and the fact that deafness occurs early in the course of the illness. Clearly, the most beneficial intervention to prevent meningogenic deafness will be immunisation against the common pathogens causing childhood bacterial meningitis. This is even more important in developing countries where meningitis is more common and carries a much greater morbidity.

## 1.6. Conclusions.

### **Towards a new paradigm of meningogenic hearing loss.**

It is clear from the preceding review that there are likely to be many mechanisms which cause hearing loss in bacterial meningitis. The current paradigm is dominated by the concept that a largely frustrated host inflammatory response liberates toxic intermediates that cause end-organ damage. This does not really explain the much worse prognosis in meningitis due to *S. pneumoniae* as opposed to meningococcal or Hib meningitis, other than to assume (without a lot of evidence) that Gram-positive cell wall is in general more “inflammatory”. The crucial link in this hypothesis – that inflammatory mediators are the *major* cause of brain and auditory damage – has not been satisfactorily proven. There are in fact few experimental studies of end-organ damage (as opposed to endpoints such as CSF leukocytosis) although recent studies of putative adjuvant agents have included histological data. Several studies have shown that bacterial products such as pneumolysin and pneumococcal cell wall are themselves cytotoxic, irrespective of the host inflammatory response. There are as yet few data about the role in the pathogenesis of meningitis of pneumococcal accessory virulence factors such as pneumolysin or neuraminidase.

Although it seems to be accepted that the cochlea is the site of meningogenic deafness, the available evidence is largely circumstantial. There is no published evidence that conclusively shows that the hearing loss measured in experimental bacterial meningitis reflects cochlear damage rather than brain stem disturbance. All but one clinical study has relied on brain stem recording or behavioural audiometry to assess hearing loss. Evidence from experimental rabbit meningitis does suggest that specific ultrastructural lesions of the organ of Corti underlie meningogenic deafness but more data are needed especially in different species.

In conclusion a new paradigm of hearing loss in bacterial meningitis needs to be constructed which takes into account:

- Evidence gathered from histopathological and neurophysiological studies of tissue damage which sheds light on the effects of bacterial meningitis on brain and auditory function.
- Evidence about the role of bacterial products in direct cytotoxicity and the contribution to virulence of the various proteins elaborated by *S. pneumoniae*.
- A better model of the molecular and bioelectric phenomena which underlie meningogenic hearing loss whether induced by inflammatory mediators or toxic bacterial products. This should satisfactorily explain reversible hearing loss.



**Summary of experimental data to be presented.**

The following data from a model of experimental meningitis in the guinea pig are now presented:

- The scanning and transmission electron microscopic appearance of the organ of Corti in the first twelve hours of experimental meningitis due to *E coli* or *S. pneumoniae*;
- **An** electrophysiological study of hearing loss measured by direct electrocochleography **in** experimental pneumococcal meningitis;
- Hearing measurements and cerebrospinal fluid data in experimental meningitis induced by isogenic strains of *S. pneumoniae* lacking pneumolysin, neuraminidase or hyaluronidase;
- The effects of antibiotic treatment on cochlear Potentials and ultrastructural damage to the organ of Corti after microperfusion of *S. pneumoniae* directly into the scala tympani of the inner ear.

## 2. MATERIALS AND METHODS

### 2.1 Common methods

#### 2.1.1 Overall strategy

Two different experimental models were employed.

***Meningitis model.*** Experimental meningitis was induced by *Escherichia coli* K-12, or a virulent serotype 2 *Streptococcus pneumoniae* D39, or its isogenic derivatives PLN-A,  $\Delta$ NA1 or  $\Delta$ HY1, deficient in pneumolysin, neuraminidase or hyaluronidase respectively. This work is referred to as the “meningitis model”, and is described in section 2.2 with experimental results given in chapter 3. The majority of the work was performed in guinea pigs, but meningitis was also induced in six rabbits.

***Cochlear perfusion.*** Suspensions of viable bacteria were perfused through the scala tympani of the cochlea of the guinea pig to mimic under controlled conditions what might happen when organisms invade the cochlea during bacterial meningitis. This work is referred to as “cochlear perfusion”, and is described in section 2.3 with experimental results given in chapter 4.

The two primary endpoints in all studies were:

- Hearing loss assessed by recording either auditory-evoked brain-stem far-field Potentials or the auditory nerve compound action potential.
- Ultrastructural changes in the organ of Corti observed by scanning and transmission electron microscopy.

The common methods for animal handling and bacterial preparation are now described. The composition of solutions used will be found in appendix A. The manufacture of isogenic derivatives of D39 is described in appendix B.

#### 2.1.2 Use of animals

##### ***Consideration of alternatives.***

Before undertaking any animal study one has to consider the use of alternative strategies to investigate the problem. In order to study the pathophysiological events of meningitis a whole animal model is essential. The concern of this project was to investigate how inoculation of organisms into one compartment (the CSF space) would affect the behaviour

of an organ in another compartment (the perilymphatic and endolymphatic spaces). There is no in vitro system sophisticated enough to model these events. Much of the work challenges the currently accepted dogma on which such models might be based.

### ***Minimisation of animal use***

In all parts of the project the absolute minimum number of animals was used consistent with obtaining statistically valid results. In general this implied group sizes of **4-6** for each particular organism or treatment under investigation. Experiments were carefully planned to yield the maximum data. Strong ethical and financial constraints at times prevented repetition or extension of experiments where in a less rigorous environment this may have been considered useful. In particular, our group has a policy of not allowing nor seeking permission for “recovery” experiments where mid to long term sequelae can be investigated. The investigations to be reported therefore deliberately concentrate on the acute pathophysiological events occurring within the first twelve hours of induction of meningitis.

### ***Animal welfare.***

In the first part of the project pigmented guinea pigs were bred in our own colony and housed in open pens with free access to food and water. With the implementation of real costing, in-house breeding became financially unviable and for the later parts of the project pigmented guinea pigs were purchased from a breeding colony at Leeds University. These animals were housed under similar conditions. Rabbits were purchased from a commercial supplier. All experiments were conducted under a Home Office Project Licence and Personal Investigator Licence.

### **2.1.3 Anaesthesia and conditions**

Pigmented guinea pigs of either sex weighing between 500 g and 700 g were anaesthetised by intraperitoneal injection of Urethane (**5.5 ml/kg** body weight of **25%** (w/v) ethyl carbamate in distilled water; Sigma, UK). This gave a stable deep surgical anaesthesia for up to 8 h before supplements were necessary. Animals never recovered consciousness and the level of anaesthesia was monitored regularly throughout each experiment by assessing withdrawal reflex. The rectal temperature was maintained at 38°C with a heat lamp or (in later experiments) with a **12 V DC** home-built servo-controlled heating pad based around a Maplin temperature module (FE33). Animal temperature with the latter stabilised to **38°C ± 0.3°C** within one hour. For any experiment longer than **4 h** fluid replacement was given as 0.9 % (w/v) saline by intraperitoneal injection (**66 ml/kg/24h**) (approx. **5 ml** every 3 h for a **600 g** guinea pig).

Sites for surgery and electrode contact were carefully shaved. All animals underwent tracheotomy to protect the airway from nasal secretions. A 2 cm midline incision was made above the sternal notch. The trachea was bluntly dissected free from overlying layers and sectioned transversely. A 2 mm diameter custom-made metal tracheotomy tube was inserted, tied tightly in place and the wound closed with cotton sutures. The trachea was cleared with fine tissue wicks at least hourly.

Pigmented Dutch rabbits weighing between 1.4 and 1.7 kg were anaesthetised by intravenous injection of 30 mg/kg Sagatal (pentobarbitone sodium; RMB Animal Health Ltd). They were intubated with the veterinary assistance of Mr Paul Townsend. Light anaesthesia was maintained by continuous intravenous infusion of a 1:10 dilution of Sagatal in physiological dextrose/saline, which also provided fluid replacement. Rectal temperature was maintained by use of a heat lamp.

#### **2.1.4. Bacterial preparation**

##### ***General considerations.***

*Streptococcus pneumoniae* is designated a class II pathogen by the Advisory Committee on Dangerous Pathogens. All work with *S. pneumoniae* was approved by the University Microbiological Safety Committee. All laboratories used met the required containment standard. Cultures for inoculation (max. 1 ml) and inoculated plates for viable counting were transported between locations in sealed metal containers in accordance with good microbiological practice. A full gown, mask and gloves were donned when inoculating animals or dissecting the cochleas free at the end of an experiment because of the risk of aerosol formation.

Sterile artificial perilymph (APL; see appendix A) was used as the final diluent for the inoculum in all cochlear perfusion experiments and all *E. coli* work. Pneumococcal cultures for meningitis work were washed and resuspended in filter-sterilised PBS. All bacterial cultures (broth and agar) were incubated at 37°C without shaking and with no added CO<sub>2</sub>.

Macconkey agar plates for *E. coli* growth were made in the Department of Biological Sciences. Five percent horse blood agar plates for pneumococcal isolation were purchased from the Department of Medical Microbiology, Queen Elizabeth Hospital, Birmingham. Viable counting was performed by a modification of the drop count method of Miles and Misra (1938). Serial ten-fold dilutions of the inoculum or CSF or blood were made (10 µl into 90 µl of sterile APL or 0.9% saline) and 20 µl dropped onto a quadrant of the relevant agar plate. Three quadrants were inoculated per dilution and the plates incubated for at least 18 h at 37°C.

The viable count was calculated thus:

$$\text{Viable count (log., cfu/ml)} = \log., ([\text{mean quadrant count}] \times 50 \times \text{dilution})$$

### ***Escherichia coli***

Stock cultures of *E. coli* K-12 were stored in 50% glycerol at  $-70^{\circ}\text{C}$ . For each experiment a fresh mid-logarithmic phase (3 h) culture was prepared as follows. A loopful of stock *E. coli* K-12 was plated out onto Macconkey agar and incubated overnight. Two to three colonies were scraped into 10 ml of brain-heart infusion broth (BHI) (Oxoid, Basingstoke, England) and cultured overnight. Fresh BHI (10 ml) was inoculated with 100  $\mu\text{l}$  of the overnight culture and incubated for 3 h. An aliquot of the log-phase culture was diluted 1:9 in formal:saline and bacteria were counted in a Thoma chamber. Organisms were harvested by centrifugation (4000 rpm  $\approx$  2600 g, 10 min,  $20^{\circ}\text{C}$ ) in a Mistral 2000 centrifuge. The pellet was resuspended in sterile APL to a final concentration of  $5 \times 10^9$  organisms/ml for meningitis experiments or  $5 \times 10^8$  organisms/ml for cochlear perfusion. In the first three experiments viable counts were performed by serial ten-fold dilution and overnight incubation on Macconkey agar plates.

### ***Streptococcus pneumoniae D39 and derivatives.***

*S. pneumoniae* serotype 2 strain D39 (NCTC 7466), and its derivatives PLN-A,  $\Delta\text{NA1}$  and  $\Delta\text{HY1}$ , were a generous gift from Dr Tim Mitchell, Dept of Microbiology and Immunology, University of Leicester, UK. This strain is encapsulated and fully virulent in a mouse model of pneumococcal bacteremia (Berry *et al* 1989). The method of preparing the pneumococcal inoculum was modified from that of Alwmark *et al* (1981) which allows preparation of a standardised inoculum.

Outbred MF1 mice were inoculated by intraperitoneal injection of  $10^5$  CFU of stock D39 (or its derivative) in 0.2 ml PBS (Gibco) and bled by cardiac puncture 24 h later. Blood was grown overnight on Columbia agar. Four to five colonies of the mouse-passaged pneumococci were transferred into 10 ml BHI and cultivated overnight. Erythromycin (5  $\mu\text{g/ml}$ ) was added to all subsequent liquid media when preparing PLN-A,  $\Delta\text{NA1}$  or  $\Delta\text{HY1}$  to maintain selection pressure. Bacteria were harvested by centrifugation (4000 rpm  $\approx$  2600 g, 15 min,  $20^{\circ}\text{C}$ ) in an IEC Centra 4R centrifuge and resuspended in fresh BHI to remove any autolysin present after overnight culture. Serum broth was prepared by adding as cryoprotectant 17 % (v/v) heat-inactivated fetal calf serum (Gibco) to BHI, and was filter-sterilized (0.2  $\mu\text{m}$ , Whatman). Fresh serum broth (10 ml) was inoculated with 400  $\mu\text{l}$  of pellet suspension (final  $\text{OD}_{500}=0.7$ ) and incubated for 5 h. Aliquots of 1 ml were rapidly frozen and stored at  $-70^{\circ}\text{C}$ . Viable counts were performed in triplicate on one of the aliquots 24 h later.

Table 2.2 (page 59) lists the batches of *S. pneumoniae* which were used in the study. Batches were given consecutive letters irrespective of the intended phenotype. Batches *A* and *F* through *N* were prepared as above in Leicester. Batches *B* through *E* were subcultured in Birmingham. Batch *B* was prepared from an agar plate growth of batch *A*. Batch *C* was prepared from an agar plate growth of pneumococci recovered from the CSF from experiment D39 (8). Batch *D* was prepared from an agar plate growth of Batch *C*. Batch *E* was prepared from an agar plate growth of PLN-A obtained from Leicester. It only later became clear that for reliable in vivo growth, organisms needed to be animal passaged before the final overnight culture (see section 3.2.1).

***Derivatives of S.pneumoniae D39 deficient in accessory virulence factors: PLN-A, ANA1 & ΔHY1.***

Three isogenic mutants of D39 were used in this study and full details of their construction are given in appendix B. This work was approved under the Genetically Modified Organisms (Contained Use) Regulations 1992 as ACGM Containment level II.

Name:	Deficient in	Erythromycin resistance	Assay
<b>PLN-A</b>	pneumolysin	<b>R</b>	Haemolytic
<b>ΔNA1</b>	neuraminidase	<b>R</b>	MUAN cleavage fluorescence
<b>ΔHY1</b>	hyaluronidase	<b>R</b>	Albumin cleavage

**Table 2.1:** Derivatives of *S. pneumoniae* D39 used.

Wild type D39 has full haemolytic, neuraminidase and hyaluronidase activity and is fully sensitive to erythromycin (ERY). All the derivatives are fully resistant to ERY and can be tested for lack of the gene product by a specific assay (details in appendix C). Routinely the sensitivity of both the inoculum and recovered organisms from CSF and blood was tested by streaking out a 1:100 dilution onto blood agar, adding a 5 µg ERY disk (Oxoid, Basingstoke, UK) and incubating overnight. There were problems throughout the study with the purity of PLN-A and ΔNA1 cultures, hence batches *E*, *G*, *H* and *K* were found to be partially or fully sensitive to erythromycin. When this occurred, further phenotypic assays were performed in Leicester by Dr Mitchell's staff. These problems were finally traced to a clerical problem with the archive strains in Leicester and further batches *J* and *L* proved satisfactory. Recovered organisms from guinea pigs infected with PLN-A (Batch *J*) and ANA1 (Batch *L*) were also assayed for the gene product to ensure the mutation was still

present. The titre of  $\Delta$ HY1 batch *M* dropped rapidly on storage due to a problem with the fetal calf serum. The final inoculum obtained with batch *N* of this derivative was also slightly less than desired.

#### ***Preparation of final inoculum***

Prior to inoculation an aliquot was allowed to thaw completely at 20°C, centrifuged in a bench top microfuge (12,000 g, 1 min, 20°C), washed with ice-cold sterile **APL** (or PBS for the later meningitis experiments), recentrifuged and then resuspended in fresh ice-cold **APL** (or PBS) to an estimated concentration of  $3 \times 10^8$  CFU/ml for the meningitis experiments and  $5 \times 10^8$  CFU/ml for cochlear perfusion. The inoculum was held on ice until required (usually less than 1 h). Viable counts were not reduced after holding the inoculum on ice for up to 3 h. Dilutions of the inoculum for viable counting were plated shortly after inoculation in all experiments.

#### **2.1.5 Pneumococcal cell wall preparation.**

Highly purified intact pneumococcal cell wall material (PCW) containing teichoic acid was a kind gift of Professor Alexander Tomasz, Rockefeller Institute, New York. Full details of the preparation of PCW from strain **R36A** are given in Tuomanen *et al* (1985). This strain is the non-encapsulated derivative of type D39 used elsewhere in this study. PCW (100-200  $\mu$ g) reliably induces CSF inflammation in rabbits (Tuomanen *et al* 1985) and rats (Pfister *et al* 1992a; Pfister *et al* 1992b, personal communication Prof A Tomasz). For experiment PCW (1), PCW (1 mg) was suspended in sterile **APL** (1 ml) and sonicated for 2 min in a water bath sonicator before use. For subsequent experiments, this suspension was re-sonicated in a cup-horn sonicator (20 s) and dialysed overnight against 1000 volumes of **APL** at 4°C before storing in aliquots at -20°C.

Batch	Intended genotype	Actual phenotype <sup>(1)</sup>	Passaged <sup>(2)</sup>	Experiments
<b>A</b>	D39	w/t	mouse	D39 (1) – D39 (8) D39 Perf 1 – Perf 9
<b>B</b>	D39	w/t	subcultured Batch A	D39 Perf 10 – Perf 19
<b>C</b>	D39	w/t	subcultured CSF of D39(8)	D39 (10) & D39 (11)
<b>D</b>	D39	w/t	subcultured Batch C	D39 (12) & D39 (13)
<b>E</b>	PLN-A	prob w/t (not assayed)	(subcultured in non-selective media)	PLN-A (1)
<b>F</b>	D39	w/t	mouse	D39 (14) – D39 (19) RAB 36 – 38
<b>G</b>	PLN-A	PLY(+)	mouse	PLN-A (2) (included as w/t)
<b>H</b>	PLN-A	mixed (not assayed)	mouse	PLN-A (3) & PLN-A (4) PLN-A Perf 3
<b>J</b>	PLN-A	PLY (-)	mouse	PLN-A (5) – PLN-A (15) RAB 39-41
<b>K</b>	$\Delta$ NA1	w/t (NA+)	mouse	NA+ (1) & NA+ (2) (included as w/t)
<b>L</b>	$\Delta$ NA1	NA (-) HY(+) PLY(+)	mouse	NA( 1) – NA (6)
<b>M</b>	$\Delta$ HY1	HY (-) (low titre)	mouse	HY1 (1) & HY1 (2)
<b>N</b>	$\Delta$ HY1	HY (-) NA(+) PLY(+)	mouse	HY1 (3) – HY1 (8)

w/t = wild type; PLY = pneumolysin; NA = neuraminidase ; HY = hyaluronidase; PLN-A = PLY deficient mutant;  $\Delta$ NA1 = NA deficient mutant ;  $\Delta$ HY1 = HY deficient mutant.

(1) See appendix C for details of phenotype testing.

(2) Some batches were prepared in Birmingham by subculture. Mouse passage (cardiac puncture 24 h after intraperitoneal injection) preceded the final broth culture.

**Table 2.2:** Batches of *S. pneumoniae* used.

## 2.2. Meningitis model

### 2.2.1. Experimental design.

The main purpose in establishing a new model of meningitis in the guinea pig was to examine the importance of accessory pneumococcal virulence factors in causing meningogenic deafness. A new method of measuring hearing loss was developed during the course of the investigation which allowed the final comparative studies to be performed.

Subsidiary aims were:

- (i) To investigate the difference between pneumococcal and *E. coli* meningitis in terms of ultrastructural changes in the organ of Corti and hearing loss.
- (ii) To examine the effect of cefotaxime-treatment on the morphology of *E. coli* in vivo.
- (iii) To investigate whether hearing loss would occur as a result of sterile inflammation induced by pneumococcal cell wall material.

The guinea pig meningitis work divided into two main parts: initial studies to perfect techniques and the final comparative study. For the initial studies with *E. coli* and *S. pneumoniae* D39, animals were killed at different times after inoculation. The final comparative study compared groups of guinea pigs infected with the different isogenic derivatives of *S. pneumoniae* with those infected by wild-type D39. Animals were killed at a predetermined time-point of 12 h after inoculation. This was chosen because in the initial experiments all animals infected with wild-type D39 had lost some hearing by this time. Animals that died earlier than 9 h were excluded from the hearing loss analysis. The tables of results given in chapter 3 include details of experimental numbering, duration and inoculum.

#### *Experimental numbering*

Guinea pig experiments were numbered serially (see table 2.3 overleaf). Some batches of the inocula of isogenic mutants were subsequently found to contain wild type phenotype organisms (*see* section 2.1.4 above). Therefore some experiments labelled as PLN-A or NA1 were included in the analysis as wild-type experiments. The work with *E. coli* was performed before the work with pneumococci because of delays in gaining safety approval for the latter.

<b>Intended inoculum</b>	<b>Experiment number</b>
<i>E. coli</i>	K-12(1) to K-12(24)
<i>S. pneumoniae</i> D39	D39(1) to D39(19)
<i>S. pneumoniae</i> PLN-A (pneumolysin-deficient)	PLN-A(1) to PLN-A(15)
<i>S. pneumoniae</i> ΔNA1 (neuraminidase deficient)	NA1(1) to NA1(6)
<i>S. pneumoniae</i> ΔHY1 (hyaluronidase-deficient)	HY1(1) to HY1(8)
Pneumococcal cell wall (from R36A)	PCW(1) to PCW(4)

**Table 2.3:** Numbering of guinea pig experiments

### *CSF sampling*

One of the major disadvantages of the guinea pig model compared to the traditional Dacey and Sande rabbit model is that because of the low volume of CSF it is difficult to sample CSF sequentially. With practice it became possible to place a cisternal cannula (23G Butterfly, Abbot) using a stereotactic guide but it was difficult to maintain the position for the full **12 h** without a CSF leak developing. Although **only** a small volume of CSF was required for analysis, a substantial dead space (some 100-200  $\mu$ l) needed to be flushed. Removing a substantial fraction of the free CSF at regular intervals might well have altered the course of the inflammatory response, so an indwelling cisternal cannula was inserted in only a few experiments. Another way of establishing in vivo growth curves and the time course of the CSF inflammatory response would have been to kill several guinea pigs at each of several time points. It was considered inappropriate to do this as some of this information was already published for the rabbit (Friedland *et al* 1995) and these data remained secondary endpoints. However, a terminal CSF sample was obtained in most animals and (for the comparative study) quantitative culture, white cell count and protein concentration were compared between the groups.

### *E. coli meningitis (table 3.1).*

One animal each was killed at 3 h, **4.5h**, 6 h, 7 h, 9 h, and 12 h post inoculation (p.i). Additional animals were killed at 3 h and 7 h. One animal inoculated with sterile APL was killed at 7 h. Five animals died within **4 h** of inoculation; CSF measurements from these animals are included in the results but because of delayed fixation the cochleas were poorly preserved.

***Cefotaxime-treated E. coli meningitis (table 3.2).***

Cefotaxime was chosen because it is commonly used as blind monotherapy for acute childhood bacterial meningitis. In experimental rabbit meningitis cefotaxime (amongst other antibiotics) induces a transient rise in CSF free endotoxin concentration (Tauber *et al* 1993). The usual paediatric dose is 200 mg/kg/day in two divided doses. Doses of 100 mg/kg body weight and 10 mg/kg body weight were used in this work. Cefotaxime (Claforan, Roussel, UK) was purchased from the Pharmacy, Queen Elizabeth Hospital, Birmingham and once opened the vial was stored sealed under desiccation at -20°C. Cefotaxime was diluted in 5 ml 0.9% w/v saline and administered by intraperitoneal injection 3 h **after** inoculation to allow infection to become established and organisms to reach the scala tympani. The half life of cefotaxime is some three times shorter in the guinea pig compared to man (Personal communication, Dr J Edwards, Zeneca Pharmaceuticals, Macclesfield, UK) so for experiments which lasted more than 6 h, cefotaxime was also administered 6 h and 9 h post inoculation. The morphological appearance of cefotaxime-treated *E. coli* in vivo was investigated by examining the surface of the basilar membrane facing scala tympani with high-resolution scanning electron microscopy. Other endpoints were the CSF parameters (viable count, leukocyte count, protein) and hearing loss assessed by click-evoked response testing as above.

1) *Cefotaxime 100 mg/kg body weight*: Two animals were killed at 1 h, 2 h, and 3 h post antibiotic (4 h, 5 h and 6 h p.i.) and one each at 4 h, 5 h and 6 h post-antibiotic.

2) *Cefotaxime 10 mg/kg body weight*. One animal each was killed 1 h and 3 h post antibiotic.

***Initial study of untreated pneumococcal meningitis (tables 3.4 & 3.5).***

Three animals were used for dose-finding. Subsequently, one animal each was killed at 4.5 h, 6 h and 12 h p.i. and two each at 9 h and 10 h p.i. One control animal was inoculated with sterile PBS and was killed at 10 h p.i.

***Comparative study between 039 and derivatives (tables 3.6 – 3.9).***

**039:** Eight animals were inoculated with wild-type D39; 7 were sacrificed 12 h later and 1 died early.

**PLN-A:** Fourteen animals were inoculated with PLN-A. Five were sacrificed 12 h after inoculation and evaluated for hearing loss. In 2 animals the inoculum leaked back and failed to induce meningitis. A further 7 animals were not evaluated either because the phenotype of the inoculum was in question (see section 2.1.4) or because they died prior to 12 h.

***ΔNA1***: Six animals were inoculated with **ΔNA1** of which **5** were evaluated for hearing loss. Four were sacrificed after 12 h; a fifth was sacrificed at 7 h p.i. after losing all detectable hearing and another animal died 9 h p.i.

***ΔHY1***: Eight animals were inoculated with **ΔHY1** of which **5** were evaluated. Two received a low inoculum and a third died 7 h p.i.

### ***Pneumococcal cell wall material (table 3.10)***

Meningitis was induced by introducing 0.1 ml (100 µg) of the PCW suspension into the subarachnoid space through a drill hole (as above) or (for expt PCW(2)) via an indwelling cisternal cannula (Butterfly-23). All animals had an indwelling cisternal cannula inserted and CSF samples (approx. 30 µl) were withdrawn at intervals of 3 h for the duration of the experiment.

### **2.2.2. Consideration of inoculum and antibiotic doses**

Guinea pigs are known to be susceptible to at least some strains of *S. pneumoniae* when inoculated intracisternally (Edwards and Nairn, 1992). Three inocula were tested: (5.0, 7.5 and 9.0 log<sub>10</sub> CFU) and 7.5 log<sub>10</sub> CFU was chosen for subsequent experiments (see results section 3.2.2). It was found that 0.1 ml was sufficient diluent to allow reliable injection so the final concentration of the inoculum was adjusted to **8.5 log<sub>10</sub> CFU/ml** PBS.

*E. coli* K-12 is a disabled laboratory strain which has poor serum survival and produces no known cytolytic toxins. As will be seen in section 3.1.2 it also survives poorly in the CSF space of guinea pigs. Previous work in the laboratory with a rabbit model of meningitis suggested that a high inoculum (9.0 log<sub>10</sub> CFU) would be necessary to generate a significant inflammatory response. Work by Levy *et al* (1978) showed that *E. coli* K-12 was approximately 1000-fold less virulent for mouse bacteremia than a virulent *E. coli* strain. Therefore an inoculum of 9.0 log<sub>10</sub> CFU total in 0.2 ml APL was used.

### **2.2.3. Induction of meningitis**

#### ***Subarachnoid inoculation***

The anaesthetised, tracheotomized guinea pig was transferred to an electrically-screened and sound-proofed laboratory where all experiments were performed. Subarachnoid inoculation was favoured over intracisternal inoculation because the arachnoid membrane covering the cisterna tended to leak CSF once punctured and this would reduce the chance of organisms penetrating the inner ear. A midline incision was made extending from the vertex of the skull to the occiput. The periosteum was scraped clean with a scalpel and a

burr hole 1 mm in diameter was drilled in the outer table of the left parietal skull bone with a hand-held dental drill. The inner skull table was carefully pierced with a 25 G needle. A slight give could be felt as the subarachnoid space was entered. The inoculum (0.2 ml for *E. coli*, total inoculum  $1 \times 10^9$  organisms; modified to 0.1 ml for *S. pneumoniae*, total inoculum  $3 \times 10^7$  CFU) was gently instilled over 1 min. The needle was left *in situ* for 5 minutes and the drill hole then plugged with a smear of silicone sealant (this was found to adhere easily). No attempt was made to withdraw CSF from the drill hole and the injection was never forcible.

The contiguity of this route of injection with the intracisternal route was verified on two guinea pigs after death by injecting methylene blue dye via the parietal skull drill hole. This flowed immediately through the punctured arachnoid membrane overlying the *cisterna magna*.

#### ***Analysis of CSF and blood***

At the end of the experiment blood (1 ml) was taken by intracardiac puncture and serial dilutions prepared for viable counting. The *cisterna magna* was exposed by extending the midline scalp incision and dividing the recti from the occipital ridge. A 23G butterfly (Butterfly-23; Abbot Venisystems, Kent, UK) was used to pierce the arachnoid covering and up to 150  $\mu$ l CSF withdrawn gently. The brain stem was then destroyed. CSF leukocytes were counted in an improved Neubauer chamber after suitable dilution and nuclear staining with a counting fluid (acidic crystal violet; see appendix A) (10  $\mu$ l CSF in 10  $\mu$ l or 90  $\mu$ l counting fluid). Another 10  $\mu$ l aliquot of CSF was used to determine the viable bacterial count as above. The remainder of the CSF was centrifuged (13,000 g, 5 min, 20°C) in a bench-top microfuge and the supernatant stored at -20°C or -70°C for up to four months prior to protein assay. Protein concentration was measured with a standard BioRad microassay (BioRad, Munich, FRG), a colorimetric dye-binding assay (Bradford, 1976). The assay was run on four occasions. CSF (5  $\mu$ l) was diluted in PBS (795  $\mu$ l) (Gibco 042-04200), and BioRad Dye reagent (Cat no. 500-0006) (200  $\mu$ l) added. The optical density at 595 nm was read after 10 min incubation. A standard curve was constructed with bovine serum albumin (BioRad) (1 g/l to 10 g/l). A regression line was fitted using the LINEST function in Excel and used to calculate the approximate protein concentration of the CSF samples.

#### ***Brain histology.***

In some experiments brains were removed, rinsed in 0.9 % w/v saline in 0.2 M phosphate buffer, fixed by immersion in 10% (v/v) formalin in 0.2 M phosphate buffer (see appendix A) and routinely processed through to paraffin wax. Sagittal sections (5  $\mu$ m) were cut,

mounted on glass slides, stained with haematoxylin and eosin, and examined with a Zeiss photomicroscope.

### ***Fixation of cochleas.***

Immediately after death both temporal bones were removed and the cochleas fixed as described on page 72.

### **2.2.4. Hearing loss assessment**

The methods for assessment of hearing loss changed substantially between groups of experiments. In *E. coli* experiments, hearing loss was determined by click-evoked auditory brain stem response testing. In the initial pneumococcal experiments, tone-pip evoked brain stem response testing was used to give an estimate of hearing loss at both high and low frequencies. In the final technique the transducer was closely coupled to the meatus via hollow ear bars and the auditory nerve compound action potential (CAP) induced by a tone-pip was recorded from the round window membrane. The reasons for this evolution are laid out fully in section 3.2.3. A strict comparison of hearing loss between experimental pneumococcal and *E. coli* meningitis was not therefore possible.

#### ***Click-evoked auditory brain-stem responses***

Auditory click-evoked brain stem responses were recorded using commercial clinical apparatus (The Screener, Medelec, Surrey, UK) originally designed for use with neonates. This is calibrated in terms of normal human threshold (**nHL**) and prints a paper strip bearing the evoked response tracing. The ear piece (Medelec) was coupled loosely to the external auditory canal with a neonatal eartip. The reference electrode (a gold-plated Crocodile clip) was attached to the vertex and a good electrical contact ensured by using conducting jelly. Another gold-plated crocodile clip attached behind the stimulated ear served as the ground electrode. Clicks of 100  $\mu$ s duration were presented at 10 **Hz**. Far-field Potentials were bandpass filtered (150 **Hz**-2 **kHz**). The sweep time was 12 ms and 1024 presentations were averaged. No attempt was made to mask the unstimulated ear. Because of the time taken for data acquisition and printing it was impractical to find the visual detection threshold and still be able to measure hearing every hour. Therefore a set of control readings were obtained for each ear at 60, 40, 20 and 0 dB above normal human threshold (**nHL**). Every hour thereafter the response to a 40 dB **nHL** stimulus was recorded in both ears. Later, all printouts were analysed without reference to the experimental conditions and compared with their respective controls. Hearing loss, expressed as dB, was defined as the difference between the applied stimulus and the stimulus which had produced the control trace most closely matching the experimental tracing. Selected printouts were scanned into an Apple

Mac Quadra 800 and digitised with "DataThief" software before illustrations were prepared with Deltagraph software (see fig 3.3). The designation of waves I to V was derived from Jewett and Williamson (1971) and Buser and Imbert (1992).

***Tone specific recording with a MacLab and PowerMac: general description of equipment.***

The equipment for recording tone-pip induced responses is shown in fig 2.1 and described below; the MacLab settings for recording evoked brain stem responses or round window compound action Potentials are given later. Sine-wave pure tones generated by a Farnell LFM-4 oscillator were gated by a home-made ramp-gate modulator. The onset of the pulse was phase-locked to 0° with a rise and fall time of <0.1 ms. Pulses were attenuated with a variable attenuator (Hatfield Model 2109, amplified by a home-built low noise audio driver (Maplin LM505), and delivered to the ear by a Motorola piezo-electric ceramic transducer. Recorded Potentials were amplified by a FET headstage (NL100, Neurolog, UK) and an AC preamplifier (NL104, Neurolog) and filtered (NL115, Neurolog). Electronic data acquisition was performed with a MacLab 2e (AD Instruments, Australia) connected to a PowerMac 6100/60 (Apple, UK). A sweep was triggered by the outgoing pulse. Incoming amplified Potentials were recorded via the second input and stored for on-line averaging. The maximum time base with this equipment was 40 kHz over a 5 ms window. A standard oscilloscope (Telequipment D63, UK) monitored the outgoing pulse and incoming signal.

***Brain stem evoked responses.***

The guinea pig was anaesthetised, inoculated as above, and laid on the heating pad. The transducer was held in an adjustable clamp and coupled to the outer ear canal via 4 cm of plastic tubing and a neonatal eartip. The tip rested at the entrance to the external ear canal. Tone pips (10 kHz or 1 kHz; 1 ms) were delivered at 10 **Hz**. Gold plated crocodile clips were positioned as for click-evoked response testing. To reduce stimulus artefact from the transducer, the transducer was screened with foil and a grounded wire mesh screen placed beneath the animal. Satisfactory signals were then obtained in single-ended mode rather than with common-mode rejection, with the active electrode at the vertex. Far-field Potentials were amplified 20,000 times, bandpass filtered (100 Hz–10 kHz) and notch filtered at 50 **Hz**. The output was AC coupled to the MacLab with sensitivity set to 20 mV and 512 sweeps of 10 ms were averaged. The resulting data were smoothed by the software (this has the effect of a low pass filter of approximately 5 *MIZ* at the time base used). If a poor signal was obtained 1024 or 2048 sweeps were averaged but this rarely improved the resulting waveform; careful attention to electrical connections and screening was always more rewarding.

This equipment was not formally calibrated in terms of sound pressure level so only relative changes in stimulus intensity were recorded.

***Recording the compound action potential from the round window.***

The guinea pig was anaesthetised and tracheotomized and the neck and skull shaved. A midline incision was made from the vertex to the occiput. Two **2** cm transverse skin incisions were made parallel to the occipital ridge. The temporalis and occipital muscles were reflected and the outer cartilaginous meati cut close to the skull with careful attention to haemostasis. The occipital ridge and the posterior ridges of both bullae were cleared of muscle attachments. The animal was transferred to a stereotactic frame (Bonetti) and secured with two custom-machined hollow brass ear bars which were inserted into the meati. These also served to earth the animal. Each bulla was opened with bone forceps at the posterior ridge at the level of the meatus and enough bone removed with dissecting forceps to gain a view of the round window. The defect measured approximately **5 mm x 5** mm. Great care was taken to avoid damaging the tympanic membrane. With the dissecting microscope illuminating the bulla the tympanic membrane appeared transilluminated with white light. The presence of this white light reflex was checked before each recording to ensure fluid or blood had not accumulate on or behind the tympanic membrane.

Silver electrodes (**8** thou (**203  $\mu$ m**) in diameter) were coated with epoxyite insulating resin (EPR-4, Clark Electromedical, UK), soldered to stainless steel wire and mounted in a perspex holder. The electrode assembly was secured in a Bonetti micromanipulator and connected to the FET headstage in single-ended mode as above. The ground connection was made via the ear bars. Before each recording the round window membrane and middle ear cavity were carefully mopped dry with fine tissue wicks and the transducer was securely coupled to the ear bar with a **2** cm length of plastic tubing. Tone pips of 1 ms duration at 1 kHz intervals between **3** kHz and 10 kHz were delivered at a rate of **10 Hz**. The silver electrode was advanced so that the tip of the wire rested on the round window membrane. Potentials were amplified (x 20,000), bandpass filtered (**100 Hz–6** kHz) and notch-filtered at **50 Hz**. The output was **AC** coupled to the MacLab (set to a sensitivity of **2 V**) and **16** sweeps of **5** ms duration were averaged. The intensity of the stimulus was adjusted with the attenuator to give a mean peak to peak potential of the **N<sub>1</sub>–P<sub>1</sub>** wave of **2 V**, equivalent to **100  $\mu$ V** at the electrode (see fig 1.1). The choice of criterion level is fully discussed in section **3.2.3**.

***Cochlear microphonic.***

The cochlear microphonic could also be recorded from the round window electrode. Tone pips (**3** kHz, 100 ms) were delivered at **2 Hz**. The stimulus intensity was increased in 10 dB

steps from 82 dB SPL to 112 dB SPL. The **CM** was recorded as the mean peak-to-peak height of **4** sweeps in a **5** ms sweep triggered **5** ms post-stimulus. The maximum peak-to-peak **CM** amplitude was used for analysis.

### ***Calibration.***

The transducer/ ear bar assembly was calibrated with a Bruel and Kjaer amplifier (2606) coupled with plastic tubing to a microphone (**B+K 4134**) at the position of the tympanic membrane. At 0 dB attenuation and a stimulus of **4 V** peak-to-peak, a **3 kHz** tone yielded 112 dB SPL re 20  $\mu$ Pa and a **10 kHz** tone yielded 102 dB SPL re 20  $\mu$ Pa.

### **2.2.5. Rabbit meningitis.**

The rabbit experiments were performed in conjunction with Dr **MP** Osborne and Dr **SD Comis** to investigate whether the differences in hearing loss and ultrastructural damage observed between meningitis due to **D39** and that due to PLN-A would be maintained in a different species. Animals were inoculated via a hole drilled in the skull exactly as for the guinea pig. Three rabbits were inoculated with wild type **D39** (**RAB 36–RAB 38**) and three rabbits were inoculated with pneumolysin-deficient *S. pneumoniae* (**RAB 39–RAB 41**) (PLN–A). Hearing was assessed by recording click-evoked brain stem auditory responses with the Medelec Screener. Rabbits were killed between 10 and 11 h after inoculation. A terminal **CSF** sample was taken when possible and the cochleae fixed exactly as for the guinea pig, albeit after a more difficult dissection. Blood samples were not taken. Results are shown in section **3.9** and table **3.17**.

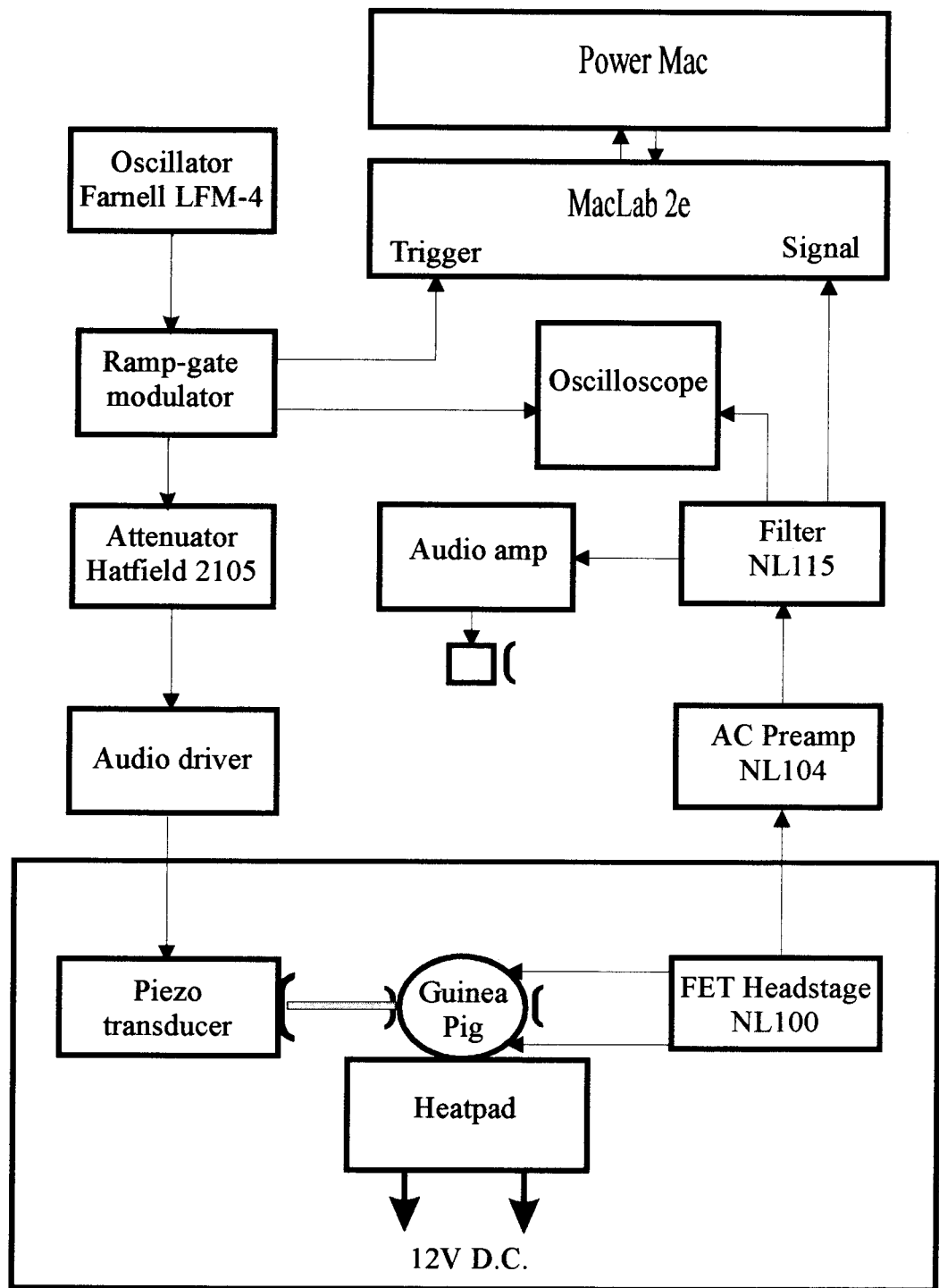


**Figure 2.1:** Tone-evoked response recording: equipment diagram  
 The same basic setup was used for recording far-field potentials from surface electrodes or the CAP from an electrode positioned on the round window membrane.

## 2.3. Cochlear perfusion

### 2.3.1. Experimental design

In this series of experiments the effect of microperfusion of live bacterial suspensions through the scala tympani was investigated. The aims were:

- i) to investigate whether suspensions of live bacteria were directly ototoxic and if so over what time course;
- ii) to investigate whether pretreatment of the animal with bacteriolytic antibiotics would exacerbate any ototoxicity by releasing cell wall material and intracellular toxin (the so-called antibiotic-induced inflammatory burst).

Groups of guinea pigs were compared as follows:

---

<i>E. coli</i> K-12	(untreated)	(n=4)
<i>S. pneumoniae</i> D39	(untreated)	(n=4)
<i>S. pneumoniae</i> D39	(cefotaxime-treated)	(n=4)
<i>S. pneumoniae</i> D39	(amoxycillin-treated)	(n=4)

---

### 2.3.2. Preparation of the animal

The inferolateral approach to the cochlea has been fully described by **Comis** and Leng (1979). Guinea-pigs were anaesthetised and tracheotomized as described above. The area over the left mandible and the whole of the neck was shaved. **An** incision was made along the inferior margin of the left mandible extending to the angle of the jaw, dividing the left masseter to reach the mandible. All the muscles attached to the left mandible were cleared and the mandible removed. The left bulla was exposed by blunt dissection beneath the styloid and digastric muscles. The meati were exposed and sectioned as described above (round window recording, page 67). The arachnoid membrane covering the *cisterna magna* was exposed and slit with a sterile 19 G needle to reduce CSF fluid flow through the opened cochlea (see discussion). The animal was mounted left side uppermost in a stereotactic frame and held by hollow brass ear bars inserted into the meati. The styloid process was removed and the bulla cautiously opened at its lower margin with artery forceps. A window was cut in the bulla sufficient to expose the cochlea. A hole 50  $\mu\text{m}$  in diameter was drilled in the basal turn of the cochlea 2 mm from the round window and a hole about 100  $\mu\text{m}$  in diameter was drilled at the apex to allow the perfusate to escape. A

machine-pulled tapered glass recording pipette containing a platinum wire electrode was filled with **APL** with the aid of a Treonic microinfusion pump (**IP-3**), and mounted in a Bonetti micromanipulator. The inoculum was drawn into a 1 **ml** syringe which was mounted in a home made micrometer device and attached to a second micropipette by a short length of plastic tubing. The bacterial suspension (10  $\mu\text{l}$ ) was perfused into the scala tympani over 1 min. For *E. coli* experiments the concentration of the inoculum was  $5 \times 10^8$  organisms/ml (amount delivered =  $5 \times 10^6$  organisms); for *S. pneumoniae* experiments the concentration was  $5 \times 10^8$  CFU/ml (amount delivered =  $5 \times 10^6$  CFU). Immediately after perfusion, the micropipette was removed and the recording pipette was inserted in the basal hole. Because of the taper a good seal was usually obtained and little perilymph escaped. Recordings were normally first obtained within 5 min of perfusion. The best recording achieved in the first 20 min after perfusion was taken as the baseline. Measurements were then made every 20 min for the first hour, and every 30 min for the remaining 2 h. The experimental (left) cochlea was then fixed in vivo as described below (page 72).

### 2.3.3. Recording techniques

The equipment for delivering the tone pips was identical to that described above. The transducer was coupled to the ear bar with a 5 cm length of rubber tubing. The CAP was elicited with a 10 **KHz**, 1 ms tone pip delivered at 1 **Hz**. Potentials at the pipette tip were amplified by an identical system. The peak to peak height of the  $N_1$ - $P_1$  wave of the CAP was measured on an oscilloscope (Teleequipment **D63**, UK) or by computer averaging as described above and a value of 2 **V** taken as the reference (equivalent to 100  $\mu\text{V}$  at the pipette tip); this is approximately 14 dB above the visual detection threshold (Comis *et al* 1993). Before each reading the bulla was carefully mopped dry. The CAP loss (and for brevity in description, hearing loss) was defined as the dB increase in the intensity of the stimulus needed to restore the  $N_1$ - $P_1$  height to the reference value.

The CM was elicited with a 5 kHz, 500 ms tone pulse. Data were stored on a Gould digital storage oscilloscope (Model 1602) and four tracings averaged. Stimulus response curves were plotted in 10 dB steps and the maximum peak-to-peak CM amplitude was used for subsequent analysis. The shape of the stimulus-response curve was altered if there was a conductive deafness (e.g. bleeding onto the tympanic membrane) and such guinea pigs were not included in the electrophysiological analysis.

The equipment was calibrated as described above (page 68). A 5 kHz tone yielded 129 dB SPL re 20  $\mu\text{Pa}$ ; a 10 kHz tone 110 dB SPL re 20  $\mu\text{Pa}$ .

## **2.4 Electron microscopy and photo-micrography**

### **2.4.1. Fixation**

A 1 ml syringe was filled with ice-cold fixative (buffered 2.5% glutaraldehyde; see appendix A), mounted in a home-made micrometer device, and connected to a glass micropipette via Polyethylene tubing. In cochlear perfusion experiments, the left cochlea was intravitaly fixed by perfusing 100 µl fixative via the drill hole in the basal turn. The brain stem was then destroyed. Both temporal bones were removed shortly after death and the bullae opened carefully with bone forceps. The apex of the right otic capsule was sectioned with a scalpel, and the scala tympani of the right cochlea was perfused via the round window with 100 µl fixative. Both temporal bones were then immersed in fixative. In meningitis experiments both cochleas were fixed in this way immediately after death.

### **2.4.2. Scanning electron microscopy.**

Specimens were fixed in glutaraldehyde for at least one week. Some specimens were prepared for scanning electron microscopy (SEM) after post-fixation with 1% osmium tetroxide (see appendix A) for 15 min. The modiolus was dissected out and trimmed above the second turn. Batches of eight to ten cochleas were dehydrated in graded acetone dilutions (1 h each in **50%**, 70%, **80%**, 90%, **95%**, 100%, 100% (v/v) in dH<sub>2</sub>O). Great care was taken to avoid premature drying. The modioli were critical point dried in liquid CO<sub>2</sub> (Emscope CPD750 or Polaron E3000). Specimens were attached with Araldite (apex upright) onto copper SEM holders, sputter coated with platinum (Emscope SC500) and examined in a JEOL 120CXII TEM fitted with a TEMSCAN scanning attachment. Images were obtained with a secondary electron detector and accelerating voltage of 40 kV. Photomicrographs were taken onto Kodak Pan-X roll film. To examine the under surface of the basilar membrane (bordering scala tympani), specimens were carefully prised off the SEM holder, inverted, and remounted so that the basal surface of the first cochlear turn was upright. The specimen was then recoated with platinum.

### **2.4.3. Transmission electron microscopy.**

For transmission electron microscopy (TEM) the modiolus was fixed in 2.5% (vh) glutaraldehyde (see appendix A) overnight then post fixed in 0.1% osmium tetroxide (see appendix A) for 15 min. A wedge of the organ of Corti was cut from the basal turn. This was dehydrated in graded ethanol dilutions (15 min each in (v/v) **70%**, 90%, 100%, 100%, 100% dried) and transferred to propylene oxide (15 min **x 2**). The specimen

was immersed in a 1:1 solution of Epon-substitute resin (see appendix A) and propylene oxide for 1 h then vacuum embedded in resin overnight at 80°C. Semi-thin sections were cut at 1 µm, dried onto glass slides, stained with 1% toluidine blue and examined with phase contrast in a Zeiss photomicroscope. All bone was trimmed away. Ultrathin sections were cut at 90 nm with a diamond knife, mounted on Formvar-coated grids and stained with uranyl acetate and lead citrate in an Ultrastainer. They were examined with an accelerating voltage of 80 kV in a JEOL 120CXII TEM and photomicrographs taken onto cut film. The rest of the modiolus was usually prepared for scanning electron microscopy although as osmication alters the appearance of the stereocilia the results obtained were not as good as processing the whole modiolus for SEM. (Osborne *et al* 1984).

#### 2.4.4. Image processing

Photomicrographs were processed with standard photographic techniques. Illustrations for publication were prepared on a Macintosh Quadra 800. Black and white enlargements (6 x 4 in) were scanned into Aldus Photoshop using a flat-bed Mirror 600 scanner and enhanced as necessary to improve contrast. Scale bars and markers were added in Aldus Freehand and the final composite illustration output on a photographic quality dye sublimation printer.

## 2.5 Data analysis

For the final comparative study, data analysis was performed with Microsoft Excel v4.0 (means, confidence intervals) and Arcus Pro-Stat v3.01 (checks for normality, comparisons of means and medians, linear regression and analysis of covariance, correlation). Confidence interval analysis was preferred as this gives more information about the size of differences between groups and is less reliant on an arbitrary P value. In brief, the 95% confidence interval of the difference between the two sample means is the range of values in which it is **95%** certain the true difference between the populations should lie. Confidence interval formulae were derived from Gardner and Altman (1989) p 21:

$$95\% \text{ CI} = x - (t_{1-\alpha/2} \times \text{SE}) \quad \text{to} \quad x + (t_{1-\alpha/2} \times \text{SE})$$

where SE is the standard error of the mean and  $t_{1-\alpha/2}$  is the appropriate value from the  $t$  distribution with  $n - 1$  degrees of freedom associated with a confidence of 100(1- $\alpha$ )%. In an Excel worksheet this is rendered as the following formula:

$$=\text{TINV}(0.05,\text{COUNT}(\text{B3}:\text{K3})-1) * \text{STDEV}(\text{B3}:\text{K3})/\text{SQRT}(\text{COUNT}(\text{B3}:\text{K3}))$$

where B3:K3 contain the data and the result is the 95% CI for the mean of that data.

Data were tested for normality with the Shapiro-Wilk test. For comparison between groups, the null hypothesis was that there was no difference expected in any parameter measured. The major quantitative endpoint in the meningitis model was the difference between hearing loss (judged by CAF recording) induced by **D39** wild type and that induced by the isogenic mutants (PLN-A,  $\Delta$ NAI,  $\Delta$ HY1) at 10 kHz and 3 kHz. CAP losses all fitted a normal distribution. Independence between left and right ears within each group was confirmed with Spearman's rank correlation coefficient (**p**) so the data were pooled. Differences were compared by Student's t-test if the variances were similar or a Mann-Whitney test if variances were unequal. The minimum number of significance tests was performed and hearing loss was not compared between groups infected with the different mutants. Confidence limits at 95% significance (or as close as possible for the Mann-Whitney test) for the difference between the means were calculated using Arcus ProStat. Normal data for the audiograms were expressed as means with 95% confidence limits.

Quantitative bacterial counts and CSF white cell counts were log transformed and the geometric mean calculated. Significance was assessed by Student's t-test. Protein concentrations did not normalise with log transformation; the geometric mean is however given. Significance was assessed by the Mann-Whitney test.

Cochlear microphonic loss was non-normal and not log-transformable. The significance of a difference between the medians was compared with a Mann-Whitney test. The relationship between CM loss and CAP loss was assessed by calculating Spearman's rank correlation coefficient (**p**).

Non-normal data were obtained from auditory evoked response testing in the rabbit experiments (these results were discontinuous variables of 0, 20, 40, 60 or 80 dB loss). Medians were compared with the Mann-Whitney test and an approximate 95% confidence interval calculated.

In the cochlear perturbation study, the main endpoint was the difference in CAP loss at 10 kHz 3 h after perturbation between the 4 groups of guinea pigs (*E. coli*; *S. pneumoniae* with or without cefotaxime or amoxicillin pretreatment). Comparisons were with multiple t-tests. The rates of change of CAP loss over time during the period 60–180 min were tested for linearity and analysed by group linear regression and variance to determine whether the slopes were significantly different.

## 3. EXPERIMENTAL MENINGITIS.

### 3.1. *E. coli* K-12 meningitis.

#### 3.1.1. Overview

This section includes data obtained from the experiments where meningitis was induced by subarachnoid inoculation of *E. coli* K-12. Experiments were numbered sequentially as they were performed as K-12 (n). Some animals received cefotaxime (100 mg/kg or in two cases 10 mg/kg) i.p. 3 h after inoculation; for ease the two groups are sometimes referred to as “treated” and “untreated”. In the tables, data is given in order of duration of the experiment, Because these were the first meningitis experiments performed some techniques were not optimised, and several of them (particularly for electrophysiological recording) were improved for the pneumococcal meningitis studies. The CSF data were subsidiary endpoints, and no attempt has been made to group or analyse the data statistically.

These initial experiments were highly investigative with no particular defined endpoints. Animals were studied until they succumbed to meningitis, or hearing loss became profound. It must be emphasised that all animals remained deeply anaesthetised. Early deaths (before 4 h) were due to respiratory arrest and occurred in five of 12 untreated animals. In later work, the initial urethane bolus was given in two divided doses separated by 10 min and the tracheal cannula was kept meticulously clear of secretions. The use of a stereotactic apparatus to support the animal’s head in subsequent pneumococcal meningitis experiments also helped to reduce this early mortality. Late deaths (>4 h) occurred in two of five untreated animals and two of 10 treated animals. These deaths were assumed to be due to overwhelming infection as before death the respiration rate and heart rate became irregular and sometimes terminal convulsive movements were observed.

#### 3.1.2. Bacteriological preparation and CSF bacterial counts.

The inoculum of  $1 \times 10^9$  organisms was chosen because in the rabbit meningitis model this caused cochlear damage without killing the animal (Osborne *et al*, 1995). A fresh log-phase culture was prepared on the morning of each experiment (animals were normally used in pairs) and the bacterial concentration adjusted to  $5 \times 10^9/\text{ml}$  after counting organisms. Viable counting of serial dilutions of the inoculum on one occasion confirmed the count to be  $9.1 \log_{10}$  CFU/ml, some 0.6 log units below that intended. It was assumed this would make little difference to the course of meningitis. In this initial work viable counting of the inoculum was not routinely performed for each experiment. The surface of the brain beneath

the drill hole was inspected in several animals at the time of dissection, and on only one occasion was the drill seen to have penetrated the cortex. To prevent this in later experiments the drill was used to breach the outer skull table and the final penetration was performed with a 25G needle. To prevent organisms escaping the drill hole was sealed after inoculation. The best material for this proved to be a small plug of silicone sealant.

In most experiments a terminal CSF sample was obtained. Various venepuncture devices were tried but the optimal yield with minimal blood contamination was obtained by cisternal puncture with a 23G 'Butterfly' winged infusion device with the bevel inserted uppermost. Blood sampling for estimation of bacterial concentration was not performed for *E. coli* infection.

Bacteriological data for individual experiments are shown in table 3.1 and table 3.2 and displayed in fig 3.1 (page 83). Three points need emphasising.

- (i) Organisms were recovered from the cisternal CSF 2 h after subdural inoculation. This confirmed the contiguity of the subarachnoid and cisternal CSF spaces and means that organisms inoculated via a skull hole quickly established infection in the ventricular system. The volume of CSF in the guinea pig has not been documented to my knowledge; a working assumption of approx. 1 ml was used in this study. With an inoculum of ca. 9.0 log total CFU, a cisternal CSF concentration 2 h post-inoculation of 9.4-9.6 log CFU/ml is about that expected.
- (ii) The data constitute reasonable evidence that *E. coli* K-12 does not survive in the CSF space. Analysis is difficult because viable counts were not performed on the inoculum in each experiment, but the viable count trend seems to be downwards. This is not surprising in view of the relatively apathogenic nature of *E. coli* K-12 (see section 5.1.1).
- (iii) Cefotaxime treatment seemed to reduce the viable count as expected (fig 3.1), although viable organisms were still recovered 3 h after treatment.

### **3.1.3. Inflammatory response**

In spite of the decline in viable bacteria over time, in seven of nine untreated cases and all the treated cases the infection induced a CSF inflammatory response (fig 3.2 on page 84). All animals that survived longer than 6 h had an elevated CSF leucocyte count and a raised CSF protein concentration. Only a few protein assays were performed at this early stage. Data were insufficient to show any effect of antibiotic treatment on these inflammatory indices. Histological examination of two brains confirmed the presence of a severe leptomeningitis with acute inflammation extending into the lateral ventricles (not shown).

### 3.1.4. Electrophysiological data.

In this initial work, the intention was to perform hourly recordings of hearing loss. A typical set of brain-stem auditory evoked responses from expt K12 (18) is shown in fig 3.3 (page 85). The control traces were taken just before inoculation. These were then compared with the traces acquired 6 h post-inoculation. In the L ear (top) the 40 dB response at 6 h is clearly diminished, and resembles the 20 dB control response. However, in the R ear the 40 dB trace is identical at 0 h and 6 h. The hearing loss was therefore estimated as 20 dB (L) and 0 dB (R). For every experiment at each timepoint, a similar process yielded an approximate hearing loss. The endpoint data for all experiments are recorded in tables 3.1 and 3.2.

There were three major problems with using the Medelec Screener

- (i) It required about 30 min to acquire a set of readings, even with a large stimulus step of 20 dB. This was due to the number of repetitions required for averaging and the slow printout. In addition, the transducer was sometimes dislodged by small animal movements. Using a narrower interval (5 or 10 dB) would have increased accuracy but rendered it impossible to measure hearing more frequently than every 3 h.
- (ii) The estimation of hearing loss is very imprecise because of the large stimulus step and the crude method of visual comparison used to detect differences between traces over time.
- (iii) A click stimulus contains a broad frequency spectrum and stimulates a large proportion of the cochlea. Click-evoked responses are an insensitive way of detecting mild to moderate hearing loss. Conversely, a 40 dB loss to an auditory click represents quite profound hearing impairment.

In the untreated group there was no significant hearing loss until 6 h post inoculation. Only one of five animals surviving over 6 h lost 40 dB or more (a total of 2 out of 10 ears). In the group which received cefotaxime (100 mg/kg) three of five animals surviving more than 6 h lost 40 dB or more (in a total of 4 out of 10 ears). There was no hearing loss in one control animal (K-12(21)) studied for 7 h. No attempt was made to perform formal linear regression on the hearing loss data. Figure 3.4 (page 86) displays the hearing loss between 4 h and 7 h (as a scatter plot) for animals surviving 7 h or more. There is an impression that treated animals lost hearing earlier than untreated animals.

### **3.1.5. Ultrastructural findings (organ of Corti).**

The tables give a brief summary of the main histological findings in each experiment and plates 3.1 to 3.7 show the various lesions discussed. There were no clear differences in the pattern of damage observed in the treated and untreated groups, nor was there a consistent correlation between degree of damage observed and hearing loss as judged by click-evoked **BAEP** recording. Artefactual change caused by processing was limited to cracking deep in the inner sulcus, where the whole organ of Corti tended to curl away from the modiolus (plate 3.2). This was easily distinguishable from the specific damage seen after meningitis.

Ultrastructural changes were usually confined to the basal turn with substantial portions of the organ of Corti remaining intact as judged by SEM (plates 3.1, 3.2). Three types of damage were observed:

- Cratering of the apical surface of the border cells (BCs).
- Damage to IHC hair bundles with detachment and fusion of stereocilia.
- Some sporadic damage to OHCs.

Surface craters of the apical surface of the border cells were apparent by 5 h p.i. and were the commonest abnormality seen (plates 3.4 and 3.5). The craters were shallow circular defects with intracellular contents sometimes visible through the defect. They occurred less frequently than after pneumococcal meningitis (see section 3.2.4 and plate 3.19). The fine craters suggest genuine damage to the border cells. Such shallow lesions were never observed in control specimens both from this series and other work not shown here.

The hair bundles of IHCs adjacent to these craters were usually deformed, with fusion, splaying and detachment of stereocilia complete with rootlets (plates 3.3 & 3.4). It is possible that such detachment could be an artefact of processing. Stereocilia that are embedded more firmly than normal in the tectorial membrane would be more prone to detach when the tectorial membrane rolled back.

Abnormal OHC hair bundles were rarely found. Stereocilia were sometimes splayed apart or fused together, particularly in the longer experiments. A single TEM study was performed on the longest surviving animal, **K-12 (5)** (plates 3.6 and 3.7). Initial semi-thin sections demonstrated occasional darkened OHCs in both row 1 and row 3. At higher magnification some row 3 OHCs appeared electron dense and contained vacuoles. Mitochondria in the nerve endings at the base of these cells were also vacuolated. At all levels examined normal outer hair cells with well preserved nerve endings could also be found. Similar but more severe damage was also seen after pneumococcal meningitis (see for example plates 3.32

and 3.57) but in *E. coli* meningitis the apical surface of the sensory cells remained intact and none of the cells were torn away from adjacent supporting cells.

One of the most remarkable findings was the absence of inflammation and bacterial invasion of the scala media, given the huge number of organisms present on the undersurface of the basilar membrane (see below). No leukocytes were ever seen in scala media. Only one or two organisms were ever identified on the apical surface of the organ of Corti (not shown). As far as could be judged by the SEM and limited TEM data, the reticular lamina and the junctions between the hair cells and neighbouring phalangeal cell processes remained intact. This clearly represents a formidable barrier to invading organisms.

### **3.1.6. Ultrastructural findings (basilar membrane and bacteria).**

Bacteria reached scala tympani within 3 h of inoculation into the CSF and were able to induce a local inflammatory response. On the surface of the basilar membrane bordering scala tympani there was patchy but dense bacterial infiltration from 3 h p.i. onwards (plates 3.8 and 3.10). In untreated animals, *E. coli* appeared as regular bacilli approx.  $1.5\ \mu\text{m} \times 0.5\ \mu\text{m}$  with a roughened cell surface and variable projections. They were normally clustered in microcolonies. Bacterial density was greatest in the basal turn and declined towards the apex. The surface of the basilar membrane itself consisted of a connective tissue meshwork with many cribriform pores and was undamaged in all animals.

From 5 h onwards leukocytes were seen associated with the basilar membrane but were never numerous (plate 3.9). However, free floating white cells in perilymph would have been flushed out during fixative perfusion. The leukocytes appeared to be phagocytosing bacteria. Macrophages were rarely seen.

### **3.1.7. Effects of cefotaxime on the SEM appearance of *E. coli*.**

There are few published pictures of the in vivo appearance of antibiotic-treated organisms, although the in vitro morphological effects of beta-lactam antibiotics on Gram-negative organisms are well documented (Greenwood, 1982 p11-26) . Differences between in vivo and in vitro effects might be expected for two main reasons (Comber et al 1977):

- In vivo organisms are exposed to a continuously changing concentration of antibiotic after administration of a single bolus. In vitro organisms are exposed to a constant antibiotic concentration.
- Organisms in vivo are growing in a hostile environment and may be expressing different enzymes and cell wall constituents to those expressed by organisms growing in a rich nutrient broth.

Mer treatment with cefotaxime (100 mg/kg body weight) there were gross changes in the SEM appearance of *E. coli* K-12 within the scala tympani. It was not possible to correlate the morphological changes with local antibiotic concentration. Cefotaxime (100 mg/kg) was administered 3 h post-inoculation and plates 3.11 to 3.16 are arranged in chronological order.

One hour after treatment most organisms were elongated two to three times and had failed to separate completely during attempted cell division (plate 3.11). Plate 3.12 shows this effect more clearly 2 h after treatment, where so-called 'blunt constrictions' have appeared at the sites of attempted cell division. This implies there is predominant inhibition of penicillin-binding-protein (PBP) 3, which is needed to manufacture the spherical mucopeptide which forms the end-cap of the organism (Nanninga, 1985 p104). In addition, irregularities, blebs and grooves in the cell wall are also apparent (plate 3.13), which are features of inhibition of PBP 1a, 1b and 2, all partly responsible for formation of the cylindrical mucopeptide used in the rest of the cell wall (Spratt, 1975; Nanninga, 1985 p105). Three hours after treatment the surface of nearly all organisms was grossly deformed and convoluted, and many organisms appeared to be lysed leaving large quantities of cell debris on the surface of the basilar membrane (plate 3.14 and 3.15). Five hours after treatment most organisms appeared to be normal, but some still had obvious deformities (plate 3.16).

Plates 3.17 and 3.18 show the effect of giving 10 mg/kg cefotaxime 3 h after inoculation. Three hours after treatment, this lower dose of antibiotic induces extensive long chain formation and the formation of blunt constrictions but does not damage the rest of the bacterial cell surface. This suggests that PBP3 inhibition is predominant at this dose.

Expt no. K-12 (n)	Time (h)	CSF bacteria (log <sub>10</sub> CFU/ml)	CSF WBC (cells/μl)	CSF protein (g/l)	Estimated hearing loss (dB; L/R)*	Histological findings
9	2	9.6	–	–	0/0	Intact organ of Corti. Some organisms seen on basilar membrane.
16	2.5	–	–	–	0/0	Not examined
13	2.5	9.4	20	1.23	0/0	Intact organ of Corti.
7	3	–	8	–	0/0	Intact organ of Corti.
10	3	8.5	85	–	20/0	Intact organ of Corti. Many organisms on surface of basilar membrane
11	3.5	8.9	0	0.93	10/0	Intact organ of Corti
15	4	10.1	0	–	0/0	(Delayed fixation). Many organisms and leukocytes seen on basilar membrane.
8	4.5	7.1	–	–	0/0	Some craters in BCs. Some IHC stereocilia detached
17	6	7.7	1335	0.99	10/20	Badly curled. Dense invasion of basilar membrane
1	7	–	820	–	20/0	Craters in BCs; IHC stereocilia disrupted and detached.
12	7	8.6	40	7.3	>40/>40	(Mid turn intact organ of Corti; basal turn curled)
3	9	–	–	–	20/20	Craters in BCs and IHC stereocilia disruption.
5	12	4.5	4160	–	20/0	Some row 2 OHC R2 stereocilia damaged; IHC relatively spared.

The inoculum in all cases was 1x10<sup>9</sup> *E. coli* K-12. \*Assessed with click-evoked auditory brain stem response audiometry.  
– = data not available. IHC= inner hair cell; BC= border cells.

**Table 3.1:** Untreated *E. coli* K-12 meningitis: CSF and hearing loss data. Summary of morphological findings.

<b>Expt no. K-12 (n)</b>	<b>Time (h)</b>	<b>CTX dose (mg/kg body weight)</b>	<b>CSF bacteria (log<sub>10</sub> CFU)</b>	<b>CSF WBC (cells/μl)</b>	<b>CSF protein (g/l)</b>	<b>Estimated hearing loss (dB; L/R)*</b>	<b>SEM findings</b>
19	4	100	8.7	10	2.0	0/0	(basilar membrane only)
20	4	100	6.6	177	–	0/0	(basilar membrane only)
22	5	100	8.2	–	–	0/0	(basilar membrane only)
23	5	100	7.2	–	–	0/0	(basilar membrane only)
18	6	100	4.7	4070	4.7	20/0	Some craters in the BCs otherwise intact organ of Corti
14	6.5	100	5.9	420	3.7	>40/20	Intact organ of Corti
2	7	100	–	–	–	0/40	Splayed OHC stereocilia in patches; no craters
6	8	100	5.9	528	–	>40/>40	Craters in the BCs; mild disruption of IHC stereocilia
4	9	100	–	232	–	10/20	Intact organ of Corti
24	4	10	9.4	648	–	0/0	(basilar membrane only)
25	6	10	–	–	–	0/30	Mild disruption of IHC stereocilia; no detachment; no BC craters
21	7	100	No inoculum	0	0.48	0/0	not examined

The inoculum in all cases except K-12 (21) was 1x10(9) *E. coli* K-12. \*Assessed with click-evoked brain stem response audiometry.  
 – = data not available. OHC= outer hair cell; IHC= inner hair cell; BC= border cells.

**Table 3.2:** Cefotaxime-treated *E. coli* K-12 meningitis: CSF and hearing loss data. Summary of morphological findings.

## CSF bacterial titre

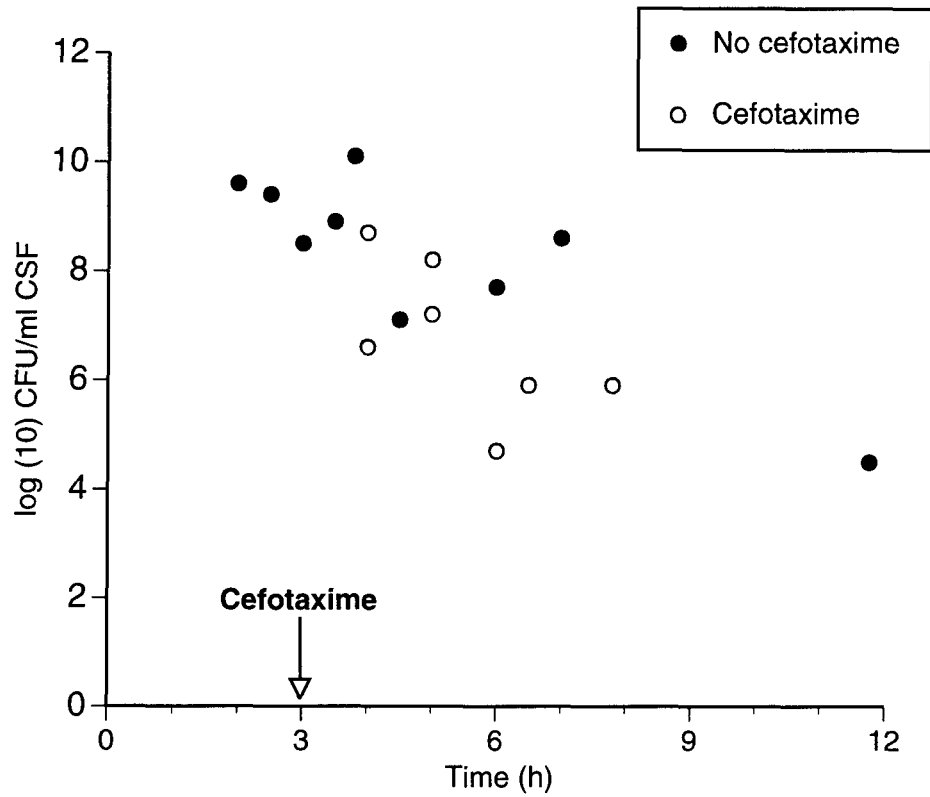


**Figure 3.1:** *E. coli* K-12 meningitis: CSF bacterial concentration. Viable counts were performed on terminal CSF samples. Cefotaxime=cefotaxime 100mg/kgi.p. 3 h post inoculation. Inoculum was nominally  $1 \times 10^9$  organisms.

## CSF white cell count

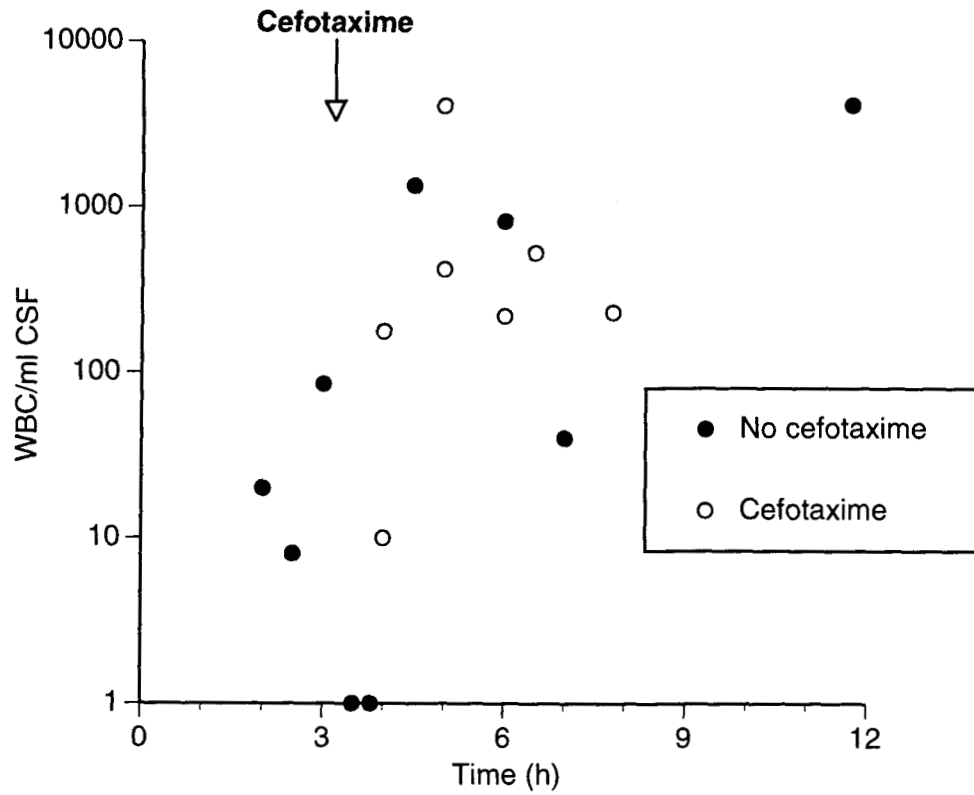
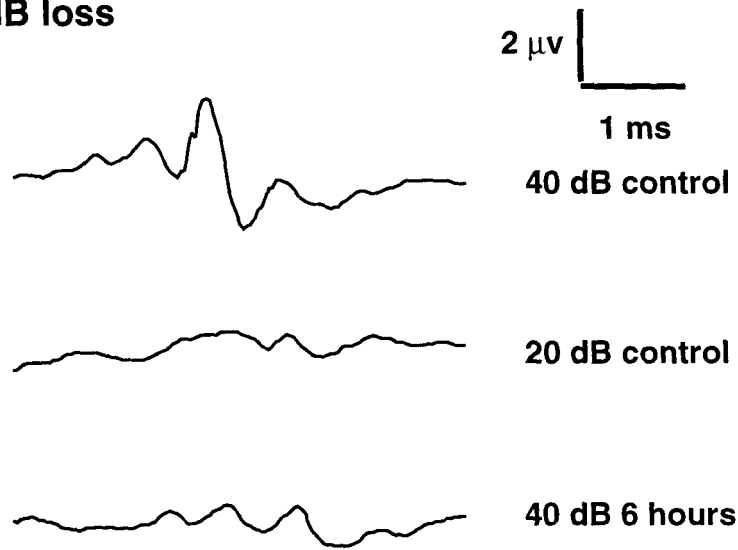


**Figure 3.2:** *E. coli* K-12 meningitis: CSF white cell count. White cells in terminal CSF samples were stained and counted microscopically. Cefotaxime= cefotaxime 100mg/kg i.p. 3 h post inoculation. Inoculum was nominally  $1 \times 10^9$  organisms.

**Left: 20 dB loss**



**Right: no loss**

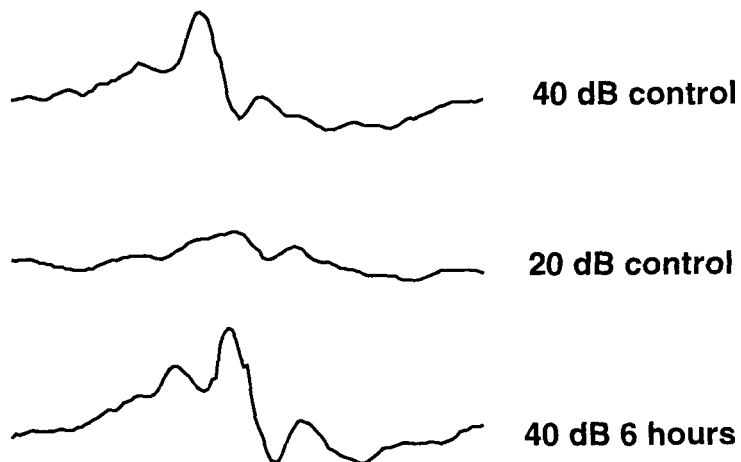


**Figure 3.3:** *E. coli* K-12 meningitis: click-evoked brain-stem auditory responses. Expt K-12 (18). Waveforms generated by the Medelec Screener were scanned, digitised and printed. Hearing loss was determined by visual comparison of control and final waveforms. 0 dB stimulus = normal human threshold (dB nHL)

### Hearing loss (evoked response)

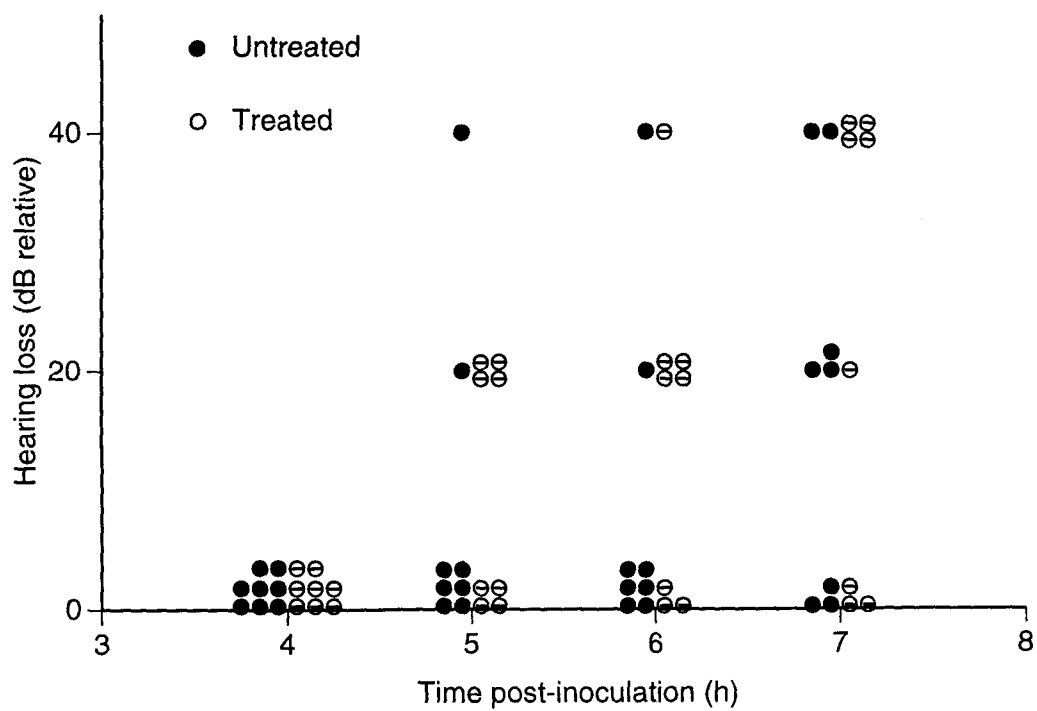


**Figure 3.4:** *E. coli* K-12 meningitis: Summary of hearing loss. Estimated hearing loss over time in animals surviving at least 7 h. Treated animals received cefotaxime (100 mg/kg) 3 h post inoculation.

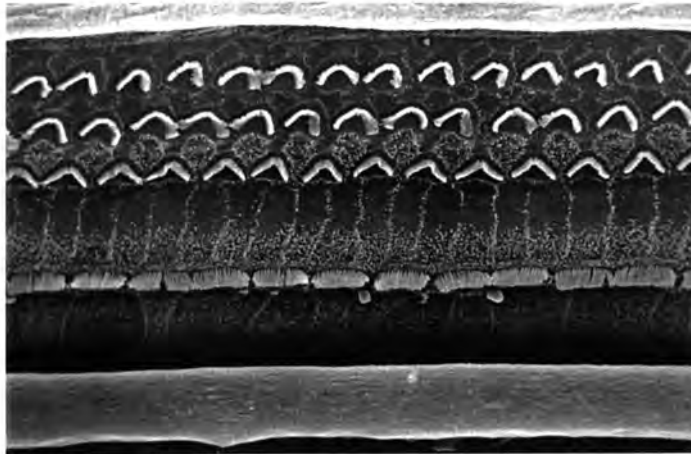


**Plate 3.1**

K-12 (1) L basal turn x800. No antibiotic treatment. 7 h p.i.  
The organ of Corti is intact at this point.  
Note the imprints of stereocilia on tectorial membrane, which has rolled back during processing.



**Plate 3.2**

K-12 (6) R basal turn x300. Cefotaxime-treated. 8 h p.i.  
The organ of Corti is intact. The cracking seen deep in the inner sulcus is a processing artefact.



**Plate 3.3**

K-12 (8) R basal turn x6,000. No antibiotic treatment. 4 h 30 p.i.  
Disruption of an IHC hair bundle. Some stereocilia have become detached from the surface of the sensory cell; lateral links between stereocilia have been lost.

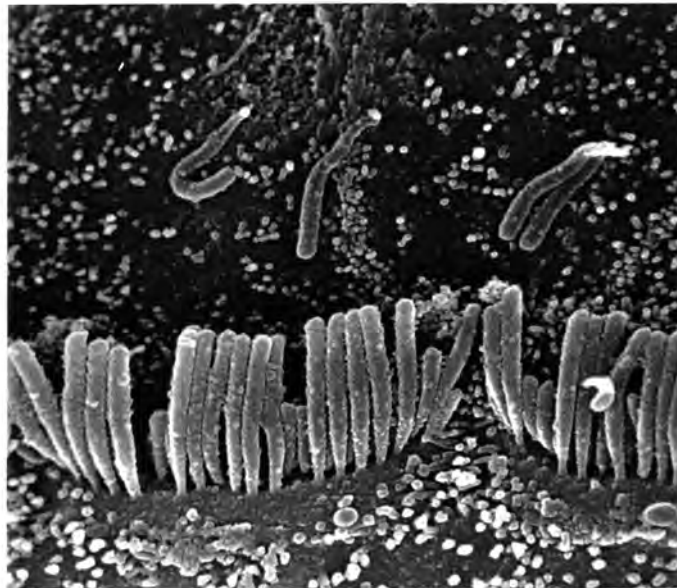


**Plate 3.4**

K-12 (1) L basal turn x6,000. No antibiotic treatment. 7 h p.i.  
Deformation of an IHC hair bundle. Stereocilia have become detached from the surface of the sensory cell. There are superficial craters in the border cells (top).



**Plate 3.5**

K-12 (6) L basal turn x15,000. Cefotaxime-treated. 8 h p.i.  
There is a crater ca. 1.5  $\mu\text{m}$  in diameter in the apical surface of a border cell.



**Plate 3.6**

K-12 (5) R basal turn x2,500. No antibiotic treatment. 12 h p.i.  
The row 3 OHC appears pyknotic and vacuolated.  
The apical surface of each OHC is intact.

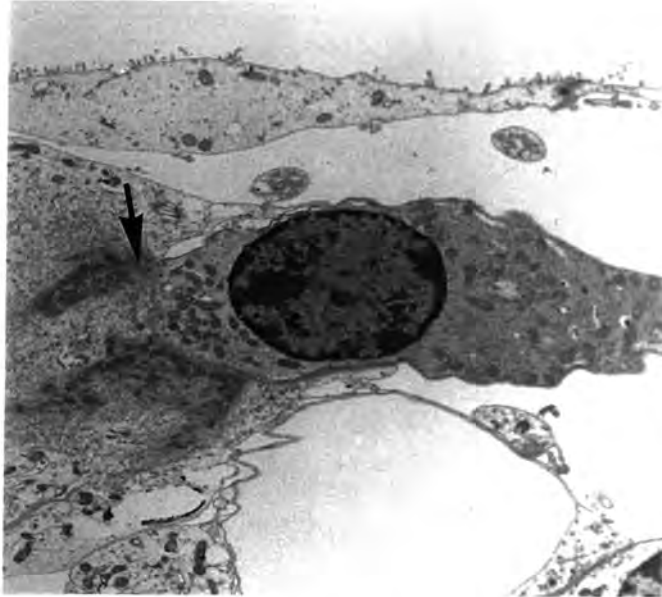


**Plate 3.7**

K-12 (5) R basal turn x4,400.

Higher power view of the base of the row 3 OHC above. Nerve endings at the base of this cell are also vacuolated and appear abnormal (arrow).

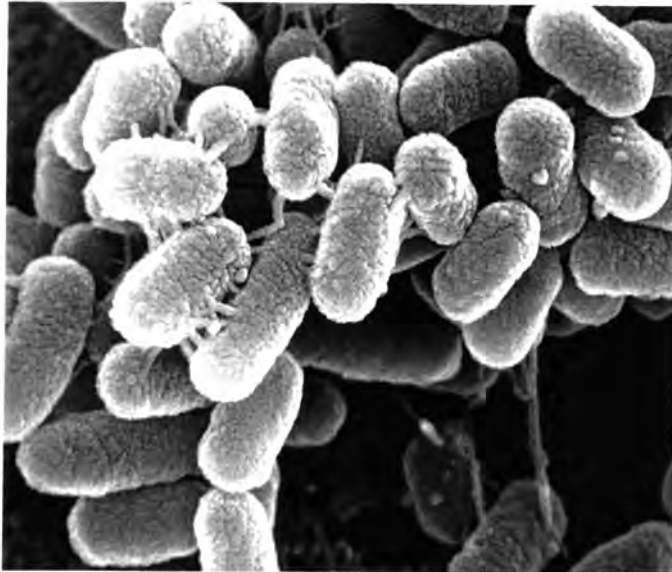


**Plate 3.8**

K-12 (1) R basal turn x15,000. No antibiotic treatment. 8 h p.i. Microcolony of *E. coli* on undersurface of the basilar membrane (facing scala tympani). Note rough surface and regular appearance.

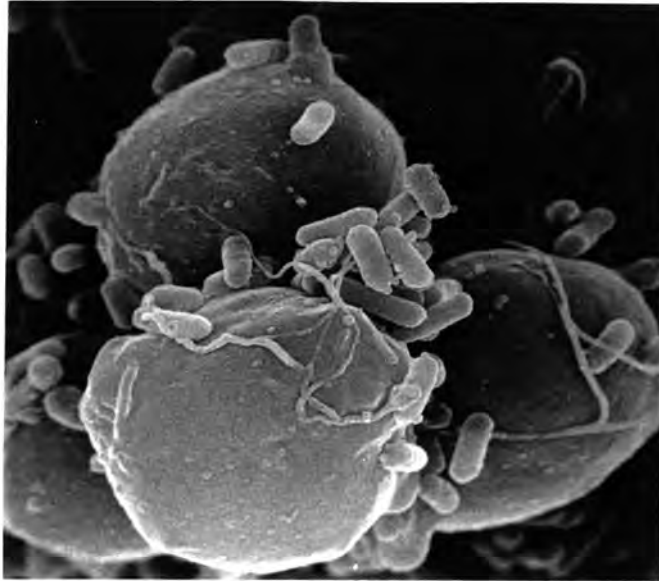


**Plate 3.9**

K-12 (1) R basal turn x5,000. No antibiotic treatment. 8 h p.i.  
Phagocytes engulfing *E. coli* on the undersurface of the basilar membrane.

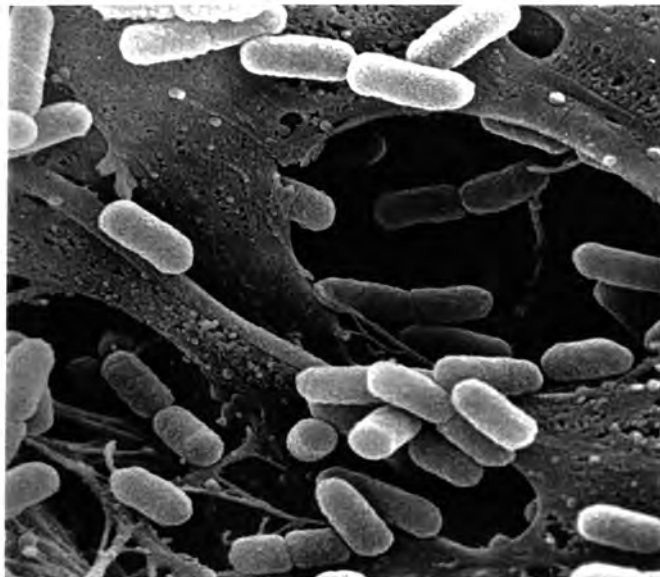


**Plate 3.10**

K-12 (1) R basal turn x8,000. No antibiotic treatment. 8 h p.i.  
*E. coli* invading the loose reticular structure of the basilar membrane.

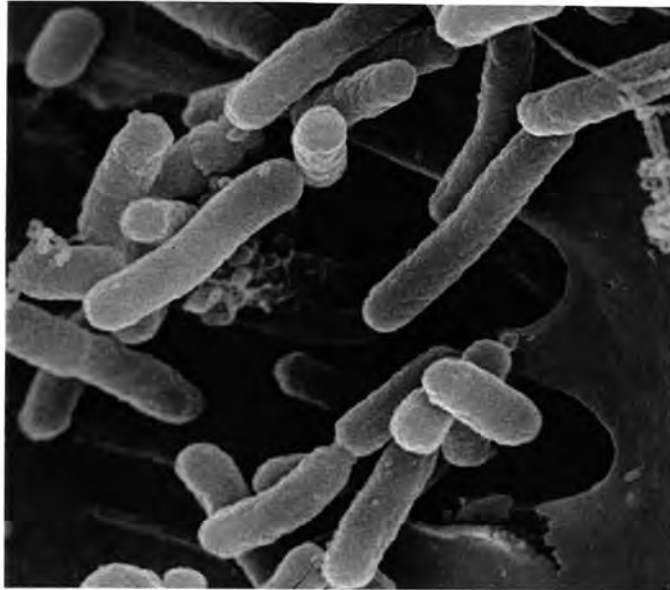


**Plate 3.11**

K-12 (19) R basilar membrane x10,000.

*E. coli* 1 h post cefotaxime (4 h p.i.).

Some elongation of organisms. There are blunt constrictions at the division points.

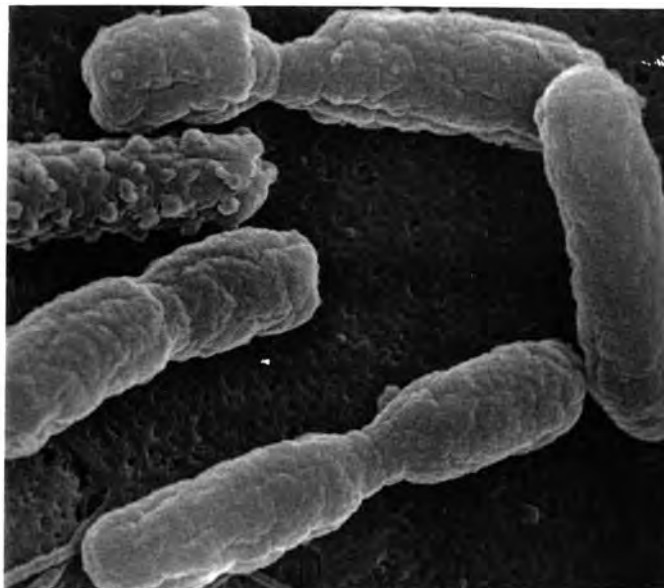


**Plate 3.12**

K-12 (22) L basilar membrane x20,000.

*E. coli* 2 h post-cefotaxime (5 h p.i.).

Blunt constrictions at the division points. Blebbing and grooving of the cell surface.

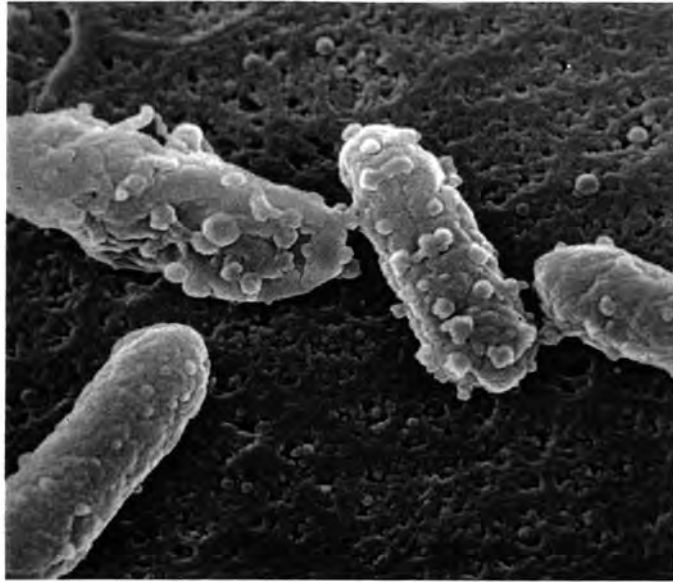


**Plate 3.13**

K-12 (22) L basilar membrane x20,000.

*E. coli* 2 h post-cefotaxime (5 h p.i.).

Convoluted surface and breakdown of the bacterial cell wall.

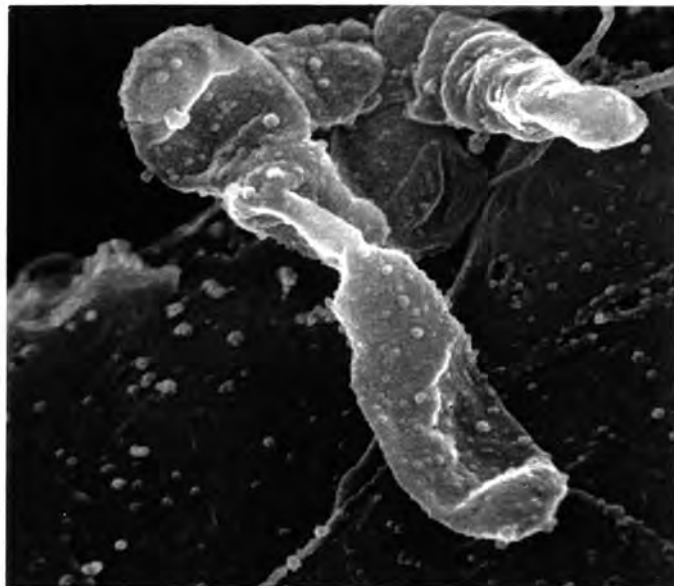


**Plate 3.14**

K-12 (14) L basilar membrane x20,000.

*E. coli* 3 h post-cefotaxime (6 h p.i.).

Gross deformation of bacterial cell surface in lysed bacterium.

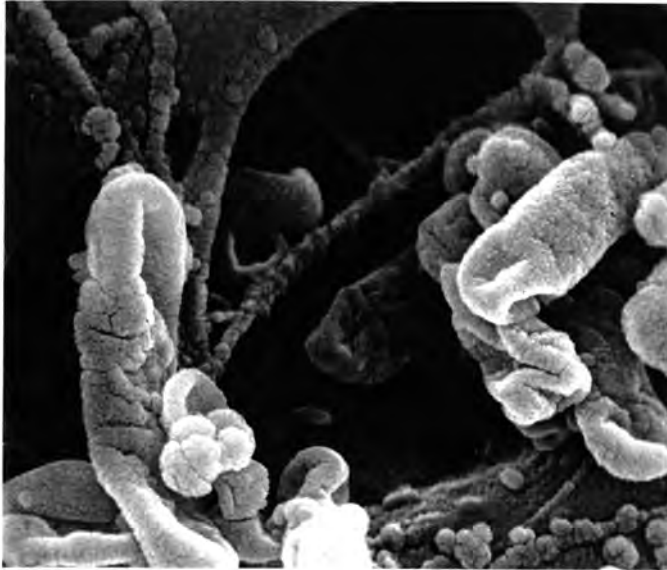


**Plate 3.15**

K-12 (2) L basilar membrane x15,000.

*E. coli* 4 h post-cefotaxime (7 h p.i.).

There is a lot of cellular debris and bacterial cell wall damage.

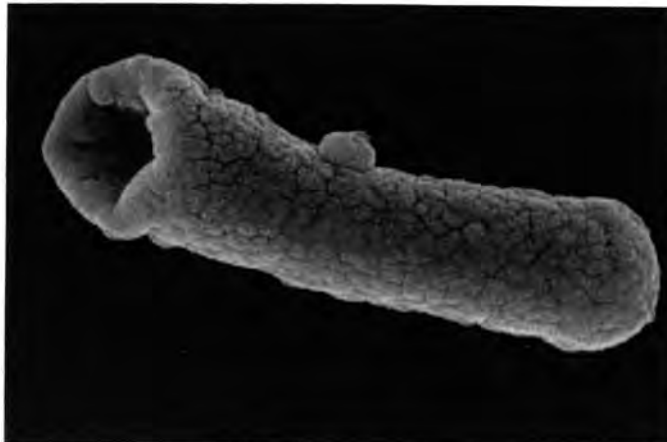


**Plate 3.16**

K-12 (6) R basilar membrane x30,000.

*E. coli* 5 h post-cefotaxime (8 h p.i.).

Deformation localised to the cap region and a single nub at the presumed site of cell division.

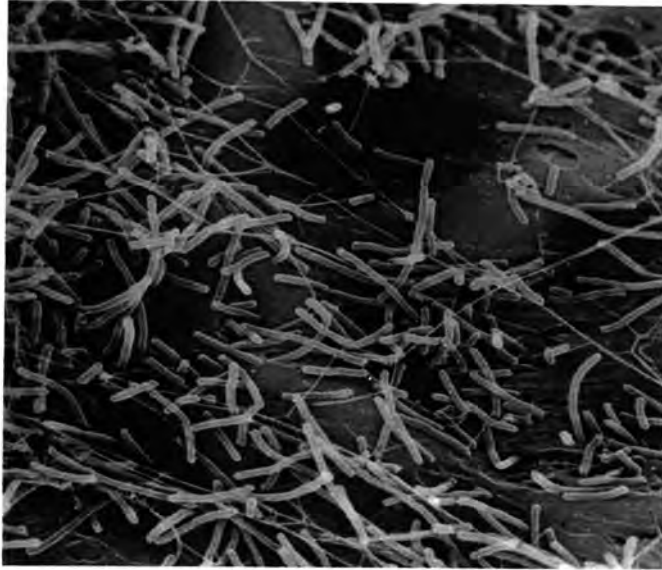


**Plate 3.17**

K-12 (25) L basilar membrane x1,500.

*E. coli* 3 h post-cefotaxime (10 mg/kg).

At this lower dose there is long chain formation but no evidence of bacterial lysis (compare plate 3.14)



**Plate 3.18**

K-12 (25) L basilar membrane x30,000.

*E. coli* 3 h post-cefotaxime (10 mg/kg).

Division point showing a blunt constriction but otherwise intact cell wall (compare plate 3.12).

### 3.2. Pneumococcal meningitis: development of recording techniques.

This section reports the preliminary part of the investigation of experimental meningitis induced by wild type *S.pneumoniae* D39. The main aims of this initial work were:

- to ensure that pneumococcal meningitis could be reliably induced in the guinea pig;
- to find an inoculum that was sufficient to cause hearing loss but that did not cause early death;
- to optimise the recording techniques for measuring hearing loss;
- to document the evolution of cochlear lesions over the first 12 hours of experimental meningitis.

#### 3.2.1. Bacteriological preparation and findings.

##### *Preparation and viability of the inocula*

The modified technique of Alwmark (1981) for preparing standard inocula of *S.pneumoniae* had been used by Dr Mitchell *et al* in Leicester for their work on experimental pneumococcal pneumonia in the mouse (Canvin, 1995). Inocula prepared in Leicester were readily transported on dry ice back to Birmingham, with suitable precautions. The only additional modification necessary to prepare inocula for experimental meningitis was to change the final diluent to PBS or (in some cases) filter-sterilized artificial perilymph. The pellet was typically resuspended in 700 to 1,400  $\mu\text{l}$  (depending on viable count). Initial viable counts on each batch were always performed after storage at  $-70^{\circ}\text{C}$  for at least 24 h. There was no noticeable decline in viable count over a period of 2-3 months, at which time inocula were discarded. The first batch (Batch **A**) had a count of 8.7 log<sub>10</sub>, CFU/ml, and was used in the experiments reported in this section.

The viable count of the inoculum was also determined in every experiment. The inocula were easily reproducible, varying between 7.1 and 7.5 log<sub>10</sub>, CFU. This confirmed the practicability of the modified Alwmark method, and the validity of the drop count method used to perform viable counting. A further benefit of the Alwmark method was that it took less than 20 min to prepare the inoculum, whereas to prepare a fresh log-phase culture of *E. coli* took around 4 h. This meant that for pneumococcal meningitis, animals could be inoculated by 9 am. In addition, the bacterial count did not significantly decline if the final inoculum was stored on ice for up to 3 h. so that two animals could be inoculated some time apart if necessary.

The in vitro growth curve of D39 is shown in figure 3.29 (page 185). Organisms harvested at 5 h are in late log phase. Inoculation of a small quantity (100  $\mu\text{l}$ ) into the CSF space (CSF

volume assumed to be 1 ml) should give a final concentration in the CSF similar to that found in mid-log phase. In vivo growth curves were not constructed.

#### *CSF bacterial counts and bacteraemia*

Table 3.4 lists all data obtained from the CSF and blood samples of experiments D39(1) to D39(13) in order of duration of the experiment. (Experiment D39(7) was used primarily to develop the round window recording technique and no CSF sample was taken.) The CSF bacterial count in animals inoculated with batch A was in all cases higher than the initial inoculum (assuming approximate CSF volume of 1 ml). This is reasonable evidence of in vivo growth. All animals in which a terminal cardiac blood sample was taken were bacteraemic, even as early as 4.5 h post inoculation.

#### *Passaging*

Batch A was prepared from organisms isolated from the blood of an MF1 mouse 48 h after intraperitoneal inoculation of stock D39. Such a passaging step had proved necessary for maximum virulence in the pneumonia model, where organisms are inoculated per-nasally. We did not want to use guinea pigs for such a passaging step for several reasons (ethical, financial, need for a license modification) and in any case it was not certain whether a similar stricture would apply to meningitis. To investigate this, batch C was grown from organisms recovered from the CSF of experiment D39(8) and used in experiments D39(10) and D39(11). Batch D was subcultured from Batch C and used in experiment D39(12). The final CSF bacterial count was in all cases was the about the same as or lower than the initial inoculum, although all animals developed a CSF leukocytosis. (Compare for example D39(10) (Batch C) with D39(6) (Batch A), both at 10 h post inoculation). These findings underlined the importance of using mouse-passaged organisms. This is not unexpected, although it is only possible to speculate what additional virulence factors are expressed by organisms having to invade the bloodstream from the peritoneum. For subsequent experiments in the comparative study all inocula were prepared in Leicester by passaging.

### **3.2.2. Inflammatory response.**

#### *Dosefinding experiments.*

The first three experiments suggested that an inoculum of 7.5 log<sub>10</sub> CFU would induce CSF leukocytosis yet allow animals to survive for 12 h (D39(2)). An inoculum of 9.0 log<sub>10</sub> CFU (D39(3)) was fatal by 6 h post inoculation (p.i.). In addition, organisms at this concentration are unlikely to enter log-phase growth. An inoculum of 5.0 log<sub>10</sub> CFU (D39(1)) evoked a minimal CSF leukocytosis (100 cells/μl) 9 h p.i. No further dose finding experiments were performed.

### ***CSF inflammation.***

In all cases inoculation of live *S. pneumoniae* D39 into the subarachnoid space provoked a CSF leukocytosis as early as 4.5 h after inoculation, as detailed in table 3.4. CSF protein concentrations seemed to be more variable, and not always consistent with the degree of CSF leukocytosis. Because of the variability in batches of inocula used this is not a firm conclusion. These experiments confirmed the feasibility of performing a comparative study with CSF data as subsidiary endpoints, and allowed refinement of the techniques used.

### **3.2.3. Electrophysiological data and development of techniques.**

This section describes the development of the techniques used to investigate hearing loss. It may be helpful to refer to methods section 2.2.4. Upgrading to the MacLab system brought two benefits:

- the evoked response to pure tones could be measured;
- data were acquired much faster and already digitised enabling rapid on-line measurement of wave height and latency.

### ***Tone-pip ramp time and frequency specificity.***

Compound action Potentials are frequency dependent when evoked by low to moderate intensity tonal stimuli (Eggermont *et al*, 1976). In order to obtain a frequency-specific CAP, the stimulus administered must trigger only that restricted population of nerve fibres tuned to that frequency. At high sound pressure levels, other fibres contribute to the CAP, so diminishing selectivity. The traditional tone stimulus has a trapezoidal envelope to reduce spectral 'splatter' associated with a fast rise time (the faster the rise time the more the wave resembles a transient click stimulus). The ramp-gate modulator had been custom built to deliver a ramp time of <0.1 **ms**. Frequency specificity was investigated by averaging eight tone-pips (1 ms duration) and subjecting them to fast fourier transform analysis at a time base of 40 **kHz** with the (default) Hamming window setting. Figure 3.5 (page 105) shows the power spectra of the unramped tone pips used in the final comparative study. Table 3.3 and figs 3.6 and 3.7 show that addition of a 0.5 ms ramp apparently improved frequency selectivity by 18 dB at both frequencies tested. But it is the initial aspect of the waveform that determines which fibres contribute to the CAP, and the addition of a 0.5 ms ramp decreased the 100  $\mu$ V threshold (see page 101) by at least 10 dB (presumably by diminishing synchronous firing). This problem was noted by van Heusden *et al* (1981) when recording CAPs in cats. They found that a gradual onset tone produced smaller and wider **APs** with a longer latency, and preferred the use of rapid onset tones.

Unramped tone pulses were therefore used for the remainder of the study. Stimuli were delivered no faster than 10 Hz to prevent adaptation occurring.

Frequency	Ramp	Relative dB (10 kHz)	Relative dB (3 kHz)
3 kHz	none	-34 dB	0 dB
3 kHz	0.5 ms	-52 dB	0 dB
10 kHz	none	0 dB	-28 dB
10 kHz	0.5 ms	0 dB	-46 dB

**Table 3.3:** Effect of ramp time on frequency specificity of tone pips.

**Evoked responses.**

Two problems remained with the evoked response technique:

- (i) **Accuracy & threshold determination.** A typical set of evoked response waveforms (from experiment **D39 (2)**) is shown in fig 3.8. Threshold determination here is still a matter of judgement by eye. The baseline visual detection threshold is clearly below **20 dB SPL**, but the visual detection threshold at **12 h** can only be approximately placed between **40 and 60 dB SPL**. Note also that the height of the largest wave (wave III) is about an order of magnitude lower than the brain-stem evoked Potentials obtained in response to an auditory click (compare fig 3.3).
- (ii) **Time to acquire data.** Although the new equipment obtained readings more quickly than with the equipment used for the *E. coli* study, stimulus steps were still limited to **10 dB** because at least **5-12** stimuli were needed for averaging.

Fig 3.9 demonstrates the course of hearing loss in expt **D39(6)**, where these two factors combine to give a rather coarse assessment of hearing loss, with apparent baseline wander in the left ear, and swings of **10-20 dB** between consecutive hours. Could quantitative analysis of the evoked response waves improve this situation? Baseline wander was initially attributed to the insecure coupling between the earpiece and the meatus. This problem was overcome by surgically exposing the meatus as for round window recording, and coupling the transducer to the meatus via hollow ear bars. Brain-stem evoked response testing and round window recording of the compound action potential (see below) were then compared. In expt **D39(11)**, the stimulus needed to maintain the *CAF'* was unchanged over a period of three hours at **70dB SPL (10 kHz)**. But figure 3.10 shows that the height of evoked response wave III (the largest wave) fell from **1.4 μV** to **0.6 μV** over the same period. However the height of Wave I at the same stimulus intensity rose from **0.6 μV** to **0.8 μV**! It is likely that the change in evoked response Potentials in the face of an

unchanging auditory nerve compound action potential reflects changes in brain stem activation particularly as the waves changed in different directions. Although these changes seem large they were most pronounced with loud stimuli and were less important with quieter stimuli. For example, the stimulus intensity required to maintain the height of wave III of the BAEP at  $0.5 \mu\text{V}$  rose from 52 dB SPL to 62 dB SPL over this same time period.

Latency analysis proved to be of little additional benefit in defining a criterion level. Wave latency is inversely proportional to sound intensity (data not shown). However this relationship flattens off at low stimulus intensity, making it difficult to define a stimulus level precisely with respect to a reference latency.

In the face of such wide variability in evoked response Potentials with a constant CAP, quantitative analysis seemed to offer little improvement over 'eyeballing' the BAEP waveform. The anticipated difference in hearing loss between the wild-type pneumococci and virulence-deficient mutants was around 30-50 dB. The lack of precision of brain-stem evoked response testing would have required many subjects in each group to demonstrate a statistical difference satisfactorily. **An** alternative technique was therefore developed.

#### ***Round window recording.***

The final method chosen was to record the auditory nerve compound action potential from an electrode positioned on the round window membrane. The height of the  $\text{N}_1\text{-P}_1$  wave was recorded (see fig 1.1). Several advantages accrued:

- Firm coupling between the transducer and the meatus eliminated one source of variability
- The response of the cochlea alone was measured with no possibility of interference from the opposite ear or from the effects of CSF inflammation on the brain stem. Therefore any hearing loss observed could confidently be ascribed to cochlear damage.
- As discussed below, the 'auditory threshold' could be determined to  $\pm 1$  dB SPL and more frequent readings were possible.
- Animals supported in a stereotactic apparatus appeared to have far fewer respiratory problems and therefore longer experiments could be conducted.

Some disadvantages were encountered:

- Accumulation of fluid in the middle ear cavity and particularly on the round window membrane itself proved to be troublesome.
- The round window membrane was inadvertently punctured on a few occasions. Formation of a CSF/perilymphatic fistula would obviously affect the spread of

organisms from the subarachnoid space and almost certainly alter the function of the organ of Corti, and so ears thus affected were disregarded.

**Definition of auditory threshold.** Were one to record the response of a single-auditory nerve fibre, it would be possible to find an auditory stimulus intensity which caused a just-perceptible change in firing pattern, and define this as the threshold. But such an all-or-nothing concept is less than helpful in a situation where we are dealing with a compound action potential or far-field potentials, which represent the massed activity of many nerve units. As shown in fig 3.11, it is clear that the heights of both wave I and wave III of the brain stem evoked response are not linearly related to stimulus at low intensities. In fact it is very difficult to determine accurately the exact point at which the wave disappears into background noise. In the example given this could be anywhere from 25 to 40 dB SPL for wave I and 40 to 60 dB SPL for wave III. The auditory nerve compound action potential behaves in a similar way (see fig 3.12); here the minimum stimulus needed to generate a just-detectable CAP response at 10 kHz could be anywhere between 20 and 35 dB SPL.

One solution would be to record a series of CAPs at different intensities and plot a curve of mean intensity versus  $N_1$ - $P_1$  height, choosing the 'knee' of this curve as the genuine threshold. In fig 3.13 the apparent 'knee' of 9 dB SPL has a wide confidence interval, demonstrating the difficulty of determining this point repeatedly. Price *et al* (1978) plotted similar curves of CAP amplitude as a function of stimulus intensity and extrapolated to obtain the intensity at zero amplitude (about 2 dB for fig 3.13). This approach was thought to be too cumbersome for the meningitis study.

The solution adopted was to choose a reference (or criterion) level on the linear part of the stimulus intensity/response curve, exactly analogous to the technique for intracochlear CAP recording (*see* section 2.3.3) (Comis *et al* 1993). In this method the stimulus intensity was adjusted to return the  $N_1$ - $P_1$  height to a reference level of 100  $\mu$ V as measured at the electrode. The stimulus intensity needed to obtain the  $N_1$ - $P_1$  reference level of 100  $\mu$ V is hereafter referred to as the CAP threshold. For the example in fig 3.13, it is 16 dB SPL, 14 dB above the extrapolated 0  $\mu$ V threshold. Hearing loss at a given frequency is defined as a rise in the stimulus intensity of that frequency needed to regain the reference level of 100  $\mu$ V. With this approach it was possible to define the threshold to within 1 dB SPL. Frequent readings were possible because only 16 sweeps needed to be averaged at each intensity. A full set of threshold determinations on one ear in 1 kHz steps between 3 kHz and 10 kHz could be performed in under 10 minutes.

**Experimental results.** Because the techniques were under continuous development, none of the recorded threshold alterations in this ultrastructural study can be regarded as

accurate. However, they are noted in table 3.5. They were the first indication of the level of hearing loss potentially caused by *S. pneumoniae* D39. Note that a 1 kHz tone pip (one cycle) was used to evoke the low frequency brain-stem auditory response. The lowest frequency that could evoke a reasonably well defined CAP was 3 kHz.

#### 3.2.4. Ultrastructural findings.

Table 3.5 summarises the histological findings in each experiment of this series. Only micrographs from animals infected with the passaged organisms (batch A) are shown.

Ultrastructural damage was dramatically more extensive than that seen after a similar duration of *E. coli* meningitis (see section 3.1.5.). From 6 h p.i. onwards surface cratering of the border cells could be found (plates 3.19-3.20, page 114). Severe derangement of some hair bundles of IHCs was apparent by 9 h p.i. (plate 3.20-3.21). Two additional lesions were seen:

- (i) As well as detachment of stereocilia from the surface of the hair cell, some sensory cells were torn away from their adjacent supporting cells (fig. 3.20). Occasionally the apical surface of the whole IHC appeared to be lifted clear of the surface of the organ of Corti (plate 3.21).
- (ii) The apical surfaces of outer hair cells were susceptible to ballooning and disruption, particularly so for row 2 cells (plates 3.23-3.24). The OHC stereocilia were sometimes severely atrophied.

Structures resembling organisms were occasionally seen on the scala media surface of the organ of Corti (plate 3.22). On the scala tympani surface of the basilar membrane it was difficult to distinguish pneumococci from the large amount of cellular debris but there appeared to be more white cells present than in animals infected with *E. coli* (plate 3.25-3.26).

The nature of the 'inflammatory string' seen in plate 3.25 is uncertain, but it may be a condensation of bacterial capsule. Such 'string' was only seen in conjunction with a labyrinthitis.

A TEM section of a pneumococcus on the basilar membrane is shown in plate 3.27. The double-layered cell wall is clearly visible. Organisms fixed after *in vitro* growth in liquid media have a clearly defined capsule around the cell wall. In this case, the capsule appears to have condensed into projections. This phenomenon has also been observed in pneumococci recovered from experimental mouse pneumonia (Dr T Mitchell, personal communication).

<b>Expt no. D39 (n)</b>	<b>Time (h)</b>	<b>Inoculum (log<sub>10</sub> CFU)</b>	<b>Batch</b>	<b>CSF bacteria (CFU/ml)</b>	<b>CSF WBC (cells/μl)</b>	<b>CSF Protein (g/l)</b>	<b>Blood bacteria (CFU/ml)</b>
11	4.5	[7.5 est]	C	6.8	740	1.8	5.0
13	6	7.5	D	6.6	280	na	3.6
4	6	8.0	A	na	1,050	0.06	na
3	6	<i>9.0</i>	<i>A</i>	<i>9.5</i>	<i>14,500</i>	<i>1.86</i>	<i>na</i>
1	9	<i>5.0</i>	<i>A</i>	<i>6.7</i>	<i>100</i>	<i>0.21</i>	<i>na</i>
12	9	6.9	D	7.2	6,200	na	4.5
8	9	7.1	A	8.2	4200	1.01	3.9
5	9.5	7.5	A	8.2	17,300	1.37	5.4
<i>9 (ctrl)</i>	<i>10</i>	<i>0</i>	<i>(APL)</i>	<i>na</i>	<i>0</i>	<i>0.00</i>	<i>na</i>
10	10	7.1	C	6.8	1,325	1.24	3.7
6	10	7.5	A	8.9	7,200	na	4.1
2	12.5	7.5	A	8.8	4,200	na	na

Italics denote inocula other than ca. 7.5 log<sub>10</sub> CFU. Batch A was mouse-passaged.  
na = data not available. See also figs 3.3 –3.5.

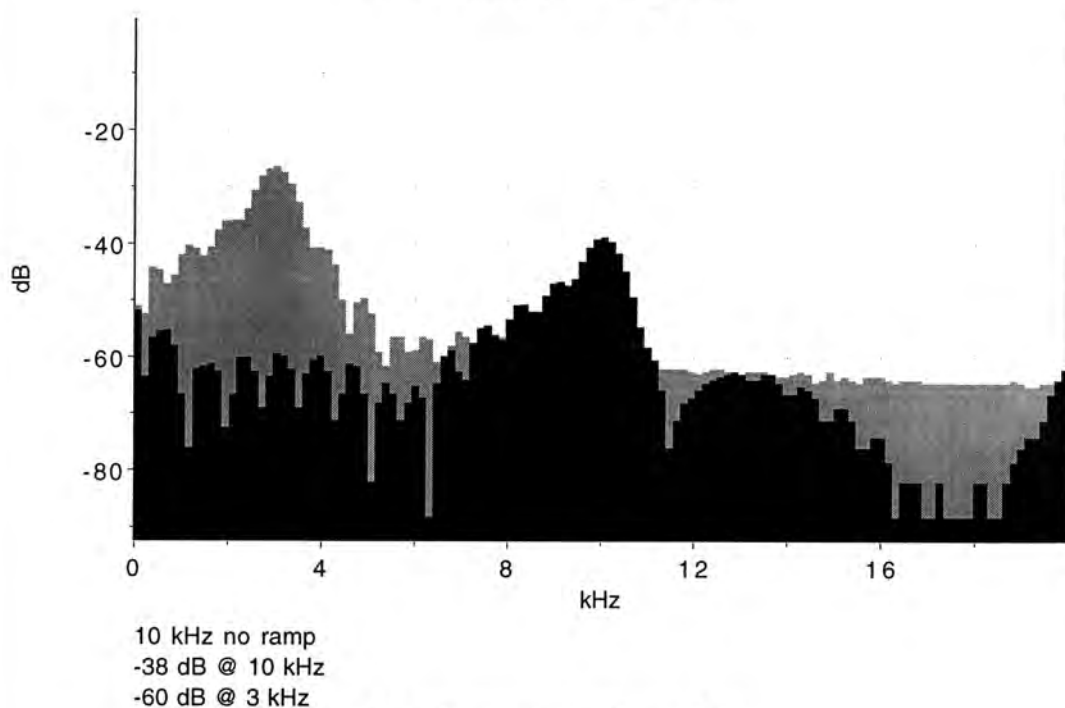
**Table 3.4:** Evaluation of pneumococcal meningitis: CSF and blood data

Expt no. D39 (n)	Time (h)	Inoculum (log <sub>10</sub> CFU)	Batch	Estimated hearing loss (dB; L/R)			Histological findings
				@ 10 kHz	@ 3 or 1 kHz #	Technique	
11	4.5	[7.5 est]	C	25/17	15/21	RW	Some row 1 OHC s/c missing.
13	6	7.5	D	-/-	-/-		not examined
4	6	8.0	A	0/0	0/0	BAEP	BC cratering; no damage to OHC/ IHC
3	6	9.0	A	-/0	-/-	BAEP	late fixation: not evaluated
1	9	5.0	A	0/0	-/-	BAEP	not examined
12	9	6.9	D	7/4	7/16	RW	not examined
8	9	7.1	A	-/54	-/-	RW	Damage to apical surfaces of row 2 OHCs; craters in BCs; IHC stereocilial disruption
5	9.5	7.5	A	40/50	30/10	BAEP	Damage to apical surfaces of row 2 OHCs; organisms in scala media
9 (ctrl)	10	0	(APL)	6/-	-/-	RW	(L) intact; (R perforated round window)
10	10	7.1	C	25/-	9/-	RW	(L) poor processing; (R perforated round window)
6	10	7.5	A	20/35	20/20	BAEP	Damage to intercellular junctions; BC craters; IHC stereocilia damage; OHC apical surfaces ballooned
2	12.5	7.5	A	40/50	30/30	BAEP	Damage to intercellular junctions; a few BC craters OHC stereocilia damage

Only batch A was animal-passaged. RW=round window recording. BAEP=tone-pip brain stem evoked responses. -/- = not evaluated. (technical problems etc.)  
 #Low frequency hearing loss: BAEP @1 kHz ; RW @3 kHz . OHC= outer hair cell; IHC= inner hair cell; BC= border cell.

**Table 3.5:** Evaluation of pneumococcal meningitis: hearing loss and ultrastructural data.

FFT tone pips : Page 15



FFT tone pips : Page 16

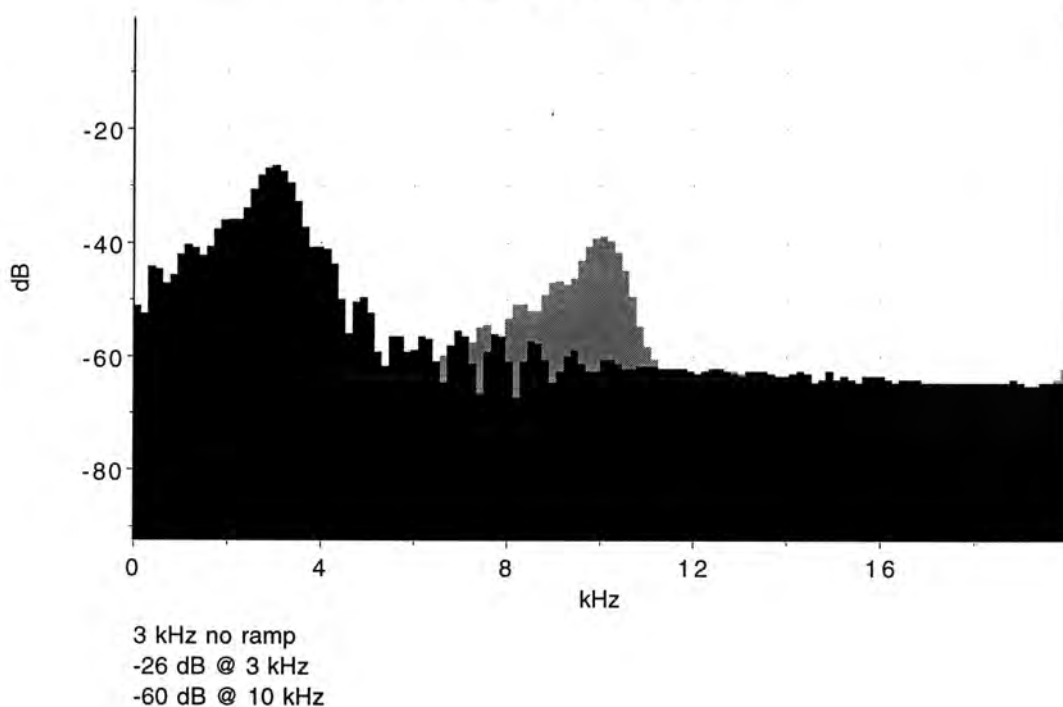


**Figure 3.5:** Spectral analysis of unramped tone pips. This diagram represents the power spectrum of the stimuli used in the comparative study. Black tracings are 10 kHz (top) and 3 kHz (bottom). Tone pips (1 ms) were averaged ( $n=8$ ) and subjected to fast fourier transform analysis. Scale in dB SPL.

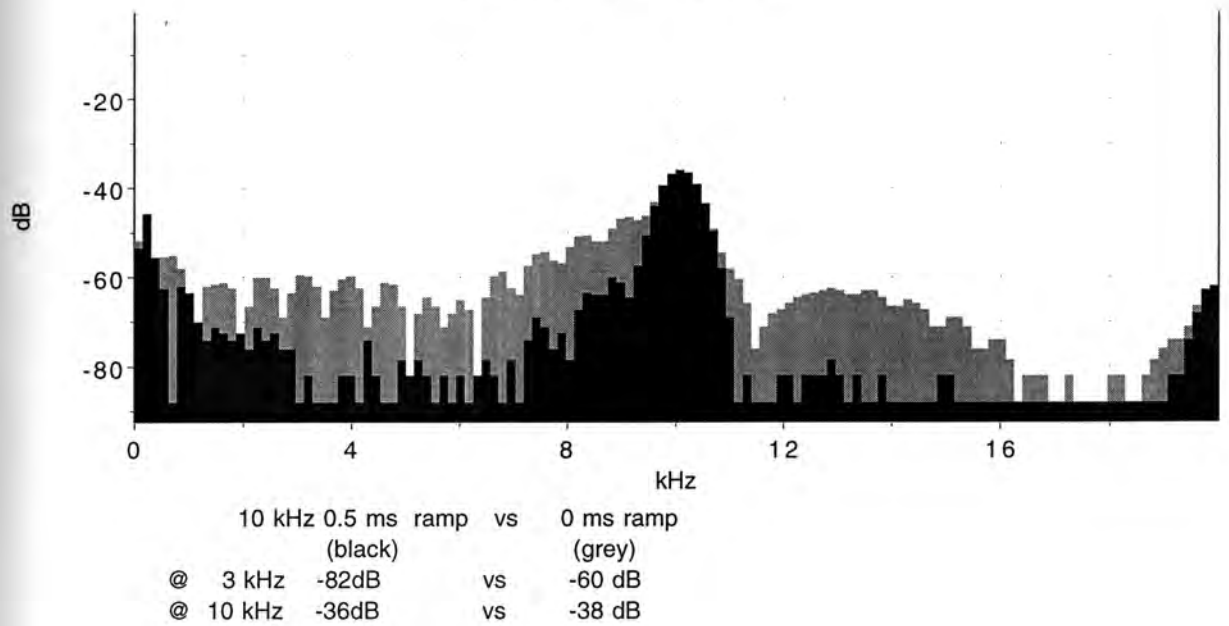


**Figure 3.6:** Spectral analysis of 10 kHz tone pip: ramped vs. unramped. Tone pips (1 ms) were averaged (n=8) and subjected to fast fourier transform analysis. Scale in dB SPL

FFT tone pips : Page 17

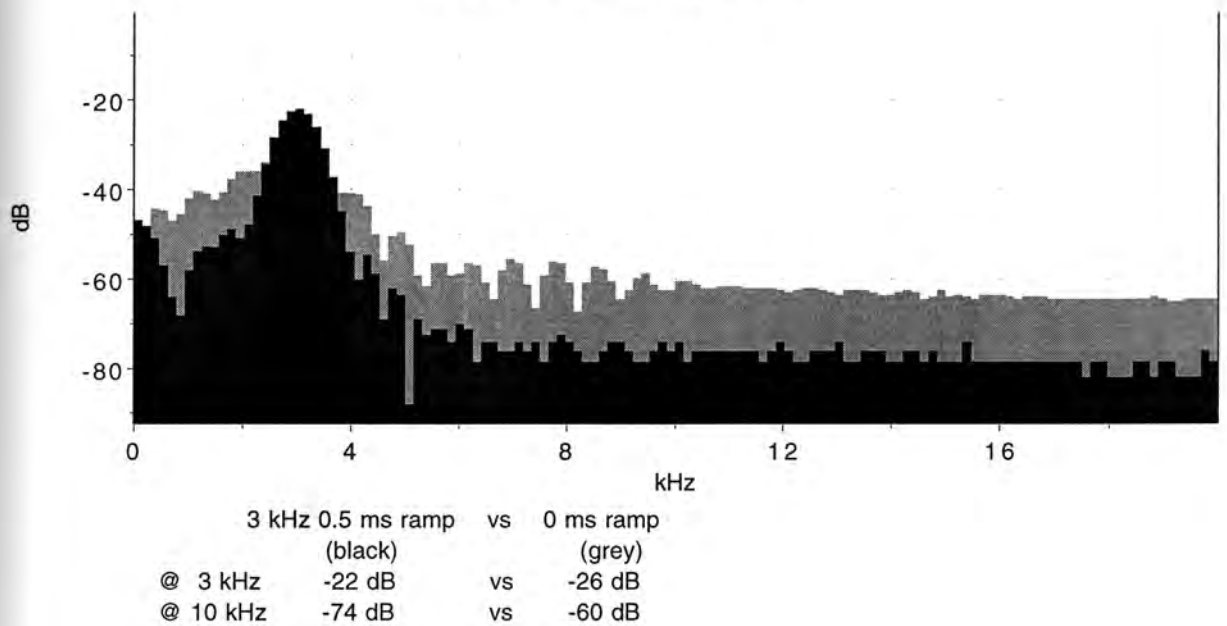


**Figure 3.7:** Spectral analysis of 3 kHz tone pip: ramped vs. unramped. Tone pips (1 ms) were averaged (n=8) and subjected to fast fourier transform analysis. Scale in dB SPL

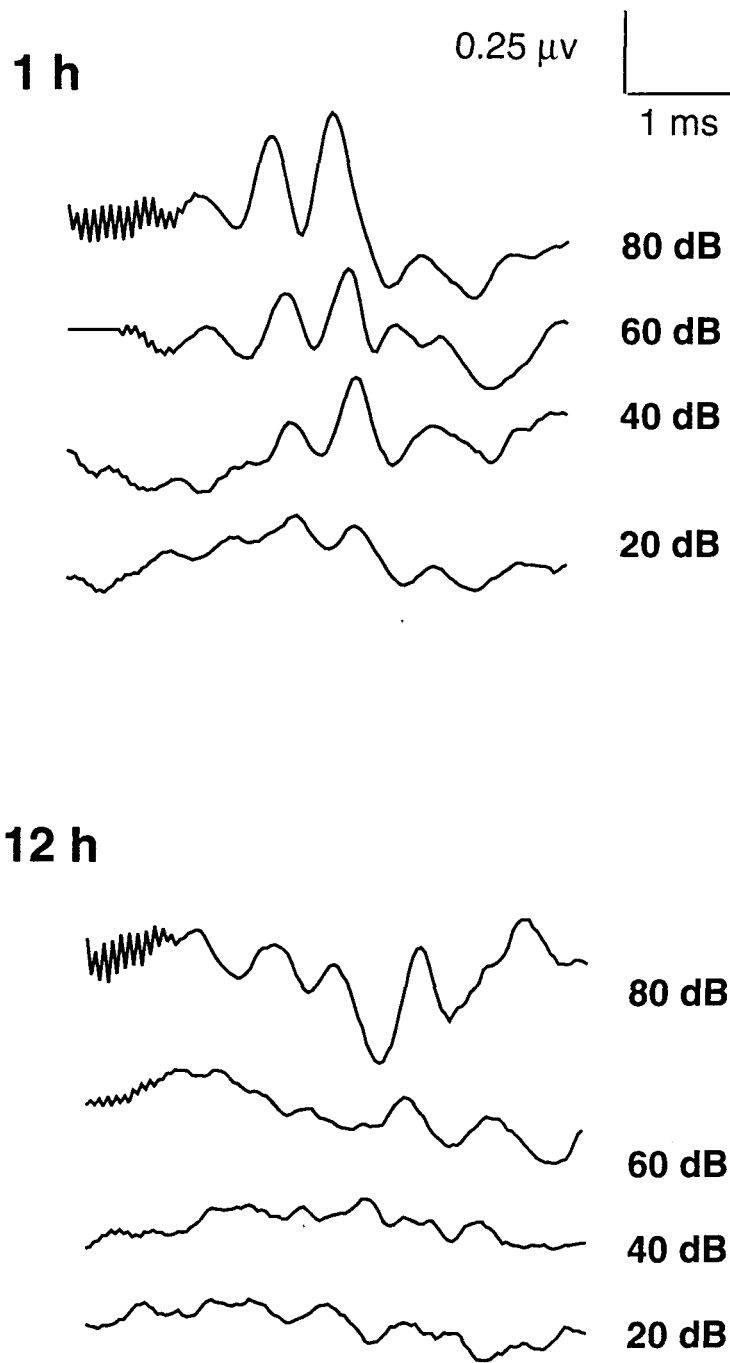
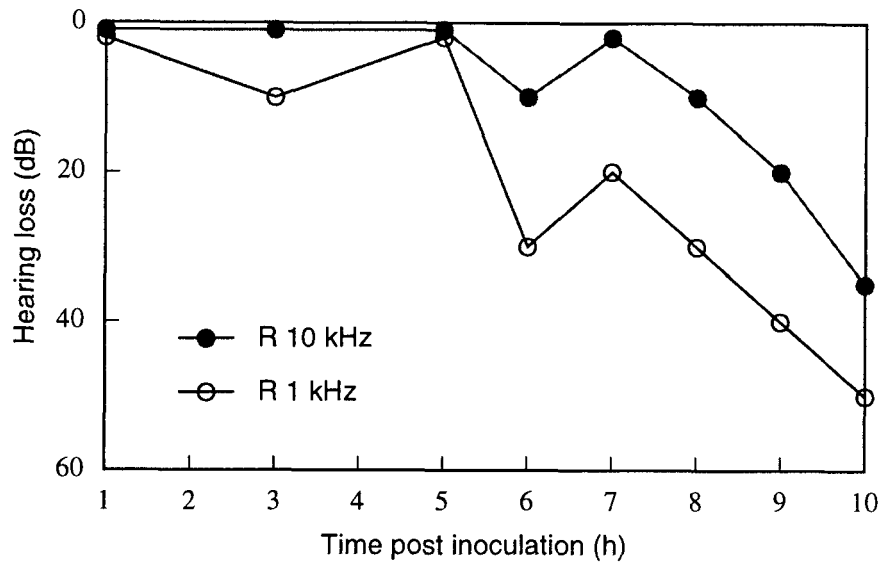


**Figure 3.8:** Pneumococcal meningitis (D39): typical tone-evoked brain stem Potentials. Data from expt D39 (2); dB=dB SPL; h=h post-inoculation.

## Right



## Left

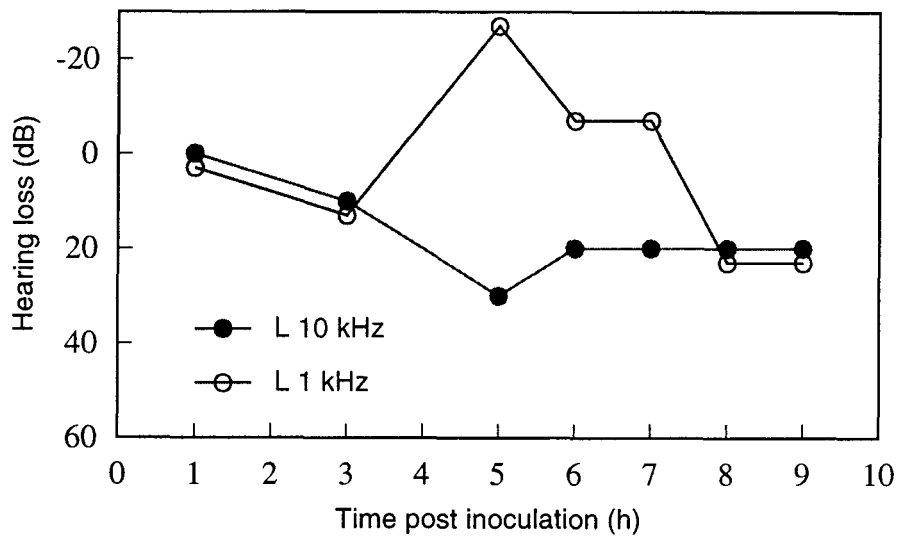
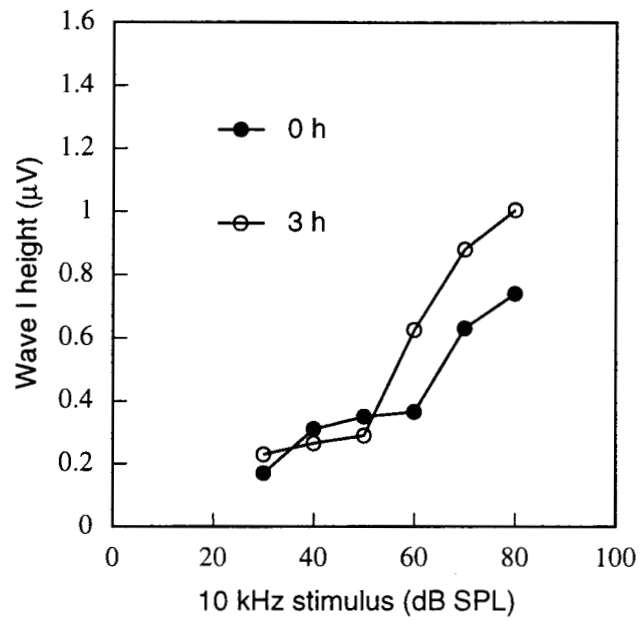


**Figure 3.9:** Pneumococcal meningitis (D39): example of hearing loss over time (BAEP). Data from expt D39(6) shows discrete steps (min 10 dB) and large fluctuations over time.

### Wave I



### Wave III

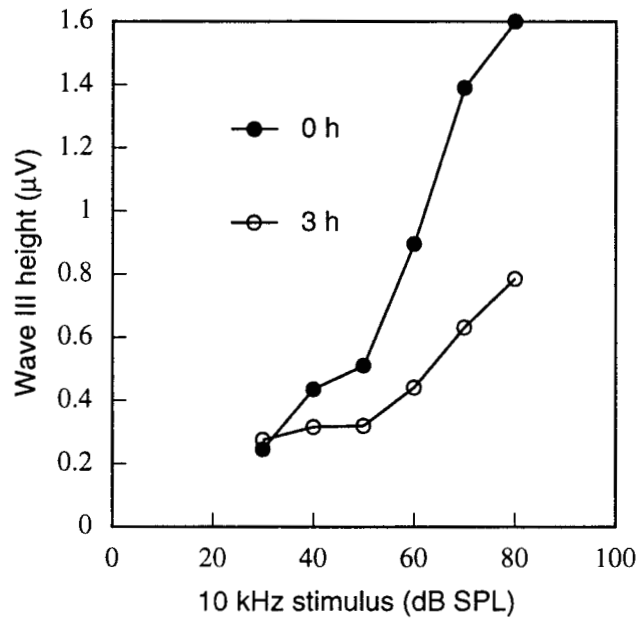
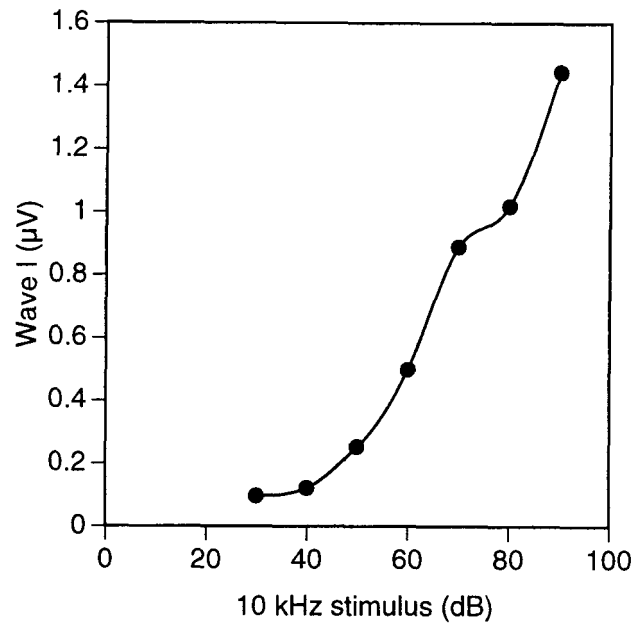


**Figure 3.10: Tone-evoked brain stem Potentials: stimulus/response curve 3 h apart. Data from expt D39(11) where the CAP threshold was unchanged at 0 and 3 h post inoculation.**

### Wave I



### Wave III

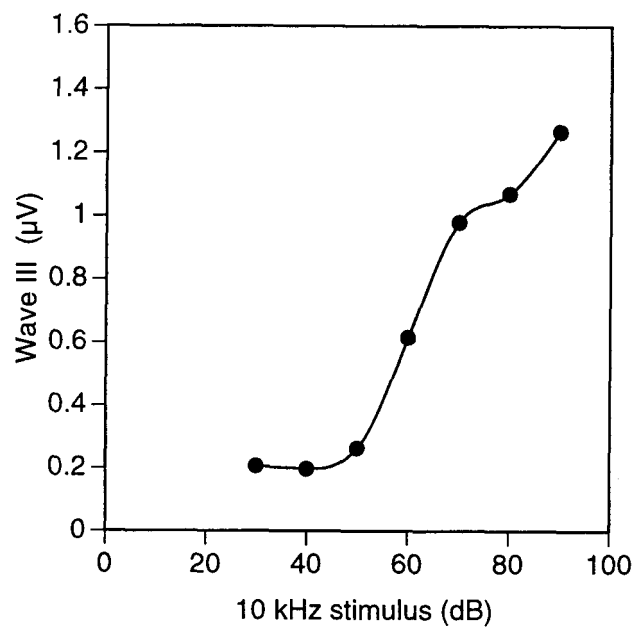


**Figure 3.11:** Tone-evoked brain stem Potentials: stimulus/response curve. Data from expt **D39(10)**; dB=dB SPL.

## Compound action potential

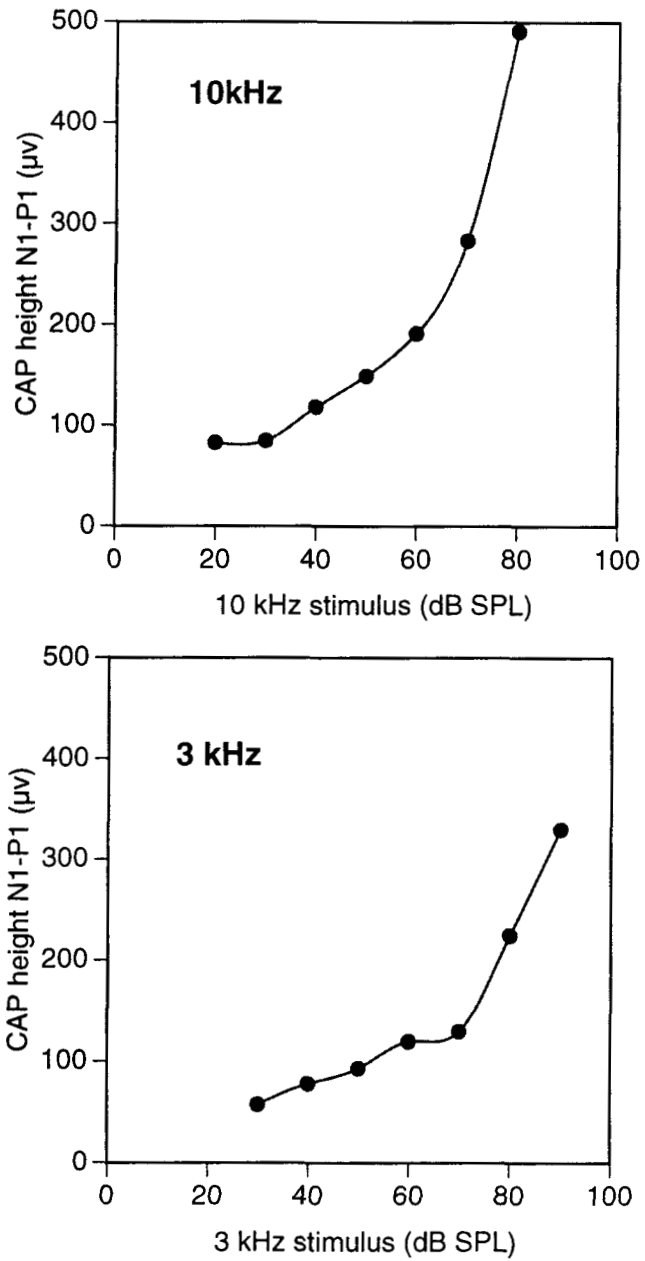


**Figure 3.12:** Tone-evoked compound action potential: stimulus/response curve. Data from expt **D39(11)**.

## Compound action potential

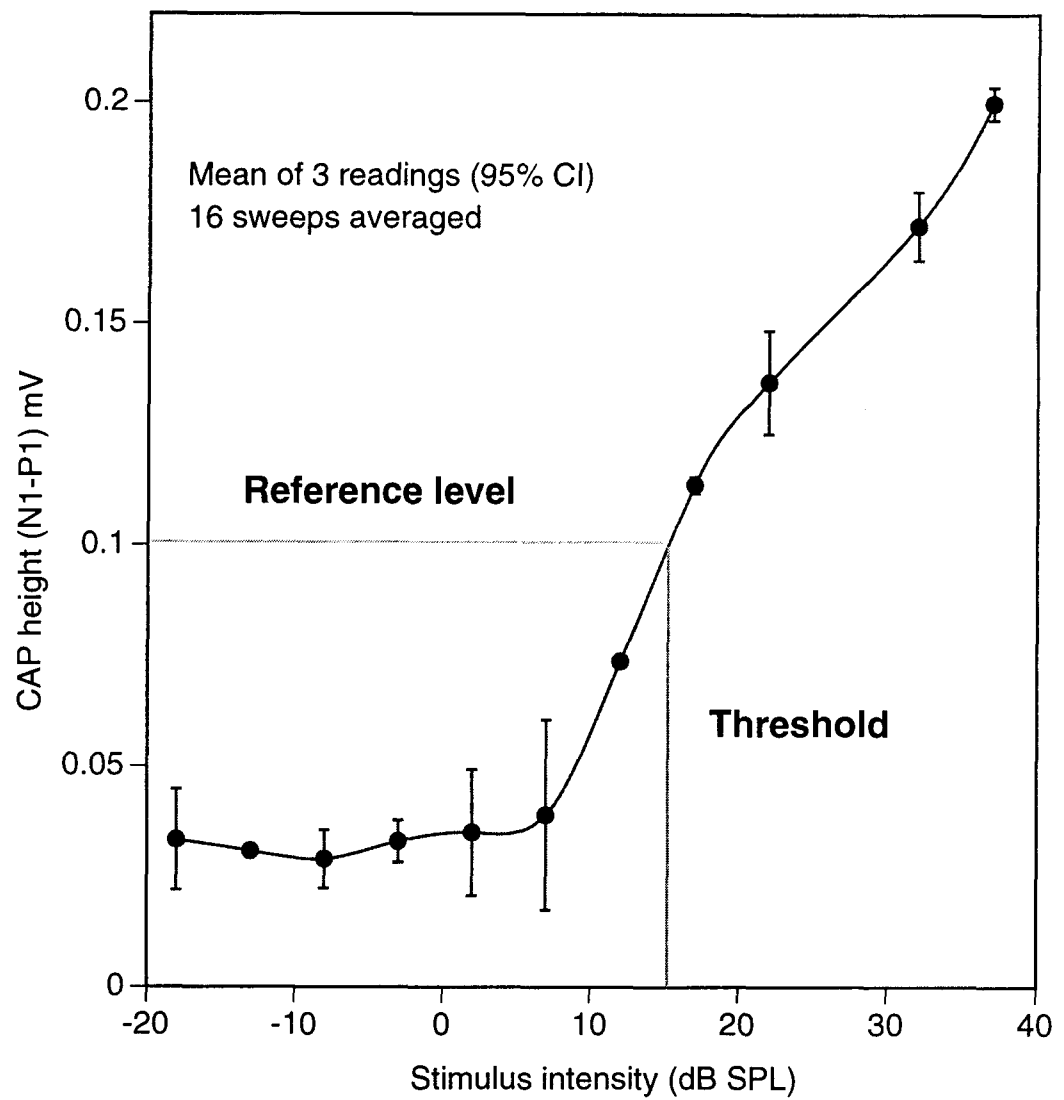


**Figure 3.13:** The definition of the compound action potential threshold in terms of a reference (criterion) level.

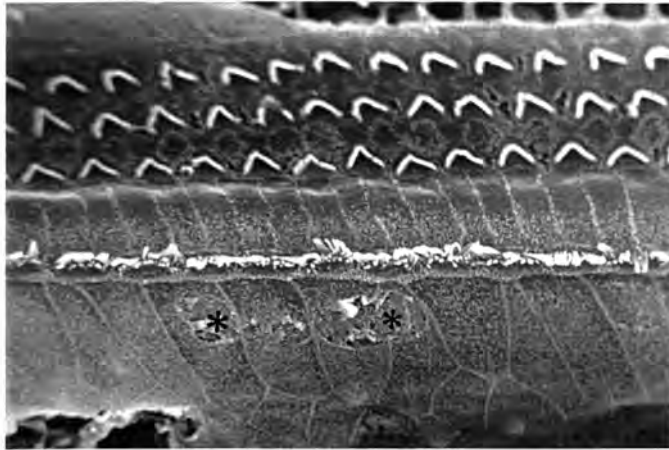


**Plate 3.19**

D39 (5) R basal turn of organ of Corti x800, 10 h p.i.  
Surface cratering of border cells (asterisks).



**Plate 3.20**

D39 (6) L basal turn of organ of Corti x5,000, 10 h p.i.  
Severe damage to IHC hair bundles. The IHCs are torn away from  
neighbouring phalangeal cells (arrow). Superficial craters are seen in  
supporting cells (arrowhead).



**Plate 3.21**

D39 (2) R basal turn of inner hair cell x20,000, 12 h p.i.  
Disruption of the intercellular tight junctions between IHC and supporting cells. The hair bundle is deformed.



**Plate 3.22**

D39 (5) R basal turn x6,000, 10 h p.i.  
Probable microcolony of pneumococci on surface of IHC. Compare plate 3.39 and plate 3.48

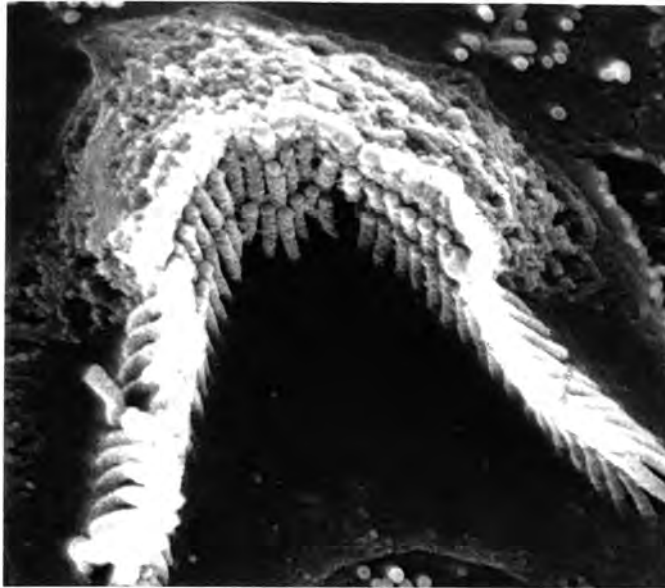


**Plate 3.23**

D39 (5) R basal turn x15,000, 10 h p.i.  
The apical surface of this row 2 OHC is pitted and the cell is torn away from its neighbour.

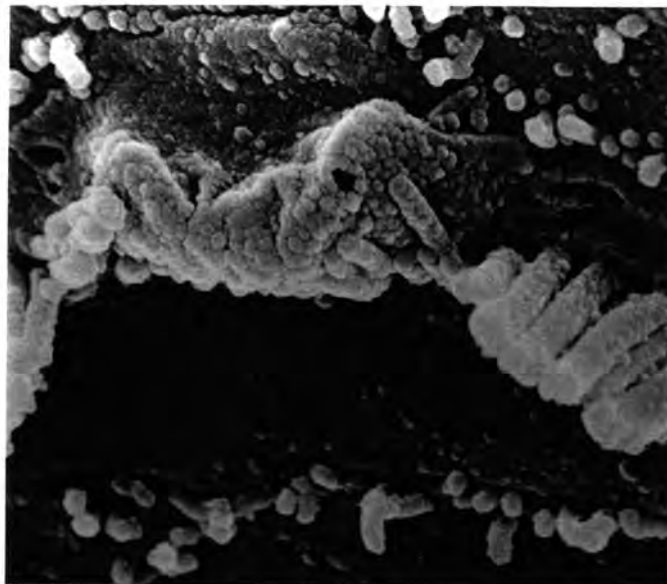


**Plate 3.24**

D39 (2) R basal turn x20,000, 12 h p.i.  
Row 2 OHC. The apical surface is grossly deformed and the hair bundle stereocilia have degenerated .

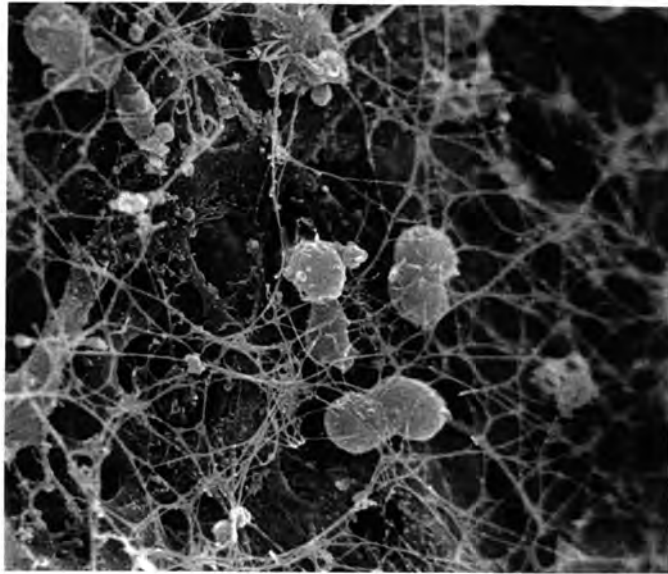


**Plate 3.25**

D39 (5) L basilar membrane x1,500, 10 h p.i.  
Leukocytes and organisms invading the basal turn of the scala tympani. Note the debris consisting mostly of 'inflammatory string'.

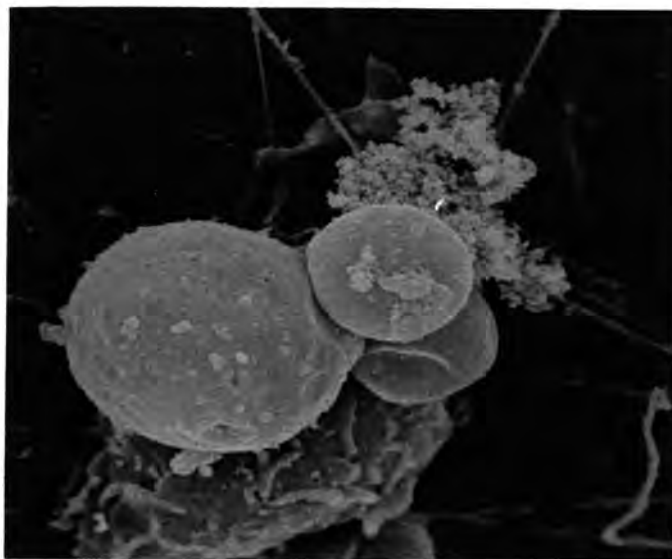


**Plate 3.26**

D39 (6) R basal turn x6,000, 10 h p.i.  
Leukocytes and inflammatory debris on the basilar membrane.

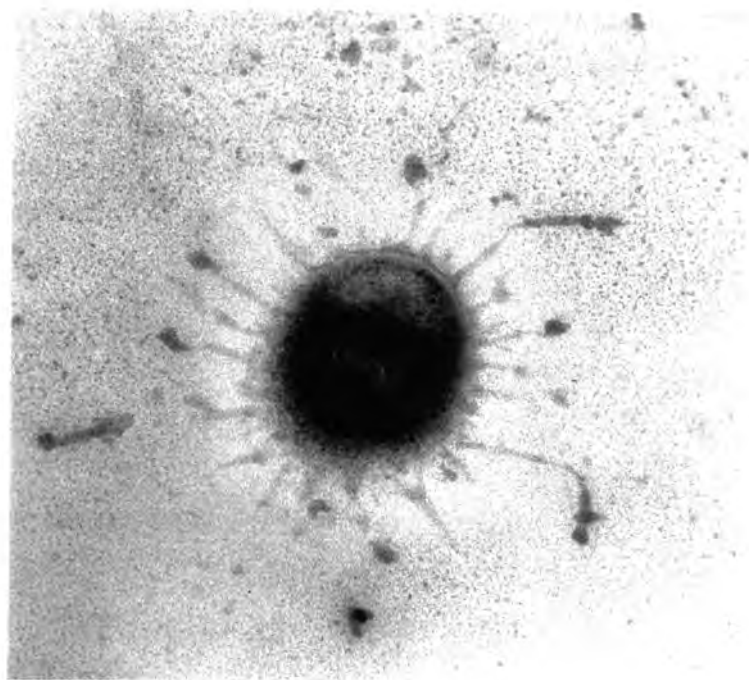


**Plate 3.27**

Cross section of *S. pneumoniae* found near the basilar membrane.

x72,500.

The capsule appears to have condensed.

### 3.3. Experimental meningitis with wild type (D39) organisms.

#### 3.3.1. Introduction and exclusions.

The experiments reported in section 3.2 laid the foundation for the final investigation of the differences between wild type and accessory virulence-factor deficient meningitis. The emphasis now was on maintaining recordings for 12 h and collecting sufficient data to allow a meaningful statistical comparison between relevant groups at this particular pre-defined time point. The data are presented for the wild type and each mutant in turn. Section 3.8 outlines the statistical comparison between the groups.

A single batch of D39 was used in experiments D39(14) to D39(19) reported here (Batch F). In addition, the wild-type data series includes animal PLN-A(2) (Batch G) which was inoculated with a pneumolysin-producing strain (wild type phenotype), rather than the intended PLN-A. Animals labelled NA+(1) and NA+(2) (Batch K) were inoculated with a strain expressing neuraminidase activity, rather than the intended NA-deficient strain, and were also included. All inocula tested were ERY sensitive as expected. Expt D39(18) was excluded because the initial CAP thresholds were over 70 dB SPL in both ears. No CSF sample was obtained in expts. D39(19) and NA+(2). The right-side round window membrane was perforated in expt D39(16). Therefore a total of 8 experiments and 15 cochleas were evaluated.

Experimental data is given in table 3.6 and figs 3.14 to 3.19. Scatter plots of all the data can be found after section 3.8 (page 186 et seq). The raw electrophysiological data for each experiment can be found in the appendix.

#### 3.3.2. Bacteriological findings.

The mean inoculum was 7.5 log<sub>10</sub>, CFU (range 7.3–7.7; n=8). The mean CSF viable count 12 h p.i. was 8.7 log<sub>10</sub>, CFU/ml (range 8.1–9.3; n=6) (fig 3.31).

In experiment D39(17), inoculated with 7.3 log<sub>10</sub>, CFU, CSF was sampled every 3 h via an indwelling cisternal needle. Viable counts were obtained as follows:

Time (h)	3	6	9	12
CSF viable count (log <sub>10</sub> , CFU/ml)	6.7	7.0	7.4	8.1
CSF WCC (cells/μl)	540	3,920	3,860	6,600

Taken together, the data support the hypothesis that the inoculum is diluted on injection into the CSF space and enters log phase growth, and constitute reasonable evidence for in vivo growth. It is likely that with this inoculum bacteria would probably have reached stationary phase by 12 h p.i. The absence of a significant lag phase in the single experiment above is in accordance with the published data for D39 meningitis in the rabbit (Friedland et al 1995).

All animals from which a terminal cardiac sample was obtained were bacteraemic with a mean viable count in the blood of  $6.6 \log_{10}$  CFU/ml (range 6.2–7.1; n=5) (fig 3.34).

### 3.3.3. Inflammatory response.

A CSF leukocytosis was seen in all animals from which a CSF sample was obtained. The geometric mean CSF white cell count 12 h p.i. was 10,500 cells/ $\mu$ l (range 1,700–32,000; n=6) (fig 3.32). The geometric mean CSF protein concentration was 1.6 g/l (range 0.4–4.0; n=6) (fig 3.33). In experiment D39(17), no white cells were observed 1 h after inoculation but a CSF leukocytosis was apparent by 3 h p.i.

### 3.3.4. Electrophysiological data.

The improved precision of round window CAP recording meant that differences in hearing loss between groups of animals could be confidently detected. For each group in this and subsequent sections the following are reported:

- Mean CAP loss (+ 95% confidence intervals) at 10 kHz and 3 kHz 12 h post inoculation;
- Mean rate of hearing loss over time at 10 kHz and 3 kHz (D39 and PLN-A **only**).
- CAP loss (mean+95% CI) in steps of 1 kHz between 3 kHz and 10 kHz at 3, 6, 9 and 12 h post inoculation (the 'audiogram').
- Mean percentage change in cochlear microphonic 12 h p.i.

Typical experimental recordings are shown in fig 3.14 (control expt PLN-A(14)) and fig 3.15 (expt D39(17) left). In the control experiment (where the inoculation failed and no CSF inflammation resulted) there is little change in peak cochlear microphonic or in CAP threshold over the course of 10 h. By contrast, fig 3.15 demonstrates the typical findings during experimental wild-type meningitis. There is hearing loss of around 45 dB at 12 h p.i. which is, in this example, evenly distributed across the frequency range tested. The cochlear microphonic is also significantly reduced 12 h p.i.

### ***Compound action potential***

All animals infected with wild type D39 had lost hearing by 12 h post inoculation. The mean CAP loss 12 h p.i. was 50 dB (range 21–75; n=15) at 10 kHz and 42 dB (range 23–70; n=15) at 3 kHz. It was sometimes difficult to elicit a clear CAP with a stimulus frequency of 3 kHz, as interference from the cochlear microphonic could be difficult to filter out. There was a strong correlation in terms of individual ears between 10 kHz CAP loss and 3 kHz CAP loss at 12 h p.i. ( $r=0.85$ , 95% CI 0.57 to 0.94,  $F=5.4$   $p=0.0001$ ). The scatter plots (see fig 3.35 and 3.36) revealed no particular differences in CAP loss between left or right ears at either 10 kHz or 3 kHz.

Figure 3.16 shows CAP loss as a function of time post-inoculation for 10 kHz and 3 kHz stimuli. By grouped linear regression over the post-inoculation period 0 h to 12 h, the mean rate of CAP loss was calculated as 4.4 dB/h at 10 kHz and 3.6 dB/h at 3 kHz.

### ***Hearing loss in relation to stimulus frequency.***

Figures 3.17 and 3.18 show what will be referred to as the 'audiogram'. CAP loss (mean+95% CI) is plotted in 1 kHz steps from 3 kHz through 10 kHz at 3 h, 6 h, 9 h and 12 h after inoculation. Full data was not collected in all wild-type experiments where n=15 for 3 kHz and 10 kHz but n=11 for other frequencies. There is a suggestion that hearing loss at 10 kHz occurred very slightly earlier than losses at other frequencies, but from 9 h p.i. onwards hearing loss most affected the frequency range 5-7 kHz. These data contradict a previous study of experimental pneumococcal meningitis in the rabbit which had suggested that high frequency hearing loss would occur substantially earlier than low-frequency loss (Bhatt, 1993).

### ***Cochlear microphonic***

Cochlear microphonics elicited at 3 kHz declined steadily in almost all experiments from 3 h p.i. onwards. The median final CM amplitude was just 18% of baseline (range 0-90%; n=15). All five animals with unrecordable cochlear microphonics had a CAP loss of at least 54 dB. Cochlear microphonic amplitude at 12 h p.i. (as percent of baseline) correlated inversely with the amount of CAP loss at 10 kHz (Spearman's  $\rho=-0.71$ , 95% CI  $-0.90$  to  $-0.32$ ;  $p=0.004$ ; *scatter plot* fig 3.37). There was less correlation with CAP loss at 3 kHz (perhaps because at this frequency reliable CAPs were more difficult to elicit).

### ***Shape of the CAP waveform***

The shape of the CAP was noted to change during an experiment as a greater stimulus was needed to regain the reference level. In normal ears and ears with a moderate CAP loss (fig 3.19a), successive compound action Potentials were uniform, with a small initial  $P_0$  and

identical  $N_1$ - $P_1$  waves occurring with precisely the same latency. In ears which had lost substantial hearing ( $>50$ dB), the CAP sometimes 'dropped out' for every third or fourth stimulus, and could not be elicited. This phenomenon was not usually apparent until 9 h p.i. Closer inspection of successive CAP recordings (fig 3.19b) in such an affected ear demonstrates two important findings:

- i) Successive CAPs are dissimilar. The height of the  $N_1$ - $P_1$  wave varies markedly, although the mean peak-peak height is of course  $100 \mu\text{V}$ . The latency also varies slightly, and this would have a significant effect on the averaging process.
- ii) In several recordings a prominent  $P_0$  is apparent. This wave is thought to represent massed synaptic depolarisation at the base of the sensory cells, and is normally dwarfed by the subsequent action potential response (Eybalin, 1993 p 323).

Reasons why the compound action potential might become non-uniform include impairment of the cochlear filter (in the light of the pronounced OHC damage) allowing varying groups of fibres to contribute to the CAP, disturbance of synaptic transmission at the base of the hair cell, and axonal pathology such as spontaneous firing that would mean some axons were refractory and could not be recruited by the stimulus.

### **3.3.5. Ultrastructural findings.**

Nine cochleas were examined by SEM (of which two were not evaluated because the organ of Corti had curled during processing). One cochlea was subjected to a detailed TEM study. A summary of the histological changes is detailed in table 3.6. The same pattern of damage was observed as in the preliminary study, namely cratering of border cells with associated disruption of IHC stereocilia (plate 3.28) and damage to the apical surface of outer hair cells and their hair bundles (plates 3.29-3.34).

Damage to outer hair cells 12 h p.i. was strikingly more extensive than in the preliminary study. In general, row 1 and 2 OHCs were more affected than row 3 OHCs, and the basal turn more affected than the mid turn. Four main categories of damage were seen:

- i) There were gross defects in the apical cell membrane (plates 3.30, 3.31), which was usually breached at the site of the basal corpuscle (plate 3.32) at the apex of the 'V' formed by the stereocilia. A higher power view (plate 3.33) shows what appear to be cell contents extruding from a row 2 OHC. The bordering phalangeal process appears to be intact.

- ii) Many hair bundles were devastated (plate 3.31). Stereocilia were detached from the sensory cell or had degenerate plasma membranes (plate 3.33). Other stereocilia were fused together (plate 3.34).
- iii) OHCs appeared to be swollen and ballooned with breaks in the basal plasma membrane (plates 3.32 & 3.40). Mitochondria were abnormal and vacuolated. Intercellular junctions were also damaged; at times the cuticular plate seemed to be lifted clear of the bordering phalangeal cell processes (plate 3.34).
- iv) Nerve endings suffered pathological damage as judged by TEM (plate 3.32). Mitochondria within nerve endings were vacuolated and highly abnormal.

Hair bundles of IHCs were also affected. Stereocilia were sometimes fused together (plate 3.35). In other cells, the lateral links were disrupted and the hair bundle had collapsed onto the cell (plate 3.36). The rootlets appeared to be stretched at the insertion into the cuticular plate (plate 3.37).

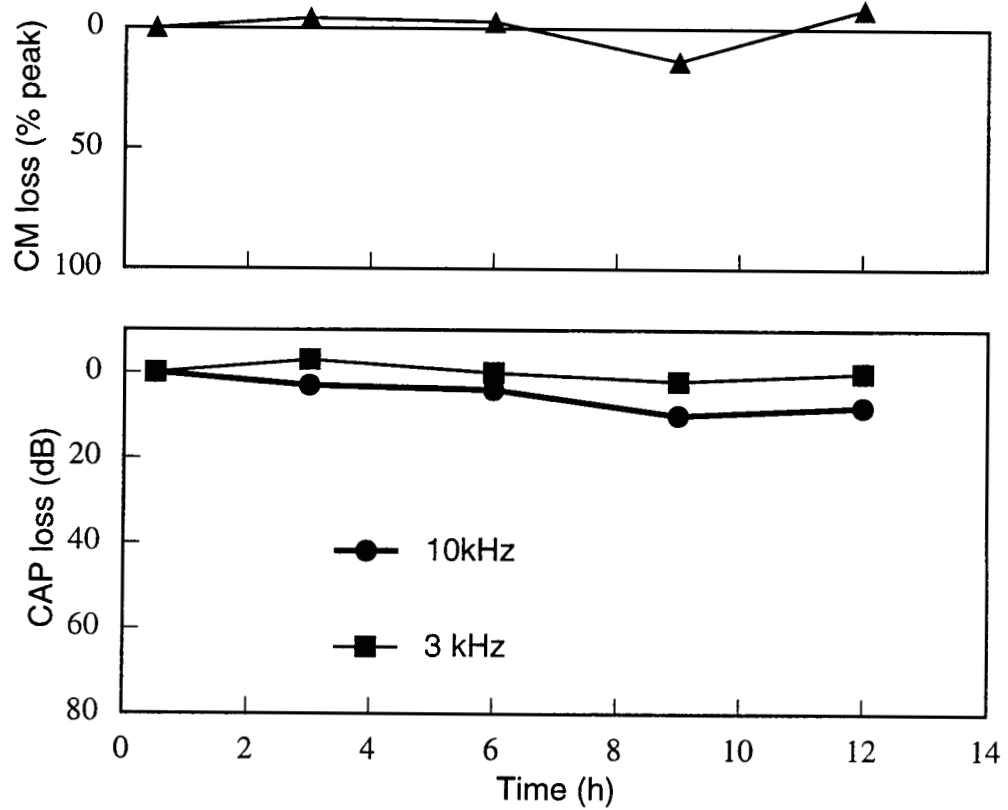
Border cells and phalangeal cells were also damaged with craters in their apical surfaces seen by SEM (plate 3.38.). Sometimes the contents of a phalangeal cell could be seen extruding into scala media (plate 3.40). These cells also appeared to be swollen and contained abnormal mitochondria. Colonies of what appeared to be pneumococci could sometimes be found closely associated with the inner hair cell surface (plate 3.39).

Expt no.	Batch	Inoculum (log <sub>10</sub> CFU)	CSF CFU (log <sub>10</sub> /ml)	Blood CFU (/ml)	CSF WBC (cells/μl)	CSF protein	Estimated hearing loss (dB; L/R)		CM ratio (L/R)	Histological findings
							@10 kHz	@ 3kHz		
D39 (14)	F	7.6	9.3	7.1	13,850	4.0	56/62	54/44	0.00/0.00	(R) & (L): Many ISC craters; OHC apical surface and s/c damage. TEMs show breaches in OHC apical surface, nerve ending damage and blown supporting cells.
D39 (15)	F	7.3	8.7	6.2	32,000	–	24/66	37/57	0.32/0.00	Leukocytes on (R) basilar membrane (organ of Corti not examined); (L) all curled.
D39 (16)	F	7.4	8.2	6.2	1,700	1.1	37/–	23/–	0.30/–	Widespread OHC damage worse on (L), detachment of IHC s/c and ISC craters. No organisms seen in scala media.
D39 (17)	F	7.3	8.1	6.7	6,600	0.4	45/42	43/34	0.39/0.18	(L): IHC s/c fusion and ISC craters. (R): basal turn all curled but mid-turn has no damage.
D39 (19)	F	7.5	–	–	–	2.2	21/65	25/48	0.53/0.26	(L): Some IHC s/c fusion and ISC craters. OHC less affected.(R) is similar.
PLN-A(2)*	G*	7.3	9.0	6.6	30,500	1.9	37/31	31/27	0.90/0.24	–/–
NA+ (1)*	K*	7.7	9.0	–	9,450	2.3	49/54	30/33	0.13/0.00	–/–
NA+ (2)*	K*	7.7	–	–	–	–	70/75	59/70	0.12/0.00	–/–
<b>Means</b>	–	<b>7.5</b>	<b>8.7</b>	<b>6.6</b>	<b>10,500g</b>	<b>1.6g</b>	<b>50</b>	<b>42</b>	<b>0.18med</b>	

All expts. lasted 12 h. Hearing loss data from round window recordings of CAP. \*D39 phenotype (see text). –/– = not evaluated. *g*= geometric mean. *med*=median. OHC=outer hair cell; IHC= inner hair cell; s/c=stereocilia; ISC= border cell. TEM=transmission electron micrograph.

**Table 3.6:** D39 (wild-type) meningitis experiments included in comparative study.

## Cochlear microphonic and CAP loss over time



## Audiogram

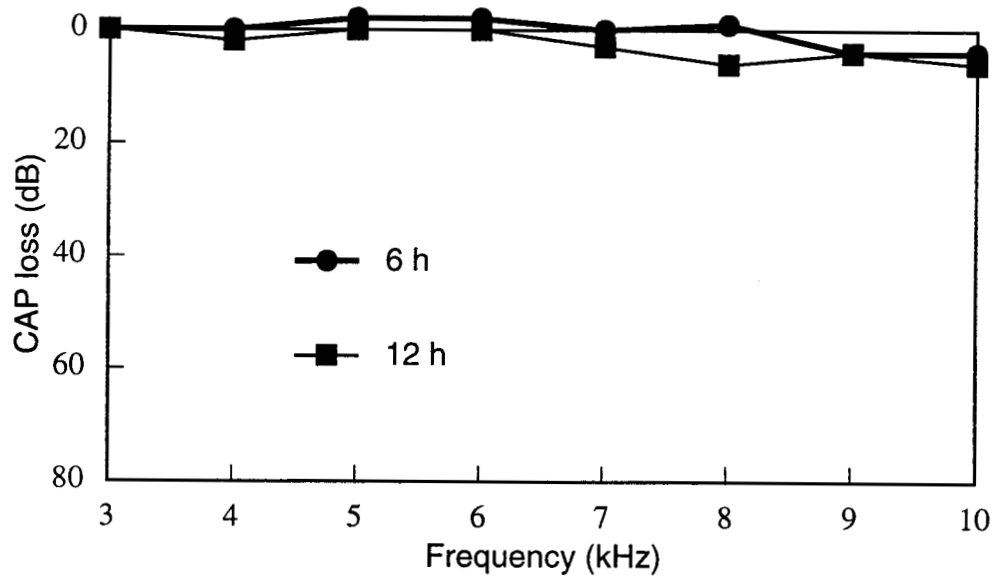
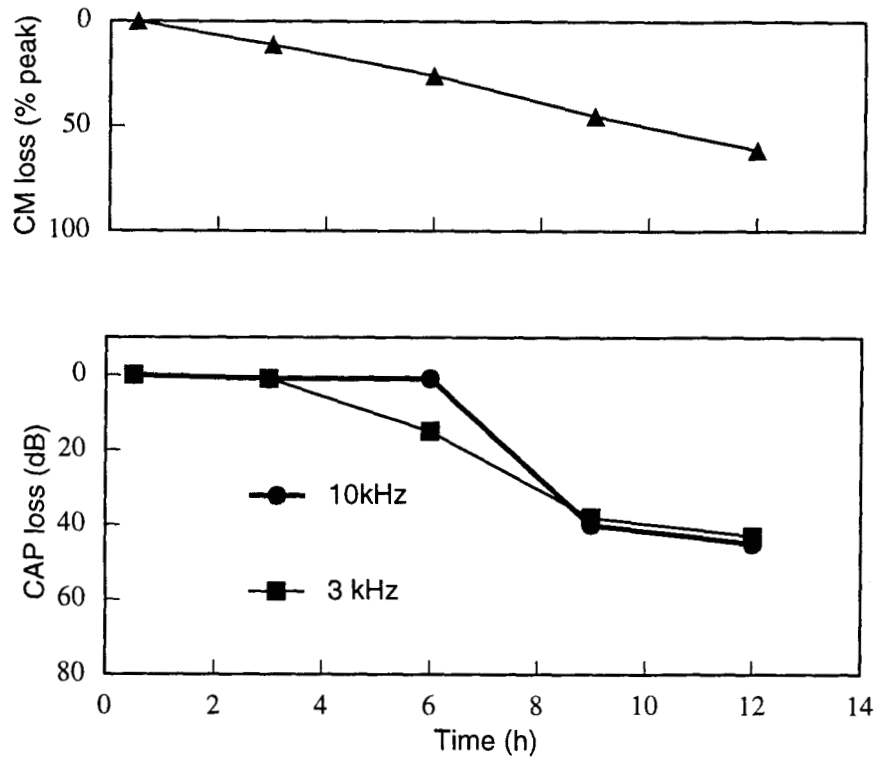


**Figure 3.14:** Control round window recording. Typical data from a control experiment (here **PLN-A(14)**) showing no loss of CAP or CM over time.

### Cochlear microphonic and CAP loss over time



### Audiogram

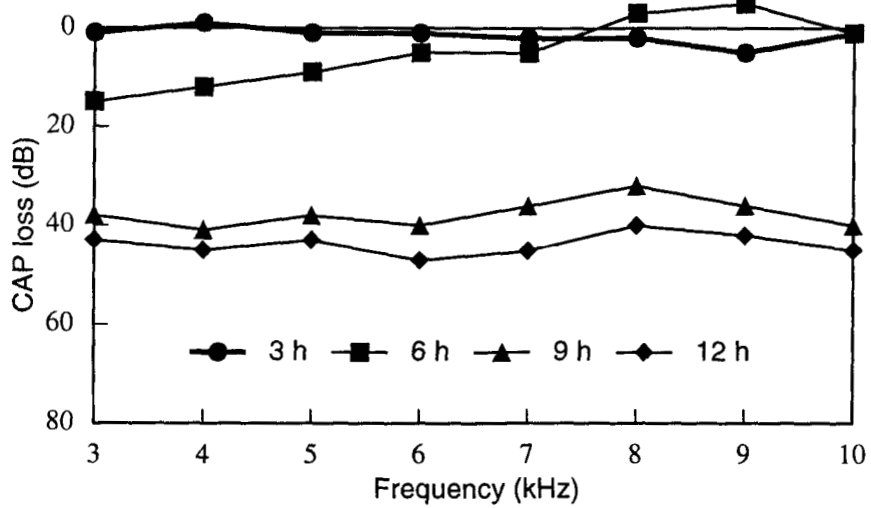


**Figure 3.15:** D39 meningitis: hearing loss over time in a typical experiment. Data from expt D39(17). h=hours post inoculation.

### D39

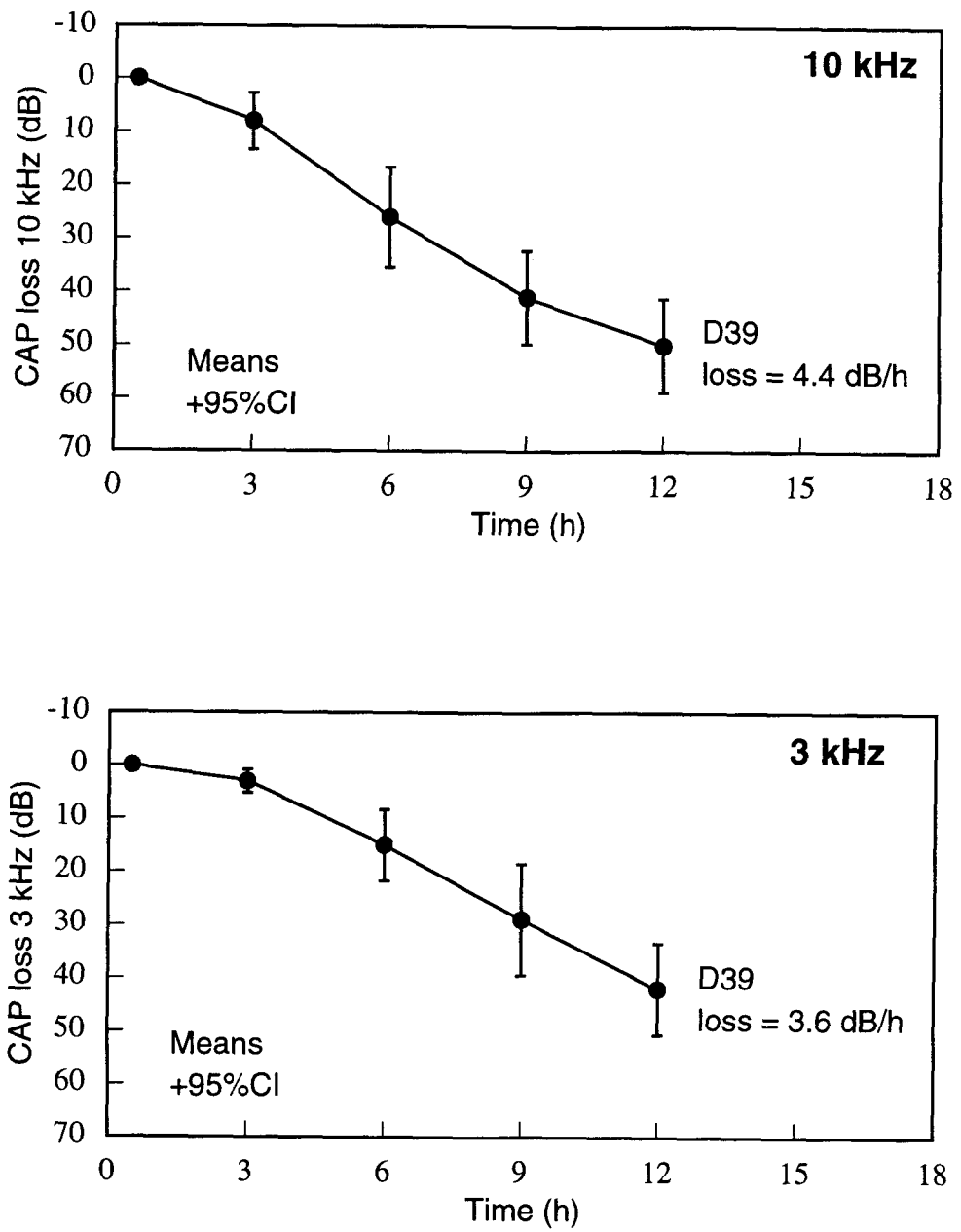
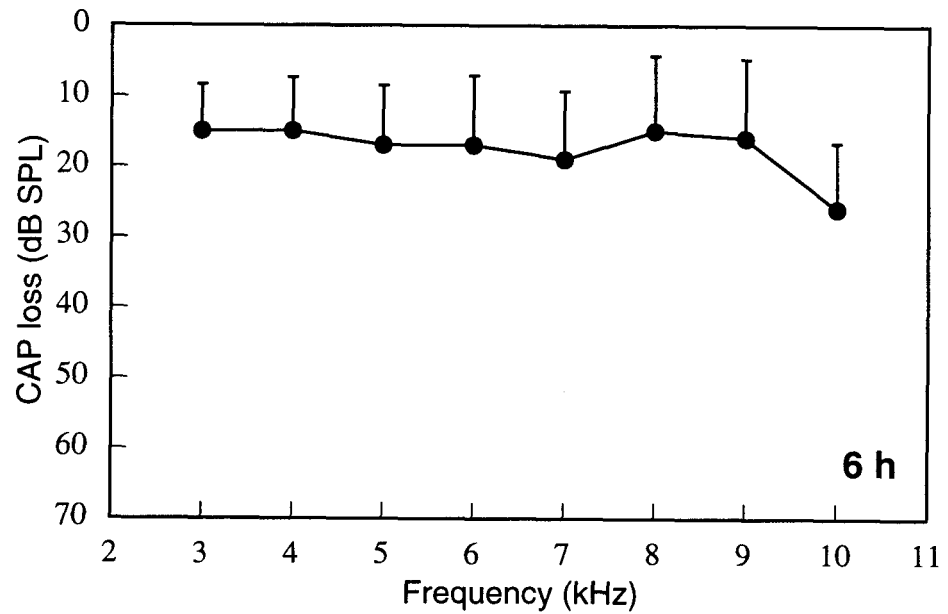
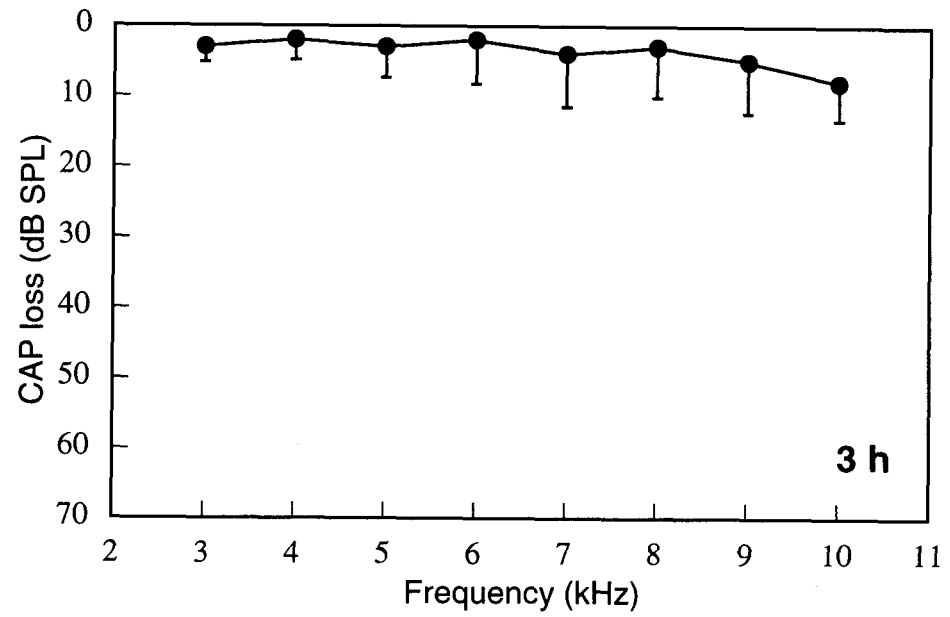


Figure 3.16: D39 meningitis: mean hearing loss over time.

### D39



**Figure 3.17: D39 meningitis: audiograms (3 h and 6 h)**  
Frequency-specific CAP loss; h=h post inoculation.;  
means + 95% CI

### D39

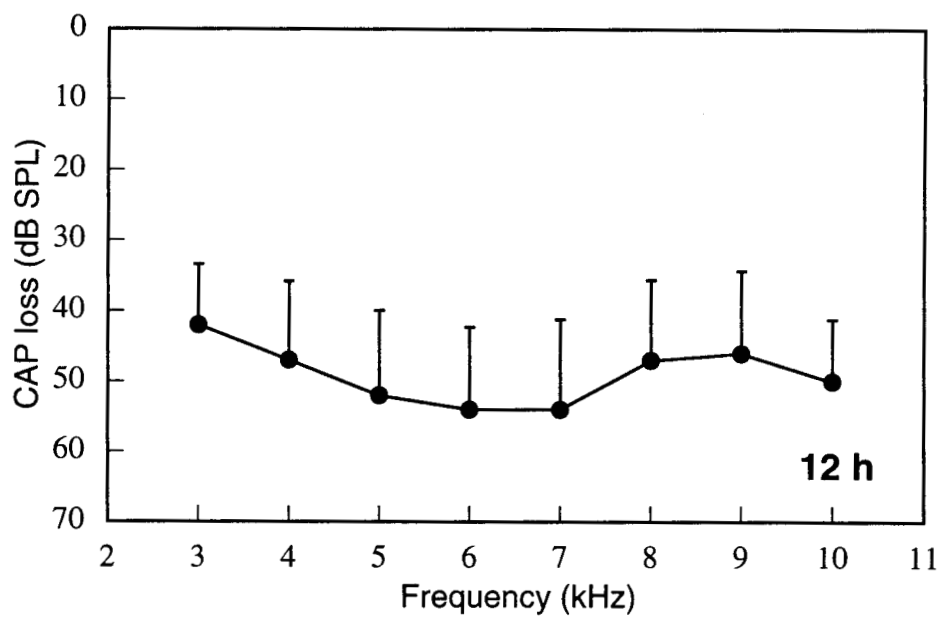
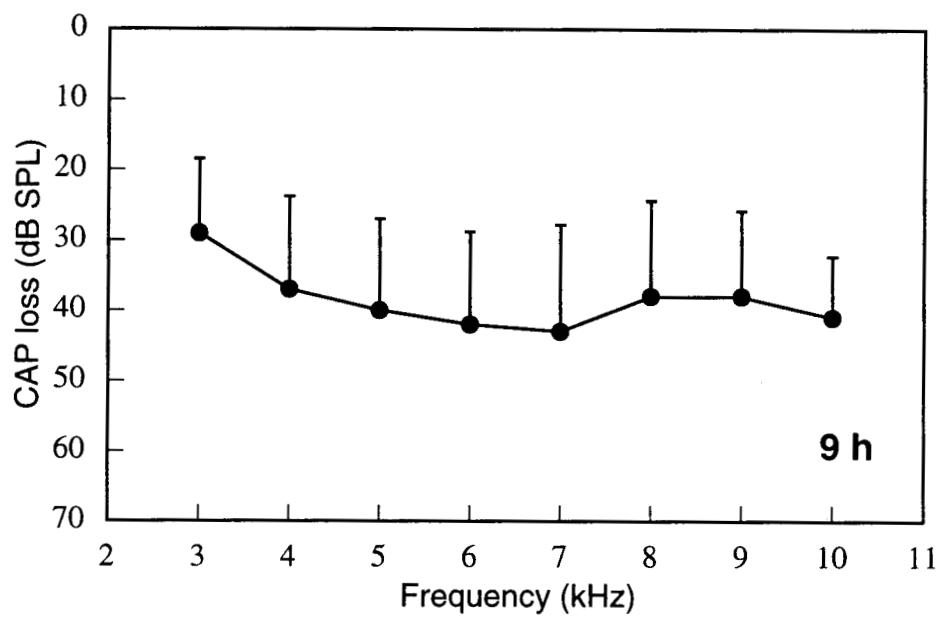


**Figure 3.18: D39 meningitis: audiograms (9 h and 12 h)**  
Frequency-specific CAP loss; h=h post inoculation.;  
means + 95% CI

### Successive CAP recordings at 100 ms intervals

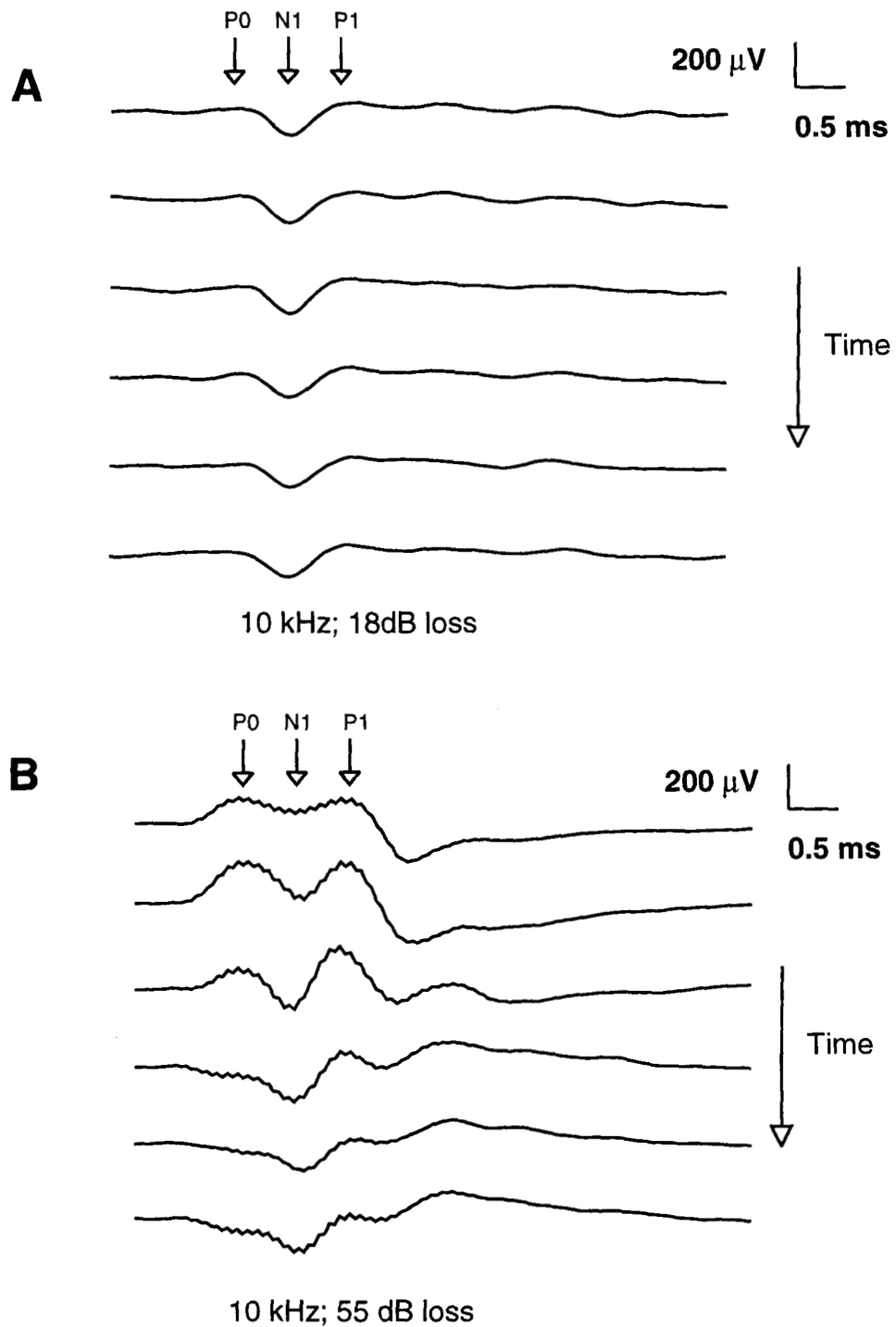


**Figure 3.19:** Serial CAP recordings from unaffected and affected ears. Composite recordings from experiment D39 (19).

**A:** (18 dB loss) successive CAPs are uniform;

**B:** (55 dB loss) successive CAPs are variable, some have a prominent  $P_o$  wave.

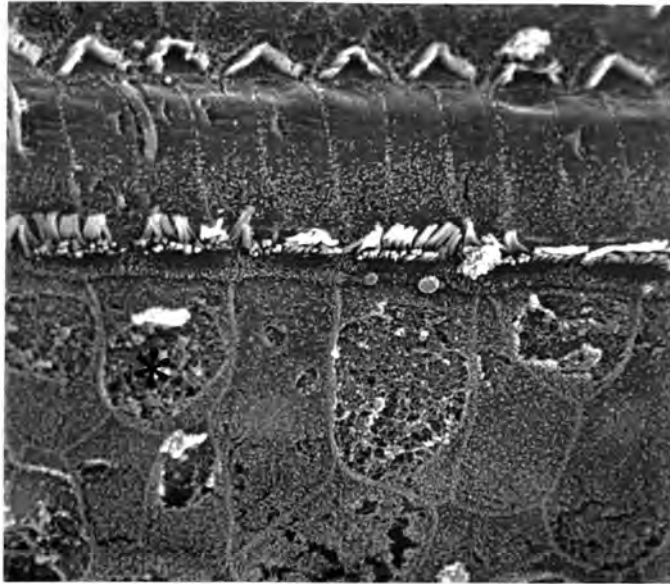


**Plate 3.28**

D39 (14) R basal turn x1,500, 12 h p.i.

There is extensive cratering of the border cells and inner sulcus supporting cells (asterisk). IHC hair bundles are deformed. The apical surface of a row 1 OHC is distorted.

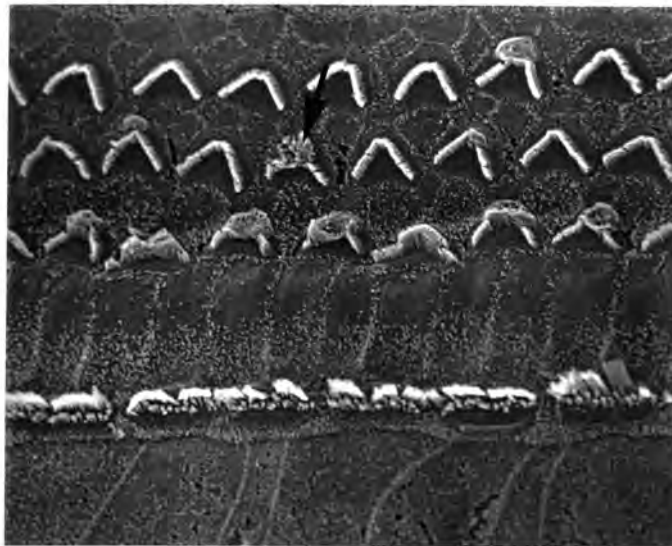


**Plate 3.29**

D39 (16) L basal turn x1,500, 12 h p.i.

There is ballooning and loss of integrity of the apical surface of many OHCs, particularly in row 1.

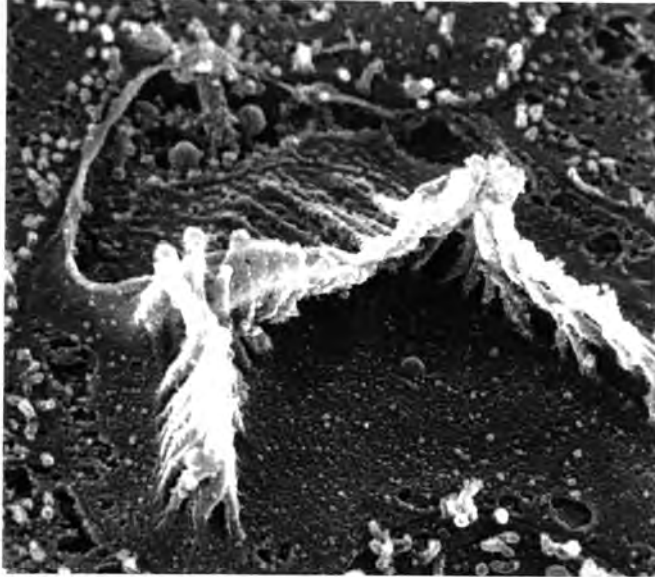


**Plate 3.30**

D39 (14) R basal turn x15,000, 12 h p.i.

The apical surface membrane of this row 2 OHC is torn at the apex of the 'V' of the stereocilia. Some stereocilia have fused together.

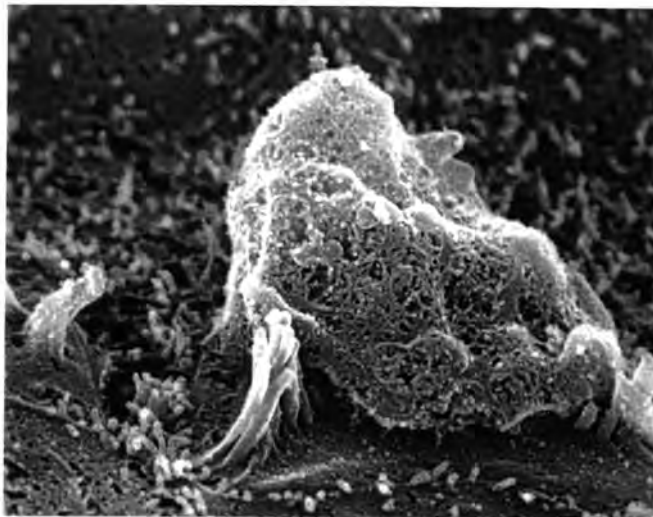


**Plate 3.31**

D39 (14) R basal turn x10,000, 12 h p.i.

Stereocilia of this row 1 OHC are fused together

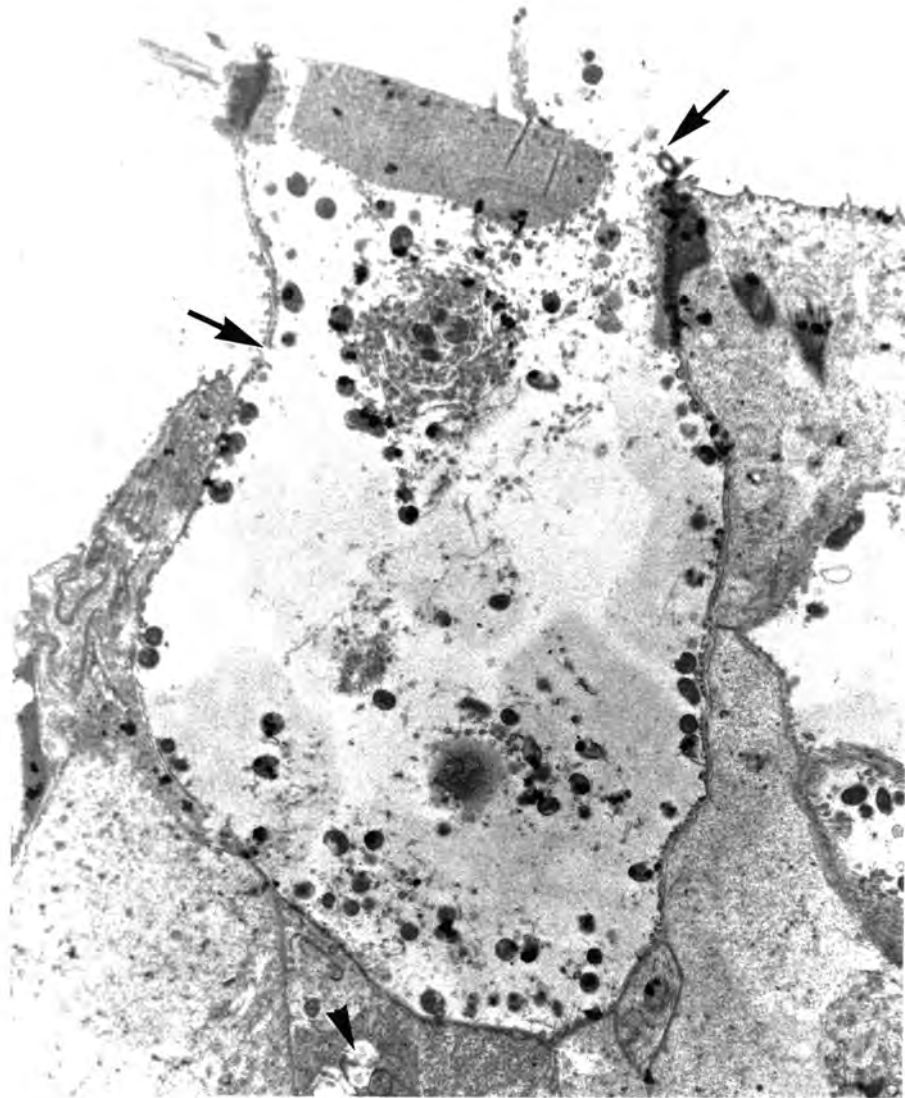


**Plate 3.32**

D39 (14) R basal turn x8,250, 12 h p.i.

Row 2 outer hair cell. There are breaks in the plasma membrane (arrows) and the apical surface is disrupted. Mitochondria in both the nerve endings and in the hair cell are vacuolated (arrowhead).

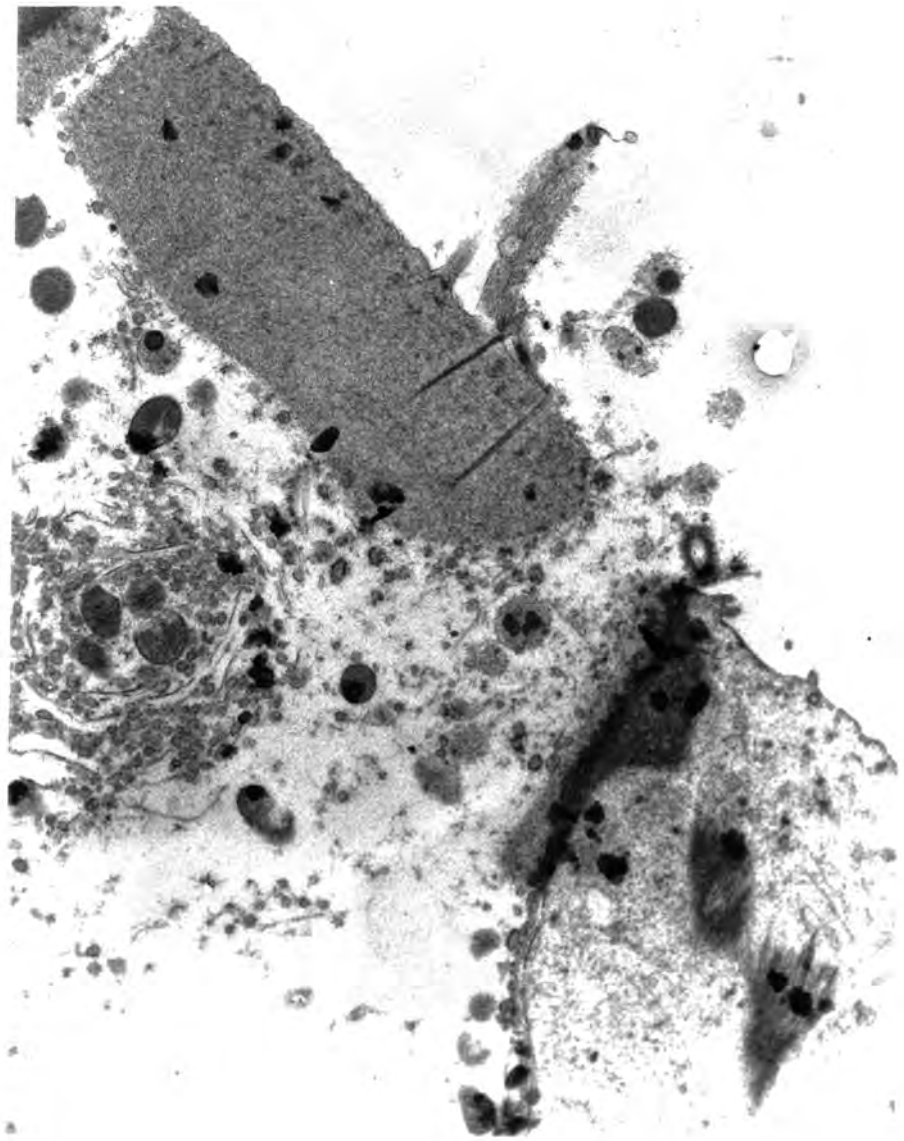


**Plate 3.33**

D39 (14) R basal turn x16,500, 12 h p.i.

A higher power view of plate 3.32. The apical cell membrane has been breached at the site of the basal corpuscle and cellular debris released. The stereocilia are indistinct and their attachments severed.

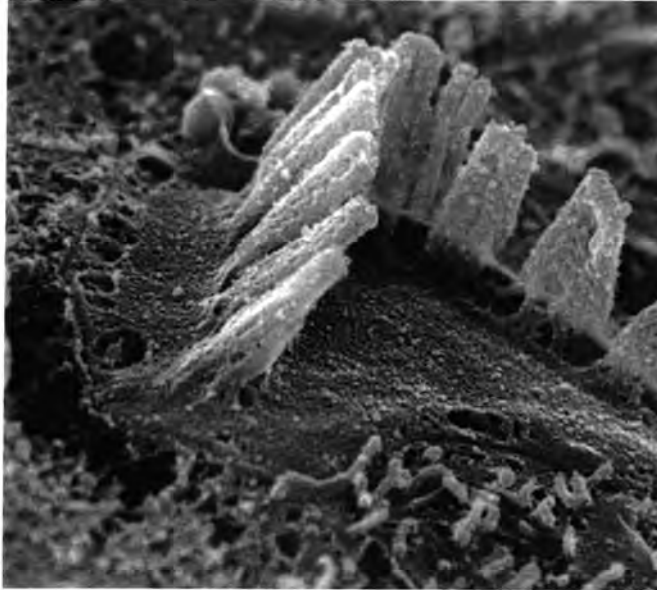


**Plate 3.34**

D39 (14) R basal turn x15,000, 12 h p.i.  
Another row 2 OHC with disintegrating intercellular junctions and fusion of the stereocilia.

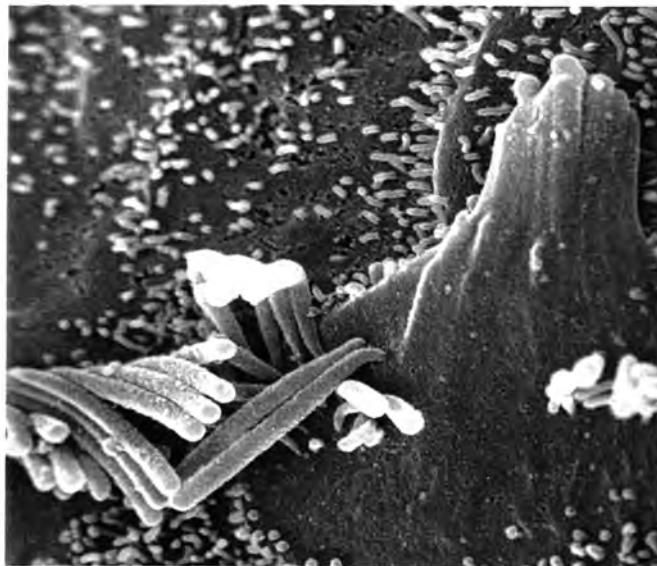


**Plate 3.35**

D39 (17) L basal turn x10,000, 12 h p.i.  
Here the plasma membranes of the stereocilia of this IHC hair bundle have fused together.

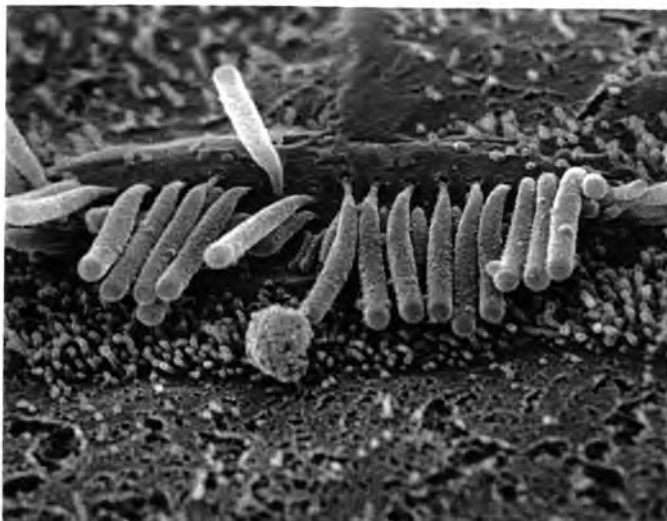


**Plate 3.36**

D39 (16) L basal turn x10,000, 12 h p.i.  
Disruption of the insertion of stereocilia into the surface of the IHC  
and loss of the lateral links between them.

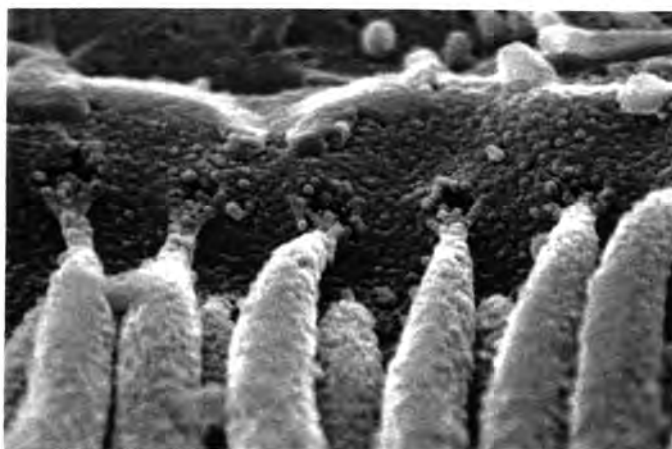


**Plate 3.37**

D39 (16) L basal turn x10,000, 12 h p.i.  
A higher power view of the roots of the IHC stereocilia which are  
stretched and appear to be detaching from the surface of the sensory  
cell.

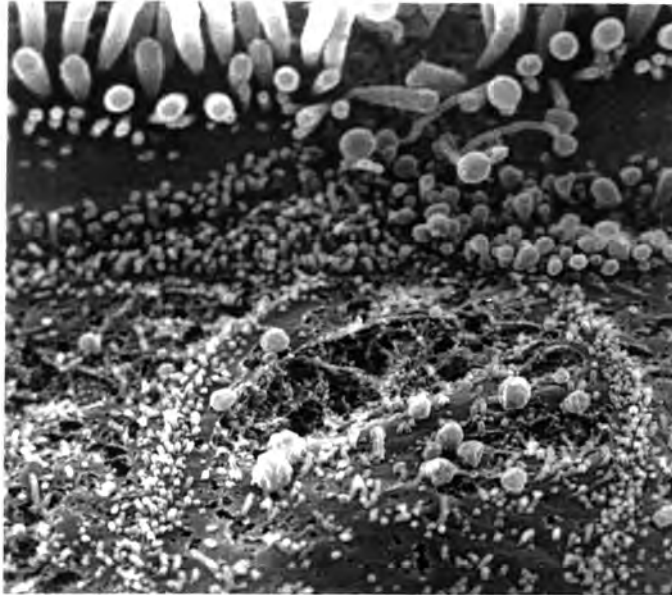


**Plate 3.38**

D39 (14) L basal turn x8,000, 12 h p.i.

A higher power view of a typical 'crater' in the surface of a border cell, revealing cellular debris and intracellular organelles.

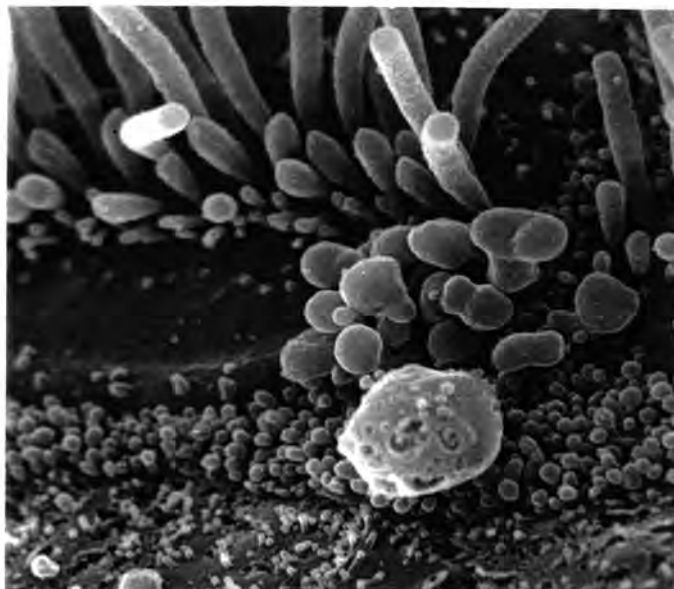


**Plate 3.39**

D39 (14) L basal turn x10,000, 12 h p.i.

Possible microcolony of pneumococci at the base of IHC stereocilia.  
Such objects were only ever seen in this location.

(Compare plates 3.22 and 3.48.)

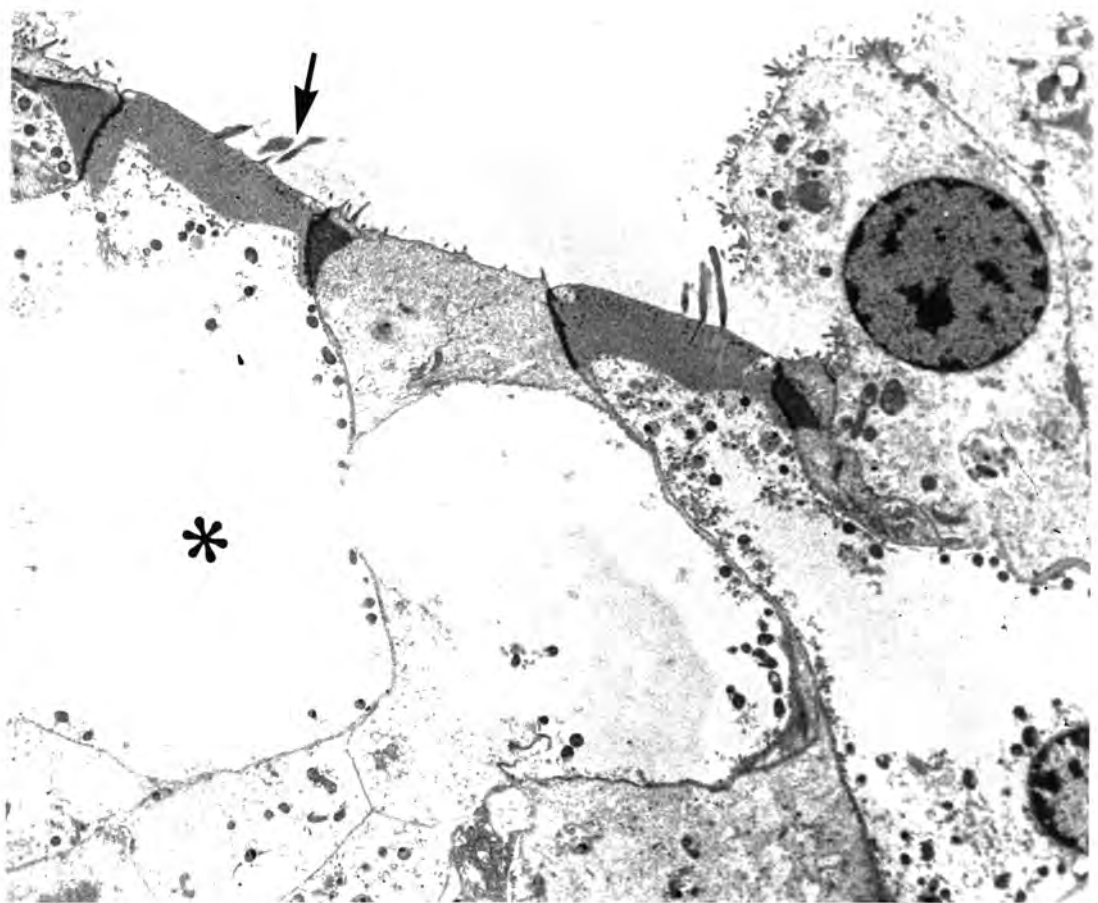


**Plate 3.40**

D39 (14) R basal turn x5,600, 12 h p.i.

On the right, the contents of an inner phalangeal cell are extruding through its apical surface. The row 2 OHC on the left is swollen (asterisk) with defects in its plasma membrane and pathological stereocilia (arrow). Mitochondria in both hair cells and neighbouring supporting cells are abnormal and vacuolated.

### 3.4. Experimental meningitis with pneumolysin-deficient organisms (PLN-A).

#### 3.4.1. Introduction and exclusions.

Five experiments were evaluated from fifteen performed. Four animals died before the endpoint of 12 h was reached. It is unclear why a run of animals died early. No significant CAP loss was noted in these animals, so their exclusion is unlikely to have materially influenced the hearing loss comparison. Four animals received an inoculum of indeterminate phenotype (discussed below). In two animals the inoculation failed to induce a leukocytosis and no organisms were recovered from the CSF. These exclusions are summarised below:

---

PLN-A (1),	Low inoculum (6.6 log <sub>10</sub> , CFU) of batch <b>E</b>
PLN-A (2)	wild-type phenotype (Batch <b>G</b> ) (included in wild type series)
(3), & (4)	Batch H. Indeterminate phenotype; mostly ERY sensitive. Mean 10 kHz CAP loss 15 dB (range 4–29; n=4)
PLN-A (6) to (8)	these four animals all died of respiratory failure between 2 h and 7 h p.i.
PLN-A (12)	Maximum recorded CAP loss at 10 kHz was 8 dB.
PLN-A (9), (14)	Failed inoculation. PLN-A(9) bacteraemic (7.1 log <sub>10</sub> , CFU/ml)

---

A formal comparison of PLN-A and D39 wild type infection is given in section 3.8.

#### 3.4.2. Bacteriological findings.

Batch E was grown in Birmingham without erythromycin selection pressure, which would encourage the loss of the genetic insert. Batch **G** was obtained from Leicester and (like Batch H) found to be fully erythromycin sensitive (rather than resistant) on checking in Birmingham, with zones of 2 cm in diameter around a 5 µg ERY disk. CSF recovered from expt PLN-A(2) was analysed in Leicester. The proportion of ERY sensitive (likely D39) to resistant (likely PLN-A) colonies was estimated at about 100:1 by colony picking. A cell lysate of recovered CSF organisms had full haemolytic activity. Although this would be consistent with reversion to wild type *in vivo*, where the genetic insert falls out and the wild-type emerges as dominant, further tests on the inoculum suggested that the organisms inoculated were in fact wild-type phenotype. It emerged that the 'stock' inocula might in fact have been animal passaged several times. Batch H experiments were therefore also excluded, although the zone of inhibition around the ERY disk was not completely clear suggesting a mixed inoculum, and hearing loss was not as great as with wild type infection. Batch J was then prepared from original stock PLN-A from Adelaide (Berry *et al* 1989) as

detailed in the methods and the resulting standard inocula found to be free of haemolytic activity and fully resistant to 60 µg ERY. It was used for the experiments listed in table 3.6. All organisms isolated from the CSF and blood in animals inoculated with batch J were ERY resistant.

The mean inoculum in animals included in the analysis was 7.5 log<sub>10</sub> CFU (range 7.4–7.7; n=5). The mean CSF viable count 12 h p.i. was 8.1 log<sub>10</sub> CFU/ml (range 7.7–8.6; n=5) (fig 3.31).

All included animals from which a terminal cardiac sample was obtained were bacteraemic with a mean viable count in the blood of 6.0 log<sub>10</sub> CFU/ml (range 4.2–8.0; n=4) (fig 3.34).

### **3.4.3. Inflammatory response.**

A CSF leukocytosis was seen in all included animals from which a CSF sample was obtained. The geometric mean CSF white cell count 12 h p.i. was 4,790 cells/µl (range 2,025–10,950; n=5) (fig 3.32). The geometric mean CSF protein concentration was 0.6 g/l (range 0.4–0.8; n=5) (fig 3.33).

### **3.4.4. Electrophysiological data.**

Animals infected with PLN-A had lost little hearing by 12 h post inoculation. The mean CAP loss 12 h p.i. was 12 dB (range –3 to 27; n=10) at 10 kHz and 18 dB (range 6–26; n=10) at 3 kHz. Successive action Potentials were always uniform. The median final CM amplitude was 65% of baseline (range 30–102%; n=10). There was no correlation between the final CM (as a proportion of baseline) and CAP loss (Spearman's  $\rho$ : –0.3,  $P=0.19$ )

Figure 3.20 shows CAP loss as a function of time post-inoculation for 10 kHz and 3kHz stimuli. The mean rate of CAP loss over the post-inoculation period 0 h to 12 h was 1.0 dB/h at 10 kHz and 1.4 dB/h at 3 kHz, significantly lower than in meningitis due to D39 (see section 3.8).

Figures 3.21 and 3.22 show the 'audiogram'. It is clear that at every frequency tested, PLN-A caused significantly less hearing loss than the parent D39 strain.

The two animals in which the inoculum failed to induce a meningitis lost almost no hearing over the course of 12 h. For these animals, mean CAP loss was 6 dB (range 0–10; n=4) at 10 kHz and 5 dB (range 0–13; n=4) at 3 kHz. The data for PLN-A(14) are shown in fig 3.14.

### **3.4.5. Ultrastructural findings.**

Eight cochleas were examined by SEM of which two were not evaluated because the organ of Corti had curled. Two cochleas were subjected to a detailed TEM study.

All six cochleas observed appeared to be virtually intact as judged by SEM (plate **3.41**). Organisms were seen on the scala tympani surface of the basilar membrane (plate **3.42**), and a gross labyrinthitis was evident in several specimens on initial dissection. Therefore the absence of damage is not because PLN-A failed to invade scala tympani.

Close inspection of OHCs revealed pitting at the site of the basal corpuscle in some cells (plate **3.43**), but the breakdown of the apical surface membrane characteristic of wild type infection was never observed. Most OHCs and their associated hair bundles appeared to be completely intact (plate **3.44** and **3.46**). Inner hair cell hair bundles were usually regular (plate **3.46** and **3.49**). Just one border cell crater was found, and here there was some disruption of the lateral links of the stereocilia on the adjacent IHC, some of which had collapsed (plate **3.47**). Organism-like structures were occasionally observed adjacent to the IHC/border cell junctions with localised disruption of the **IHC** stereocilia (plate **3.48**)

Transmission electron microscopy however revealed some specific damage to OHCs:

- i) There was some evidence of loss of sensory cell turgor (plate **3.45**)
- ii) Nerve ending damage was apparent (plate **3.50** and **3.51**). Mitochondria within the nerve ending were vacuolated, as were some within the basal region of the OHC itself.

There was however no breakdown of the junctions between sensory cells and adjacent phalangeal cells, and the apical cell surface of the OHCs and IHCs was spared (plates **3.45**, **3.50**, **3.52**).

As far as could be assessed by SEM and TEM, the critically important reticular lamina appeared to remain intact.

Expt no.	Batch	Inoculum (log <sub>10</sub> CFU)	CSF CFU (log <sub>10</sub> /ml)	Blood CFU (log <sub>10</sub> /ml)	CSF WBC (cells/μl)	CSF protein (g/l)	Estimated hearing loss (dB; L/R)		CM ratio (L/R)	Histological findings
							@10 kHz	@ 3kHz		
PLN-A (5)	J	7.6	8.0	8.0	10,950	0.8	11/7	25/13	0.58/0.30	(L) and (R): Intact organs of Corti. No ISC craters, stereocilial disruption or change in OHC/IHC surface. Organisms and few leukocytes present on BM. TEMs show intact reticular lamina and hair cells.
PLN-A (10)	J	7.7	8.1	7.0	7,260	0.7	19/-3	15/6	0.70/1.02	not examined
PLN-A (11)	J	7.4	8.6	4.7	3,730	0.4	10/10	17/18	0.84/0.68	(L): badly curled; (R): intact basal and mid turn organ of Corti.
PLN-A (13)	J	7.4	8.3	–	4,200	0.4	19/27	24/26	0.50/0.40	(R): Organisms (?) seen near IHC, no damage to OHC or IHC. (L): only one crater only seen in mid turn, TEMs show intact hair cells but damaged nerve endings.
PLN-A (15)	J	7.4	7.7	4.2	2,025	0.8	9/12	15/16	0.65/0.65	(L) intact organ of Corti. (R) curled.
<b>Means</b>		<b>7.5</b>	<b>8.1</b>	<b>6.0</b>	<b>4,790g</b>	<b>0.6g</b>	<b>12</b>	<b>18</b>	<b>0.65<sub>med</sub></b>	

All expts. lasted 12 h. Hearing loss data from round window recordings of CAP. -- = not evaluated. (technical problems etc.). *g* = geometric mean. *med* = median. OHC = outer hair cell; IHC = inner hair cell; ISC = border cell; TEM = transmission electron micrograph.

**Table 3.7:** PLN-A (pneumolysin-deficient) meningitis experiments included in comparative study..

# PLN-A

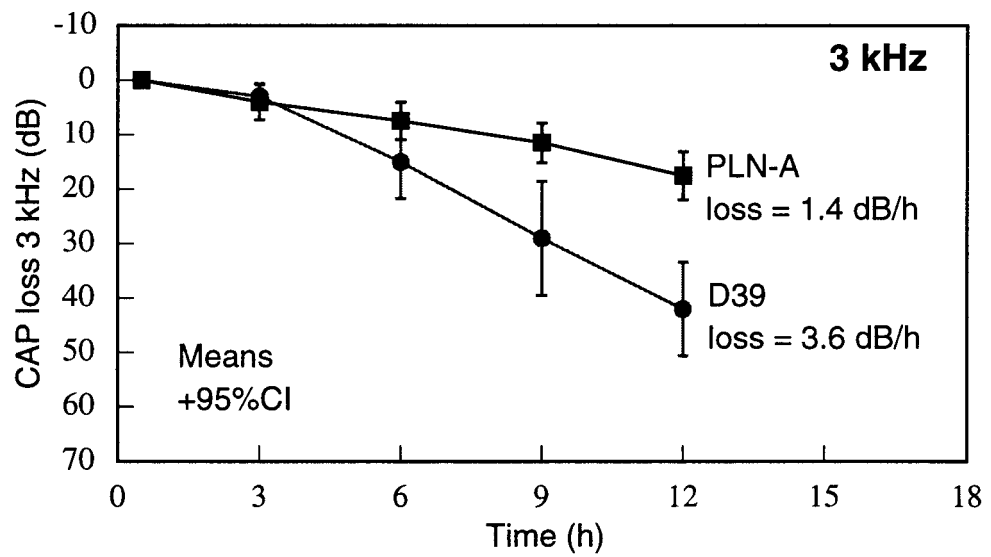
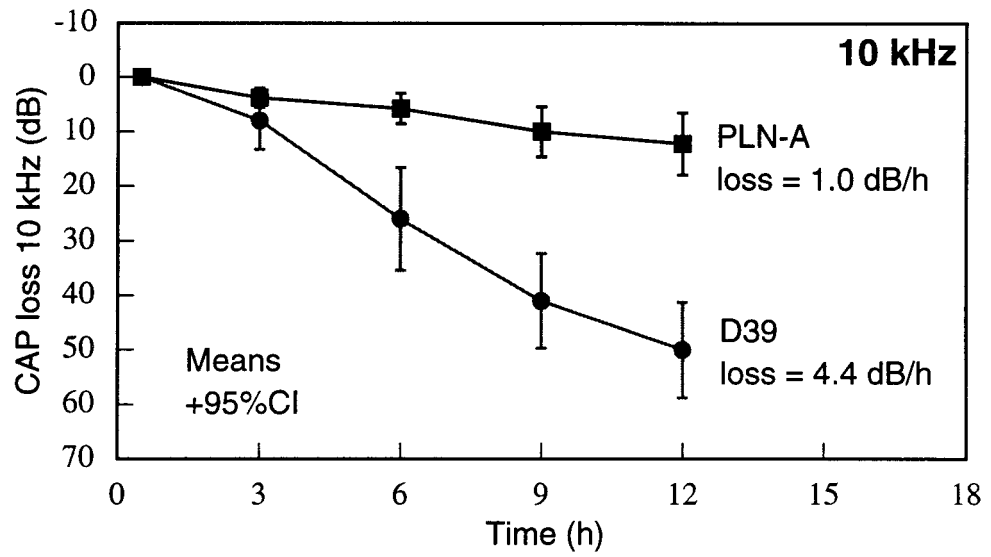


Figure 3.20: PLN-A meningitis: mean hearing loss over time.

## PLN-A

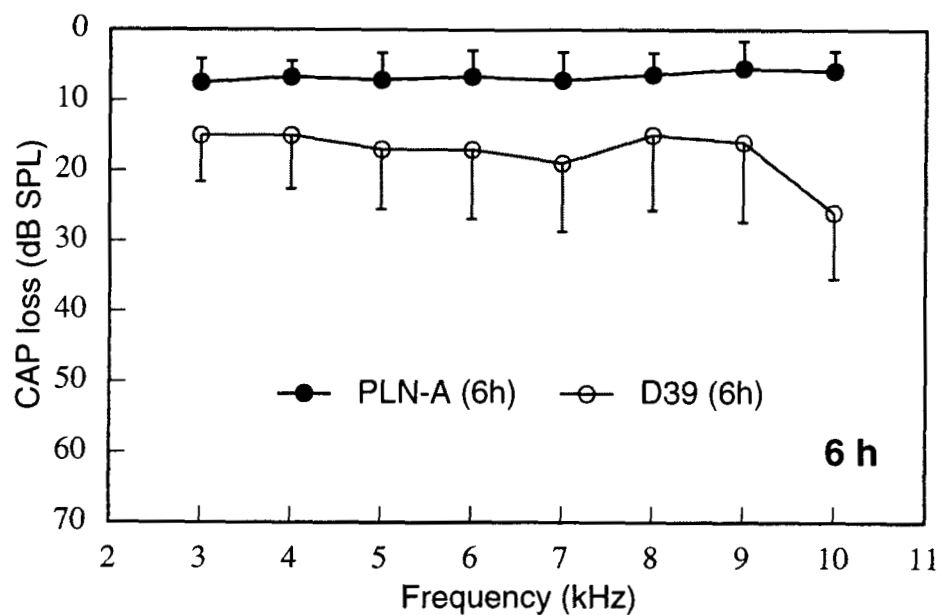
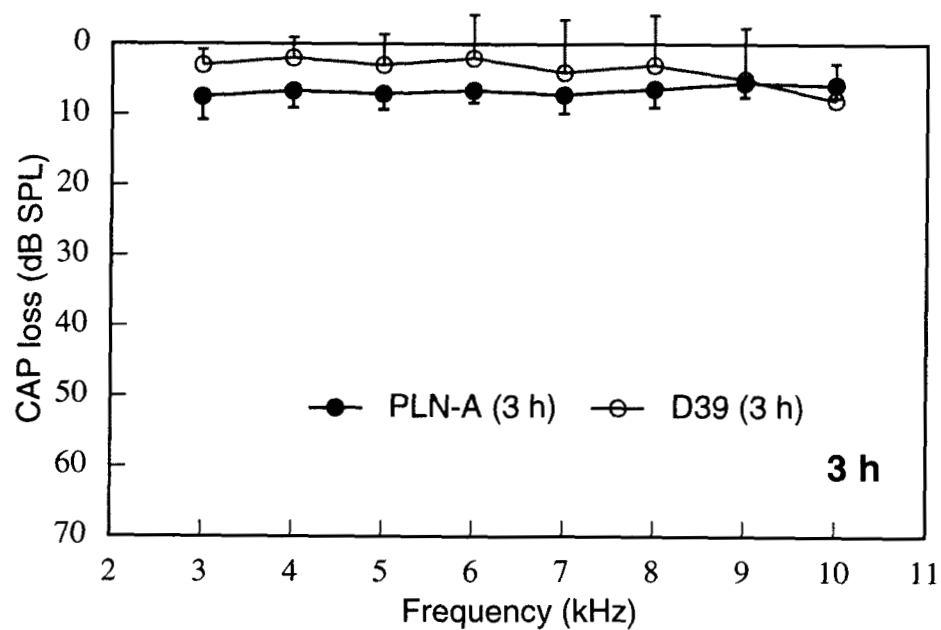
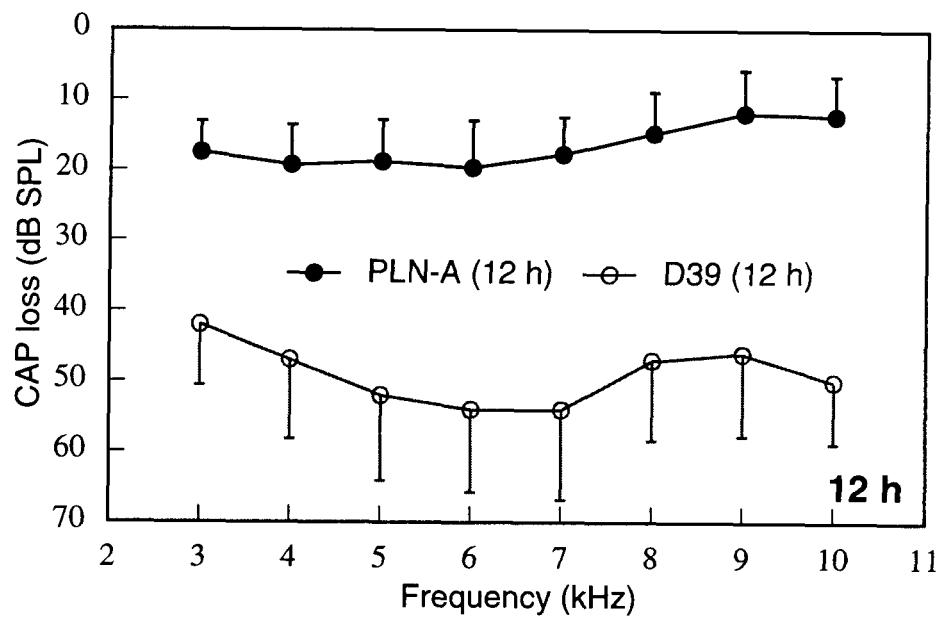
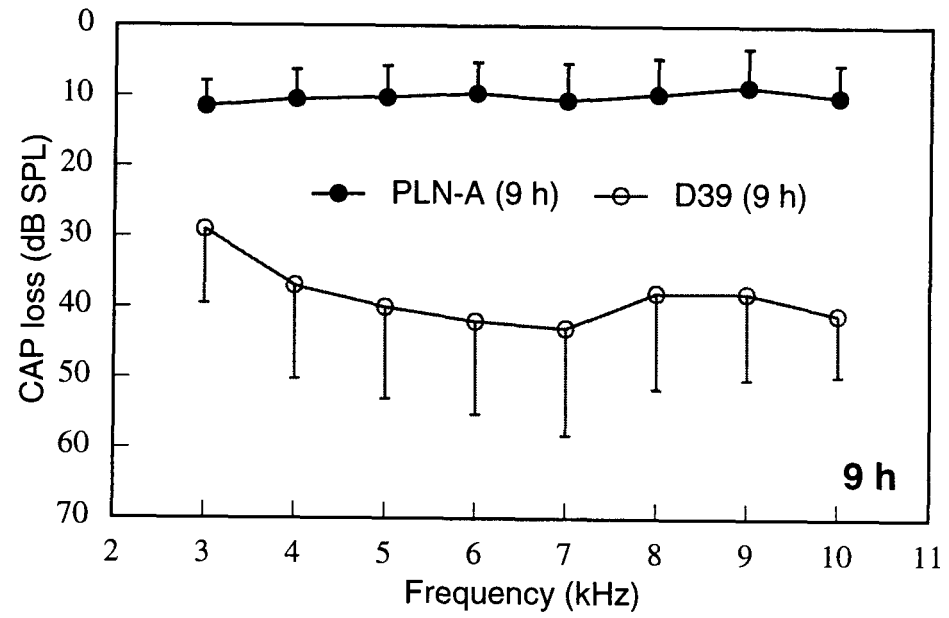
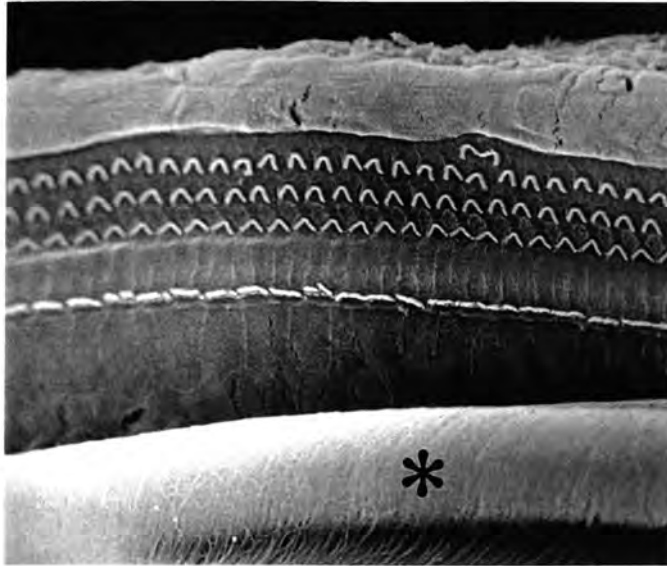


Figure 3.21: PLN-A meningitis: audiograms (3 h and 6 h)  
Frequency-specific CAP loss; h=h post inoculation.;  
means + 95% CI

## PLN-A



**Figure 3.22: PLN-A meningitis: audiograms (9 h and 12 h)**  
Frequency-specific CAP loss; h=h post inoculation.;  
means + 95% CI



**Plate 3.41**

PLN-A (5) L basal turn x500, 12 h p.i.

No lesions are seen in this well-preserved specimen. Note also the delicate lace-like texture of the rolled-back tectorial membrane (asterisk).

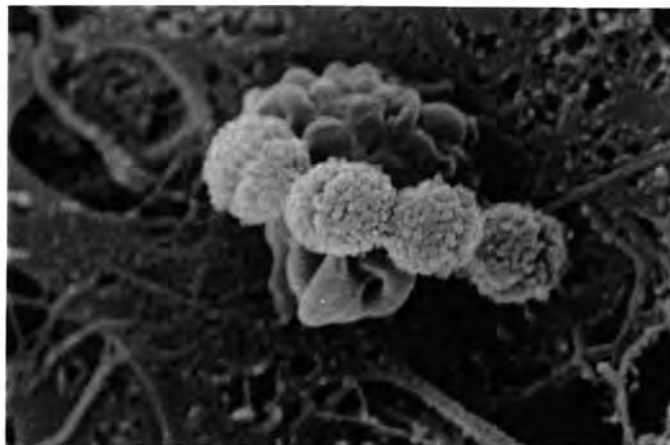


**Plate 3.42**

PLN-A (5) L basilar membrane (undersurface) x15,000, 12 h p.i.

A short chain of cocci, demonstrating that PLN-A invaded scala tympani.

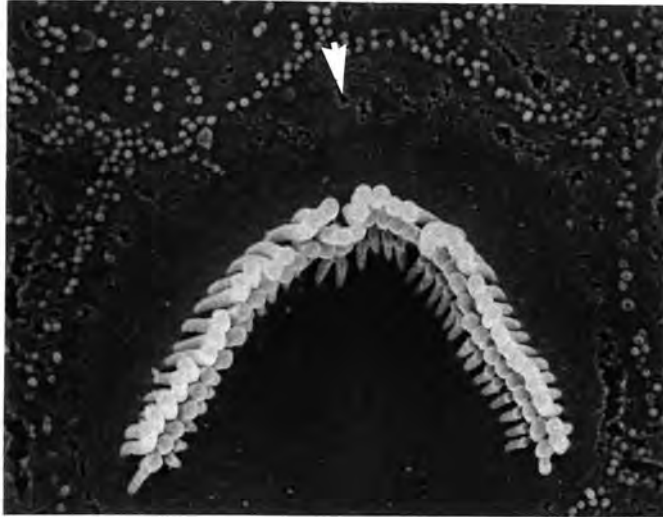


**Plate 3.43**

PLN-A (5) L basal turn x10,000, 12 h p.i.

There is some probably artefactual pitting of the apical surface of the sensory cell (arrow) but no gross defect. Compare plate 3.30.



**Plate 3.44**

PLN-A (5) L basal turn x10,000, 12 h p.i.

A lower power view shows good preservation of OHC stereocilia.

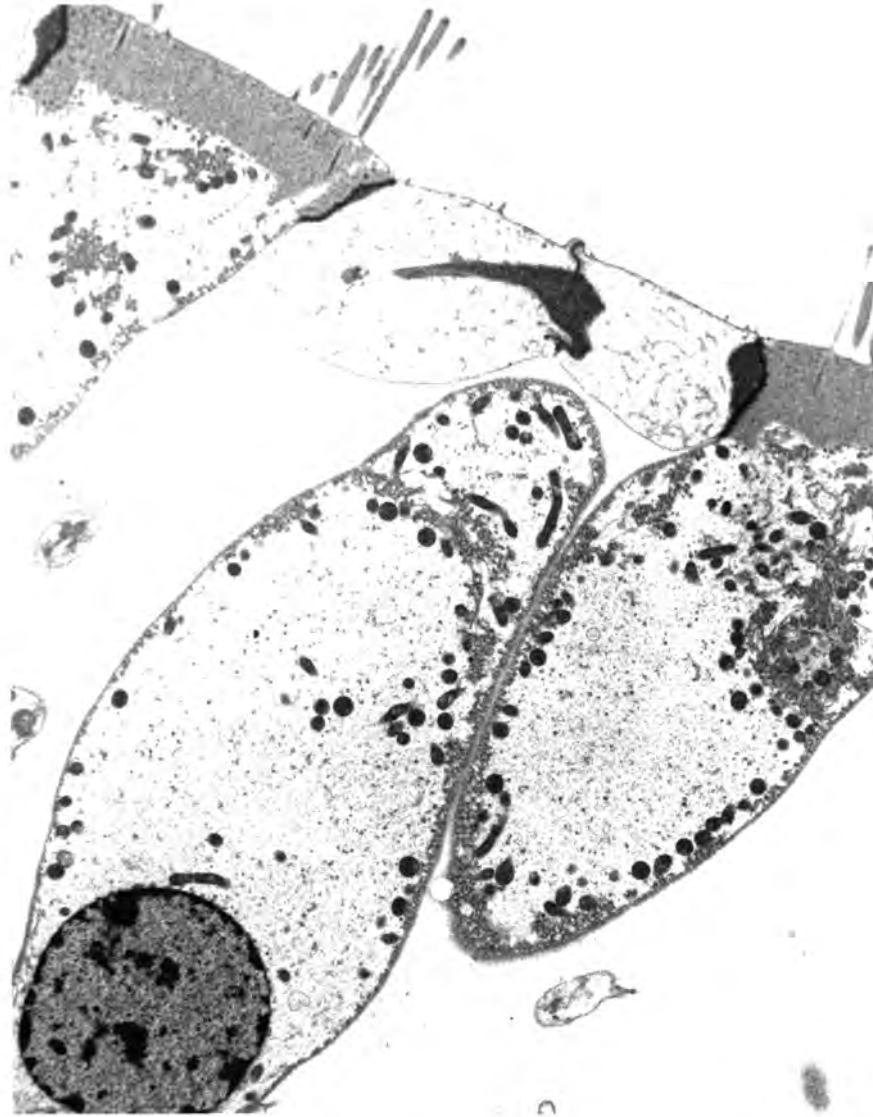


**Plate 3.45**

PLN-A (5) L basal turn x6,700, 12 h p.i.

The OHCs have perhaps lost a little turgor but there are no defects in the plasma membrane or the apical surface. The stereocilia are intact.

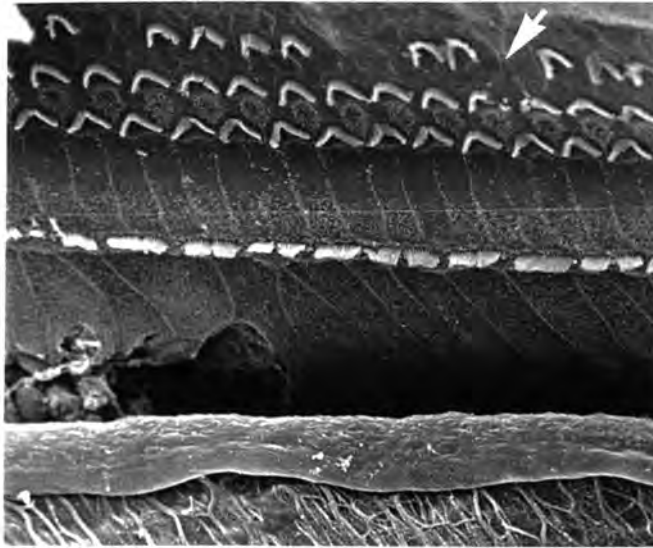


**Plate 3.46**

PLN-A (13) R basal turn x1,000, 12 h p.i.

There are no gross stereocilial abnormalities. The missing row 3 cells have been replaced by a phalangeal scar (arrow) and this damage is unlikely to be acute.



**Plate 3.47**

PLN-A (13) R basal turn x3,000, 12 h p.i.

A small crater in a border cell was seen in this specimen.

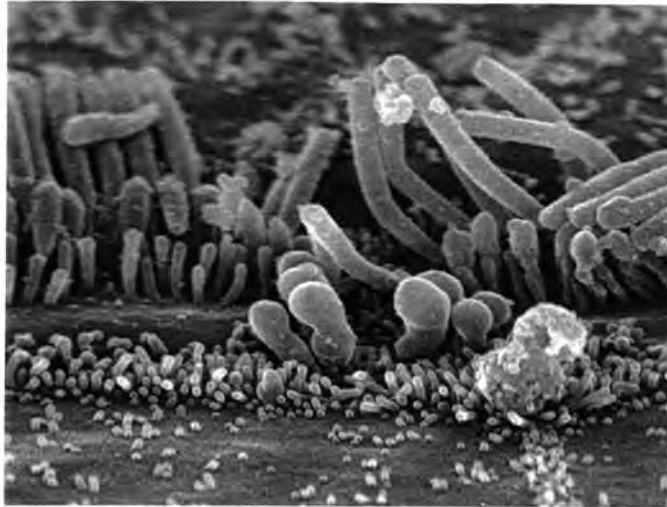


**Plate 3.48**

PLN-A (13) R basal turn x10,000, 12 h p.i.  
Organism-like structures near an area of slight disruption of IHC  
stereocilia



**Plate 3.49**

PLN-A (11) R basal turn x4,000, 12 h p.i.  
IHC stereocilia and intercellular junctions are intact.

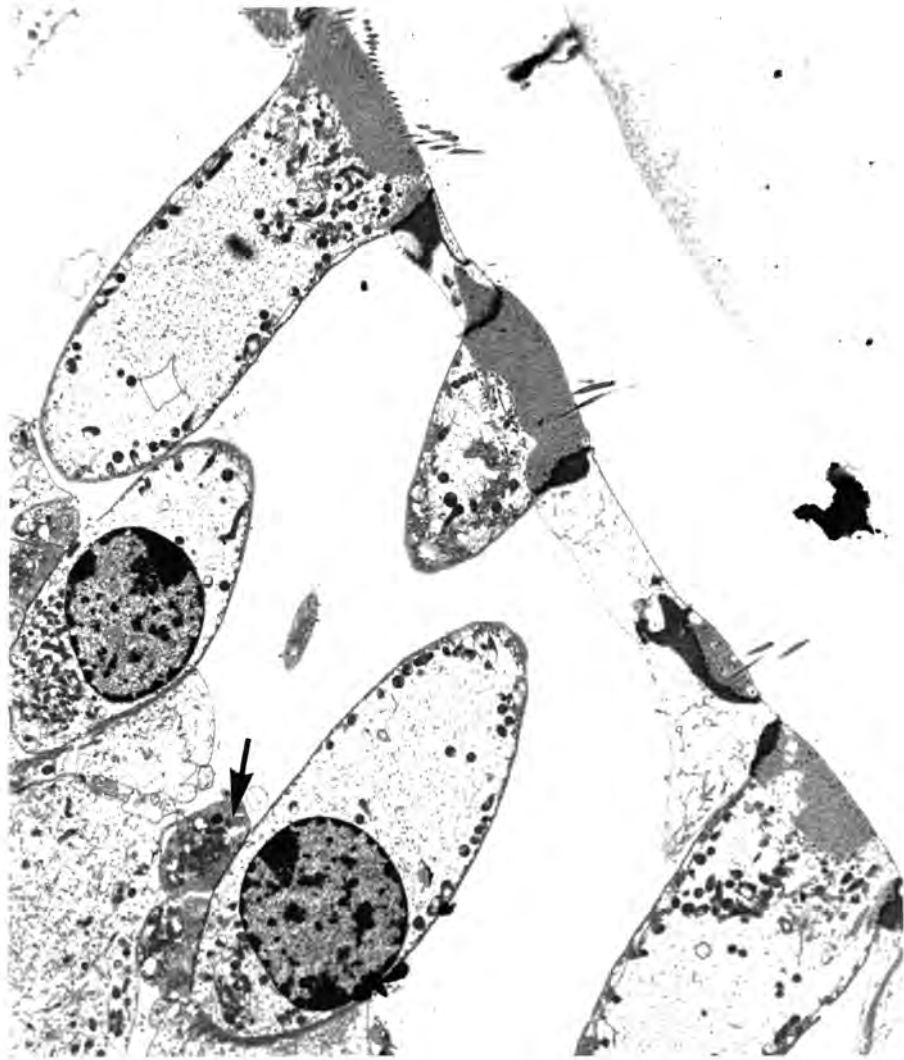


**Plate 3.50**

PLN-A (13) L basal turn x4,400, 12 h p.i.

The reticular lamina and associated tight junctions are clearly intact across the entire width of all 3 outer hair cells. The nerve endings at the base of the row 2 OHC are abnormal (arrow). Some mitochondria are vacuolated. The tectorial membrane is seen upper right.

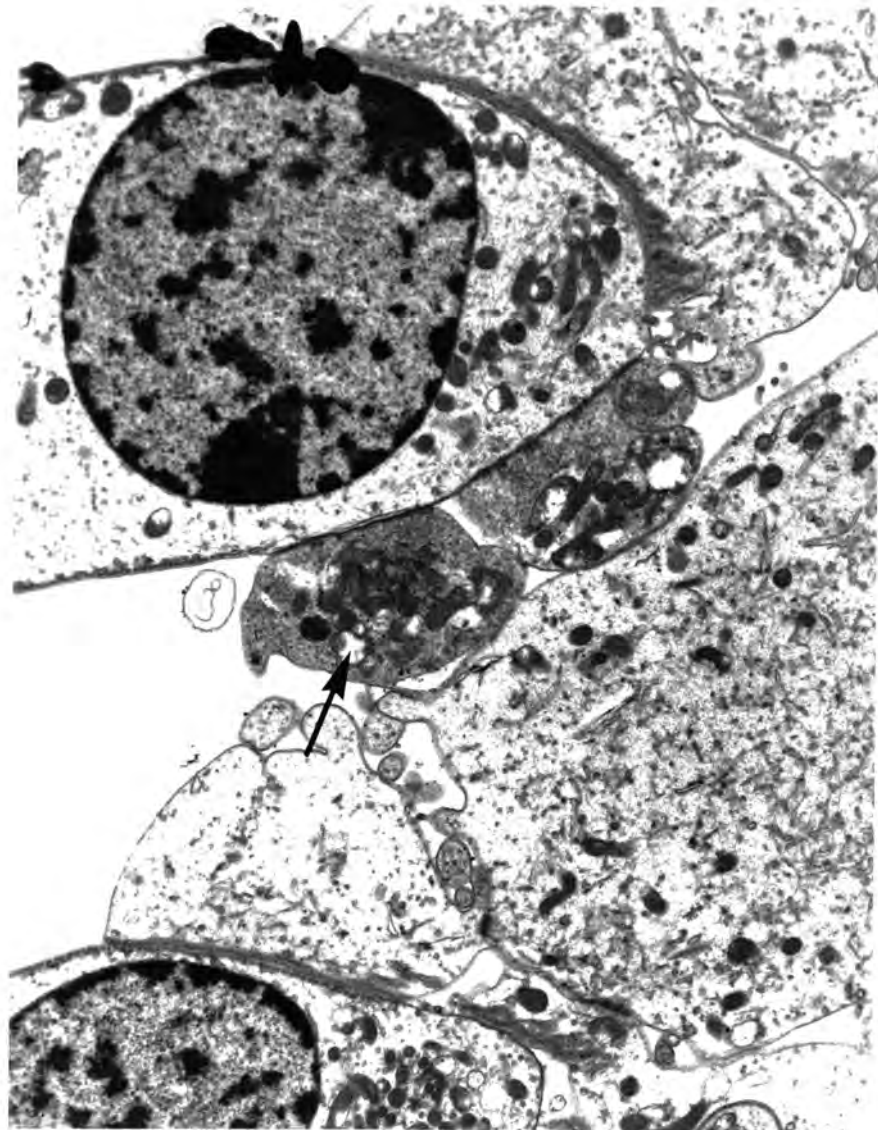


**Plate 3.51**

PLN-A (13) L basal turn x11,500 12 h p.i.

This shows the base of the same row 2 OHC (plate 3.50) at higher power. Most mitochondria within the efferent nerve endings are vacuolated (arrow), as are a few within the OHC itself. The cell plasma membranes are however intact.

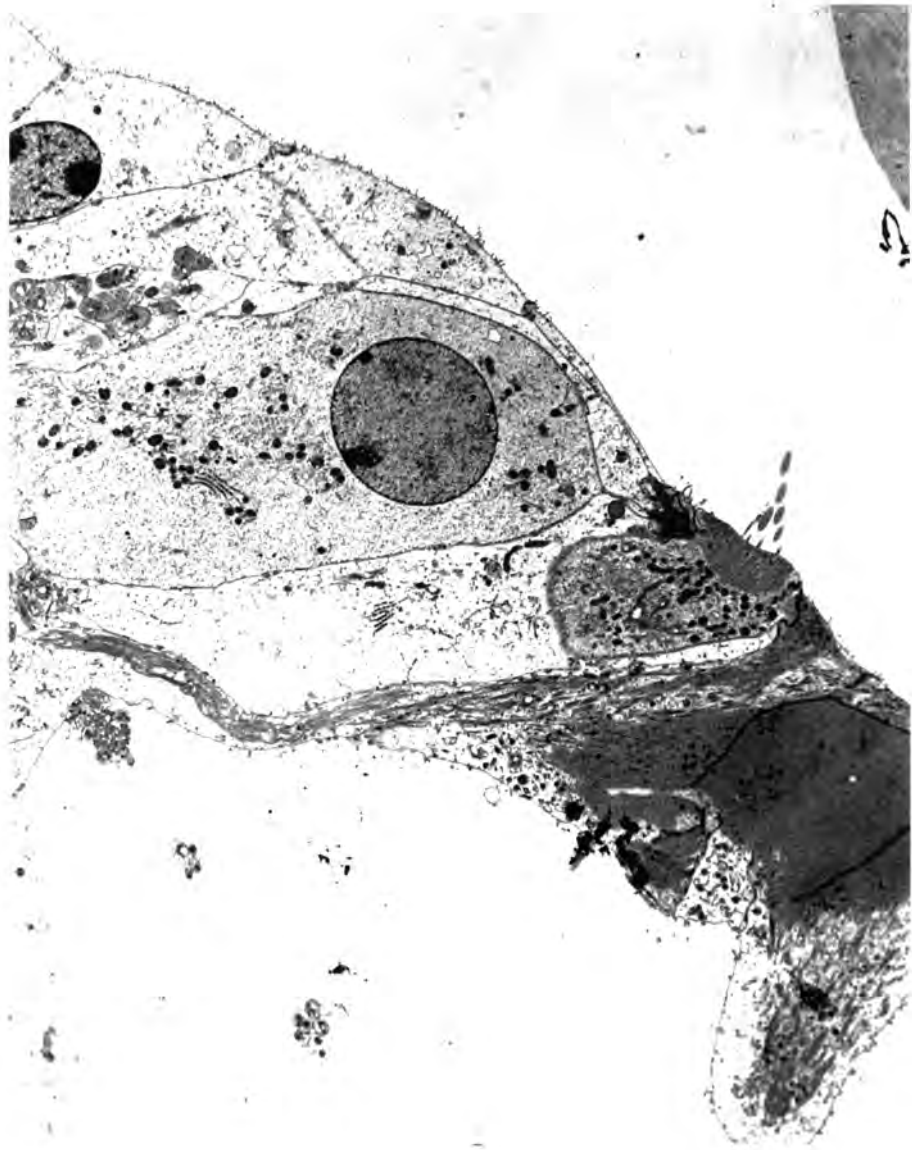


**Plate 3.52**

PLN-A (13) L basal turn x3,200, 12 h p.i.  
The apical surfaces of the border cells and inner sulcus cells are intact. The IHC and its stereocilia appear healthy.

### **3.5. Experimental meningitis with neuraminidase-deficient organisms ( $\Delta$ NA1).**

#### **3.5.1. Introduction and exclusions**

Eight experiments were performed. Two animals were inoculated with batch K and included in the wild-type series (see section 3.3.1). One animal (NA1(2)) was killed 7 h p.i. after losing all detectable hearing. The hearing loss data were included (assuming there would have been no recovery) but the CSF and blood findings were excluded. Another animal (NA1(4)) died 9 h p.i (before hearing was assessed). Data from the terminal CSF sample were included in the analysis. No CSF could be obtained from expt NA1(3), although pneumococci were isolated from a brain smear and the animal was bacteraemic. A formal comparison with wild type infection is given in section 3.8.

#### **3.5.2. Bacteriological findings.**

All animals included in the analysis were inoculated with batch L ( $\Delta$ NA1). This batch expressed both haemolytic (i.e. pneumolysin) and hyaluronidase activity. Neuraminidase activity by the *MUAN* cleavage fluorescence assay (see appendix C) was found to be 0.41 mU/mg cell protein when organisms were grown in non-selective medium, and 0.55 mU/mg cell protein after growth in selective medium (5  $\mu$ g/ml erythromycin). This is at the lower limit of detection for this assay (about 0.5 mU/mg). As a control, Batch N ( $\Delta$ HY1) expressed 6.4 mU neuraminidase activity per mg cell protein, about that expected by wild type organisms. Organisms recovered from the CSF of expt NA1(5) and NA1(6) expressed no neuraminidase activity (<0.5 mU/mg cell protein) after growth in either selective or non-selective media. This is good evidence for the stability of the mutant in vivo.

The inoculum was 7.5 log<sub>10</sub> CFU in all 6 evaluated experiments. The mean CSF viable count 12 h p.i. was 9.0 log<sub>10</sub> CFU/ml (range 9.0–9.5; n=4) (fig 3.31).

All animals from which a terminal cardiac sample was obtained were bacteraemic with a mean viable count in the blood of 6.1 log<sub>10</sub> CFU/ml (range 5.9–6.7; n=3) (fig 3.34).

#### **3.5.3. Inflammatory response.**

A CSF leukocytosis was seen in all animals from which a CSF sample was obtained. The geometric mean CSF white cell count 12 h p.i. was 19,700 cells/ $\mu$ l (range 9,500–27,600; n=4) (fig 3.32). The geometric mean CSF protein concentration was 2.1 g/l (range 1.1–3.3 n=4) (fig 3.33). In experiment NA1(2) at 7 h p.i. the CSF WCC was already as high as 11,000 cells/ $\mu$ l.

These data suggest that the absence of neuraminidase expression in no way impedes the in vivo growth of serotype 2 *S. pneumoniae* and does not modify the host inflammatory response, at least in the CSF space (see section 3.8.2).

#### 3.5.4. Electrophysiological data.

All animals infected with  $\Delta$ NA1 lost hearing as judged by CAP recording. The mean CAP loss 12 h p.i. was 52 dB (range 19–75; n=10) at 10 kHz and 45 dB (range 10–66; n=10) at 3 kHz. The median final CM amplitude was just 12% of baseline (range 0–39%; n=10). Final CM amplitude (as a proportion of baseline) did not correlate with CAP loss (Spearman's  $\rho = -0.33$ ,  $P = 0.4$ ).

Figure 3.23 shows CAP loss as a function of time post-inoculation for 10 kHz and 3 kHz stimuli. The mean rate of CAP loss over the post-inoculation period 0 h to 12 h was 4.3 dB/h at 10 kHz and 3.4 dB/h at 3 kHz. Figures 3.24 and 3.25 show that if anything,  $\Delta$ NA1 induced a more rapid hearing loss in the first 6 h of infection than did wild type D39.

The pattern of loss across the frequencies tested at 12 h p.i. is absolutely indistinguishable from that due to wild type infection. This reflects the reproducibility of the inocula and recording techniques used especially as the D39 experiments were performed some six months prior to the  $\Delta$ NA1 series.

Changes in the CAP waveform were similar to those during wild type infection, with a progressive loss of uniformity and the appearance of a prominent  $P_0$  wave.

### **3.5.5. Ultrastructural findings.**

Nine cochleas were examined by SEM of which five were not evaluated because the organ of Corti curled during processing. Both cochleas from expt  $\Delta$ NA1(1) were subjected to a detailed TEM study. Table 3.8 summarises the histological data for each experiment.

Plates 3.53 to 3.56 show that the pattern of ultrastructural damage was identical to that seen in wild type infection, with cratering of the border cells, deformation of the apical surface of OHCs and disruption of their hair bundles. However, the organ of Corti in one specimen (NA1(6)) was relatively undamaged.

The TEM findings confirmed the pattern of damage seen with wild type infection. The normal space between sensory cells was sometimes enlarged and filled with an electron dense material (plate 3.57 and 3.60). Some hair cells themselves appeared to be swollen and filled with extremely abnormal vacuolated mitochondria (plate 3.58). This damage extended to the neighbouring phalangeal cells (plates 3.58 and 3.60). Pathologically damaged nerve endings were more obvious than with wild type infection (plate 3.59). In some sections the apical surfaces of the neighbouring supporting cells were themselves ballooned out (plate 3.60).

The basilar membrane itself appeared to be relatively normal (plate 3.61). No convincing evidence was obtained with TEM that organisms had penetrated through this layer and into the spaces surrounding the hair cells. Some of the cells adjacent to the basilar membrane do however show signs of pathological damage.

Expt no.	Time (h)	Inoculum (log <sub>10</sub> CFU)	CSF CFU (log <sub>10</sub> /ml)	Blood CFU (/ml)	CSF WBC (cells/μl)	CSF protein (g/l)	Estimated hearing loss (dB; L/R)		CM ratio (L/R)	Histological findings
							@10 kHz	@ 3kHz		
ΔNA1 (1)	12	7.5	9.5	–	25,600	1.1	61/75	60/66	0.00/0.00	TEMs show vacuolation of OHCs and nerve endings, and damaged apical surfaces. (L) SEM reveals damaged intercellular junctions.
ΔNA1 (2)	7	7.5	8.4	5.2	11,000	1.8	69/69	60/66	0.23/0.00	(L):Extensive BC craters and OHC surface ballooning. Some irregularity of IHC stereocilia. (R): curled
ΔNA1 (3)	12	7.5	+	5.9	–	–	19/43	34/58	0.12/–	Both (L) and (R) curled
ΔNA1 (4)	9	7.5	9.2	–	22,300	3.3	–/–	–/–	–/–	(last hearing recording at 6 h)
ΔNA1 (5)	11	7.5	9.1	6.7	27,600	1.4	43/52	37/27	0.11/0.39	(L): curled (R): Damage to apical surface of OHCs in basal turn. Craters in BCs
ΔNA1 (6)	12	7.5	9.0	6.7	9,500	3.9	37/40	42/10	0.12/0.16	(L) curled. (R): intact organ of Corti
<b>Means</b>		<b>7.5</b>	<b>9.0</b>	<b>6.1</b>	<b>19,700<sub>g</sub></b>	<b>2.1<sub>g</sub></b>	<b>52</b>	<b>45</b>	<b>0.12<sub>med</sub></b>	

All experiments used batch L. Hearing loss data from round window recordings of CAP. Data not included in analysis appears in italics. –/– = not evaluated. *g*=geometric mean. *med*=median. OHC=outer hair cell; IHC=inner hair cell; BC= border cell; TEM=transmission electron micrograph. +=pneumococci isolated but not quantified.

**Table 3.8:** ΔNA1 (neuraminidase-deficient) meningitis experiments included in comparative study..

# NA1

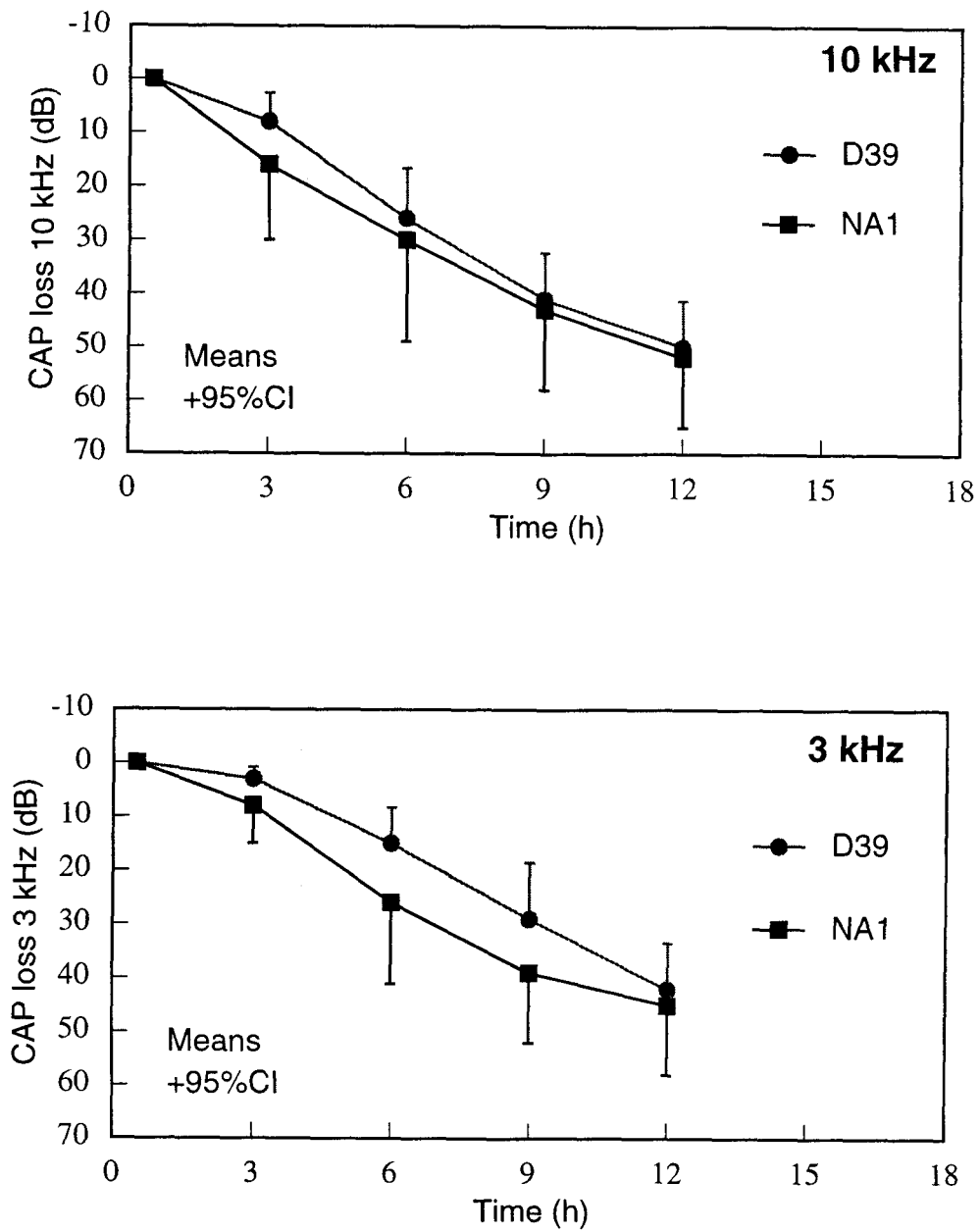
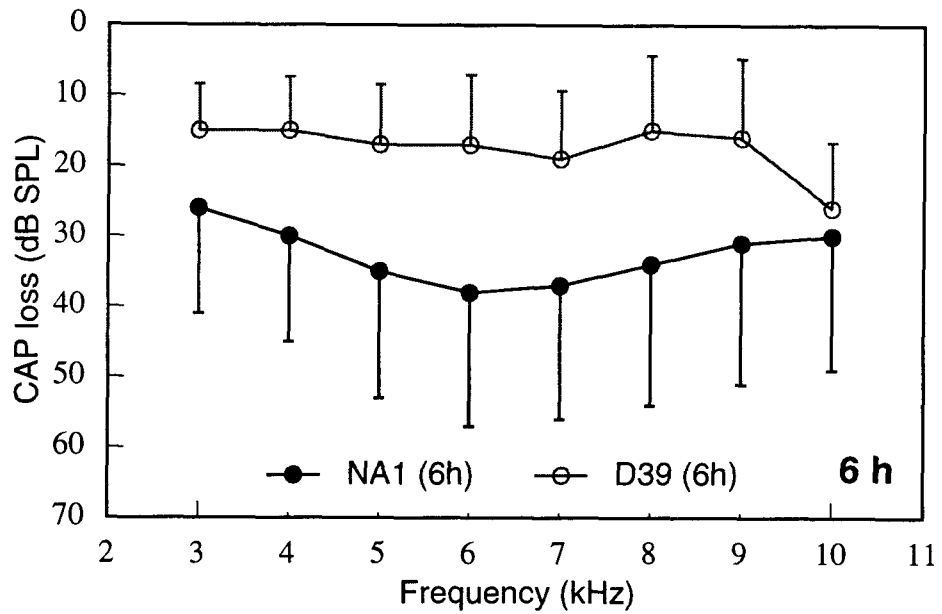
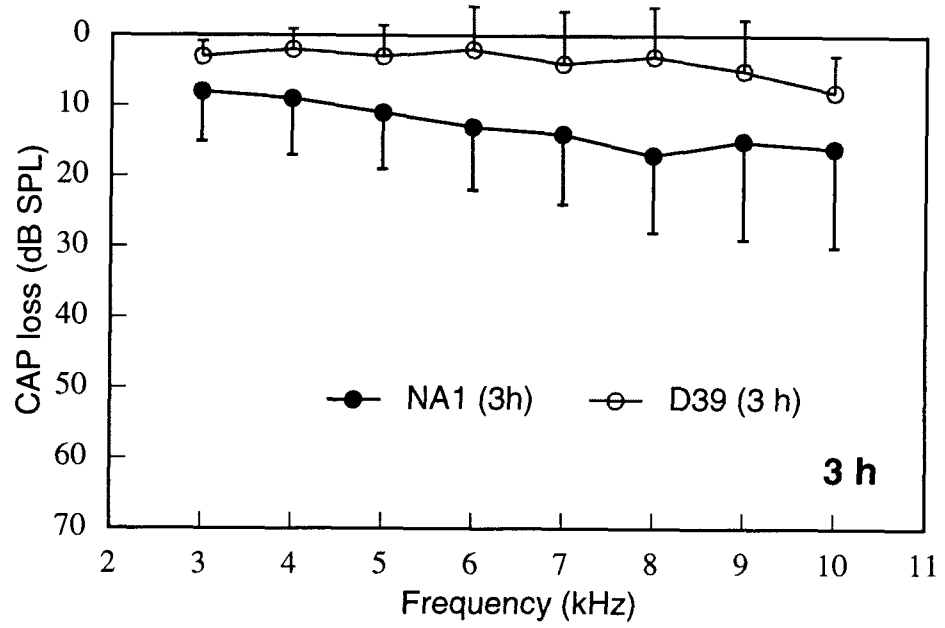


Figure 3.23: ANA1 meningitis: mean hearing loss over time.

# NA1



**Figure 3.24: ANA1 meningitis: audiograms (3 h and 6 h)**  
Frequency-specific CAP loss; h=h post inoculation.;  
means + 95% CI

# NA1

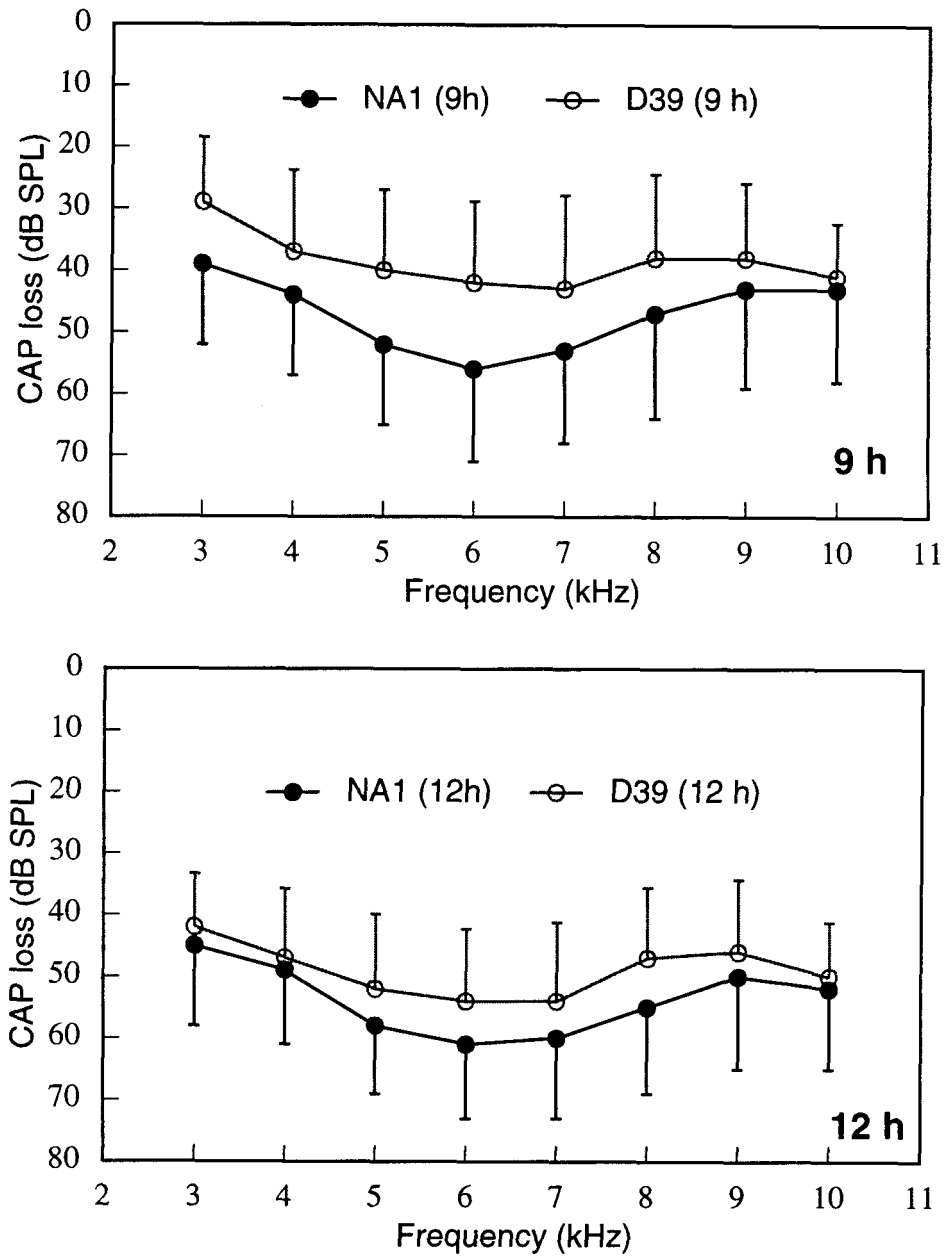


**Figure 3.25: ANA1 meningitis: audiograms (9 h and 12 h)**  
Frequency-specific CAP loss; h=h post inoculation.;  
means + 95% CI

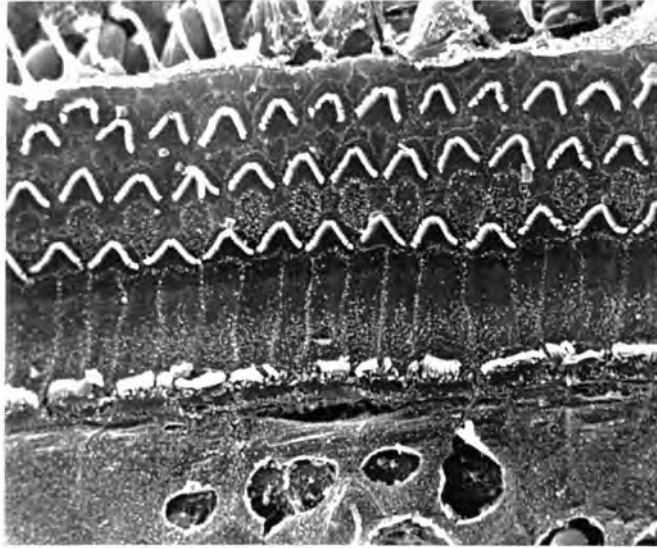


**Plate 3.53**

$\Delta$ NA1 (2) L basal turn, x1,000, 12 h p.i.

There are craters in the border cells. IHC hair bundles are irregular.



**Plate 3.54**

$\Delta$ NA1 (2) L basal turn, x1,000, 12 h p.i.

Row 2 OHC with deformed apical surface, which appears to be ballooning out.

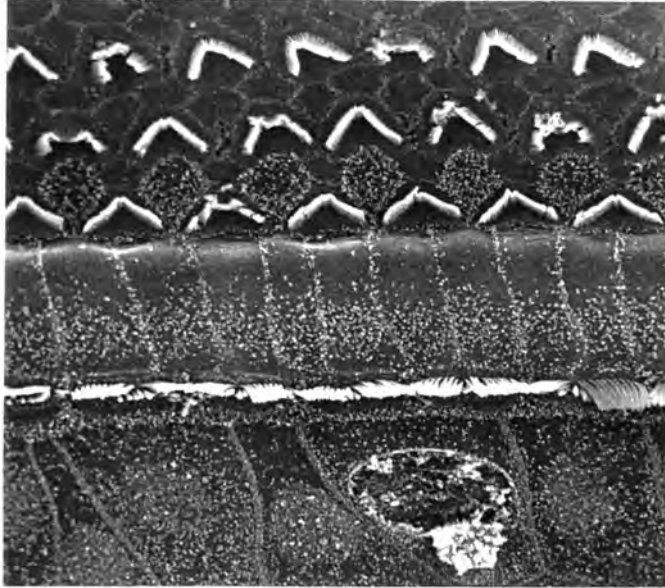


**Plate 3.55**

$\Delta$ NA1 (5) R basal turn, x1,500, 12 h p.i.

Many OHCs are damaged with deformed hair bundles and disruption of their apical surfaces. There is a large crater in the surface of a border cell.

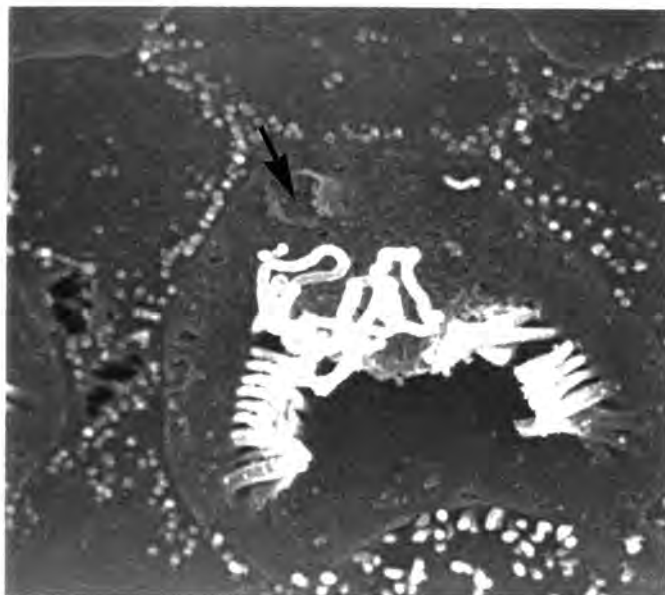


**Plate 3.56**

$\Delta$ NA1 (5) R basal turn, x10,000, 12 h p.i.

The hair bundle of this row 2 OHC is deformed. Some stereocilia have become detached from the cell surface. There is a defect in the apical surface (arrow).

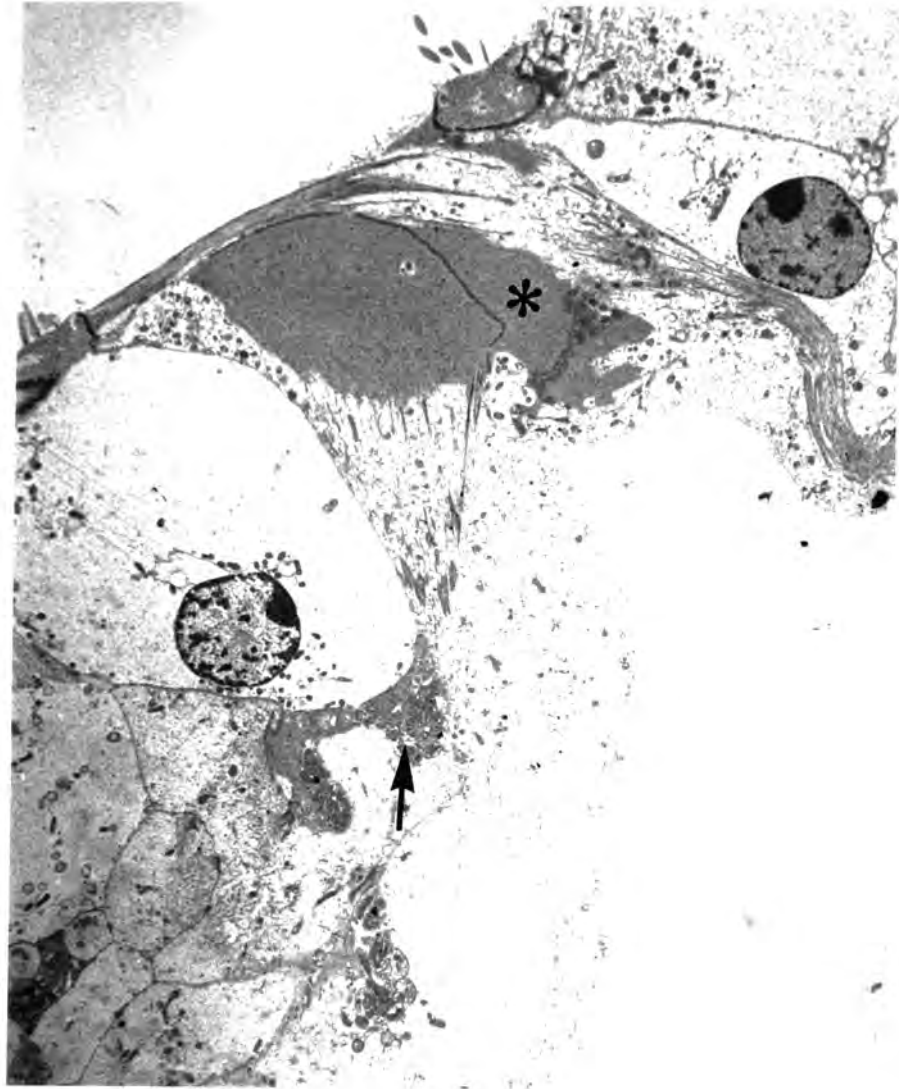


**Plate 3.57**

$\Delta$ NA1 (1) L basal turn, x6,700, 12 h p.i.

The space between the hair cells and phalangeal cells is swollen and filled with a electron dense material (asterisk). The OHC has ballooned out and the nerve endings at the base appear severely damaged and pyknotic (arrow).



**Plate 3.58**

$\Delta$ NA1 (1) L basal turn, x6,700, 12 h p.i.

This row 1 OHC is filled with grossly vacuolated mitochondria. The stereocilia however appear intact. Cellular organelles in the neighbouring supporting cells are also damaged.

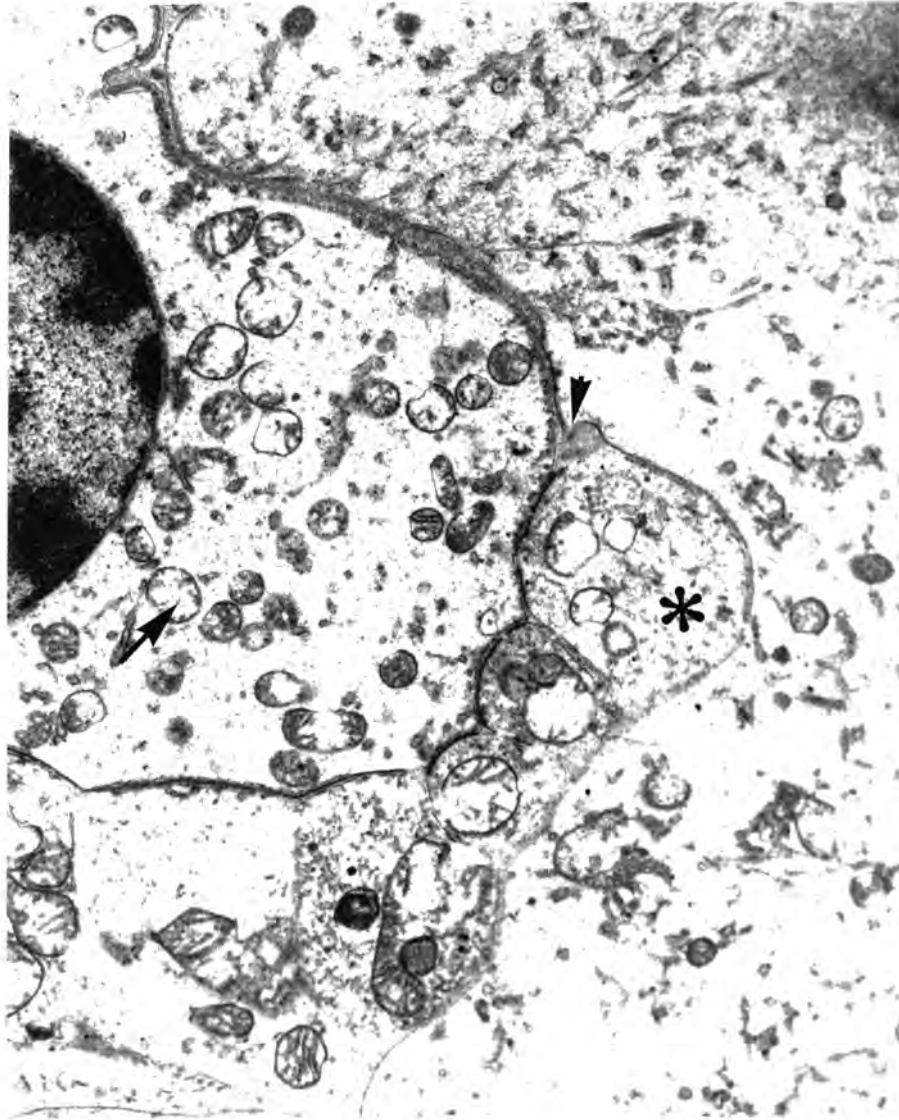


**Plate 3.59**

$\Delta$ NA1 (1) R basal turn, x7,200, 12 h p.i.

Nerve endings at the base of this OHC are damaged (asterisk), with vacuolated mitochondria in the nerve ending and in the OHC itself (arrow). The plasma membrane of the nerve ending is fragmented in places (arrowhead). There is flocculent material in the intercellular space.



**Plate 3.60**

$\Delta$ NA1 (1) R basal turn, x6,700, 12 h p.i.

The apical surface of a supporting cell has ballooned out. The intercellular spaces are filled with electron dense extracellular material and mitochondria in both the hair cell and supporting cell appear vacuolated.

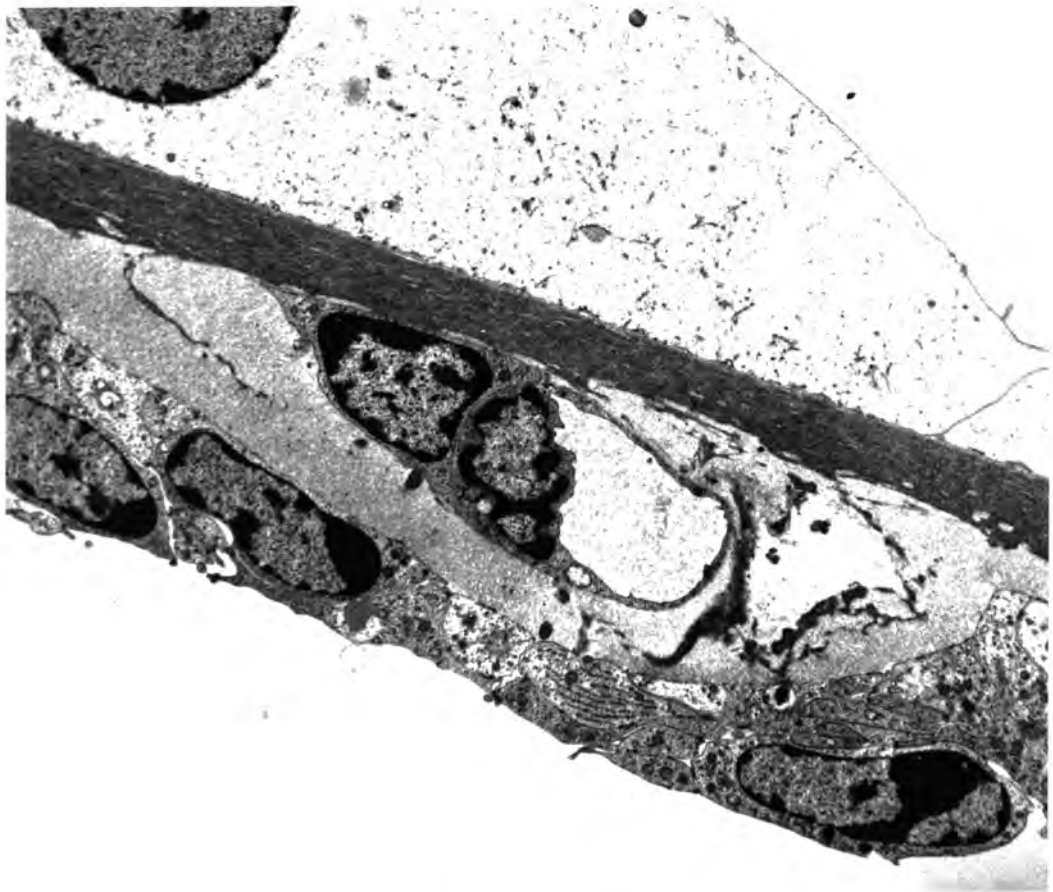


**Plate 3.61**

$\Delta$ NA1 (1) L basal turn, x6,700, 12 h p.i.

The basilar membrane itself is intact although a few cells show signs of pathological damage.

### 3.6. Experimental meningitis with hyaluronidase-deficient organisms ( $\Delta$ HY1).

#### 3.6.1. Introduction and exclusions

Eight experiments were performed. Exclusions included:

- (i)  $\Delta$ HY1(1) and (2) low inoculum
- (ii)  $\Delta$ HY1(3) last recording 6 h p.i., died at 7 h;
- (iii)  $\Delta$ HY1(5) R initial auditory threshold > 100 dB SPL;
- (iv)  $\Delta$ HY1(7) L bleeding into auditory bulla;
- (v)  $\Delta$ HY1(8) L+R last recordings 6 h p.i., died 9 h p.i.

Therefore recordings from only six cochleas were included in the analysis

#### 3.6.2. Bacteriological findings.

##### *Viability of the inocula and evidence for maintenance of the phenotype.*

The in vitro growth curve for  $\Delta$ HY1 is shown in fig 3.29. The first batch of  $\Delta$ HY1 (batch **M**) used to inoculate expts.  $\Delta$ HY1(1) and (2) had a viable count of only 6.3 log<sub>10</sub> CFU/ml after storage at -70°C, a 99% loss of viability. This was attributed to the use of a defective batch of fetal calf serum as cryoprotectant. A second batch (batch **N**) also had a low count (fig 3.30), and the mean inoculum in animals included in the analysis was only 7.1 log<sub>10</sub> total CFU (see section 3.8.1 for comparison). A sample of this batch had no detectable hyaluronidase activity, but did express neuraminidase with a specific activity of 6.4 mU/mg cell protein, some 20-fold higher than that expressed by  $\Delta$ NA1 (see section 3.5.2).

Organisms recovered from the CSF of expt  $\Delta$ HY1(5) were grown overnight on blood agar plates and transported to Leicester. Colonies were inoculated into both selective and non-selective media (BHI with or without erythromycin (5 µg/ml)), cultivated overnight at 37°C, and cell lysates prepared (see appendix C). There was no detectable hyaluronidase activity in either lysate.

##### *CSF count and bacteraemia.*

Table 3.9 and fig 3.31 show data from expts.  $\Delta$ HY1(4) to (8) which were included in the comparative analysis. The mean CSF bacterial count 12 h p.i. was just 6.2 log<sub>10</sub> CFU/ml (range 5.4–7.2; n=5). Expts.  $\Delta$ HY1(1) and (2) were inoculated with 5.4 total CFU (batch **M**) and yielded viable counts of 6.5 and 4.6 log<sub>10</sub> CFU/ml CSF respectively. Experimental animal  $\Delta$ HY1(3) died 7 h p.i. following a prolonged episode of respiratory irregularity. The CSF bacterial viable count was only 5.1 log<sub>10</sub> CFU/ml.

Only two of six animals had detectable bacteraemia 12 h post inoculation (4.7 and 4.0 log<sub>10</sub>, CFU/ml). The lower limit of detection was approximately 1.7 log<sub>10</sub>, CFU/ml blood.

In spite of the small numbers, these data suggest that :

- (i) In contrast to wild type infection with D39,  $\Delta$ HY1 survives poorly in vivo in cerebrospinal fluid and the blood stream.
- (ii) Under these experimental conditions there is no evidence that the phenotype reverts to wild type.

### 3.6.3. Inflammatory response.

Among included animals, the geometric mean CSF WCC 12 h p.i. was 2,000 cells/ $\mu$ l (range 100–7,600; n=5). In expt  $\Delta$ HY1(6) the CSF WCC was just 100 cells/ $\mu$ l, even though the CSF bacterial count was 7.0 log<sub>10</sub>, CFU/ml. There were no obvious reasons why this inoculum had failed to induce an inflammatory response. No leukocytes were seen in the CSF of one of the two animals inoculated with 5.4 log<sub>10</sub>, CFU; the other animal developed a moderate meningitis (CSF WCC=1200 cells/ $\mu$ l). In contrast, in the animal which died unexpectedly early (expt  $\Delta$ HY1(3)), there was a huge CSF leukocyte response (CSF WCC=28,000 cells/ $\mu$ l).

The geometric mean CSF protein concentration was 0.3 g/l (range 0.15–0.30; n=3).

### 3.6.4. Electrophysiological data.

Mean CAP loss 12 h p.i. was 40 dB (range 11–94; n=6) at 10 kHz and 24 dB (range 1–52; n=6) at 3 kHz. Figure 3.26 shows CAP loss as a function of time post-inoculation for 10 kHz and 3 kHz stimuli. The mean rate of CAP loss over the post-inoculation period 0 h to 12 h was 3.4 dB/h at 10 kHz and 2.2 dB/h at 3 kHz. The median final CM amplitude was 65% of baseline (range 25–90; n=6). Final CM amplitude (as a proportion of baseline) did not quite significantly correlate with CAP loss (Spearman's  $\rho = -0.83$ ,  $P = 0.06$ ).

Audiograms are displayed in figs 3.27 and 3.28, where it is clear that the pattern of loss across the frequencies tested at 12 h p.i. is broadly similar to that due to wild type infection. The confidence limits are wide because of the small numbers and because the range of measured hearing loss was greater in this group than in animals infected with D39,  $\Delta$ NA1 or PLN-A.

The pattern of the change in CAP waveform was similar to that of wild type with a progressive loss of uniformity and the appearance of a prominent  $P_0$  wave.

The two animals inoculated with the low inoculum ( $\Delta$ HY1(1) and (2)) lost almost no hearing (mean **CAP** loss 9 dB at 10 **kHz** and 15 dB at 3 kHz (**n=4**)).

### **3.6.5. Ultrastructural findings.**

A total of seven cochleas were examined by SEM. Labyrinthitis was noted to be particularly severe in the left cochlea of expt  $\Delta$ HY1(4) (94 dB loss), which disintegrated on dissection. Table 3.8 summarises the other findings shown in plates 3.62 to 3.65.

Ultrastructural damage was more patchy than with wild type infection. Some areas of the organ of Corti in some experiments were intact (plate 3.62). But in other experiments, all the characteristic lesions were present: damage to apical surface of **OHCs** and **OHC** hair bundles (plate 3.63), craters in the apical surface of border cells (plates 3.64 and 3.65) and irregularity, collapse and detachment of **IHC** stereocilia (plate 3.65).

No TEM study was undertaken.

Expt no.	Time (h)	Inoculum (log <sub>10</sub> CFU)	CSF CFU (log <sub>10</sub> /ml)	Blood CFU (/ml)	CSF WBC (cells/μl)	CSF protein (g/l)	Estimated hearing loss (dB; L/R)		CM ratio (L/R)	Histological findings
							@10 kHz	@ 3kHz		
ΔHY1 (4)	11	7.1	5.6	<1.7†	4,000	0.30	94/39	52/36	0.54/0.31	(L): disintegrated with severe labyrinthitis; disruption of mid-turn OHC s/c and surfaces. (R): no damage seen.
ΔHY1 (5)	12	7.2	7.2	<1.7†	7,100	–	44/–	27/–	0.25/–	(L): disruption of OHC apical surfaces (R): Craters in BCs.
ΔHY1 (6)	12	7.1	7.0	4.7	100	–	25/11	4/1	0.78/0.90	(L) no damage to basal turn (R): curled basal turn; mid-turn intact.
ΔHY1 (7)	12	6.8	5.4	<1.7†	7,600	0.15	–/29	–/26	–/0.76	(R): A few craters in BCs and disruption of OHC stereocilia.
ΔHY1 (8)	9	7.1	5.8	4.0	1,500	0.40	–/–	–/–	–/–	
<b>Means</b>		<b>7.1</b>	<b>6.2</b>	<b>(1.7)</b>	<b>2,000g</b>	<b>0.3g</b>	<b>40</b>	<b>24</b>	<b>0.65med</b>	

All exits used batch N. Hearing loss data from round window recordings of CAP. –/– = not evaluated. (technical problems etc.). *g*= geometric mean. *med*=median. OHC=outer hair cell; BC= border cell; Blood bacterial count: †= minimum detectable in assay.

**Table 3.9:** ΔHY1 (hyaluronidase-deficient) meningitis experiments included in comparative study..

# HY1

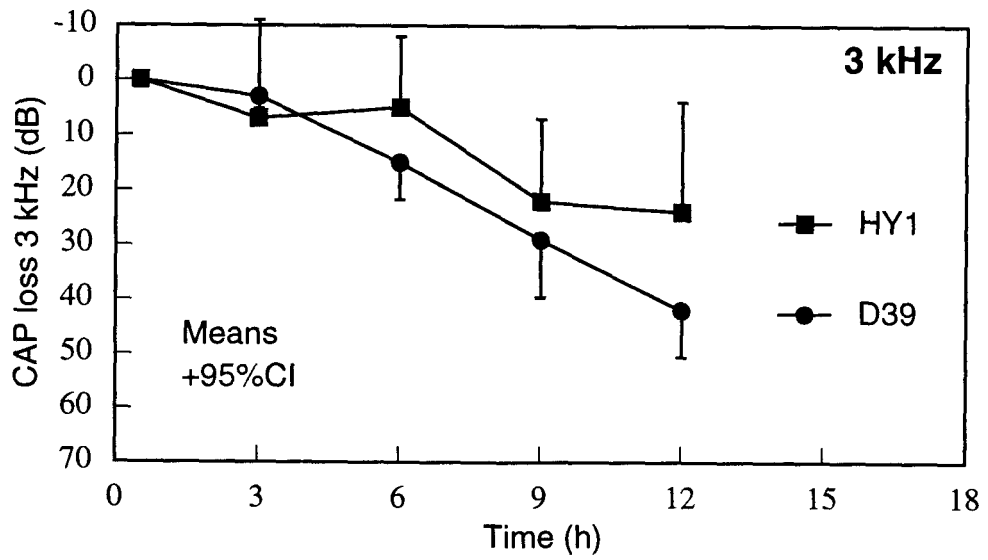
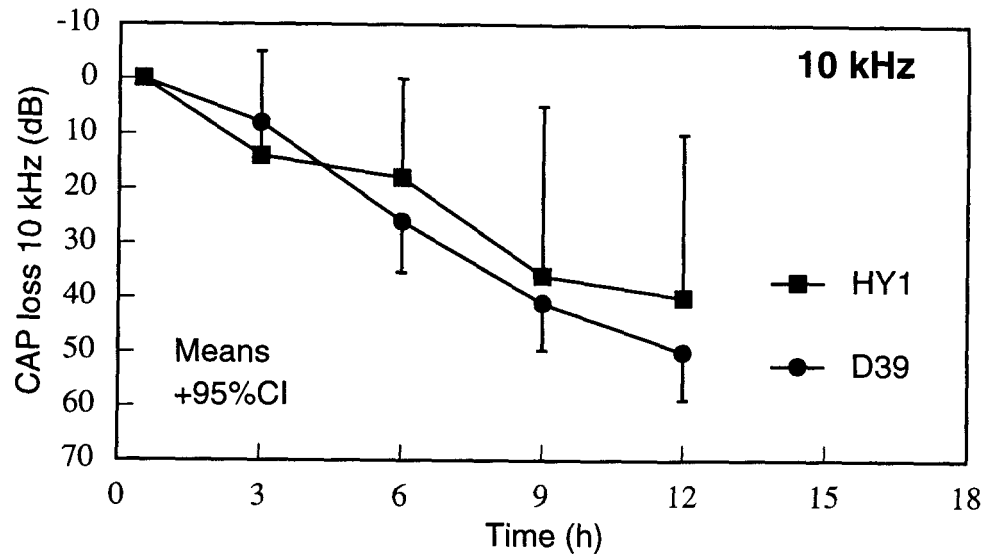
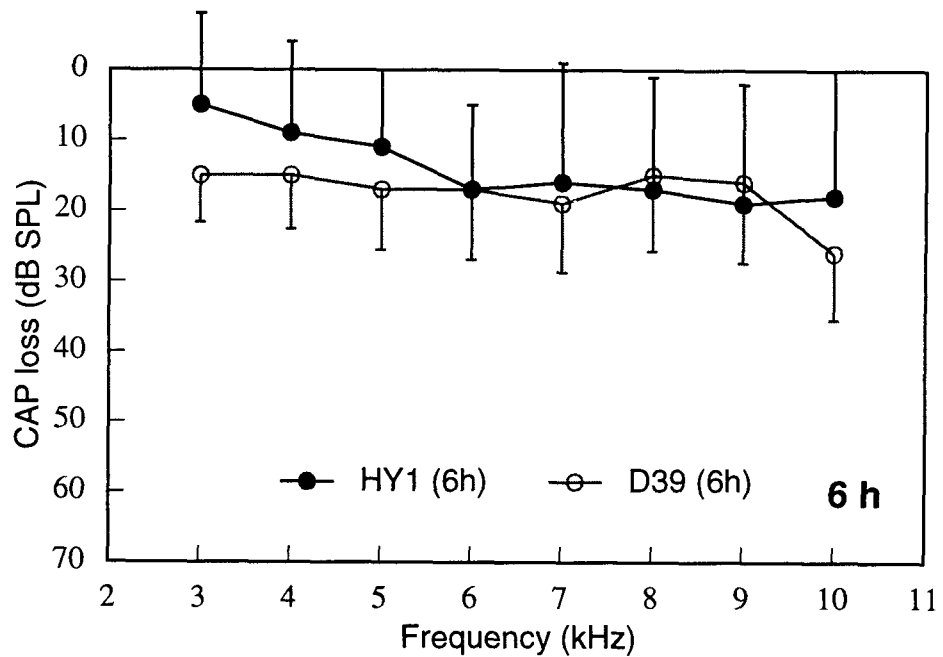
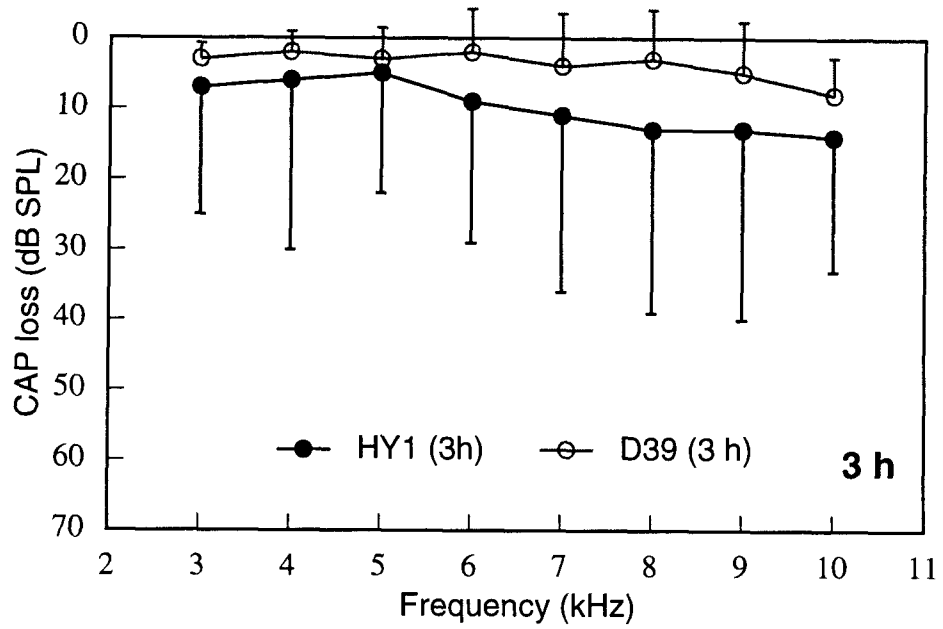


Figure 3.26: AHY1 meningitis: mean hearing loss over time.

# HY1



**Figure 3.27:**  $\Delta$ HY1 meningitis: audiograms (3 h and 6 h)  
Frequency-specific CAP loss; h=h post inoculation.;  
means + 95% CI

# HY1

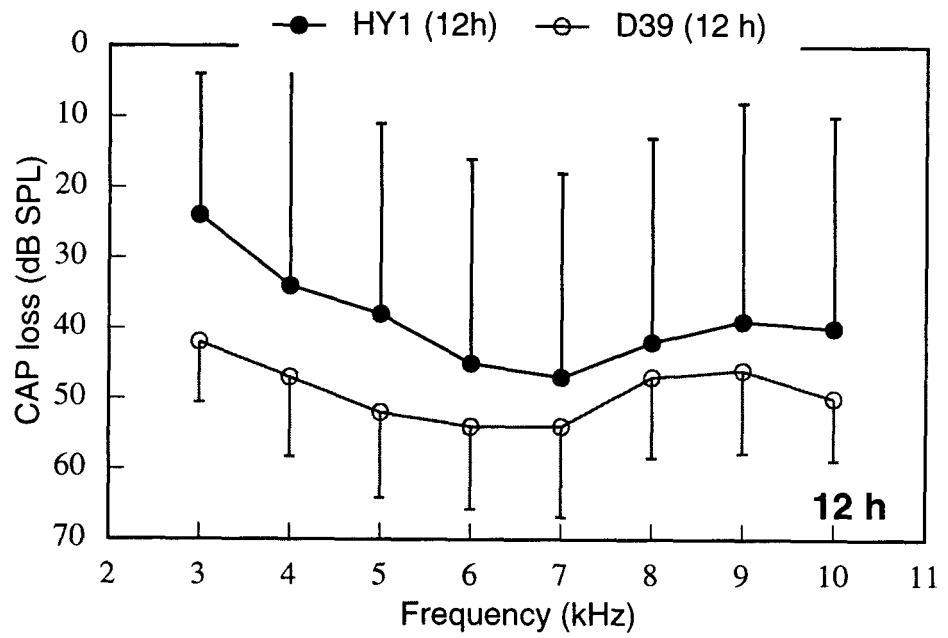
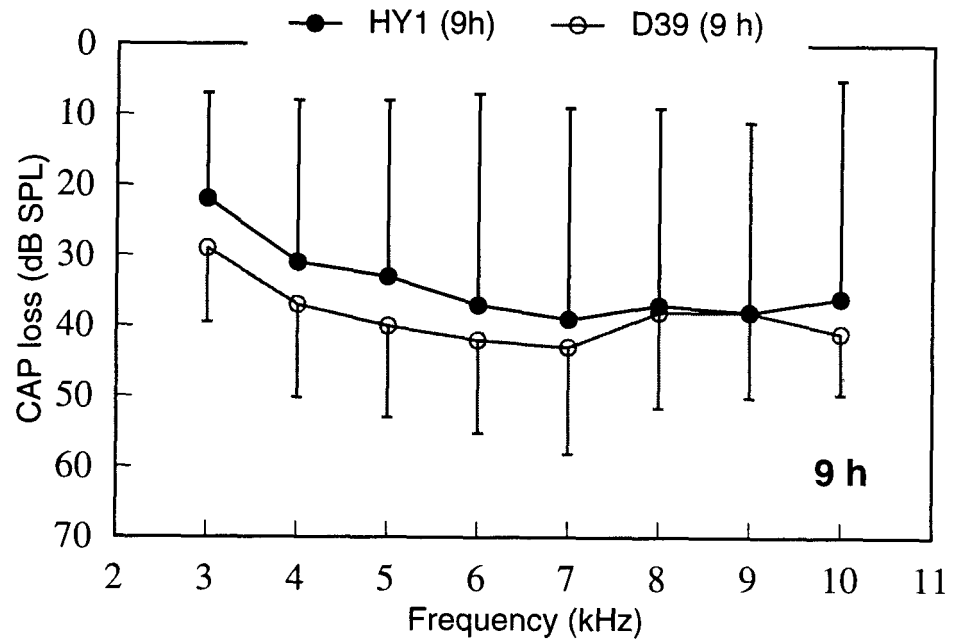


**Figure 3.28:**  $\Delta$ HY1 meningitis: audiograms (9 h and 12 h)  
Frequency-specific CAP loss; h=h post inoculation.;  
means + 95% CI

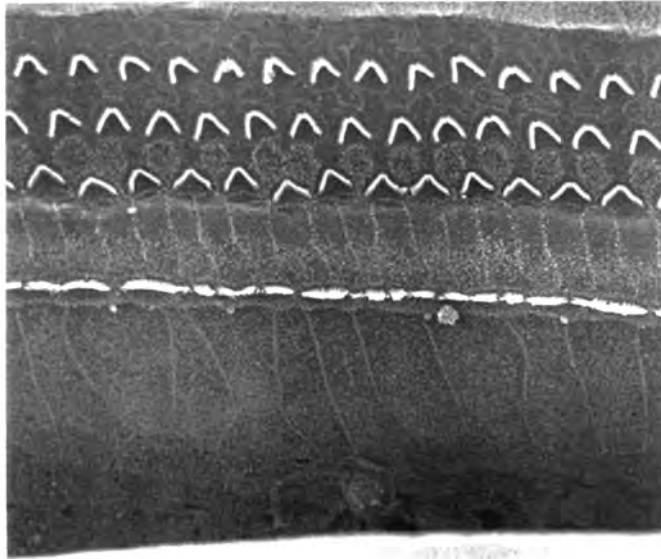


**Plate 3.62**

$\Delta$ HY1 (4) R basal turn x800, 12h p.i.  
The organ of Corti is intact at this point.



**Plate 3.63**

$\Delta$ HY1 (5) L high basal turn x4,000, 12 h p.i.  
Damage to OHCs particularly affecting row 1 cells.

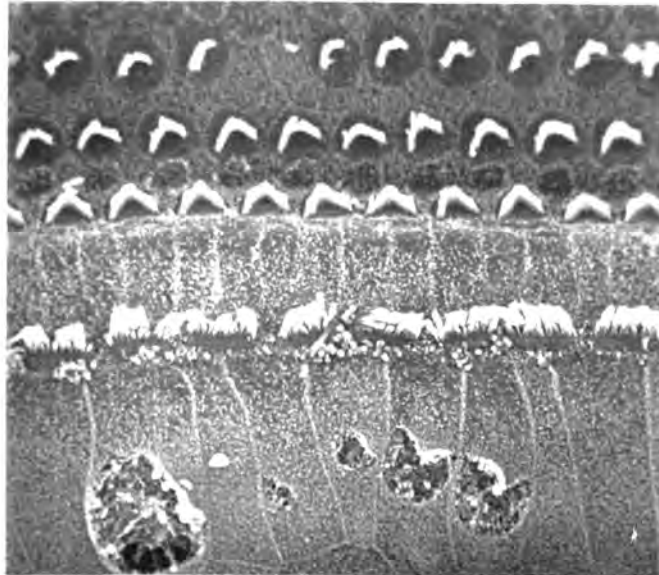


**Plate 3.64**

$\Delta$ HY1 (5) L mid turn  $\times 1,000$ , 12 h p.i.  
Extensive cratering of the apical surface of border cells.



**Plate 3.65**

$\Delta$ HY1 (7) R basal turn  $\times 5,000$ , 12 h p.i.  
There is a large crater in a border cell. IHC hair bundles are irregular. Some have collapsed onto the surface of the cell and some stereocilia have fused together (arrow).

### **3.7. Induction of meningitis by purified pneumococcal cell wall.**

#### **3.7.1. Introduction.**

Four animals were challenged with 100 µg of pneumococcal cell wall injected either via the skull drill hole into the subarachnoid space (expts PCW(1), (3), (4)) or via an indwelling cisternal needle (PCW(2)). Animal PCW(1) died at 6 h p.i. Animal PCW(2) also died prematurely at 10 h p.i. after developing a significant CSF leukocytosis. It appeared to have developed a peritonitis, probably from a contaminated batch of anaesthetic. For the purposes of this analysis the data are included as 12 h p.i. The round window membrane of the right cochlea of PCW(4) was perforated by the electrode.

#### **3.7.2. Inflammatory response.**

Table 3.10 summarises the course of the inflammatory response. No CSF leukocytosis developed in PCW(1) by 6 h p.i.. The PCW material did not suspend well and so for subsequent experiments the suspension was re-sonicated in a more powerful cuphorn sonicator. Only expt PCW(2) developed a meningitis of comparable severity to wild type infection, probably because the challenge was delivered directly into the cisternal CSF. In the other two experiments a mild meningitis developed (compared to wild type live infection) which in one experiment (PCW(4)) appeared to peak and then begin to resolve.

The geometric mean CSF WCC 12 h p.i. (expts PCW(2) to (4)) was 3,400 cells/µl. The CSF protein concentration was elevated only in expt PCW (2) (0.74 g/l).

#### **3.7.3. Electrophysiological data.**

No animal lost more than 18 dB as judged by CAP recording. The mean CAP loss 12 h p.i. was 9 dB (range 0–15; n=5) at 10 kHz and 11 dB (range 6–18; n=5) at 3 kHz. Cochlear microphonics were unaffected (median final CM as a proportion of baseline=84%; range 66–92%; n=5).

#### **3.7.4. Ultrastructural findings.**

Four cochleas were examined by SEM. No organ of Corti was clearly visible because all had curled during processing. However, the undersurface of the basilar membrane was examined in expt PCW(2) (plate 3.66) and PCW(4) (plate 3.67). In both cases, leukocytes could be found, although such inflammation was patchy, limited to the basal turn and less pronounced than in meningitis due to viable pneumococci (compare plates 3.25 and 3.26)

<b>Expt:</b>	<b>PCW-1</b>	<b>PCW-2</b>	<b>PCW-3</b>	<b>PCW-4</b>	<b>Mean (Expts 2-4)</b>
<b>Inoculum (<math>\mu\text{g}</math>)</b>	100 (not well sonicated)	100	100	100	
<b>Duration of expt (h)</b>	6	10	12	12	
<b>CSF WBC (cells/<math>\mu\text{l}</math>)</b>					
3h	0	0	0	0	0
6h	0	1070	264	620	650
9h	-	11,050	800	1330	4,400
12h	-	17,700	3,600	640	7,300
<b>CSF Protein (g/l)</b>					
3h	0	0.02	0	0	
6h	0	0.007	0.02	0.16	0.06
9h	-	0.18	0.08	0.08	0.11
12h	-	0.74	0.05	0	0.26
<b>Hearing loss (CAP)</b>					
10kHz L/R		15/16	0/12	4/-	9
3 kHz L/R		12/18	5/12	6/-	11

Hearing loss data from round window recordings. -/-= not evaluated. (technical problems etc.).

**Table 3.10:** Details of experiments with pneumococcal cell wall material.

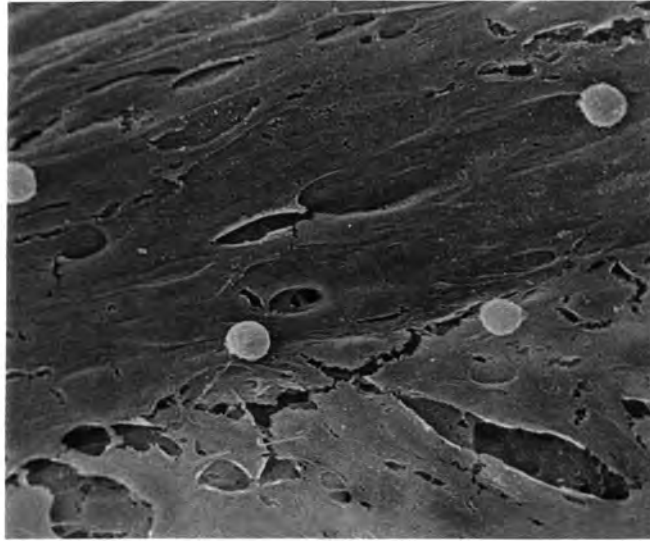


**Plate 3.66**

PCW (2) L basilar membrane (underside) x800, 10 h p.i.  
A few leukocytes are seen but the inflammatory response here is  
less marked than with live infection.

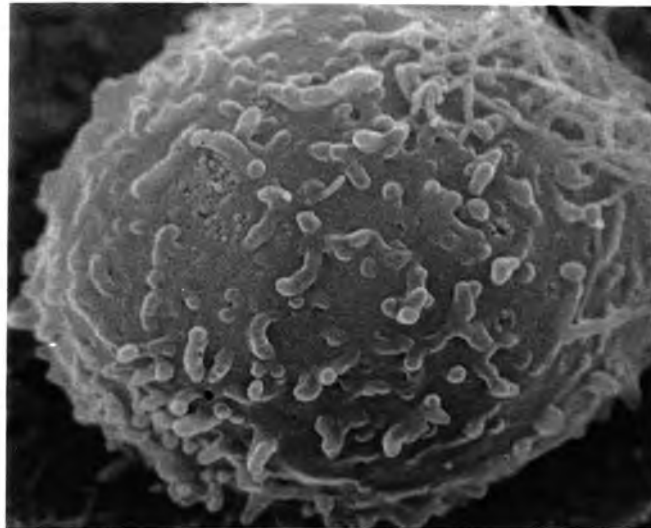


**Plate 3.67**

PCW (4) R basilar membrane (underside) x15,000, 12 h p.i.  
A leucocyte in the scala tympani.

### 3.8. Statistical analysis of the comparative experiments

In this section the data from the comparative experiments are tabulated by heading. Scatter plots (figs 3.30 to 3.38) allow easy inspection of differences between groups.

#### 3.8.1. Differences in inoculum, CSF bacterial counts and bacteremia.

There is known to be no difference between the *in vitro* growth rates of D39 and PLN-A under the conditions used in Leicester (Canvin *et al*, 1995). *In vitro* growth curves for the new mutants ANA1 and  $\Delta$ HY1 and wild type D39 are shown in fig 3.29. While the growth of  $\Delta$ ANA1 is slightly slower, this is probably not biologically significant.

The variation between the inocula given in different experiments was satisfyingly low (fig 3.30). The main problem was the concentration of batch N, which meant that the mean inoculum in the  $\Delta$ HY1 group was 7.1 log<sub>10</sub> CFU/ml. While this is statistically significantly different from the mean inocula in the other groups, this difference (0.4 log<sub>10</sub> CFU) is unlikely to be biologically significant.

There were no differences between the final (12 h) mean CSF bacterial count in infection due to D39, PLN-A and  $\Delta$ ANA1, all of which were higher than the initial total inoculum. However,  $\Delta$ HY1 did not appear to grow *in vivo*: the mean viable count 12 h p.i. was significantly lower than that in the other groups and well below the original total inoculum (fig 3.31).

CSF (12 h)	log <sub>10</sub> CFU/ml	95% CI for difference vs. D39	P
D39 (n=6)	8.7	—	—
PLN-A (n=5)	8.1	0 to 1.1	0.05 NS
$\Delta$ ANA1 (n=4)	9.0	-1 to 0.1	0.09 NS
$\Delta$ HY1 (n=5)	6.2	1.6 to 3.4	<0.0001

Students t-test (data already log transformed).

**Table 3.11:** CSF viable counts in comparative study

$\Delta$ HY1 also survived poorly in the bloodstream when compared to the other three groups. Indeed, bacteraemia was detected in only two out of six animals. There was no significant difference in the mean viable count of D39, PLN-A and  $\Delta$ ANA1 recovered from the blood 12 h p.i. (fig 3.34)

<b>.Blood (12 h)</b>	<b>log<sub>10</sub>CFU/ml</b>	<b>95% CI for difference vs. D39</b>	<b>P</b>
D39 (n=5)	6.6		
PLN-A (n=4)	6.0	-2.5 to 1.8	0.8 NS
ANA1 (n=3)	6.1	-0.6 to 0.9	0.68 NS
$\Delta$ HY1 (n=5)	(1.7)	1.9 to 7.1	0.007†

Students f-test (data already log-transformed) except †: Mann-Whitney test due to unequal variances.

**Table 3.12:** Blood viable counts in comparative study.

### 3.8.2. Differences in CSF inflammatory markers.

No significant differences were observed between the mean CSF leukocyte counts (fig 3.32). Differences in mean protein concentration were difficult to assess due to the wide scatter and small numbers. Neither PLN-A nor  $\Delta$ HY1 seemed to induce as great a protein elevation as D39 or  $\Delta$ NA1 (fig 3.33). There were insufficient numbers in the PCW group to allow a formal comparison between the inflammatory response due to PCW and that due to live infection.

<b>CSF (12 h)</b>	<b>Mean WCC (cells/<math>\mu</math>l)</b>	<b>95% CI for difference vs. D39</b>	<b>P</b>
D39 (n=6)	10,500		
PLN-A (n=5)	4,790	*	0.18 NS
ANA1 (n=4)	19,700	*	0.35 NS
$\Delta$ HY1 (n=5)	2,000	*	0.08 NS
PCW (n=3)	3,440	*	0.24 NS

Geometric means. Students t-test on log-transformed data; \* 95% CI not calculated.

<b>CSF (12 h)</b>	<b>Mean protein (g/l)</b>	<b>Approximate 95% CI for difference vs. D39</b>	<b>P</b>
D39 (n=6)	1.6		
PLN-A (n=5)	0.6	-3.2 to 0	0.04
ANA1 (n=4)	2.1	-1.2 to 2.8	0.8 NS
$\Delta$ HY1 (n=3)	0.3	not calculated	(0.04)

Geometric means. Mann-Whitney test on untransformed data.

**Table 3.13:** CSF inflammatory response in comparative study.

### 3.8.3. Comparison of CAP loss at 12 h in the comparative study groups.

This was the major predetermined endpoint of the study. Data from left and right cochleas for CAP loss at 10 kHz and 3 kHz in groups D39, PLN-A and ANA1 were found to be independent within each group by Spearman's rank correlation (P=0.72, 0.78 and 0.08 respectively for 10 kHz; P=0.3, 0.5 and 0.23 for 3 kHz) (only two pairs of ears were included in the analysis for  $\Delta$ HY1). Data from left and right ears were therefore pooled together within the groups and statistical significance between means was assessed with Student's t-test or (if variances were unequal) with a Mann-Whitney test.

Guinea pigs infected with the pneumolysin deficient isogenic mutant PLN-A lost significantly less hearing at both 10 kHz and 3 kHz than those infected with wild type strain D39. The audiograms (fig 3.21 and 3.22) confirm that the difference between wild type and pneumolysin-deficient infection was apparent across all frequencies tested. There were no significant differences in the mean CAP loss in meningitis induced by the other mutants, ANA1 and  $\Delta$ HY1, compared to wild type. Animals with meningitis induced by 100  $\mu$ g pneumococcal cell wall lost significantly less hearing than animals with live D39 pneumococcal infection.

10 kHz	Mean CAP loss (dB)	Difference vs. D39	95% CI	P†
D39 (n=15)	50	–	–	–
PLN-A (n=10)	12	38 dB less	25 to 51	<0.0001
ANA1 (n=10)	52	2 dB more	–16 to 12	0.76 NS†
$\Delta$ HY1 (n=6)	40	10 dB less	–11 to 30	0.35 NS†
PCW (n=5)	9	41 dB less	22 to 56	0.0001

3 kHz	Mean CAP loss (dB)	Difference vs. D39	95% CI	P
D39 (n=15)	42	–	–	–
PLN-A (n=10)	18	24 dB less	12-34	<0.0001
$\Delta$ ANA1 (n=10)	45	3 dB more	–17 to 10	0.64 NS†
$\Delta$ HY1 (n=6)	24	18 dB less	0.7 to 35	0.04 NS†
PCW (n=5)	11	31 dB less	18 to 47	0.0001

P by Mann-Whitney test because of unequal variances except for †: Student's t-test  
n refers to number of ears evaluated.

**Table 3.14:** CAP loss in comparative study.

### 3.8.4. Comparison of rates of CAP loss.

Data for each time point within each group were pooled to determine the approximate rate of hearing loss. Grouped linear regression and analysis of variance were used to assess differences between groups. At both 10 kHz and 3 kHz, the rate of CAP loss was significantly lower with infection due to the pneumolysin negative mutant than with wild type infection (fig 3.20). There were no highly significant differences in rates of CAP loss at either 10 kHz or 3 kHz between D39,  $\Delta$ NA1 and  $\Delta$ HY1 infection (fig 3.23 and 3.26). The difference between the rate of CAP loss at 3 kHz in the  $\Delta$ HY1 group compared to the D39 group is not significant given the multiple comparisons.

Although the rate of CAP loss at 3 kHz was different to that at 10 kHz in every group, this never reached statistical significance (D39, PLN-A, ANA1 and  $\Delta$ HY1; P=0.37, 0.08, 0.14 and 0.13 respectively).

10 kHz	Slope (dB/h)	Difference vs. D39	95% CI	P
D39 (n=15)	4.4			
PLN-A (n=10)	1.0	3.4	n/a	<0.0001
$\Delta$ NA1 (n=10)	4.3	0.1	n/a	0.47 NS
$\Delta$ HY1 (n=6)	3.4	1.0	n/a	0.1 NS

3kHz	Slope (dB/h)	Difference vs. D39	95% CI	P
D39 (n=15)	3.6			
PLN-A (n=10)	1.4	2.2	n/a	<0.0001
ANA1 (n=10)	3.4	0.2	n/a	0.34 NS
$\Delta$ HY1 (n=6)	2.2	1.4	n/a	0.02 NS

Grouped linear regression and analysis of variance. n refers to number of ears evaluated.

**Table 3.15:** Rate of CAP loss in comparative study.

### 3.8.5. Comparison of cochlear microphonics.

There was a clearly significant difference in CM loss (expressed as the ratio of final CM amplitude at 12 h p.i. to baseline CM amplitude) between animals infected with wild type and those infected with PLN-A. A possibly significant difference was seen between wild type and  $\Delta$ HY1 groups but no significant difference was apparent between groups infected with wild-type and ANA1 (fig 3.37).

Figure 3.38 shows the ratio of final CM amplitude to baseline CM amplitude plotted as a function of CAP loss at 12 h p.i. for all experiments. No ear completely lost CM unless there was at least a 56 dB change in CAP threshold. However, in ears with a fall in CAP threshold of less than 20 dB there was sometimes up to a 90% fall in CM. In spite of this, there was a strong overall correlation between final CM (as a proportion of baseline) and CAP loss (Spearman's rank correlation coefficient **p**: -0.7; 95% CI for **p** -0.8 to -0.5;  $P < 0.0001$ ).

	<b>Median final CM (as a proportion of baseline)</b>	<b>Approx. 95% CI for difference vs. D39</b>	<b>P</b>
D39 (n=15)	0.18		
PLN-A (n=10)	0.65	0.26 to 0.65	0.0003
$\Delta$ ANA1 (n=10)	0.12	-0.24 to 0.11	0.32 NS
$\Delta$ HY1 (n=6)	0.65	0.07 to 0.66	0.01

Mann-Whitney test because of non-normal distribution. n refers to number of ears evaluated.

**Table 3.16:** Cochlear microphonic loss in comparative study.

### Growth curves of *S. pneumoniae* in vitro

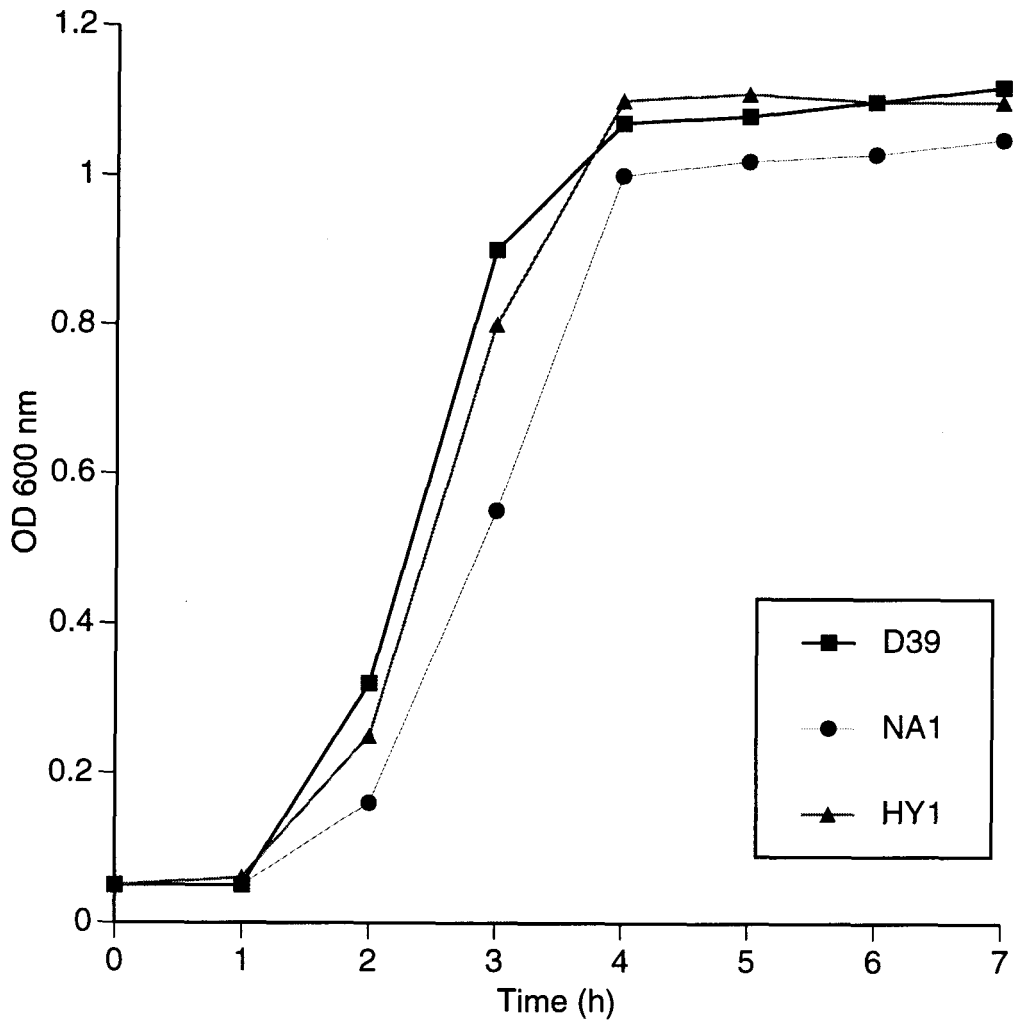


**Figure 3.29:** In vitro growth curves of *S.pneumoniae* D39,  $\Delta$ NA1 and  $\Delta$ HY1. Conditions as described in Methods; growth determined by optical density at 600 nm.

## Inoculum

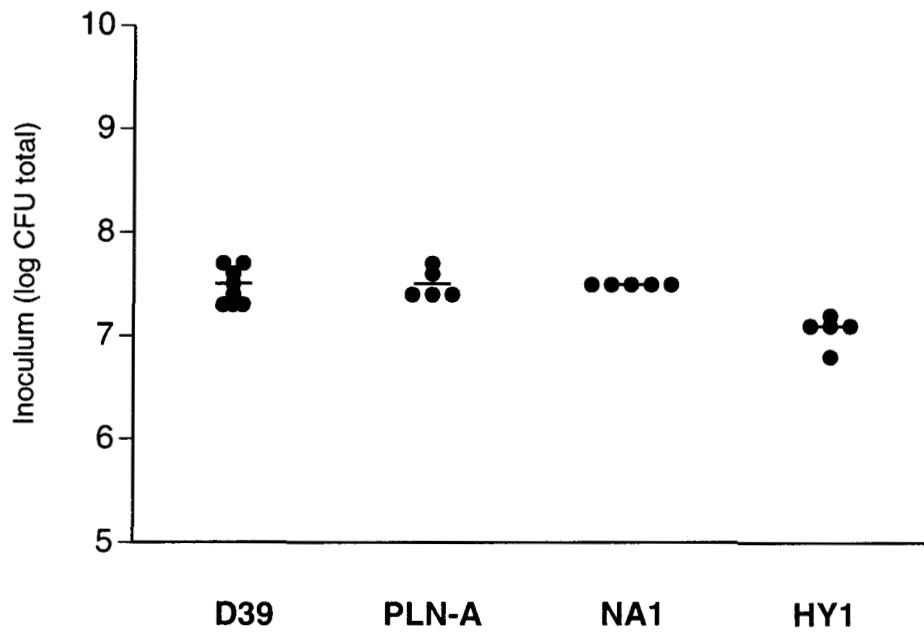


**Figure 3.30:** Pneumococcal meningitis: inoculum given.  
Bars are means.

## CSF bacterial count

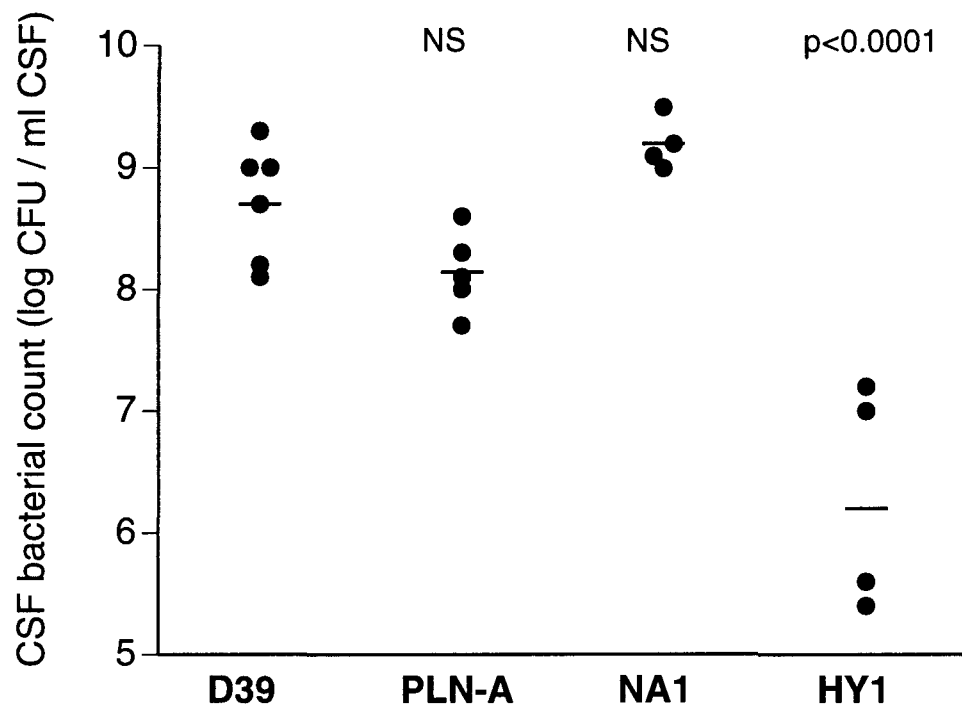
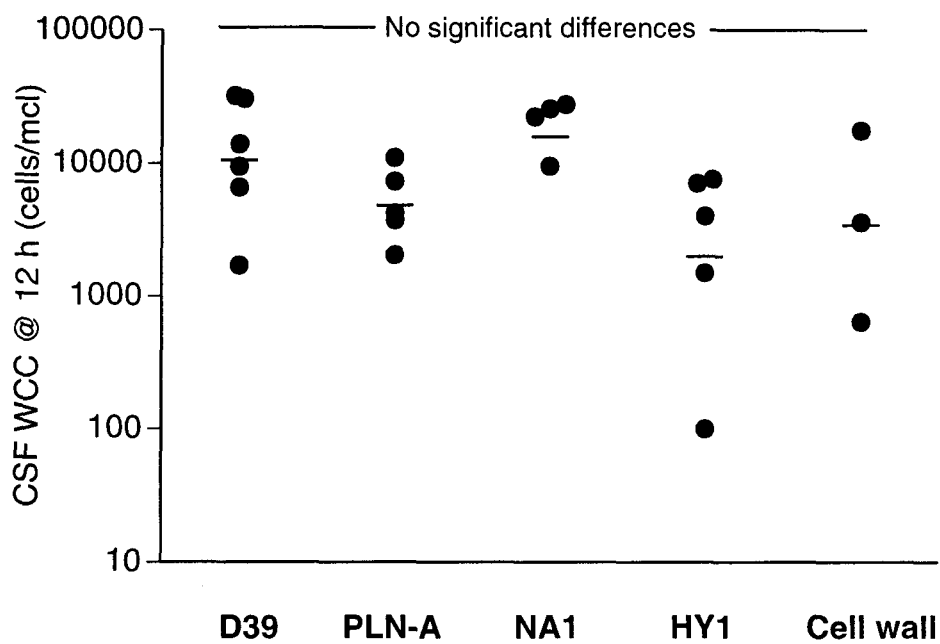


Figure 3.31: Pneumococcal meningitis: CSF bacterial count.  
Bars are means. P by Student's t-test.

### CSF white cell count



**Figure 3.32:** Pneumococcal meningitis: CSF white cell count. Bars are geometric means. P by Student's t-test on log-transformed data.

## CSF protein

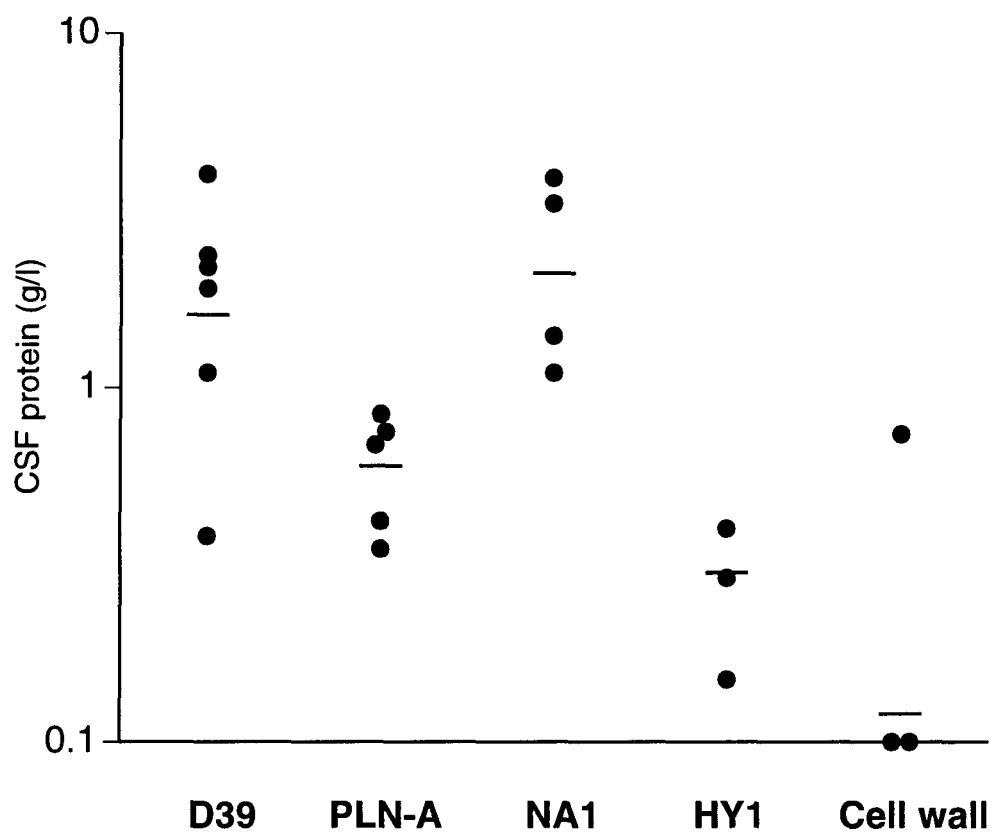


**Figure 3.33:** Pneumococcal meningitis: CSF protein concentration.  
Bars are geometric means.

## Blood bacterial count

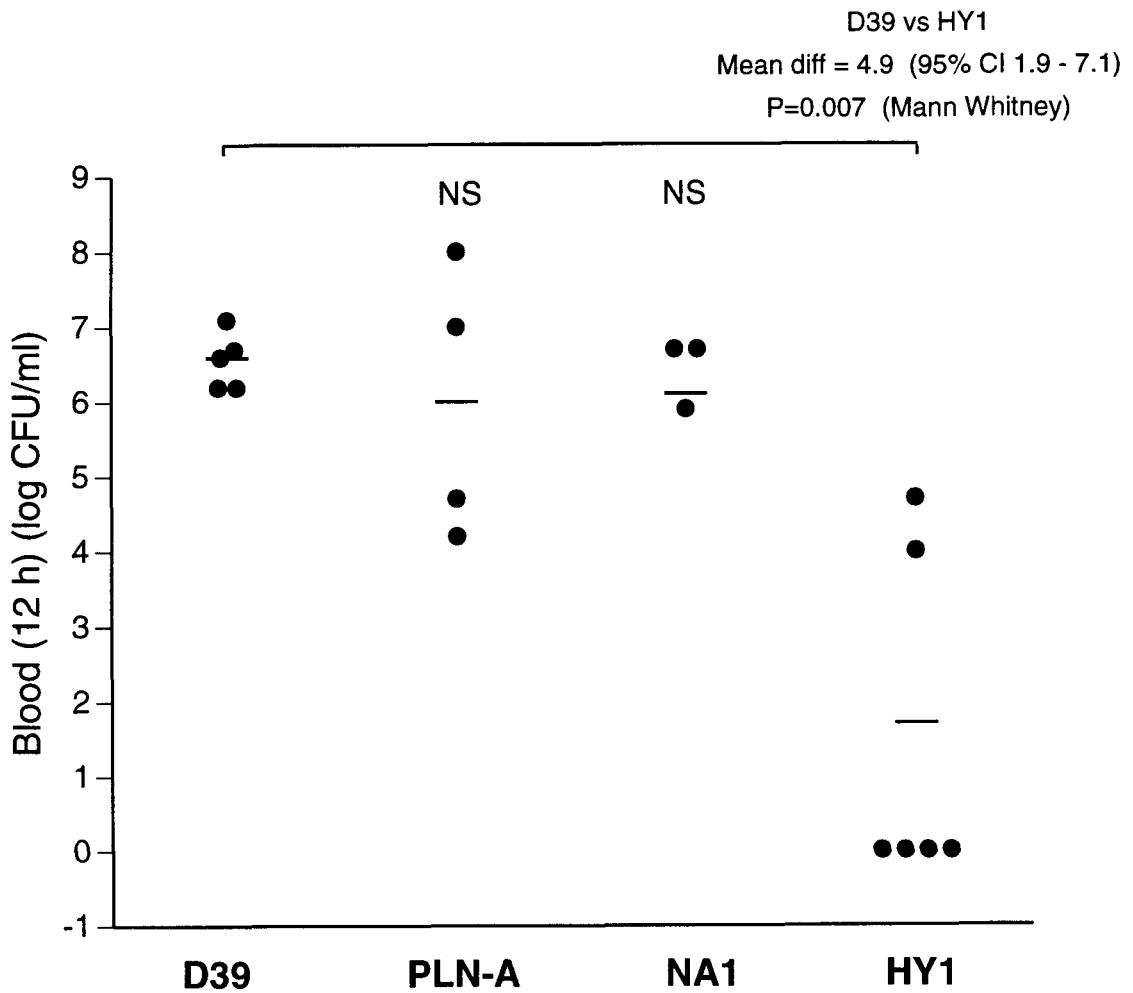


**Figure 3.34:** Pneumococcal meningitis: blood bacterial count.  
Bars are means.

## Hearing loss 10 kHz

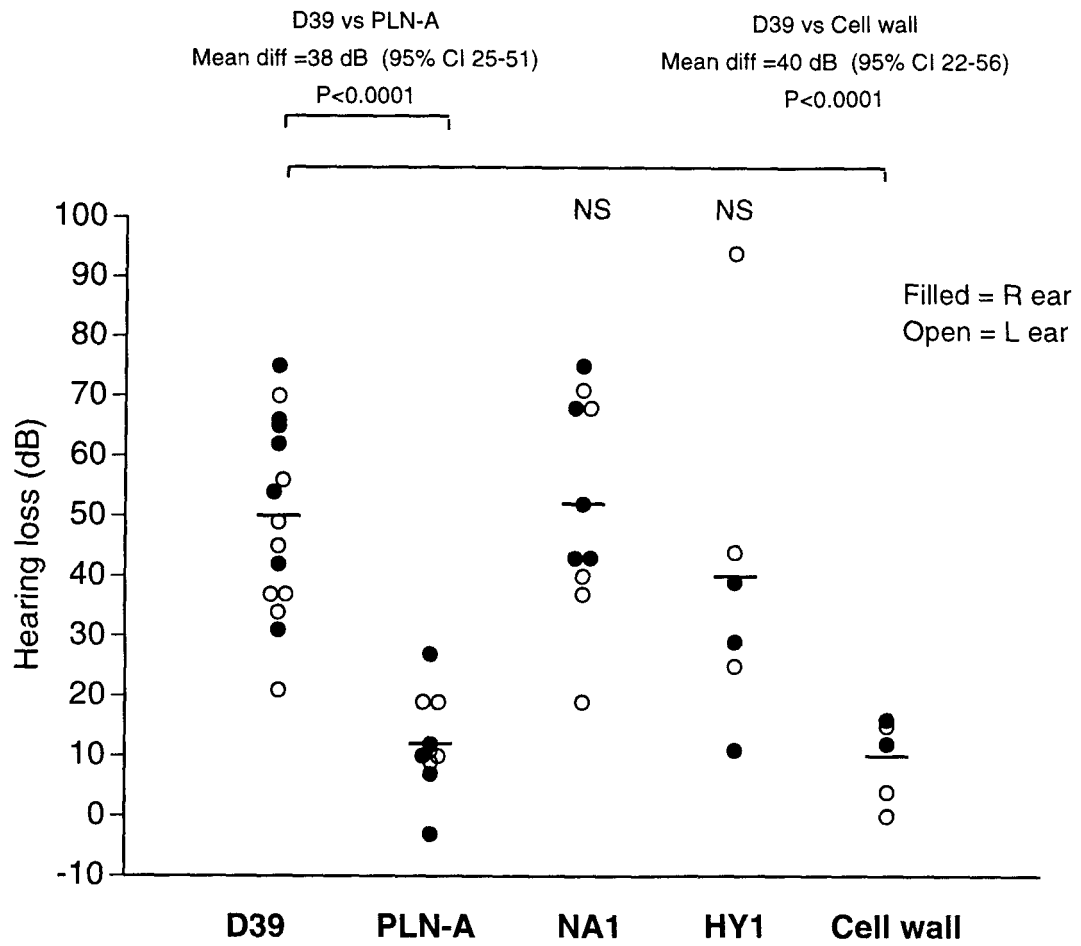


**Figure 3.35:** Pneumococcal meningitis: scatter plot of 10 kHz hearing loss. CAP recordings. Bars are means. P by Mann-Whitney test.

## Hearing loss 3 kHz

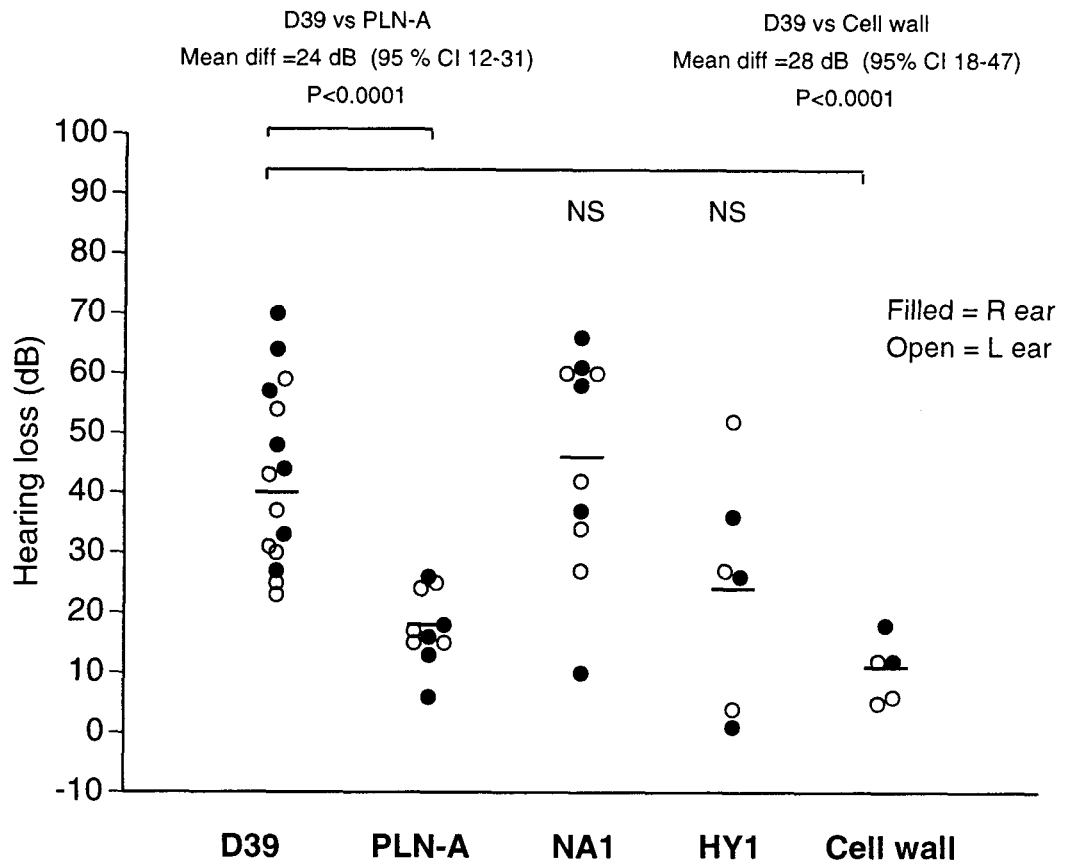


**Figure 3.36:** Pneumococcal meningitis: scatter plot of 3 kHz hearing loss. CAP recordings. Bars are means. P by Mann-Whitney test.

# CM loss

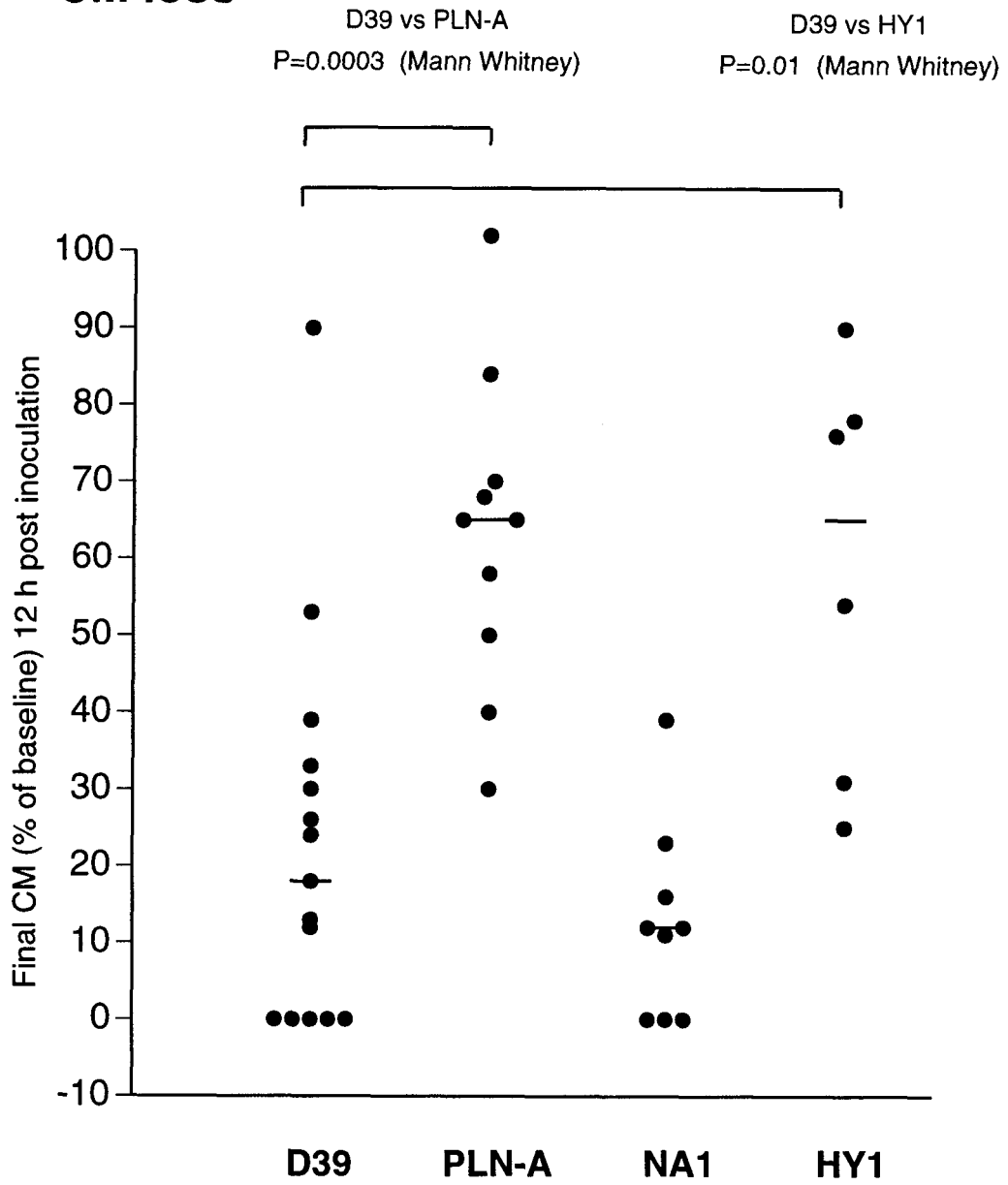
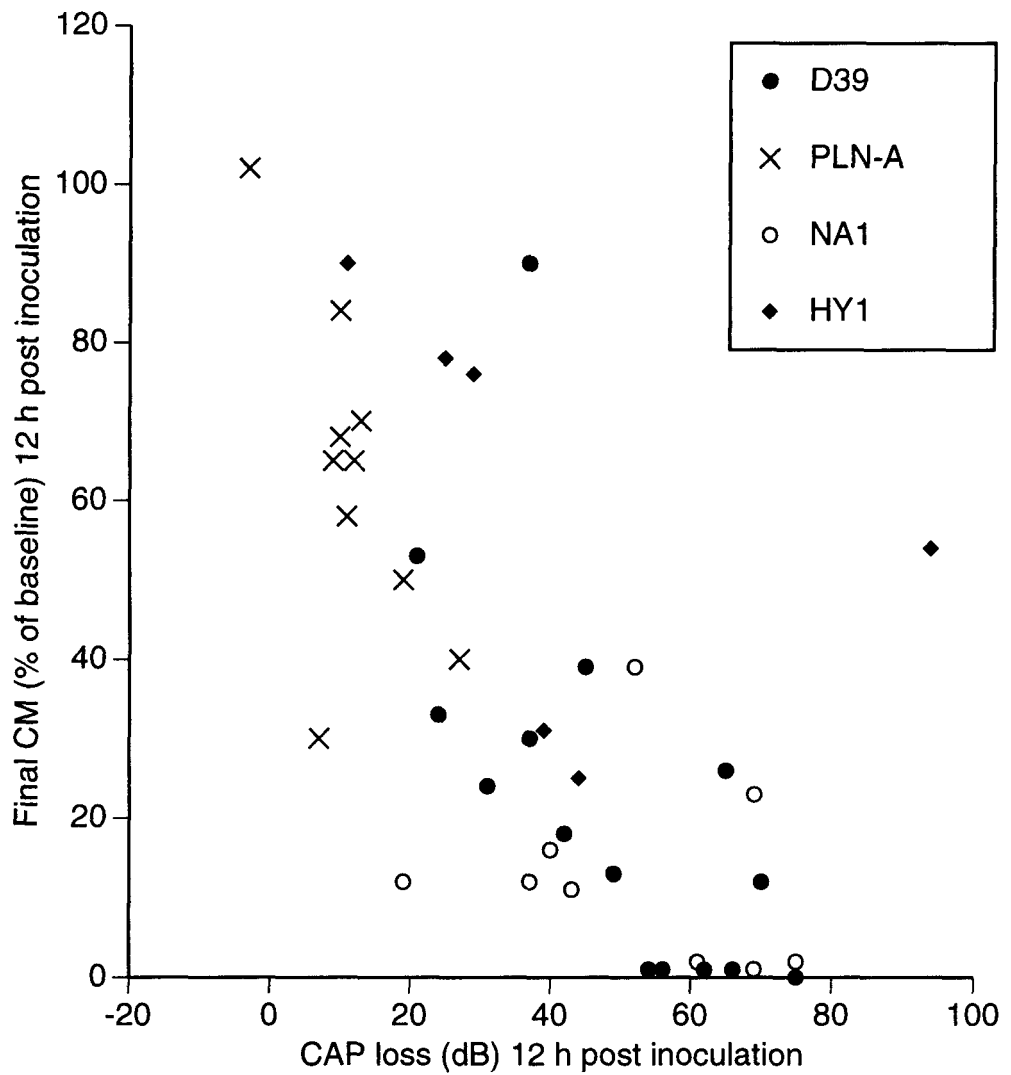


Figure 3.37: Pneumococcal meningitis: scatter plot of CM loss  
Bars are medians.

## CM loss vs CAP loss



**Figure 3.38:** Pneumococcal meningitis: scatter plot of CAP vs. CM. CM loss at 12 h p.i. is related to CAP loss, although there is a wide scatter

### **3.9. Pneumococcal meningitis in the rabbit: a comparison of wild-type (D39) and pneumolysin-deficient (PLN-A) infection.**

*These experiments were performed in conjunction with Dr Spiro Comis and Dr Michael Osborne.*

#### **3.9.1. Introduction and exclusions**

Three rabbits (RAB 36–38) were inoculated with D39 and three (RAB 39-41) with PLN-A to confirm that the differences in hearing loss and ultrastructural damage induced by these two organisms were not just limited to the guinea pig. No CSF was obtained from RAB 37 or RAB 41. Blood samples were not taken. Hearing loss was not assessed for the left ear of RAB 37. Experiments ran for between 9.5 and 11 h. All animals were successfully inoculated (mean inoculum D39, 7.9 log., CFU; PLN-A, 7.5 log., CFU) and viable organisms were recovered from all animals from which a CSF sample was obtained.

#### **3.9.2. Inflammatory response.**

Table 3.17 shows that the four animals in which a CSF sample was taken developed a CSF leukocytosis and elevated protein concentration. There appeared to be no difference between the inflammatory response in either group.

#### **3.9.3. Electrophysiological data.**

Hearing loss was assessed by tone-pip-evoked brain stem response audiometry (BAEP). Final BAEP recordings were compared with the initial control tracings and an approximate dB loss assigned. As far as possible this comparison was performed blind to the experimental group. There was a significantly greater loss in rabbits infected with D39 compared to PLN-A. Median hearing loss was 40 dB greater (97% CI 20 to 80 dB; n=5; P=0.01 by Mann-Whitney test) at 10 kHz and 30 dB greater (97% CI 20 to 40 dB; n=5; P=0.02 by Mann-Whitney test) at 3 kHz in the D39 group (see fig 3.39).

#### **3.9.4. Ultrastructural findings.**

Two cochleas in the wild type group and three cochleas in the PLN-A group were examined by SEM. Only the mid-turn of the organ of Corti could be examined except in RAB (41). This was due to curling of the basal turn during processing. A direct comparison with the guinea pig should therefore be made with caution, as the lesions characteristic of pneumococcal infection in the guinea pig occurred mostly in the basal turn, and only rarely were seen to affect higher turns. Plates are arranged in order of experiment.

In wild-type infection the following lesions were observed:

- i) Cratering of the apical surface of the phalangeal cells above the tunnel of Corti (between the inner hair cells and the first row of outer hair cells) was much more frequent than in the guinea pig (plate 3.70 and 3.71). The size and appearance of the craters were broadly similar however. Plate 3.68 shows defects in the apical surface of inner sulcus cells with intact border cells. The apical surface of the border cells seemed to be less vulnerable in the rabbit.
- ii) Disruption of the intercellular junctions between sensory cells and neighbouring phalangeal processes was seen in both cochleas examined (plate 3.69 and 3.71). However less pitting of the apical surface of the outer hair cells was observed.
- iii) In normal rabbit cochleas (historical controls), the hair bundles of inner hair cells are not quite as well preserved as in the guinea pig. But there is no doubt that plates 3.70 and 3.71 reveal severe devastation of the hair bundles of the inner hair cells. Most IHC stereocilia in plate 3.71 are missing completely and those that are still attached to the surface of the sensory cell are swollen and shortened.

In pneumolysin deficient meningitis, there was significantly less ultrastructural damage as judged by SEM. There was some irregularity of the hair bundles of inner hair cells (plates 3.72 and 3.73). A single crater was found in a border cell (plate 3.74). Outer hair cells appeared to remain intact (plate 3.75).

In conclusion there are three points:

- Experimental pneumococcal meningitis in the rabbit results in profound sensorineural deafness and induces three specific ultrastructural lesions in the organ of Corti: cratering of the apical surface of supporting cells, disruption of hair bundles and breakdown of the intercellular junctions between sensory cells and supporting cells.
- These lesions are broadly similar to those induced by experimental pneumococcal meningitis in the guinea pig. In the rabbit, border cells are spared at the expense of more damage to phalangeal cells, and inner hair cells and their hair bundles suffer more damage than outer hair cells. In the guinea pig outer hair cells are more affected.
- Infection with a pneumolysin-deficient derivative causes significantly less hearing loss and almost abolishes ultrastructural damage in both species.

Expt no.	Batch	Time (h)	Inoculum (log <sub>10</sub> CFU)	CSF CFU (log <sub>10</sub> /ml)	CSF WBC (cells/μl)	CSF protein (g/l)	Estimated hearing loss (dB; L/R)		Histological findings
							@10 kHz	@ 3kHz	
RAB 37	G	9.5	7.6	--	--	--	-/60	-/60	(L): (mid-turn) Craters in BCs, damaged intercellular junctions, IHC s/c disrupted more than OHC s/c.
RAB 36	G	10.5	7.6	8.8	1,600	2.4	90/80	80/60	not examined
RAB 38	G	10.5	8.2	9.1	3,900	1.5	80/80	40/60	(L): (mid-turn) extensive loss of IHC s/c and damage to intercellular junctions. Craters in phalangeal cells Some OHC damage.
<b>Mean (D39)</b>			<b>7.9</b>	<b>9.0</b>	<b>2,500g</b>	<b>1.9g</b>	<b>80med</b>	<b>60med</b>	
RAB 39	J	10.5	8.0	8.0	2,125	.5	60/0	40/20	(L): (mid-turn) Slight IHC s/c irregularity but OHCs are intact
RAB 40	J	11	7.3	7.2	2,275	1.2	0/40	20/40	(L): (basal and mid) Slight IHC s/c irregularity. (R): (apex only) intact
RAB 41	J	11	7.3	--	--	--	60/40	20/40	(L): Single crater seen in ISC, IHC and OHC intact
<b>Mean (PLN-A)</b>			<b>7.5</b>	<b>7.6</b>	<b>2,200g</b>	<b>0.7g</b>	<b>40med</b>	<b>30med</b>	

Hearing loss data from brain-stem auditory evoked response recording, estimated by comparison with control readings -- = not evaluated. (technical problems etc.).  
g=geometric mean; OHC=outer hair cell; IHC= inner hair cell; s/c= stereocilia; BC= border cells. med=median

**Table 3.17:** Details of rabbit meningitis experiments.

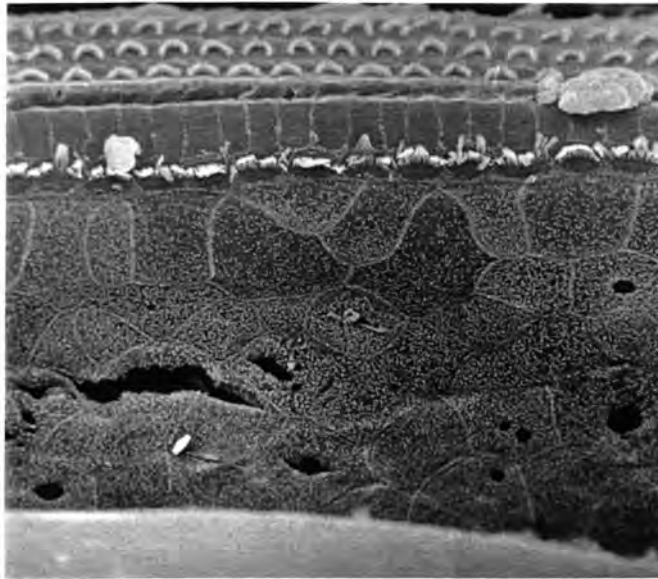


**Plate 3.68**

RAB 37 L (D39) x800, mid turn. 9 h30 p.i.

There are some small circular defects in the apical surface of some inner sulcus cells, but the border cells appear intact. There is some irregularity of the inner hair bundles.

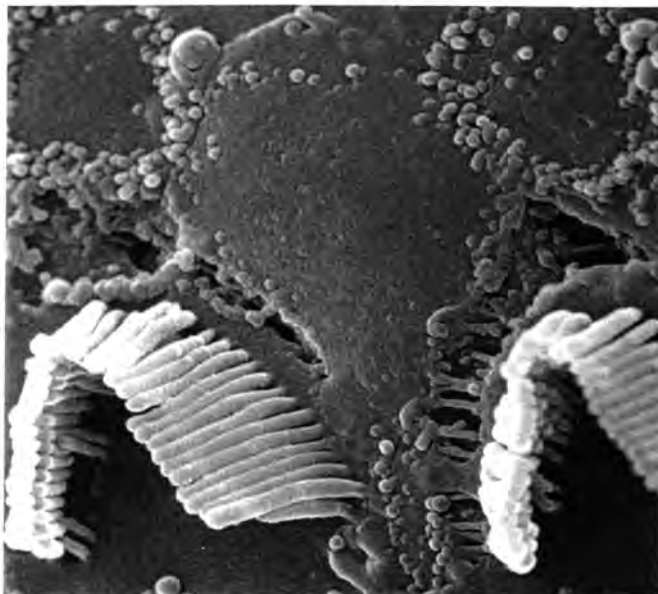


**Plate 3.69**

RAB 37 L (D39) x10,000, mid-turn, 9 h30 p.i.

These row 1 OHCs are breaking away from their neighbouring supporting cells. The hair bundles appear to be reasonably intact.

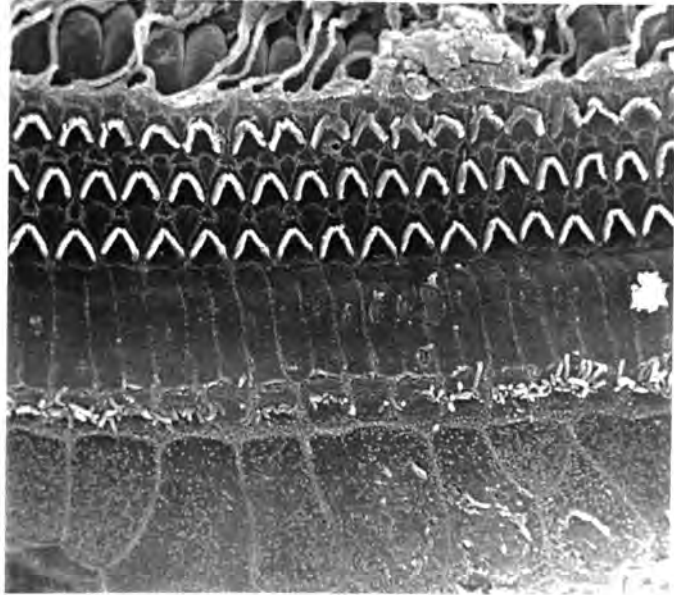


**Plate 3.70**

RAB 38 L (D39) x1,000, mid turn, 10 h30 p.i.

This low-power view reveals widespread devastation of the IHC hair bundles. There are many shallow craters in the apical surface of the phalangeal cells. However, the OHCs appear reasonably intact.



**Plate 3.71**

RAB 38 L (D39) x1,000, mid turn, 10 h30 p.i.

At higher power, the extent of devastation can be seen. Most stereocilia are missing. Remaining stereocilia are shortened and collapsed. The intercellular junctions also appear to be disrupted.

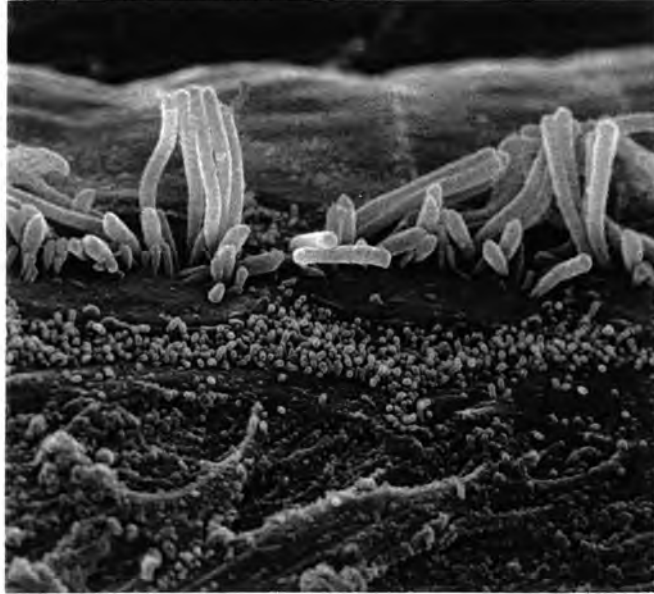


**Plate 3.72**

RAB 39 L (PLN-A) x5,000, mid turn, 10 h30 p.i.  
Although the stereocilia are irregular, the IHC cell surface itself appears intact.

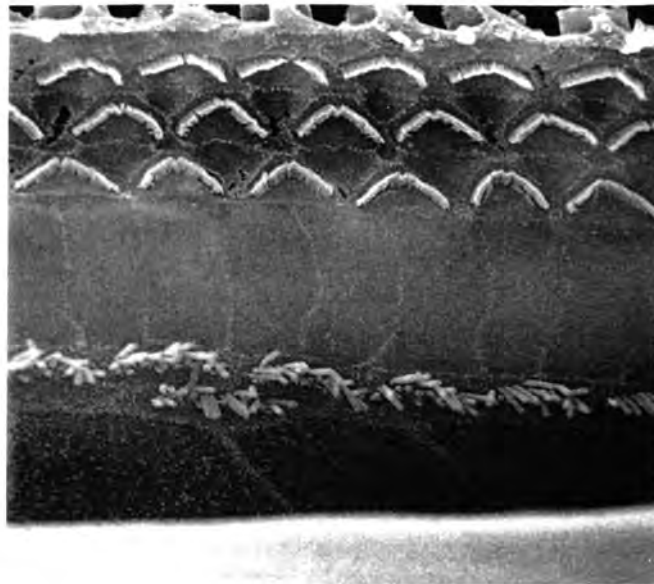


**Plate 3.73**

RAB 40 L (PLN-A) x2,000, mid turn, 11 h p.i.  
The organ of Corti is intact apart from some irregularity of IHC stereocilia.

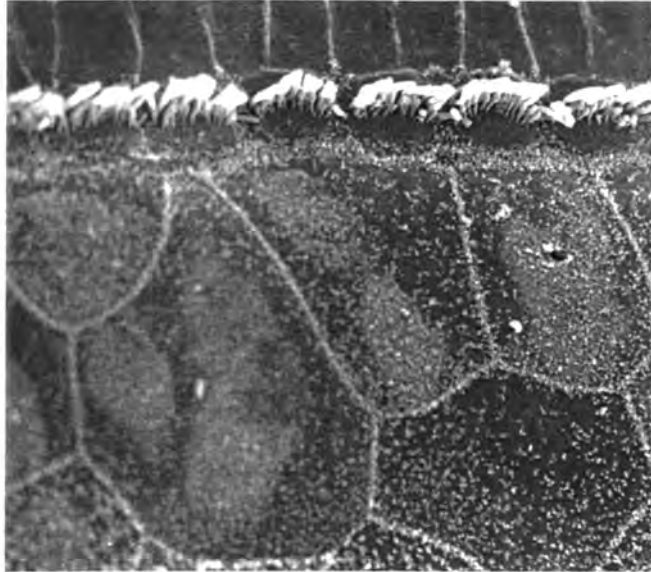


**Plate 3.74**

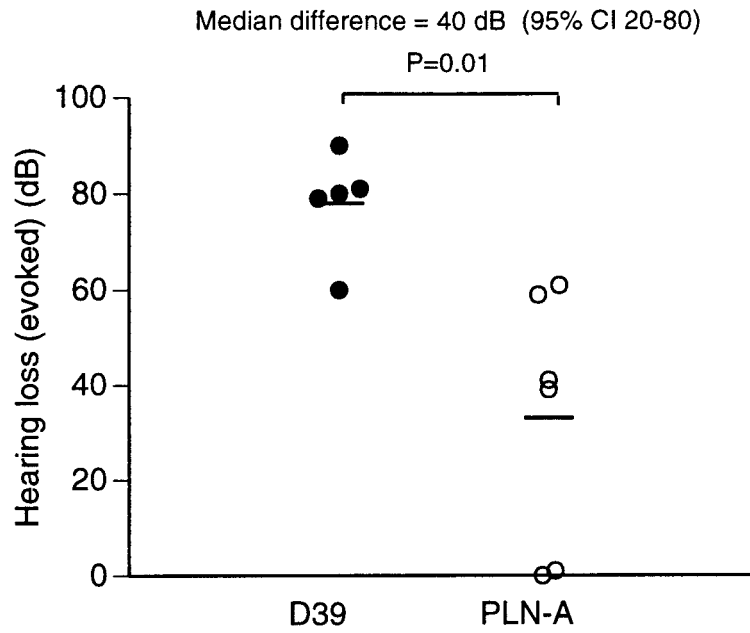
RAB 41 L (PLN-A) x2,000, basal turn, 11 h p.i.  
Intact IHC stereocilia and a tiny defect in the surface of otherwise normal inner sulcus cells.



**Plate 3.75**

RAB 41 L (PLN-A) x4,000, basal turn, 11 h p.i.  
These OHCs appear intact.

## Hearing loss 10 kHz



## Hearing loss 3 kHz

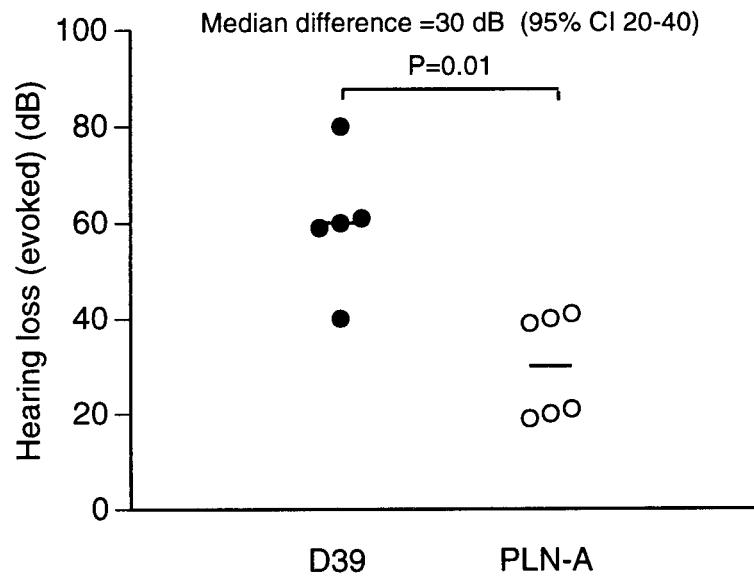


**Figure 3.39:** Rabbit pneumococcal meningitis: scatter plot of hearing loss. Hearing assessed by recording tone-evoked brain stem potentials.

## 4. COCHLEAR PERFUSION

### 4.1. Introduction.

#### 4.1.1. Overview.

In this study, a suspension of either *S. pneumoniae* or *E. coli* was microperfused into the scala tympani to model what might happen to the organ of Corti when organisms reach the inner ear during meningitis. Some animals were pretreated with antibiotics or dexamethasone. The compound action potential (CAP) evoked by a 10 kHz tone pulse, and the peak cochlear microphonic (CM) potential (at 5 kHz), were measured at intervals for 3 h after perfusion. The cochlea was then intravitaly fixed and processed for examination by scanning electron microscopy. Initial experiments were conducted with *E. coli* K-12 to perfect the techniques and ensure that the requirements for containment for *S. pneumoniae* could be met. To avoid contamination of the tubing and wire in the recording pipette the inoculum (10  $\mu$ l) was administered via a separate perfusion line and micropipette. Baseline readings taken prior to perfusion were often quite different to those obtained on reinserting the recording pipette minutes after inoculation, especially for the cochlear microphonic potential. This is likely to be due to (i) a change in coupling impedance (due to a variation in the seal obtained) and (ii) a slight change in the position of the pipette tip within the cochlea relative to the generator units. Therefore 'baseline' stimuli in the following experiments refer to readings taken within a few minutes of inoculation, rather than just before.

The arguments behind the definition of the reference level for the compound action potential (CAP) threshold are given in section 3.3.3. For brevity, the terms 'CAP loss' and 'hearing loss' are taken as synonymous with the increase in stimulus intensity needed to restore the mean height of the N<sub>1</sub>-P<sub>1</sub> wave of the CAP to its reference level of 100  $\mu$ V.

The experimental numbering is not always sequential as other workers were conducting similar work at this time (not reported here). Exclusions are listed under the relevant section.

#### 4.1.2. Inocula.

For *E. coli* experiments, a fresh 3 h log-phase culture was prepared for each experiment, and the bacterial titre was adjusted by counting organisms. An inoculum of 6.5 log<sub>10</sub> organisms was used. For *S. pneumoniae* perfusion, identical aliquots of either Batch A or Batch B were used to give a desired inoculum of 6.5 log<sub>10</sub> CFU in 10  $\mu$ l. Colony counts

were performed for each experiment. All inocula were within 0.4 log units of the desired amount. The use of reproducible inocula allowed a formal comparison between untreated and antibiotic-treated animals.

## **4.2. *E. coli* perfusion**

### **4.2.1. Electrophysiological data.**

Mean CAP loss 3 h after perfusion was just 7 dB (95% confidence interval **-5** to 19 dB) with a maximum loss of 13 dB in expt K-12 Perf 5. The mean fall in cochlear microphonic was 20% (range 62% loss to 31% gain). Table 4.1 lists all the electrophysiological data, which are shown graphically in figure 4.2 and 4.3 (page 220 et seq).

### **4.2.2. Ultrastructural findings.**

Damage to the organ of Corti assessed by scanning electron microscopy (**SEM**) was patchy and not at all severe, in keeping with the limited effects of *E. coli* K-12 on CAP loss and cochlear microphonics. The right-hand cochleae when examined were intact, and acted as controls for the processing.

***K12 Perf 2:*** This cochlea was destroyed during dissection.

***K12 Perf 5:*** The organ of Corti was mostly intact with no damage to hair cells (plate 4.1). There were occasional areas where inner hair cell (MC) stereocilia had become detached from the sensory cell and there were a few craters in the apical surface of border cells (plate 4.2). Organisms were seen on the scala tympani surface of the basilar membrane (plate 4.3). This confirmed that the micro perfusion technique used was adequate to inoculate the scala tympani. Plate 4.3 shows nicely the loose reticular structure of the basilar membrane when viewed with SEM. Organisms appeared to be dividing.

***K12 Perf 7:*** No craters were seen in the border cells, but there was some minor disruption of the lateral links of MC stereocilia (not shown).

***K-12 Perf 9:*** This cochlea was fixed 4 h after inoculation. There was some areas where IHC stereocilia appeared to be missing and some craters in the apical surface of border cells were observed (plate 4.4).

	Time (min)	<b>K12 Perf 2</b>	<b>Perf5</b>	<b>Perf7</b>	<b>Perf9</b>	<b>Mean</b>	<b>95% CI</b>
<b>CAP loss</b>	<b>5</b>	<i>0</i>	<i>0</i>	<i>0</i>	<i>0</i>	<b>0</b>	<i>0</i>
<b>10 kHz</b>							
<b>(dB)</b>	180	<b>5</b>	13	<i>0</i>	8	<b>7</b>	12
<b>Baseline stimulus</b> (N1-P1=100µV; dB SPL)		45	35	40	<b>55</b>	<b>44</b>	14
<b>CM (0 h) (mV)</b>		0.289	0.359	0.368	<i>0.605</i>		
<b>CM (3 h) (mV)</b>		0.180	0.385	0.482	0.340		
<b>CM ratio</b>		0.38	1.07	1.31	0.56	0.8	0.7

Inoculum was **5x** 10(6)organisms in 10µl of artificial perilymph. CAP=compound action potential; CM=cocNear microphonic; CI=confidence interval;

**Table 4.1:** Cochlear perfusion with *E. coli* **K-12**: electrophysiological data

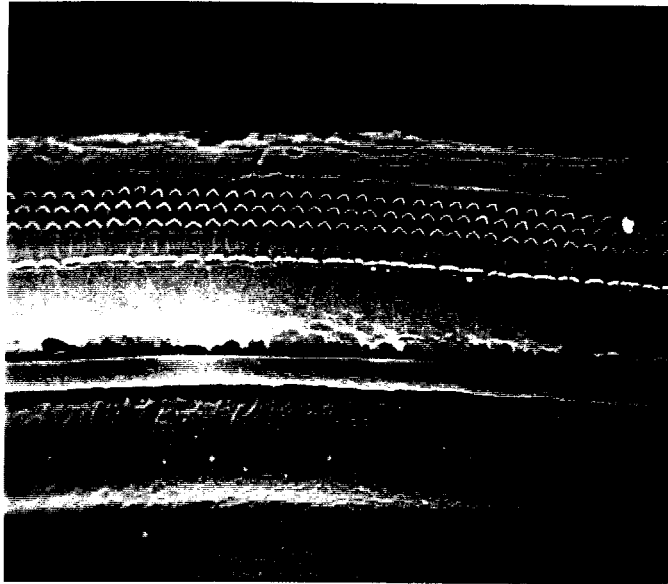


**Plate 4.1**

K-12 Perf 5 (exptl) basal turn x300

Intact organ of Corti. There is artefactual splitting deep in the inner sulcus but the surface of the border cells is intact.



**Plate 4.2**

K-12 Perf 5 (exptl) basal turn x6,000

The hair bundles are deformed, and some stereocilia have become detached from the surface of the inner hair cell (arrow). Intercellular junctions appear intact but there is a small crater in a border cell.

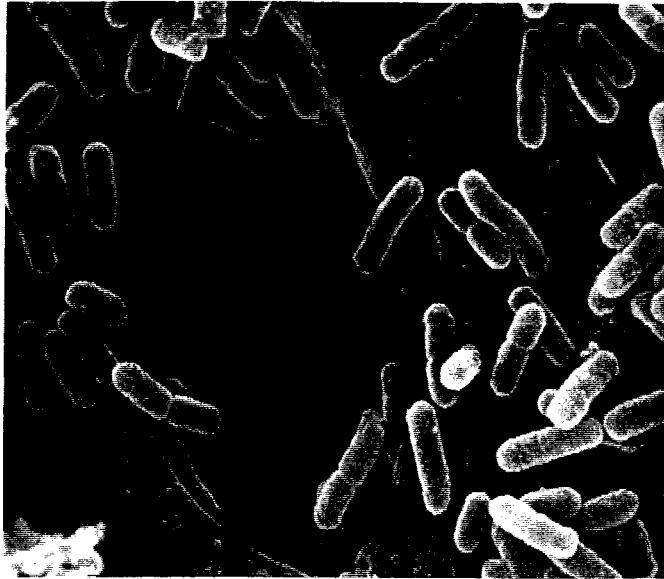


**Plate 4.3**

K-12 Perf 5 (exptl) basal turn x6,000

Organisms on surface of basilar membrane. Note the loose reticular structure of the connective tissue overlying the membrane. Compare plate 3.6.

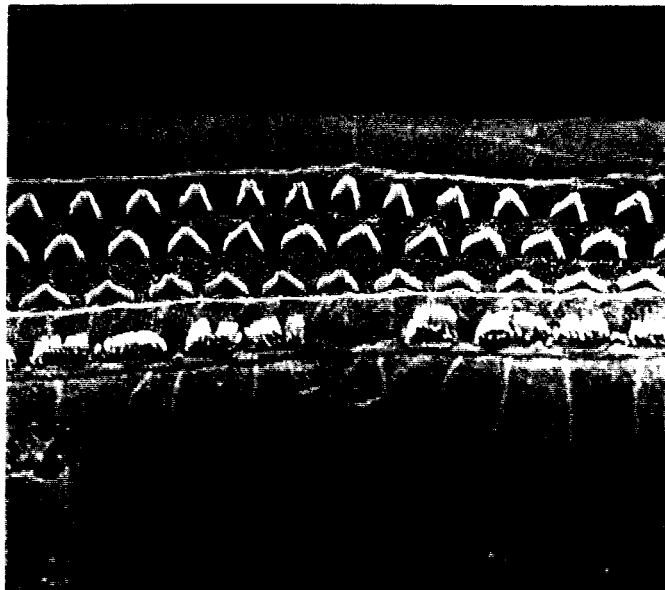


**Plate 4.4**

K-12 Perf 9 (exptl) basal turn x1,000

There are some craters in the surface of border cells. Some IHC stereocilia appear to be missing.

### **4.3. Pneumococcal perfusion alone**

#### **4.3.1. Experimental details and exclusions.**

Four animals were included in the analysis. The mean inoculum was 6.7 log<sub>10</sub> CFU (range 6.5 to 6.9). Experiment D39 Perf 3 was excluded because the cisterna magna was not opened and there was doubt whether the inoculum was successfully perfused. In expt Perf 12 the apex of the cochlea was fractured during surgery and in expt Perf 16 there was bleeding into the meatus causing conductive deafness. Both of these experiments were therefore excluded from the evaluation. The CAP losses measured in three historical control experiments (where APL alone was perfused) are included in fig 4.2 for interest. Because of the minimal CAP loss after perfusion with *E. coli* K-12 additional APL-only perfusions were not conducted.

#### **4.3.2. In vitro growth.**

Assessing the in vivo growth of organisms in the perilymphatic space would seem almost impossible due to the tiny volume of fluid. It was not known whether APL could support the growth of D39. An aliquot of *S. pneumoniae* D39 (batch B) was prepared exactly as for a perfusion experiment, but then inoculated into 4 ml sterile APL at 37°C and incubated (no shaking, no additional CO<sub>2</sub>). Every hour, an aliquot (10 µl) was removed and the titre determined. Fig 4.1 (page 211) shows a steady decline in viable counts over 6 h. This information merely suggests that D39 may not grow well in perilymph, but as artificial perilymph may well lack trace nutrients interpretation is tricky.

#### **4.3.3. Electrophysiological data.**

These are summarised in table 4.2 below, and in figures 4.2 to 4.5 on pages 220 to 223. Mean CAP loss at the 3 h endpoint was 44 dB (95% confidence interval 32 to 56 dB). The pattern of CAP loss was consistent in all four experiments. Apart from the initial variation in baseline, there was little change in CAP during the first 60 min post-perfusion. Over the subsequent 30-60 min there was a rapid fall in CAP which then levelled out. The mean rate of CAP loss over the post-perfusion period 60-180 min was 19 dB/h (see section 4.4.2 for detailed discussion of this analysis).

There was no change in mean peak cochlear microphonic potential over the course of the experiments (range 14% loss to 14% gain).

#### **4.3.4. Ultrastructural findings.**

Two specific ultrastructural lesions in the organ of Corti were noted: (i) disruption and detachment of hair cell stereocilia and (ii) cratering of the apical surface of the border cells. Three cochleae were examined after pneumococcal perfusion and all had extensive areas of damage with gross deformation of stereocilia and much debris scattered over the surface of the organ of Corti in both basal and mid turns. Damage was predominantly limited to inner hair cell stereocilia. In contrast to the damage incurred during experimental pneumococcal meningitis (see section 3.3.4 et seq), there was only some pitting of the apical surface of the hair cells rather than frank cratering.

*D39 Perf 1:* This cochlea was badly curled but in one area of the basal turn the IHC stereocilia were clearly detached from the cuticular plate. However, when examined by transmission electron microscopy the hair cell plasma membranes, nerve endings and the surfaces of the border cells all appeared intact (not shown).

*D39 Perf 2:* Both types of damage were seen (plates 4.5 and 4.6). On the scala tympani side of the basilar membrane, micro colonies of what appeared to be pneumococci could be observed (plate 4.11 and 4.12).

*D39 Perf 4:* The control (right) cochlea is shown here to demonstrate the appearance of undamaged stereocilia after osmication (plate 4.7). There were widespread areas of damage in the experimental cochlea (plate 4.8). Plates 4.9 and 4.10 show at higher power the devastation wrought on the stereocilia. Many hair bundles were disrupted and some were collapsed on the cell surface.

*D39 Perf 10:* This cochlea was not examined.

	Time (min)	Perf1	Perf2	Perf4	Perf10	Mean	95%CI
<b>CAP loss</b>	<b>5</b>	0	5	0	0	<b>1</b>	4
<b>10 kHz</b>	<b>20</b>	<b>5</b>	0	0	0	<b>1</b>	4
<b>(dB)</b>	<b>40</b>	0	3	0	4	<b>2</b>	3
	<b>60</b>	8	3	0	7	<b>5</b>	6
	<b>90</b>	28	18	25	20	<b>23</b>	7
	<b>120</b>	35	22	38	37	<b>33</b>	12
	<b>150</b>	41	32	34	51	<b>40</b>	14
	<b>180</b>	46	40	35	53	<b>44</b>	12
<b>Baseline stimulus</b> (N1-P1=100µV;dB SPL)		25	40	40	36	<b>35</b>	11
<b>CM (0 h)</b> (mv)		0.580	0.228	0.499	0.359		
<b>CM (3 h)</b> (mv)		0.499	0.228	0.570	0.315		
<b>CM ratio</b>		0.86	1.00	1.14	0.88	<b>1.0</b>	0.2
<b>Inoculum</b> (log <sub>10</sub> CFU)		6.7	6.5	6.9	6.7	<b>6.7</b>	0.3

Inoculum in 10 µl of artificial perilymph. CAP=compound action potential; CM=cochlear microphonic; CI=confidence interval;

**Table 4.1:** Cochlear perfusion of *S. pneumoniae* D39: electrophysiological data.

## D39 in APL

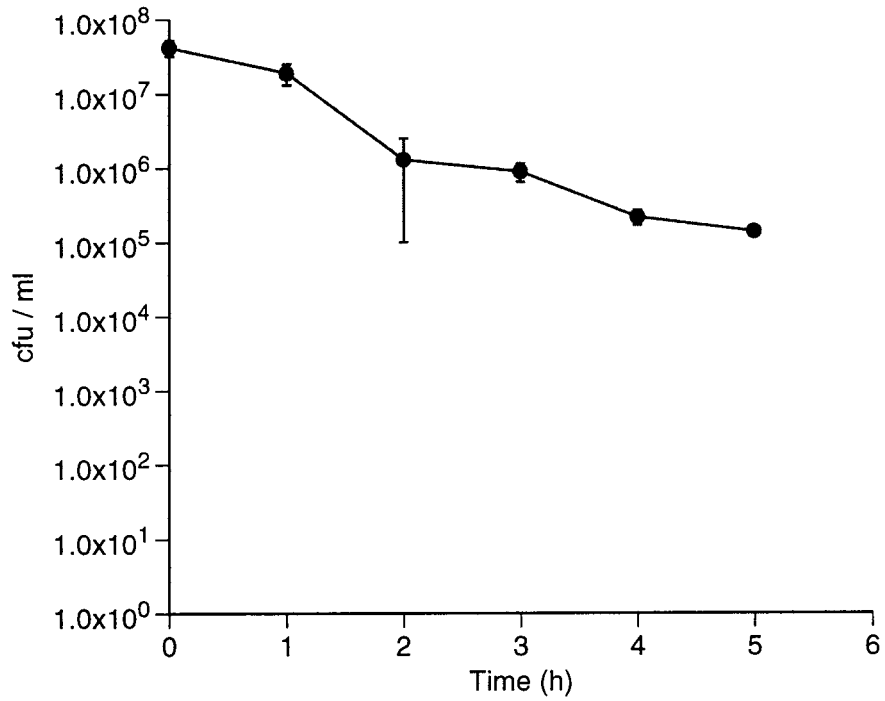


**Figure 4.1:** Growth of *S. pneumoniae* D39 in artificial perilymph. Means (95% confidence intervals) of three replicate colony counts. Incubated at 37°C with no added CO<sub>2</sub> or shaking; total volume 5 ml.

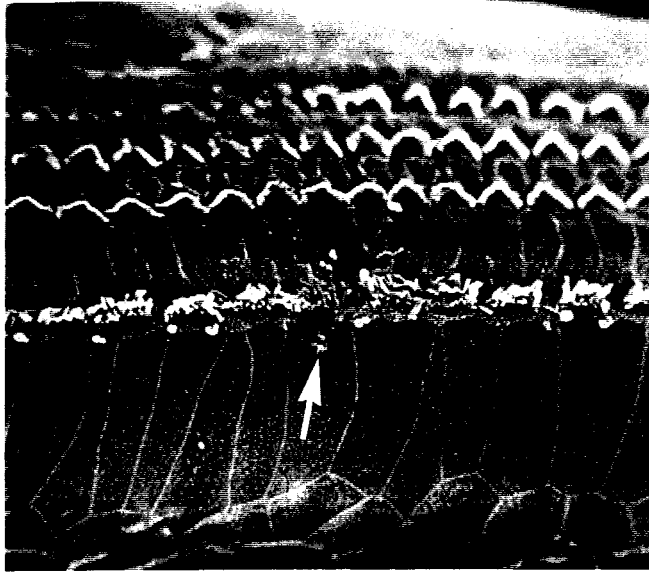


**Plate 4.5**

D39 Perf 2 (exptl) basal turn x800  
Crater in the surface of a border cell associated with  
disruption of the adjacent IHC hair bundle (arrow).



**Plate 4.6**

D39 Perf 2 (exptl) basal turn x10,000  
Damaged IHC stereocilia, some of which are detached from the cell  
surface.

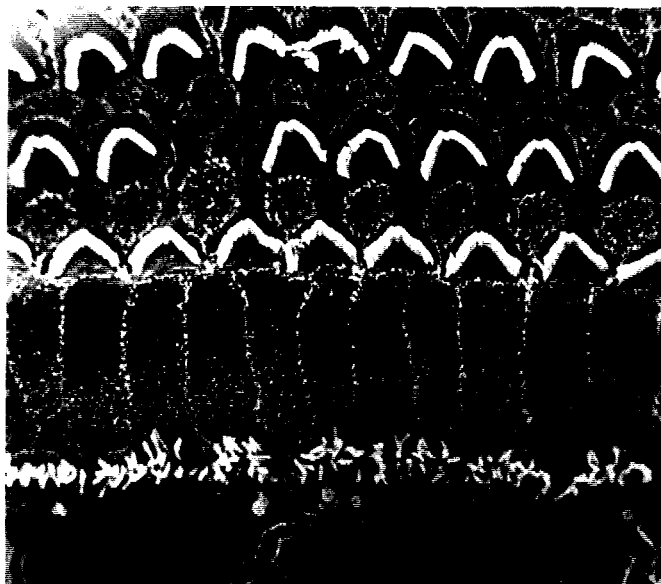


**Plate 4.7**

D39 Perf 4 (control) basal turn, x1,500 (osmicated)  
There are large artefactual cracks (but no small craters) in the border cells. Although the IHC stereocilia are irregular due to osmication, they are neither fused nor uprooted.

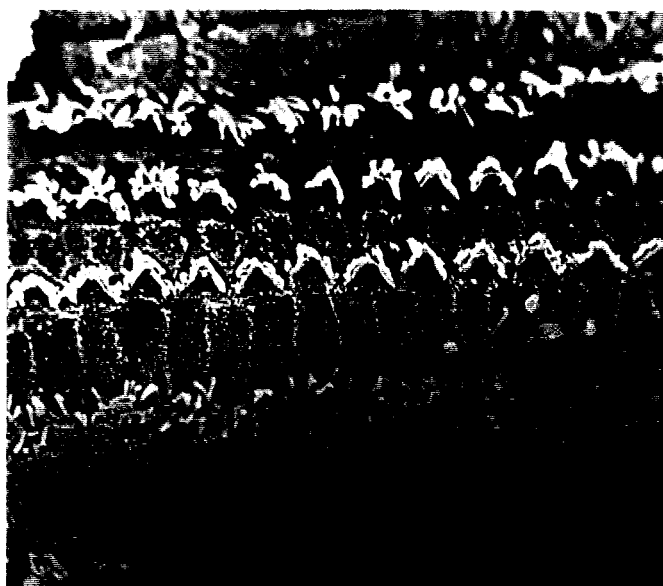


**Plate 4.8**

D39 Perf 4 (exptl) mid turn x1,000 (osmicated)  
There is extensive disruption of IHC and OHC hair bundles, cratering of the surface of border cells and a lot of debris on the surface of the organ of Corti.



**Plate 4.9**

D39 Perf 4 (exptl) basal turn x10,000  
Row 2 OHC. The hair bundle is collapsed onto the cell surface.  
Some stereocilia are detached from the cell (arrow). There is pitting  
of the apical cell surface (asterisk).



**Plate 4.10**

D39 Perf 4 (exptl) basal turn x6,000  
Inner hair cell. Fusion of stereocilia.

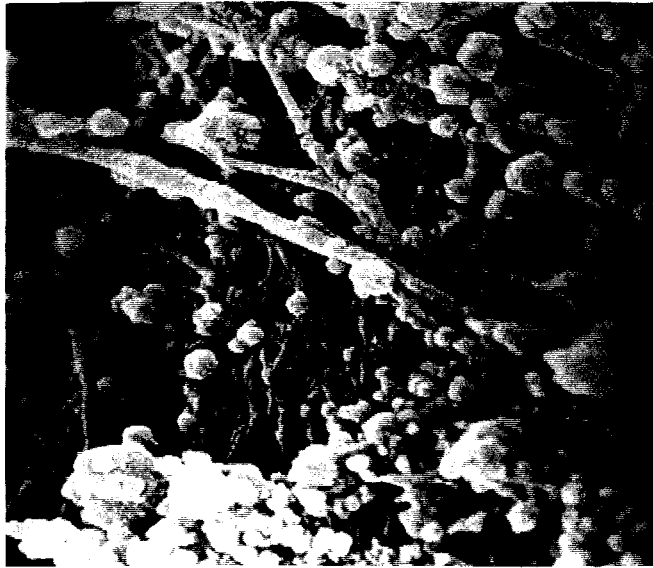


**Plate 4.11**

D39 Perf 2 (exptl) untreated x15,000. Pneumococci colonising under surface of basilar membrane.

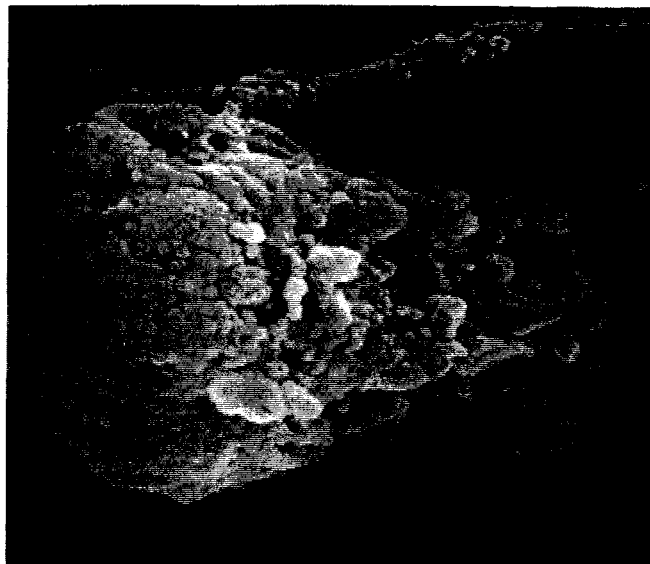


**Plate 4.12**

D39 Perf 2 (exptl) untreated x15,000  
Scala tympani. Leukocyte phagocytosing pneumococci.

## 4.4. Pneumococcal perfusion with antibiotic pretreatment.

### 4.4.1. Experimental details and exclusions

Two further groups of animals received 100 mg/kg cefotaxime (CTX, n=4) or amoxicillin (AMOX, n=4) by intraperitoneal injection 30 min prior to inoculation of the scala tympani. The mean inoculum in the cefotaxime group (6.9 log CFU) was comparable to that in the untreated group (6.7 log CFU), but was slightly lower in the amoxicillin group (6.3 log CFU). These differences are unlikely to be clinically significant. The mean baseline stimuli ( $N_1-P_1=100 \mu V$ ) did not differ between the groups. In expt D39 Perf 19, a new technique allowed the inoculum to be perfused through the recording pipette, so establishing the baseline stimulus prior to perfusion

### 4.4.2. Electrophysiological data.

Both antibiotics afforded substantial protection from CAP loss. The course of CAP loss was almost identical in the two groups. Tables 4.3 and 4.4 and figures 4.2 to 4.5 (page 218 et seq) summarise the electrophysiological data. Significance of the difference between the means was assessed by Student's t-test.

Expt	CAP loss (dB)	Difference from D39 (95% confidence interval) (dB)	Significance
D39 (n=4)	44	N/A	
CTX (n=4)	23	7 to 35	p=0.01
AMOX (n=4)	20	7 to 40	p=0.01

CTX=cefotaxime pretreatment; AMOX=amoxicillin pretreatment.

A further analysis of the rate of CAP loss was performed by grouped linear regression. This is more robust than simply fitting a single regression line to the mean data for each group. The slopes were then compared by analysis of variance. Such analysis needs to be interpreted with a great deal of caution as the data here are not strictly independent and (for the untreated group) the rate of loss over the period 60 to 180 min was barely linear (although passing the test for linearity). The mean rate of CAP loss over the post-perfusion period 60-180 min was 19 dB/h. This was significantly reduced by pretreatment with CTX (8 dB/h, p=0.003) or AMOX (6 dB/h, p<0,001). There was no significant difference between the rates of CAP loss in the CTX and AMOX groups (p=0.24).

The cochlear microphonics were again surprisingly preserved, with a mean loss of 20% in the CTX group (range 12% to 32%) and no change in the AMOX group (range 10% loss to 17% gain).

#### **4.4.3. Ultrastructural findings.**

##### ***Morphological changes in the organ of Corti***

*039 Perf 5* (CTX): In the basal turn some MC stereocilia were detached from the cell surface but the border cells remained intact. However in the mid-turn there was an area of extensive devastation (plate 4.13). Because of the extent and the quantity of debris, some of this damage is probably artefactual.

*039 Perf 6* (CTX): A single crater was found in a border cell in the basal turn. There was mild disruption of the IHC hair bundle (plate 4.14).

*039 Perf 7 and Perf 13* (CTX): The organ of Corti appeared intact.

*039 Perf 15 and 19* (AMOX): Some mild irregularity of IHC hair bundles was seen (plate 4.15) but no other damage was found. A well preserved OHC hair bundle is shown in plate 4.16

*039 Perf 14 and 17* (AMOX): These cochleae were not examined.

##### ***Morphological changes in bacteria***

The purpose of administering antibiotic 30 min prior to bacterial perfusion was to load the tissues of the inner ear and perilymphatic spaces with a bactericidal concentration of either cefotaxime or amoxicillin. Perilymph was not collected for antibiotic assay. In expt D39 Perf 18 (an animal pretreated with 100 mg/kg of amoxicillin) the experimental cochlea was intravitaly fixed 75 minutes after pneumococcal perfusion and the scala tympani surface of the basilar membrane examined by SEM. Plates 4.18 through 4.20 demonstrate typical morphological effects of cell-wall active antibiotics on gram-positive organisms: long filamentous forms, cell wall irregularity and chain formation. (Compare chapter 3.2.4 for similar effects in gram-negative bacteria.) This is qualitative evidence that antibiotic penetrated the inner ear and could be having a biologically relevant effect such as inducing cell wall shedding and arresting bacterial growth. One possible result of antibiotic treatment is that the organisms can be cleared more effectively. Plate 4.17 shows that few organisms were found on the underside of the basilar membrane 3 h after CTX treatment (compare plate 4.11).

	Time (min)	Perf5	Perf6	Perf7	Perf13	Mean	95% CI
<b>CAP loss</b>	<b>5</b>	12	0	<b>5</b>	0	<b>4</b>	9
<b>10 kHz</b>	<b>20</b>	0	0	8	3	<b>3</b>	6
<b>(dB)</b>	<b>40</b>	<b>5</b>	12	3	0	<b>5</b>	8
	<b>60</b>	<b>5</b>	10	0	6	<b>5</b>	7
	<b>90</b>	30	8	3	4	<b>11</b>	20
	<b>120</b>	17	6	8	22	<b>13</b>	12
	<b>150</b>	20	12	12	28	<b>18</b>	12
	<b>180</b>	22	16	17	35	<b>23</b>	14
<b>Baseline stimulus</b> (N1-P1=100µV; <b>dB</b> SPL)		25	40	35	33	<b>36</b>	10
<b>CM (0 h) (mV)</b>		0.665	0.725	0.525	0.755		
<b>CM (3 h) (mV)</b>		0.585	0.499	0.359	0.585		
<b>CM ratio</b>		0.88	0.69	0.68	0.77	<b>0.8</b>	<b>0.1</b>
<b>Inoculum (log<sub>10</sub> CFU)</b>		6.9	7	7	6.6	<b>6.9</b>	0.3

Inoculum perfused into scala tympani in 10 µl of artificial perilymph. Cefotaxime 100 mg/kg given i.p. 30 min pre-inoculation.. CAP=compound action potential; CM=cochlearmicrophonic; CI=confidence interval.

**Table 4.2:** Cochlear perfusion of *S. pneumoniae* D39 with cefotaxime pretreatment: electrophysiological data.

	Time (min)	Perf14	Perf15	Perf17	Perf19	Mean	95%CI
<b>CAP loss</b>	<b>5</b>	0	0	-20	12†	<b>-2</b>	21
<b>10 kHz</b>	<b>20</b>	10	2	0	7	<b>5</b>	7
<b>(dB)</b>	<b>40</b>	15	2	<b>5</b>	<b>5</b>	<b>7</b>	9
	<b>60</b>	20	2	10	3	<b>9</b>	13
	<b>90</b>	25	6	1	8	<b>10</b>	17
	<b>120</b>	30	15	7	<b>5</b>	<b>14</b>	18
	<b>150</b>	32	16	8	8	<b>16</b>	18
	<b>180</b>	35	15	<b>20</b>	9	<b>20</b>	18
<b>Baseline stimulus</b> (N1-P1=100µV; dB SPL)		30	56	30	35	<b>38</b>	20
<b>CM (0 h)</b> (mv)		0.499	0.865	0.490	0.464		
<b>CM (3 h)</b> (mv)		0.490	0.780	0.482	0.545		
<b>CM ratio</b>		0.98	0.90	0.98	1.17	<b>1.0</b>	0.2
Inoculum (log,, CFU)		6.2	6.3	6.4	6.3	<b>6.3</b>	0.1

Inoculum perfused into scala tympani in 10µl of artificial perilymph. Amoxicillin 100 mg/kg given i.p. 30 min pre-inoculation. CAP=compound action potential; CM=cochlear microphonic; CI=confidence interval. †: Baseline from pre-perfusion reading (see text)

**Table 4.3:** Cochlear perfusion of *S. pneumoniae* D39 with amoxicillin pretreatment: electrophysiological data.

## Compound action potential

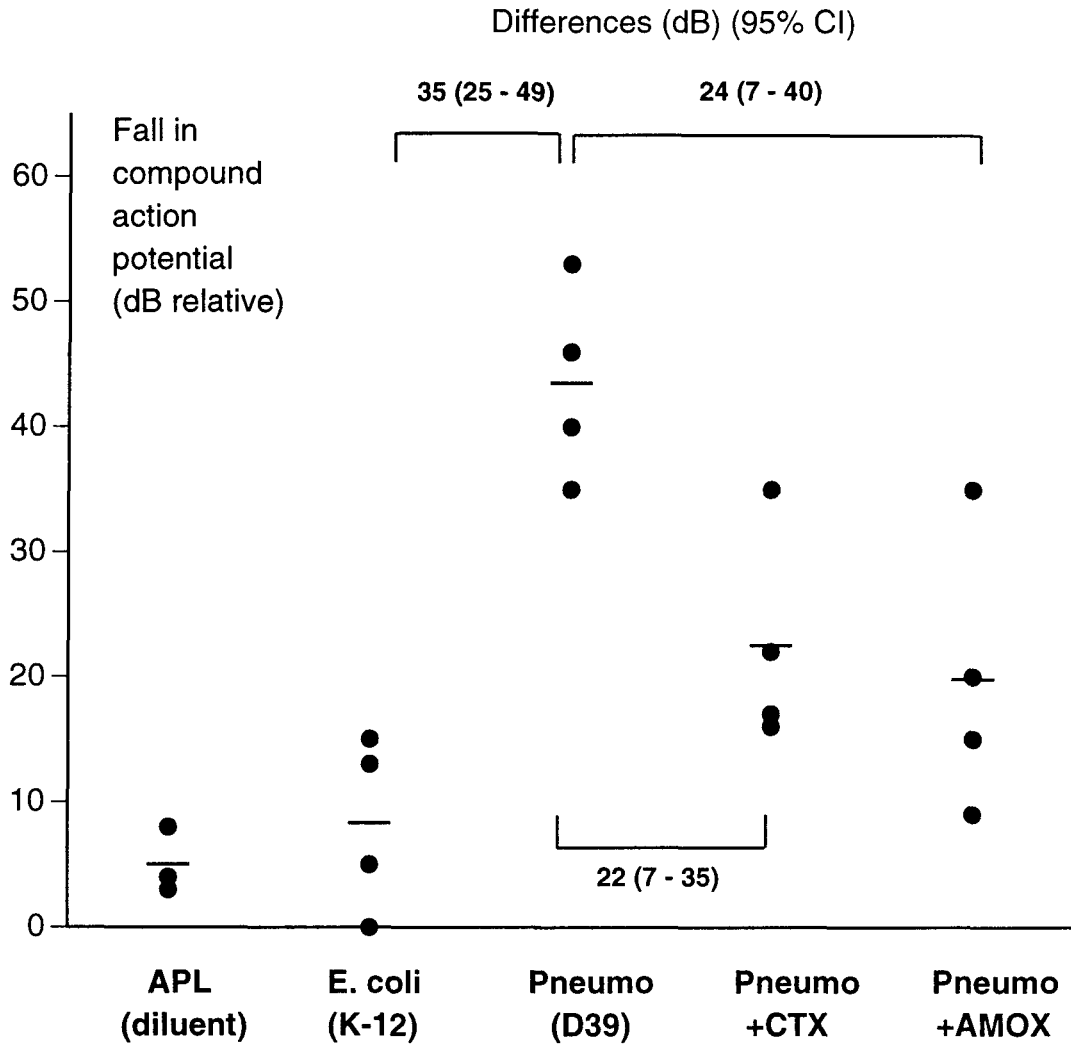


**Figure 4.2:** Cochlear perfusion: scatter plot of change in compound action potential. CAP loss (mean) 3 h after inoculation with: (i) 6.5 log<sub>10</sub> CFU *S. pneumoniae* D39 with no treatment (D39) 100 mg/kg cefotaxime (+CTX) or 100 mg/kg amoxicillin (+AMOX) given 30 min prior to inoculation; (ii) 6.5 log<sub>10</sub> *E. coli* K-12 or (iii) artificial perilymph alone (APL, historical controls included for interest only).

## Cochlear microphonic

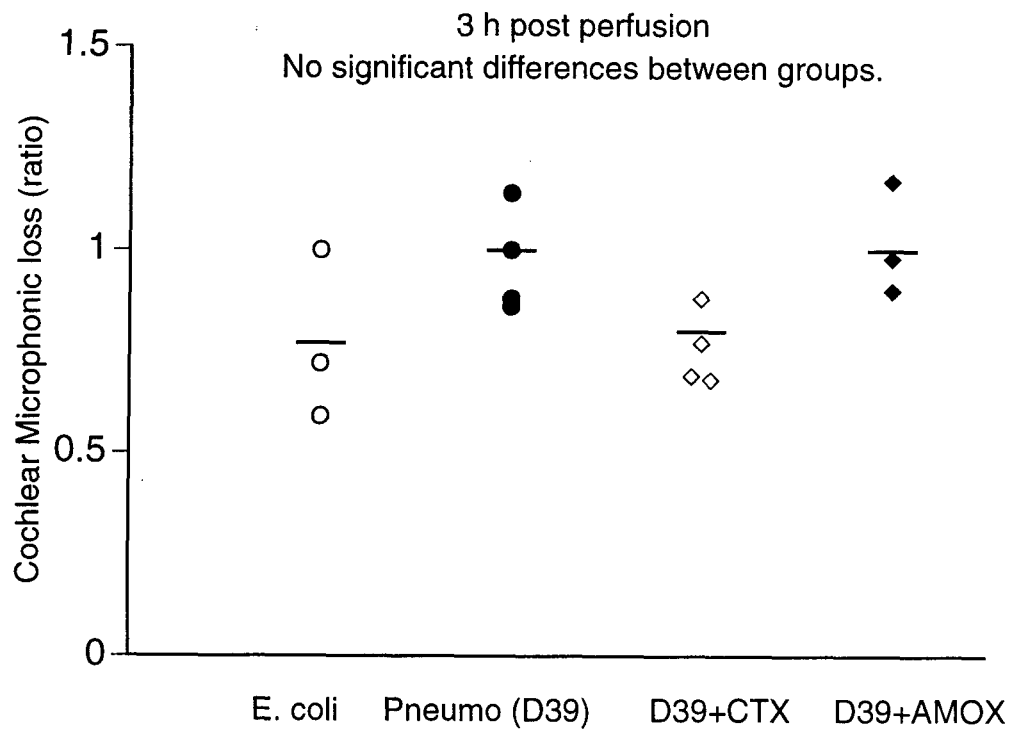


**Figure 4.3:** Cochlear perfusion: scatter plot of change in cochlear microphonic. CM loss (mean) 3 h after inoculation with: (i) 6.5 log<sub>10</sub> CFU *S. pneumoniae* D39 with no treatment (D39), 100 mg/kg cefotaxime (+CTX) or 100 mg/kg amoxicillin (+AMOX) given 30 min before or (ii) 6.5 CFU log<sub>10</sub> *E. coli* K-12

## Cefotaxime

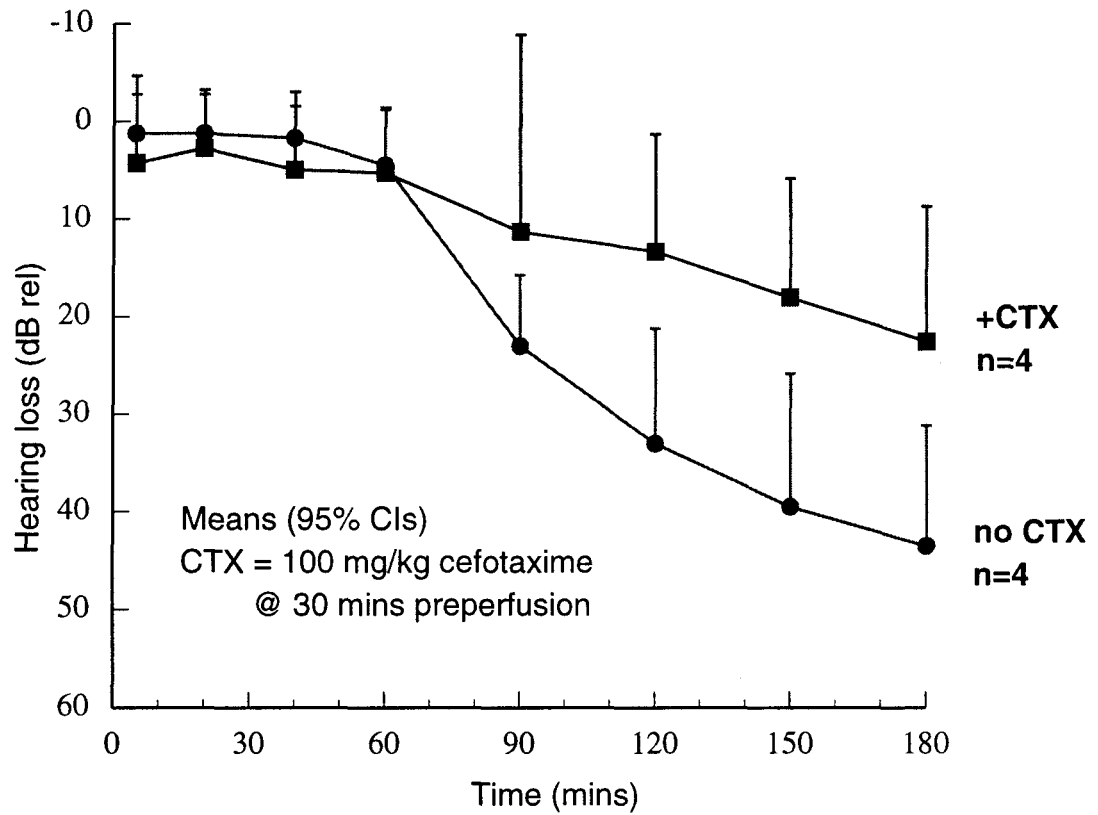


**Figure 4.4:** Effect of cefotaxime on pneumococcal-induced hearing loss. Mean CAP loss (bars: 95% confidence interval).

## Amoxicillin

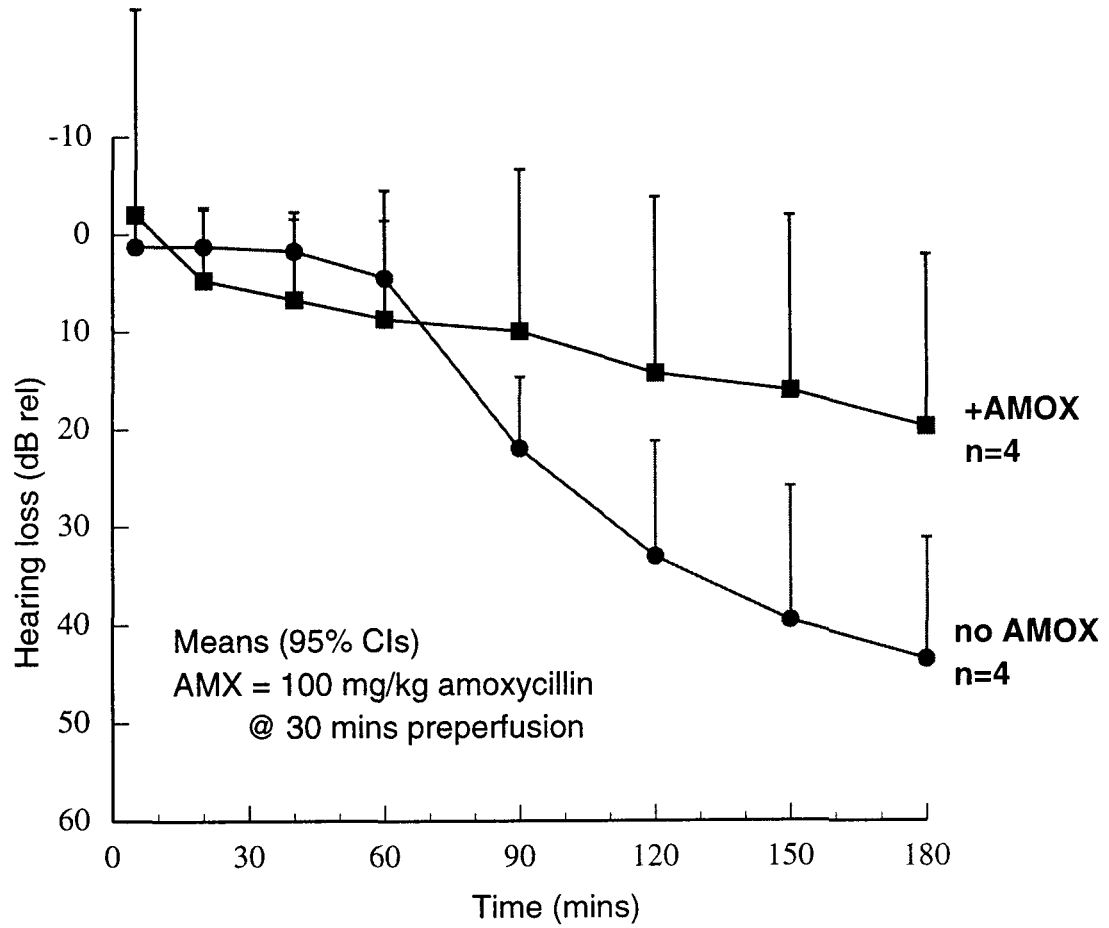


**Figure 4.5:** Effect of amoxicillin on pneumococcal-induced hearing loss. Mean CAP loss (bars: 95% confidence interval).

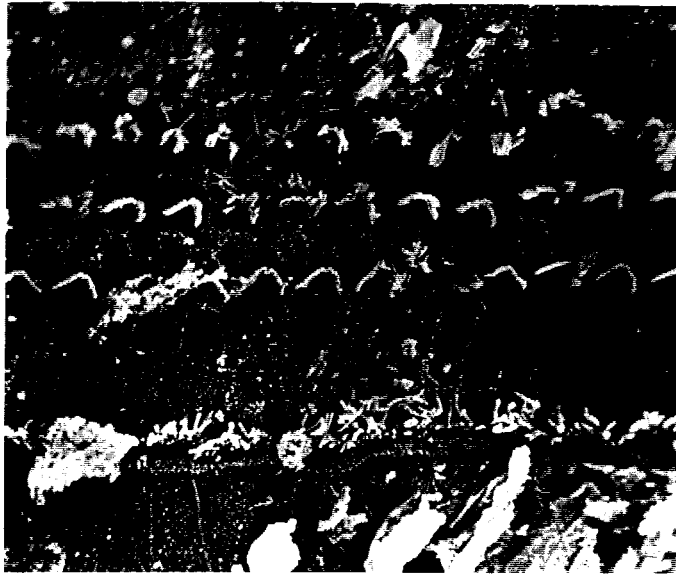


**Plate 4.13**

D39 Perf 5 (exptl) basal turn x1,500. Cefotaxime pretreated.  
There is extensive devastation of the organ of Corti with debris covering the surface and detachment of IHC and OHC stereocilia from the cell surface. Some of this damage is probably artefactual.

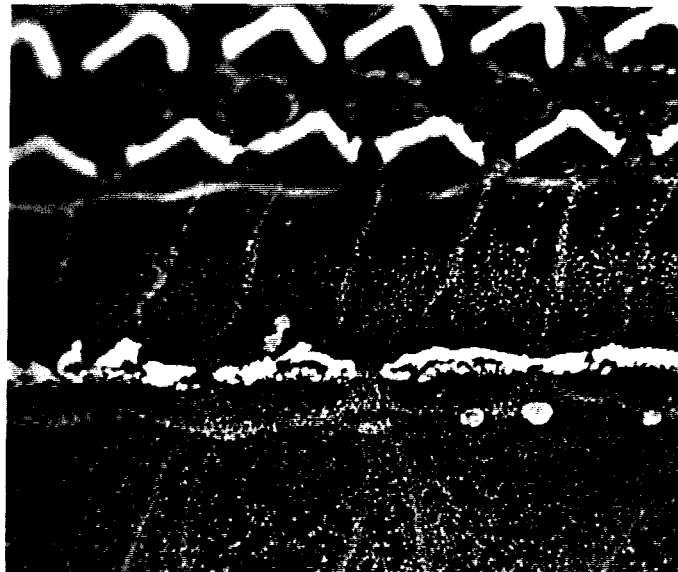


**Plate 4.14**

D39 Perf 6 (exptl) basal turn x2,000. Cefotaxime pretreated.  
Some disruption of IHC stereocilia.

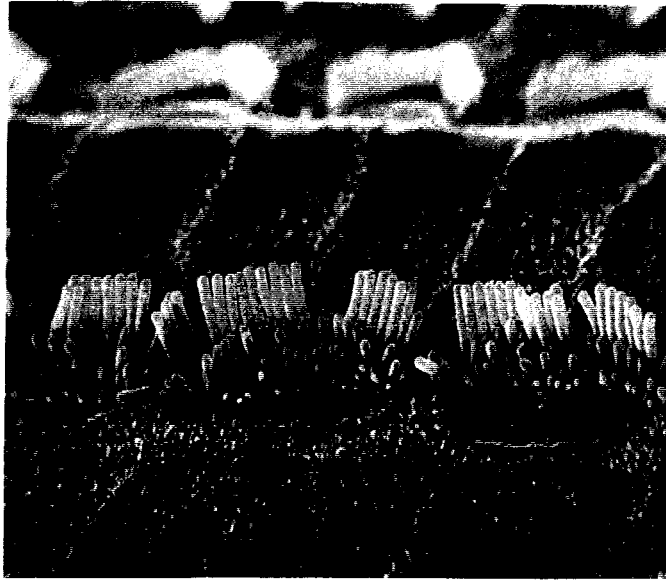


**Plate 4.15**

D39 Perf 19 (exptl) basal turn x4,000. Amoxicillin pretreated.  
Some disruption of lateral links of IHC stereocilia which are  
otherwise reasonably intact.

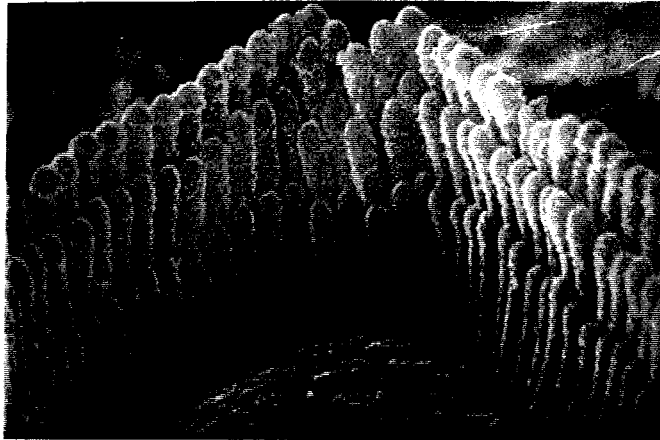


**Plate 4.16**

D39 Perf 19 (exptl) basal turn x20,000. Amoxicillin pretreated.  
Intact OHC stereocilia



**Plate 4.17**

D39 Perf 6 (exptl) x800 .

Cefotaxime pretreated.

There are a few organisms and one leukocyte visible on the basilar membrane 3 h after perfusion.

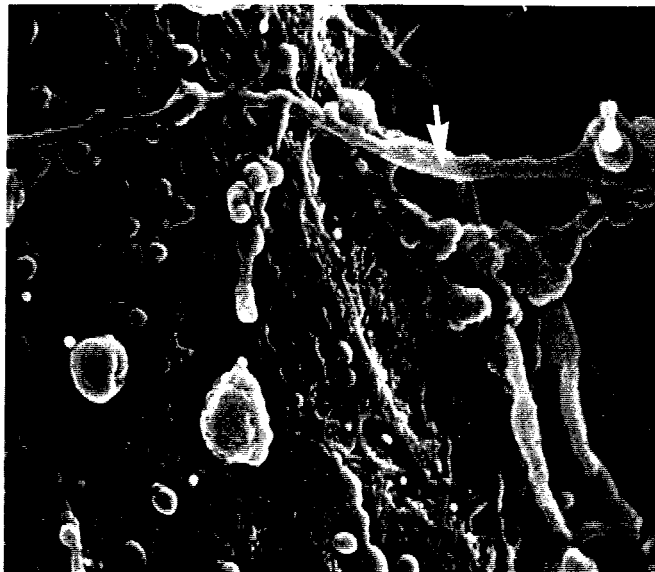


**Plate 4.18**

D39 Perf 18 (exptl) x15,000.

Amoxicillin pretreatment **75 min post perfusion**.

There is distortion of the bacterial surface and some bacteria have formed into long chains (arrow). Such morphological changes confirm that the antibiotic is active in the perilymphatic space.

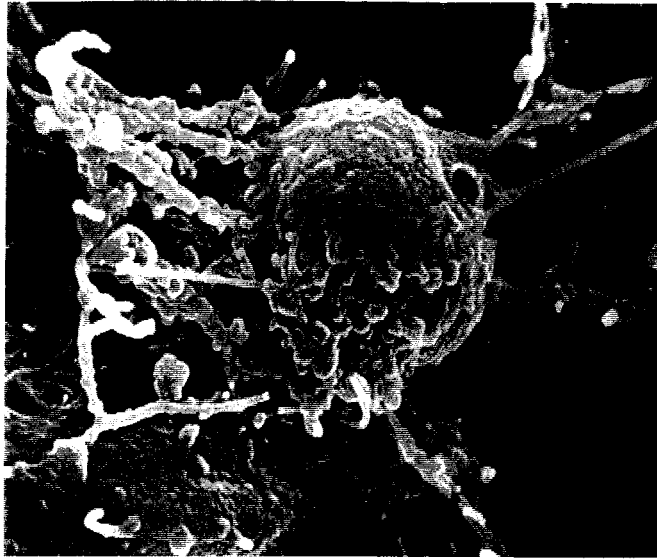


**Plate 4.19**  
D39 Perf 18 (exptl) x10,000.  
Amoxicillin pretreatment **75 min post perfusion.**  
Leukocyte on basilar membrane phagocytosing organism debris.

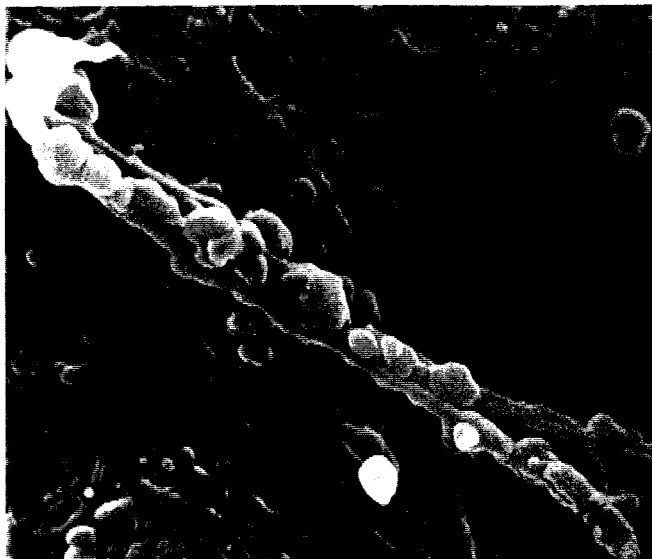


**Plate 4.20**  
D39 Perf 18 (exptl) x20,000  
Amoxicillin pretreatment **75 min post perfusion.**  
Filamentous forms of pneumococci.

## 4.5. Pneumococcal perfusion with dexamethasone pretreatment.

### 4.5.1. Experimental details.

In an uncompleted study, two animals received dexamethasone (1 mg/kg body weight by intraperitoneal injection) 90 minutes prior to cochlear perfusion to find out whether such anti inflammatory adjuvant treatment would also diminish hearing loss. The dose is higher than that used in clinical practice (around 0.4 mg/kg; Schaad et al, 1995).

### 4.5.2. Results

The electrophysiological data suggested that dexamethasone was unable to prevent at least some damage to the organ of Corti. The cochlear microphonics were once again preserved.

	Time (min)	D39 Perf 8	Perf 9
<b>CAP loss</b>	<b>5</b>	<b>0</b>	<b>0</b>
10 kHz (B)	<b>180</b>	<b>32</b>	<b>19</b>
<b>Baseline stimulus</b> (N1-P1=100 $\mu$ V; B SPL)		<b>32</b>	<b>36</b>
<b>CM (0 h) (mV)</b>		0.447	0.359
<b>CM (3 h) (mV)</b>		0.510	0.315
<b>CM ratio</b>		<b>1.14</b>	<b>0.88</b>
<b>Inoculum (log<sub>10</sub> CFU)</b>		<b>6.7</b>	<b>6.2</b>

CAP=compound action potential; **CM=cochlear** microphonic;

**Table 4.4:** Cochlear perfusion of *S. pneumoniae* D39 with dexamethasone pretreatment: electrophysiological data.

In expt D39 Perf 8, a few craters were found in the apical surface of border cells (plate 4.21) but hair cells appeared intact by SEM. No damage was seen in expt D39 Perf 9 (plate 4.22). Dexamethasone may therefore offer some protection against or defer the onset of pneumococcal-induced ultrastructural damage.

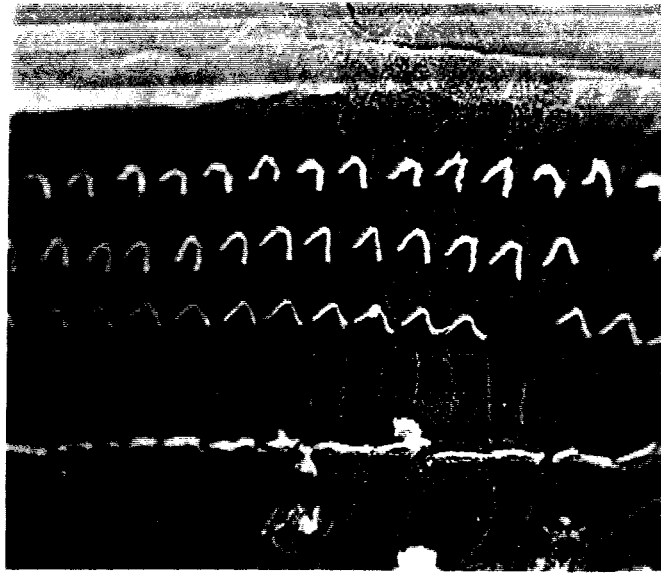


**Plate 4.21**  
D39 Perf 8 (exptl) basal turn x1,000  
Dexamethasone pretreated.  
Crater in the surface of border cells but little other damage.

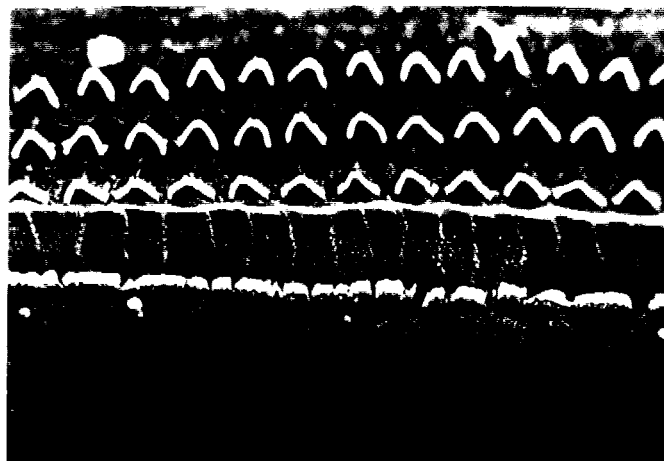


**Plate 4.22**  
D39 Perf 9 (exptl) basal turn x1,000  
Dexamethasone pretreated.  
Intact organ of Corti

## 5. DISCUSSION

The main experimental results can be summarised as follows:

- Experimental pneumococcal meningitis in guinea pigs causes a profound cochlear hearing loss as judged by electrocochleography;
- Both pneumococcal and *E. coli* meningitis cause ultrastructural lesions of the organ of Corti. Damage is more severe after pneumococcal meningitis;
- Infection with pneumolysin-deficient pneumococci (PLN-A) causes significantly less hearing loss but does not reduce the meningeal inflammatory response. Ultrastructural damage is confined to nerve endings and supporting cells; sensory cells and hair bundles remain undamaged;
- The course of hearing loss and the meningeal inflammatory response after infection with neuraminidase-deficient pneumococci ( $\Delta$ NA1) is indistinguishable from that due to wild-type *S.pneumoniae*;
- Hyaluronidase-deficient pneumococci ( $\Delta$ HY1) survive poorly in the CSF and the bloodstream, but are still able to induce hearing loss during meningitis;
- Perfusion of viable pneumococci into the scala tympani of the cochlea leads after a short delay to hearing loss accompanied by ultrastructural damage to the organ of Corti. Antibiotic pretreatment partially protects the cochlea against the effects of pneumococcal perfusion.

The following discussion will consider criticisms of the meningitis model and other studies of hearing loss in experimental meningitis; interpret data arising from infections with the defined pneumococcal mutants; examine the ultrastructural and electrophysiological findings in the light of other studies of cochlear pathology; and outline the clinical implications of the findings.

### 5.1. Experimental meningitis model.

#### 5.1.1. Clinical relevance of this experimental meningitis model

Extending conclusions from an animal experimental model to the clinical situation needs suitable caution. This issue was addressed in section 1.4. The main criticisms that can be levelled at the model used in this thesis are:

### ***The route of administering the inoculum***

Administering organisms by intracranial injection bypasses the normal immunological events associated with establishing bacteraemia and invasion through the blood-brain barrier. However these events are unlikely to influence the development of cochlear pathology. Organisms must still penetrate the cochlear aqueduct, which forms an immunological barrier in the guinea pig (Blank *et al* 1994) (see section 1.3.2). The reasons for choosing intracranial inoculation are summarised in section 1.4.1.

### ***Species variation in the sensitivity of the cochlea to insults***

Most of the work establishing the normal physiology of the inner ear and the effects of ototoxic drugs has been conducted in guinea pigs. Thus data now obtained in experimental meningitis may be compared with existing data about cochlear structure and function. It is assumed that the basic physiology and structure of the mammalian cochlea is conserved across species, in spite of variations in size, peak frequency sensitivity and hearing threshold. There are subtle differences between the pattern of ultrastructural damage caused by meningitis in the rabbit and the guinea pig (see section 5.2.2.). Another example of species difference is that carboplatin preferentially attacks **IHCs** in chinchillas but **OHCs** in guinea pigs (Takeno *et al* 1994). Such differences are relatively minor. Should it be shown, for example, that the main afferent neurotransmitter differs in humans and guinea pigs, then much of our understanding of cochlear function would be overturned, and the clinical relevance of this study would be reduced. But at present it is likely that the mechanisms of damage advanced in section 5.5 would be applicable to the human cochlea.

The patency of the cochlear aqueduct in the guinea pig and in humans has been fully discussed in section 1.2.3. Ample evidence of cochlear damage in cases of meningitis has been cited in section 1.5.2.

#### **5.1.2. Preparation and administration of the inoculum**

At least six reported techniques have been used to prepare *S. pneumoniae* for intrathecal inoculation. Differences between these techniques include:

- whether the inoculum is animal passaged;
- the phase of growth of organisms;
- whether organisms are grown in liquid or on solid media;
- whether organisms are cryopreserved prior to inoculation.

It is important to recognise these differences as they might influence the development of meningitis and the course of the inflammatory response. The constitution of bacterial cell walls (in Gram-positive organisms) and lipopolysaccharide (in Gram-negative organisms) changes according to the phase of growth (Cross *et al* 1993). Evidence has been presented in this thesis that passaging *S. pneumoniae* D39 through mice enhances the ability of the organisms to establish meningitis in guinea pigs, although the mechanism is unclear (section 3.2.1). Contaminants from the culture medium including expressed bacterial products may be inadvertently introduced unless the inoculum is washed and resuspended. Misleading results may arise from failure adequately to protect organisms from freeze-thaw damage (Nau *et al* 1994), or from using overnight cultures of *S. pneumoniae* where many organisms will have autolysed (Scheld and Brodeur, 1983; Dacey and Sande, 1974). Such inocula are likely to contain a large amount of bacterial debris, liberated pneumolysin and other expressed products as well as viable organisms.

Late log phase organisms subcultured from an overnight broth culture were used for the experiments presented in this thesis, in common with most investigators (O'Donoghue *et al* 1974; Tuomanen *et al* 1985b; McCracken, Jr. and Sakata, 1985). Replicate inocula were prepared by a modification of a technique described by Alwmark *et al* (1981), who demonstrated that pneumococci rapidly frozen in log phase in serum broth maintained viability for up to 6 months at  $-80^{\circ}\text{C}$ . This approach underpinned the comparison between different isogenic derivatives, for which replicate experiments were essential. Pneumolysin within the cells also survives freeze-thawing (TJ Mitchell, personal communication). The reproducibility of such a technique is clearly shown by the extremely small variability between inocula in the comparative experiments (fig 3.30), and the astonishing similarity in terms of rate and degree of hearing loss between the group infected with wild-type D39 and the group infected with neuraminidase-deficient  $\Delta\text{NA1}$ , prepared in batches many months apart.

The preliminary work with *Escherichia coli* was conducted with the relatively non-pathogenic laboratory strain K-12, which was rapidly cleared from the CSF. An inoculum of  $10^9$  CFU was used in accordance with previous work by Levy (1978), who found that the inoculum required to induce meningitis in mice by intracranial injection was about 1000-fold more for K-12 than for a known pathogenic strain of *E. coli*. As far as is known, K-12 does not express any cytolytic toxins. Therefore any hearing loss and pathological damage found was assumed to be due to an endotoxin-mediated host inflammatory response.

In the experimental meningitis model presented in this thesis, a relatively large inoculum was used in order to generate hearing loss and cochlear damage within a reasonable time scale, given that recovery experiments were not permitted. The use of a large inoculum does

slightly complicate the interpretation of the findings. Cross (1993) has made the distinction between a true infection model, where few organisms are inoculated and then undergo replication *in vivo*, and a challenge/toxicity model where a large number of organisms or a high concentration of bacterial product is presented to the animal. In the former case, host-immune reactions more closely mimic those in clinical infection, responding to a gradually increasing stimulus. But if too few organisms are inoculated, many animals fail to develop a meningitis, so wasting resources. In one clinical study, children presenting with pneumococcal meningitis had CSF viable counts of between  $10^7$  and  $10^8$  CFU/ml, so an inoculum of  $3 \times 10^7$  CFU is not unrealistically high (Feldman, 1976). Depending on the intention of the study, other investigators have used intrathecal inocula varying from  $10^3$  to  $10^8$  CFU (Tauber and Zwahlen, 1994).

### **5.1.3. Documenting the induction of meningitis**

A meningeal inflammatory response was clearly shown by CSF white cell counting and estimation of protein concentration according to standard techniques. Culture of CSF always yielded pure cultures of pneumococci with no contamination. Because the main focus of the study was to record hearing loss, changes in other CSF constituents such as lactate and glucose were not evaluated. In early experiments the meninges were also examined histologically to confirm the induction of an extensive leptomeningitis after subarachnoid inoculation of organisms.

Two other key problems remain with the current guinea pig model: CSF and intravenous access. In the traditional Dacey and Sande rabbit model, adequate CSF is available to allow a small aliquot to be removed every few hours. Even with special adaptations, this approach was never very successful in the guinea pig model, because of CSF leakage around the cisternal needle and trauma to the brain-stem. In one recent study of antibiotic pharmacokinetics in guinea pigs the external jugular vein was cannulated (Sun *et al* 1996). No similar attempt was made in the experiments reported in this thesis, although it is recognised that intraperitoneal injections can be unreliable due to inadvertent penetration of the gut.

In conclusion, the model of experimental meningitis in the guinea pig presented in this thesis proved to be technically straightforward and reproducible, helped by careful attention to the preparation of the inoculum. The main disadvantages were the limited duration of infection, lack of an intravenous route to administer drugs and the small amount of CSF available which made repeated sampling difficult.

## **5.2. Cochlear damage in experimental meningitis and other conditions.**

### **5.2.1. Data from other experimental meningitis models.**

Five groups have published data on cochlear damage in experimental meningitis of which three have developed various techniques for measuring hearing loss. Their work was introduced in section 1.5.2. and is now discussed in more detail to highlight the differences between previous techniques and those presented in this thesis.

#### ***Infant rat model of pneumococcal and H. influenzae meningitis (Kaplan)***

Wiedermann *et al* (1986) inoculated 150 5-day old infant rats with *H. influenzae* type B ( $10^3$  – $10^5$  CFU) by intraperitoneal injection and sought the development of labyrinthitis for up to 6 days by light microscopy. All but one animal developed a positive CSF culture. Leukocytic infiltration was seen in the scala tympani and scala vestibuli but not in the scala media. In 26% of specimens there was a suggestion that inflammation was more severe in the basal turn of the scala tympani. Labyrinthitis peaked 48 h after inoculation. Bacteria detected by a fluorescent antibody technique were not seen in the inner ear until 48 h after inoculation, when organisms were distributed both in the perilymphatic space and the endolymphatic space. No changes in cellular morphology or cochlear architecture were observed. There were no inflammatory changes in other perineural or perivascular channels and animals did not develop retrograde middle ear disease. A further study found no difference in the ability of *H. influenzae* type B strains to invade the inner ear, whether or not they were strains derived from clinical cases who had become deaf (Kaplan *et al* 1989).

Systemic induction of pneumococcal meningitis in infant rats proved to be more difficult, with only half of a group of 24 5-day old rats developing bacteraemia and meningitis after three intraperitoneal injections of *S. pneumoniae* type 6 ( $>10^8$  CFU) (Rodriguez *et al* 1991). Animals were examined 24 h after the final inoculation. Inflammation was found in the scala tympani (86%) and the scala vestibuli (55%) but not in the scala media. Bacteria were only found in the inner ear of 2 animals (18%) but examination by Gram stain is not as sensitive as using a fluorescent antibody stain. These studies in infant rats suggest that inflammation in the scala tympani extends from the subarachnoid space via the cochlear aqueduct and might precede bacterial invasion. It is not known how such suppurative labyrinthitis affected the inner ear as hearing was not measured nor the ultrastructure of the organ of Corti examined.

#### ***Guineapig model of Streptococcus suis meningitis (Kay)***

The technique for measuring brain stem responses in small animals by averaging far-field potentials in response to an auditory click was pioneered by Kay *et al* (1984). Stimulus

intensity was decreased in discrete steps of 5 dB and the hearing threshold was defined as the minimum stimulus level at which an obvious evoked response appeared. This technique was then applied to a study of experimental *Streptococcus suis* meningitis in guinea pigs (Kay, 1991). Hearing was assessed prior to inoculation and then re-assessed once signs of meningitis became evident. Animals were inoculated with a washed overnight culture of *S. suis* via three routes: intraperitoneal ( $5 \times 10^9$  CFU; n=15); intracranial ( $10^7$  CFU; n=10) or intrabullar ( $10^9$  CFU; n=15). After the experiments the animals were perfused transcardially and the ears examined histologically. This study has a number of flaws: hearing was not assessed in many animals because they were found dead (indeed six of the ten animals inoculated intracranially died within 12 h); the hearing loss data are not presented numerically, preventing proper analysis; no controls were tested; and only click-evoked responses were evaluated giving a coarse assessment of hearing loss (see section 3.1.4). In spite of this, Kay presents the only published evidence that systemically-induced experimental meningitis (as opposed to intracranial inoculation) leads to hearing loss. Of the 15 animals inoculated i.p., seven became unwell and four of five of these animals examined sustained a bilateral and severe hearing loss. In all, a total of seventeen animals were evaluated of which fifteen had hearing loss which was invariably associated with a suppurative labyrinthitis. Inflammation was limited mainly to the scala tympani with no evidence of inflammation in the scala media, just as found in the infant rat model.

***Rabbit model of pneumococcal meningitis (Tuomanen).***

The work with which the data presented in this thesis is most closely comparable is found in a series of three publications from Tuomanen's group at the Rockefeller Institute, New York. This group have investigated hearing loss in a modification of the Dacey and Sande rabbit model of experimental pneumococcal meningitis, using click- and tone-evoked brain stem response audiometry with an accuracy of no better than  $\pm 10$  dB. In all the studies, rabbits were inoculated with  $5 \times 10^5$  CFU mid-log phase virulent type III *S. pneumoniae* by intracisternal injection. This inoculum is about 2 log units less than in the guinea pig model reported in this thesis. When infected in this way hearing loss occurred after a latent period of some 12 h, affecting all ears by 36 h after infection (Bhatt *et al* 1991). Histological examination demonstrated marked leukocytic infiltration of the scala tympani in all infected animals, with dilation of the cochlear vasculature and possible thrombosis in the stria vascularis. The cochlear aqueduct was patent but infiltrated with inflammatory cells. The organ of Corti appeared normal by light microscopy except in a few cases where degenerative changes in hair and supporting cells were invariably associated with leukocytic infiltration of the scala media. Interestingly, none of the infected animals became bacteraemic, in contrast with the experiments described in this thesis.

A subsequent study (Bhatt *et al* 1993) confirmed that hearing loss in experimental pneumococcal meningitis progressed with time and correlated with the development of a meningeal inflammatory response. Hearing was not affected until the CSF leukocyte count exceeded 2000 cells/ $\mu$ l. Regression analysis showed a similar rate of hearing loss of about 3 dB/h for all stimuli (click, 1 kHz and 10 kHz tones). However, the onset of high frequency (10 kHz) loss occurred on average about 3 h earlier than low-frequency (1kHz) loss. A single rabbit underwent light-microscopic examination of the cochlea 19 h after inoculation when it had sustained a hearing loss of just 10 dB at 10 kHz. There was an inflammatory cell infiltrate in the scala tympani and the cochlear aqueduct, and the presence of pneumococci in the scala tympani was confirmed by immunohistochemical staining. It was suggested that there was a “base-to-apex” gradient of inflammation caused by inflammation spreading upwards from the cochlear aqueduct, and that this could explain the earlier onset of high-frequency loss. No damage to the organ of Corti was observed. Because this was a light microscopic study, it is certain that many subtle changes in the organ of Corti demonstrated in this thesis and by Osborne *et al* (1995) in experimental meningitis in the rabbit would have been missed (see below).

The next study reported that ceftriaxone treatment with or without adjuvant dexamethasone could alter the course of hearing loss in an identical rabbit model (Bhatt *et al* 1995). Infected rabbits were allowed to recover and were examined up to two weeks after inoculation. This sort of work would have been impossible to conduct in Birmingham (for reasons outlined in the Methods) and so no attempt was made to duplicate these findings in the guinea pig model. Rabbits were divided into three groups of five subjects all of which were inoculated as above. Group I received sham injections, group II received ceftriaxone (75 mg/kg i.v.) at 12, 24 and 36 h post-inoculation while group III received in addition dexamethasone (0.5 mg/kg i.v.) 10 min prior to each of the three antibiotic doses. As expected all untreated animals sustained bilateral hearing loss of at least 40 dB by 30 h after inoculation. After five days, subjects treated with antibiotic alone had sustained a mean hearing loss (10 kHz) of 22 dB, while those who received adjuvant dexamethasone had lost just 18 dB. Two animals in each group went on to recover hearing by the time of the next hearing assessment two weeks after inoculation. Because of the small size of the groups and the coarse nature of the hearing measurements (with a minimum of 10 dB steps in stimulus interval) this study had far too little power to demonstrate clearly that adjuvant dexamethasone therapy was of greater benefit than antibiotic treatment alone. Reversible hearing loss has not previously been reported in experimental meningitis, simply because the long-term recovery experiments have not been performed.

***Rabbit model of E. coli and H. influenzae meningitis (Osborne).***

Osborne *et al* (1995) used high-resolution scanning and transmission electron microscopy to document ultrastructural damage to the organ of Corti during short-term experimental meningitis induced by *Haemophilus influenzae* ( $10^9$  CFU) or *E. coli* strain 2073 (a pathogenic strain isolated from a clinical case of meningitis;  $10^6$  CFU) or *E. coli* strain K-12 ( $10^6$  or  $10^9$  CFU) in rabbits. Relatively large inocula were used in order to induce cochlear damage within a reasonable time limit. No particular endpoints were specified in the study and animals were sacrificed at a variety of times and degrees of hearing loss to see at what level of hearing loss damage to the organ of Corti could be detected. Hearing was monitored by click-evoked auditory brain-stem response testing, and ranged from 40 to >50 dB over 9 to 20 h during *H. influenzae* infection, and from 20 to >60 dB during *E. coli* infection. Bacteraemia was not sought, nor was the CSF examined quantitatively.

At low levels of hearing loss (<20 dB) very little structural damage to the organ of Corti was found. However, bacteria were found to have invaded the scala media. Analysis of transmission electron micrographs suggested that organisms penetrated the basilar membrane at the level of the spiral ligament and then migrated beneath the Claudius cells to reach the stria vascularis. Bacteria were also seen in the spaces between the OHCs. With greater hearing loss (>20 dB) pathological lesions were observed in patches of the organ of Corti. Damage affected hair cells, supporting cells and nerve endings. Hair cell bundles were distorted, stereocilia were fused, and the apical surfaces of the sensory cells were sometimes ballooned out or cratered. Mitochondria within hair cells were swollen and the cell cytoplasm vacuolated. Supporting cells sustained craters to the apical surface, particularly within the inner sulcus region. Nerve endings, particularly beneath OHCs, exhibited fragmentation of the plasma membrane and loss of intracellular organelles.

The damage to the supporting cells (so breaching the reticular lamina) and lesions in the stria vascularis led the authors to propose that dissipation of the endocochlear potential could contribute to meningogenic hearing loss.

***Guineapig model of pneumococcal meningitis (Blank)***

Blank *et al* (1994) conducted a histological study of acute meningogenic labyrinthitis in guinea pigs inoculated intracisternally with various amounts of *S. pneumoniae* type 3 ( $10^3$  to  $10^7$  CFU). The highest inoculum, which is approximately the same as the one used in the experiments reported in this thesis, proved fatal within 12 h. With lower inocula, animals survived for up to 15 days. Inflammation extended to the inner ear by extension along the cochlear aqueduct. However, infection then spread to the middle ear by destruction of the round window membrane to cause a retrograde otitis media. Reactive bone formation was

observed akin to the labyrinthine osteosclerosis sometimes observed in clinical cases of meningitis who have been deafened (Johnson *et al* 1995). This work therefore complements the study reported in this thesis by examining the development of histological changes in the inner ear after experimental pneumococcal meningitis over a longer time period. It also confirms the importance of the cochlear aqueduct as a means for the spread of infection from the subarachnoid space in guinea pigs.

### ***Improving these models of meningogenic hearing loss***

Two unresolved issues stand out from this work and were directly addressed when designing the experiments reported in this thesis:

- i) Is the hearing loss observed in experimental meningitis due to cochlear dysfunction, as suggested by the ultrastructural findings and evidence of labyrinthitis?
- ii) Does ultrastructural damage to the organ of Corti occur in pneumococcal meningitis?

The data presented in this thesis constitute the first clear evidence that hearing loss in experimental pneumococcal meningitis is indeed due to cochlear dysfunction. This was achieved by modifying the technique of round-window recording of the auditory nerve compound action potential (CAP) to allow longer term recording. Cody *et al* (1980) have carefully validated CAP recording (or N<sub>1</sub> electrocochleography) in guinea pigs as an accurate measure of the functional state of the organ of Corti over the range 2 kHz to 30 kHz. They found excellent agreement between the site of mechanically induced hair cell lesions and the frequency of maximum sensitivity change in the N<sub>1</sub> audiogram. They also found that recording the CAP from the round window membrane was rapid and reproducible to within 3 dB. The development of the technique was discussed in section 3.2.3. Further refinements would include the use of a silver ball electrode rather than a fine wire (this would reduce the chance of inadvertent puncture of the round window membrane) and the use of two electrodes placed on opposite sides of the cochlea to reduce interference from cochlear microphonics. As an alternative, the gate could be designed to deliver stimuli of alternating polarity, thereby cancelling out the cochlear microphonics. This would certainly improve precision at the lower frequencies where CM is prominent. In spite of these limitations, round window CAP recording offered greatly increased precision over recording far-field potentials and therefore improved the power of this study to detect a genuine difference between groups of subjects.

### ***Comparison with hearing loss data presented in this thesis***

With wild type pneumococcal meningitis in the guinea pig, hearing loss could be detected as early as 3 h after inoculation and was progressive. Indeed, hearing loss appeared to be

decline in linear fashion. This is in contrast to the lag reported by Bhatt *et al* in the rabbit model. This is almost certainly because a larger inoculum was used in the guinea pig model, containing more pneumolysin and inducing an earlier and probably more severe meningeal inflammatory response. In one experiment (D39(17)) a CSF leukocytosis was detected just 3 h after inoculation. In addition, the cochlear aqueduct in the guinea pig is shorter than that in the rabbit, allowing earlier cochlear invasion. The rate of hearing loss (4 dBk) is a little more than that seen in the rabbit model, and again this may be explained by the higher inoculum.

Data was obtained at many more frequencies than previously reported, allowing the construction of audiograms over the range 3 to 10 kHz. The shape of these was remarkably consistent, with a peak loss between 6 and 7 kHz, the peak sensitivity for the guinea pig cochlea. There was a trend to less hearing loss at the lower frequencies. However, no evidence was found to support the findings of Bhatt *et al* that high-frequency hearing loss precedes low-frequency loss. Again, this could be a result of the higher initial inoculum inducing a severe meningitis and an overwhelming suppurative labyrinthitis, whereas in their model a more progressive invasion of the scala tympani might occur. Certainly, on inspection of the scala tympani during dissection a gross inflammatory infiltrate could be seen filling the entire scala on several occasions. It is not necessary however to invoke a “base-to-apex” gradient of inflammation, as there are longitudinal gradations of hair cell structure and metabolism and endolymphatic potential (Slepecky, 1986) in the cochlea that might cause a greater susceptibility to high frequency loss. Many other non-inflammatory insults also cause more damage in the basal turn (see section 5.2.3). If anything, the data from the guinea pig model suggest that the most sensitive area of the cochlea is the most susceptible.

No previous studies have reported changes in cochlear microphonics in experimental meningitis. Although there was great variability between animals, there was a clear trend towards loss of cochlear microphonics in animals infected with all the variants of *S. pneumoniae* D39. Cochlear microphonics predominantly reflect OHC function. Thus a fall in CM suggests significant cochlear pathology at the level of the hair cell, confirming that cochlear damage is at least partly responsible for meningogenic deafness.

### **5.2.2. Ultrastructural lesions of the organ of Corti in experimental meningitis.**

The second major aim in this study was to document ultrastructural lesions that might correlate with hearing loss. The ultrastructure of the organ of Corti had not been examined in previous studies of experimental meningitis. This work developed in tandem with ultrastructural studies of the organ of Corti in meningitis in the rabbit (Osborne *et al* 1995)

so that parallels could be sought. Light microscopic analysis of the cochlea was not performed, except to examine guiding sections prior to cutting ultrathin sections for TEM analysis. Scanning electron microscopy was performed on a transmission electron microscope fitted with a scanning attachment, resulting in a very high resolution of the order of 3 nm. Because the detector is so close to the specimen, back-scattered electrons are less of a problem than in conventional SEMs, and higher accelerations (40 kV) can be used. However, the specimen size is greatly limited, with a maximum height of 4 mm. Where necessary the apices of the modioli were trimmed away so just the first two turns of the cochlea were routinely examined with SEM.

Artefacts encountered included curling of the organ of Corti, so obscuring the surface, and cracking of supporting cells deep in the inner sulcus. With experience, these artefacts were easily distinguished from the more subtle craters in the apical surface of supporting cells, which were never seen in historical control specimens. Faults in the critical point dryer led to spoilage of several specimens (most notably the cochleas from animals challenged with pneumococcal cell wall). There is a large sampling error in TEM studies, since the ultrathin sections examined only represent a tiny fraction of the organ of Corti.

Meningitis due to *E. coli* K-12 was not expected to cause much ultrastructural damage to the organ of Corti, according to our hypothesis that intracellular toxins were important in causing cochlear damage. A number of lesions were found, although damage was very patchy and some cochleas appeared to be intact even after several hours of meningitis. With pneumolysin-producing pneumococcal infection in the guinea pig there was a clear progression of damage: 6 h after inoculation, craters developed in the apical surface of border cells; by 9 h IHC and OHC hair bundles were deformed and between 9 and 12 h the apical surface of some OHCs was ballooned out. Pathological nerve endings were found particularly affecting neural elements associated with OHCs. In the absence of pneumolysin, the only convincing damage was to the nerve endings, with the apical surfaces of the hair cells and hair bundles remaining intact. The stria vascularis was not examined. These lesions will now be discussed in turn.

#### *Specific lesions of hair bundles*

In meningitis due to *E. coli* IHC hair bundles were damaged sporadically with uprooting, splaying and fusion of stereocilia. The appearance is similar to that following perfusion of endotoxin through the scala tympani, where individual stereocilia could be found attached to the undersurface of the tectorial membrane (Tarlow et al 1991). In pneumolysin-producing pneumococcal meningitis in the guinea pig the IHC hair bundles were also damaged. In pneumococcal meningitis in the rabbit there was striking injury to IHC hair

bundles with many stereocilia being completely absent, and those remaining being grossly shortened and deformed.

Outer hair cell hair bundles were severely affected by wild type pneumococcal meningitis, with fusion of stereocilia and collapse of the hair bundle onto the surface of the sensory cell. This was not seen with infection with *E. coli* nor in the absence of pneumolysin. In the rabbit there was less evidence of damage to the OHC hair bundles but only a few specimens were examined.

Given the absence of inflammation in the endolymphatic compartment, it is at first surprising that there should be so much damage to the endolymphatic surface of the organ of Corti. TEMs clearly show pathological damage of OHC hair bundle stereocilia, with loss of the plasma membrane, fusion and disintegration. This suggests that the stereocilial lesions are secondary to metabolic changes in the sensory cell. The interaction between stereocilia and the tectorial membrane may also be disrupted. Normally, the tips of the stereocilia of the hair bundles of IHCs and the first two rows of OHCs are not firmly embedded in the tectorial membrane (Lim, 1986). Disturbance of the tectorial membrane induced by endotoxin (Comis *et al* 1991) or by a change in the potassium concentration of the endolymph (Leng and Comis, 1979) might render the tectorial membrane more sticky or swollen, causing stereocilia to become detached during specimen processing.

### ***Specific lesions of hair cells***

The IHC bodies themselves were not greatly affected in any of the guinea pig experiments; no TEM studies were performed in the rabbit. This lack of damage is surprising given the defects in the nearby border cells. The intercellular junctions between the IHCs and the adjacent phalangeal processes appeared to be damaged (as judged by SEM) during infection with pneumolysin-producing *S.pneumoniae* (D39,  $\Delta$ NA1,  $\Delta$ HY1).

In pneumolysin-producing pneumococcal infection, OHCs were severely affected. Infection with **DNA1** appeared to cause the most damage as judged by TEM, but this again could reflect sampling error. Damage consisted of breakdown of the basolateral and apical plasma membrane especially at the site of the basal corpuscle, cell swelling, and vacuolation of the mitochondria. Cytoplasmic contents could be seen spewing out of the cell. The SEM appearances are striking, with severe deformation of the whole apical surface. Sometimes the cuticular plate appeared to be lifted clear of the surrounding phalangeal processes.

Damage was almost completely confined to the first two rows of OHCs. In noise-induced damage, first row OHCs are in general more easily injured than third row OHCs (Slepecky, 1986). However after mechanical trauma to Reissner's membrane it is third row OHCs

which bear the brunt of the damage (Cody et al 1980). It is not clear why first row cells are more susceptible to the damage induced by inflammation.

Selective destruction of OHCs by kanamycin abolishes practically all of the CM and modifies the tuning curves of the IHC (Dallos et al 1972; Evans and Harrison, 1975). Zwislocki (1984) has even suggested that absence of OHCs would increase the shearing forces on most of the IHC stereocilia and cause hypersensitivity of the cochlea. Damage to OHCs will not therefore necessarily result in a fall in CAP. Inner hair cell tuning curves were not measured in the experiments presented in this thesis. In some of the meningitis experiments, the CAP thresholds improved over the first 3 h post inoculation. A similar rise in CAP threshold occurs initially when cytoplasmic fractions of *H.influenzae* type B are perfused into the inner ear (Dover et al, unpublished findings). If this is a genuine effect it may be due to an increase in synchronised firing of single units as seen when neurotransmitters such as noradrenaline are perfused into the cochlea (Comis and Leng, 1979). It could also be due to failure to obtain the best recording conditions initially. Cochlear microphonic measurements from the round window during pneumococcal meningitis declined substantially, which correlates with significant damage to OHCs and OHC nerve endings.

### ***Supporting cell damage***

A consistent finding in all of the meningitis experiments was shallow cratering of the apical surface of the border cells and sometimes the adjacent inner sulcus cells. The importance of this region is that it forms part of the boundary between the endolymphatic and perilymphatic compartments; any damage here would allow intermixing of cochlear fluids. Where craters were observed, IHC hair bundles were usually disrupted, suggesting a link between IHC pathology and the supporting cell damage. At the point where craters were most frequently seen, the border cells are reduced to a thin rim of cytoplasm where they overlie the body of the IHC and its associated nerve endings (see plate 3.52). This may render them more susceptible to excitotoxic damage (see section 5.5.3).

Cratering of the phalangeal cells between the inner and outer hair cells was prominent in rabbit pneumococcal meningitis. In the guinea pig, damage in this region appeared to be limited to fragmentation of the basolateral plasma membrane and vacuolation of the mitochondria. Surface craters could be explained by a preparation artefact at a site of pre-existing damage or, more likely, represent true loss of the apical cell membrane.

### ***Nerve ending damage***

Another consistent finding unaffected by the absence of pneumolysin was vacuolation of mitochondria in nerve endings and fragmentation of the plasma membrane. Some of the nerve endings were severely damaged and swollen. Cochleas were fixed within two minutes of removal from the animal so it is difficult to invoke post-mortem deterioration as the reason for the observed damage.

It is not possible to predict how this damage would affect neural transmission overall, given the large sampling error and the fact that single fibre recording was not performed in this study. Much of the damage in meningitis appeared to be localised to (presumably mostly efferent) nerve endings bordering OHCs, which may not therefore directly affect the CAP. However a strong clue that afferent neural transmission was affected is provided by the loss of uniformity of the CAP as pneumococcal meningitis proceeds. In addition, the presence of a large  $P_0$  wave which is thought to reflect the summed excitatory post-synaptic potentials suggests that hair cell depolarisation and synaptic release is maintained even when there is a substantial hearing deficit (*see* section 1.3.5 and Eybalin, 1993 p. 323)

### ***Resistance of the scala media to invasion and inflammation***

The resistance of the scala media to inflammation was demonstrated in the experiments presented in this thesis and is a fairly consistent feature in all of the histopathological studies of experimental meningitis. If haematogenous dissemination were the main route of bacterial invasion into the cochlea, one would expect the highly vascular stria vascularis (and hence the scala media) to be a major site of bacterial ingress. Evidence however suggests that the main route of invasion of the cochlea is by extension via the cochlear aqueduct. In fact Osborne *et al* (1995) presented evidence that organisms infiltrate through the basilar membrane and penetrate between the hair cells and around the spiral ligament. Invasion of the scala media by *H. influenzae* type B was found by Osborne *et al* (1995) in rabbits and Wiedermann *et al* (1986) in infant rats, but even then there was little inflammatory reaction. In the rabbit, organisms were found emerging onto the surface of the organ of Corti. In the guinea pig experiments reported in this thesis, some organism-like structures were also observed on the surface of the organ of Corti with both wild-type and PLN-A infection. These structures were only ever seen above the junction between the IHC and its adjacent border cell. They were not solely seen in areas where the intercellular junctions appeared to be damaged. No organisms were seen in the intercellular spaces beneath the reticular lamina, probably due to sampling error.

The resistance of the scala media to inflammation and bacterial invasion in the face of massive bacterial and leukocytic infiltration of the scala tympani is quite striking. It probably

reflects the nature of the boundaries of this compartment, designed to maintain extremely high electrochemical gradients. It is however insufficient to prevent serious damage to the organ of Corti as a whole.

### ***Comparison of findings in rabbit Hib and E. coli meningitis with data in this thesis***

There are many similarities between the damage identified in pneumococcal meningitis in the guinea pig and that induced by *H. influenzae* type B or *E. coli* meningitis in the rabbit (Osborne *et al* 1995); specifically, the appearance of the border cell craters, the ballooning of the apical surface of OHCs and the fragmentation of the plasma membrane of both the hair cells and the nerve endings. Animals were examined at about the same time intervals after induction of meningitis. Damage in the guinea pig seemed to be more widespread and in general more severe. Vacuolation of the hair cells was certainly more pronounced with  $\Delta$ NA1 infection, and many more OHCs appear to be damaged than in the rabbit as judged by SEM. However, this was not quantitatively assessed. The differences are probably because hearing loss was greater in pneumococcal meningitis in the guinea pig. Osborne *et al* recorded a hearing loss to click stimuli of less than 50 dB in eight of 10 animals whereas the mean loss in the guinea pig series was 50 dB at 10 kHz. These values are not strictly comparable, as the loss of sensitivity to click stimuli represents a more profound hearing loss than loss to a tone pip. Border cell craters occurred in a linear fashion in the rabbit that was not as apparent in the guinea pig. *E. coli* K-12 induced border cell craters in the guinea pig whereas it induced little damage to the supporting cells in the rabbit.

In conclusion there is great similarity in the specific ultrastructural lesions observed in two different species resulting from infection with three different organisms. This suggests that the organ of Corti has a limited way of responding to inflammatory insults. It also gives more confidence that the ultrastructural lesions observed are genuinely a result of the meningitis.

### **5.2.3. Cochlear lesions in other conditions**

It is clearly important to distinguish changes due to delayed or defective fixation from those due to genuine pathological damage. Osborne and Comis (1990) have carefully investigated the time-course of post-mortem changes in the guinea pig cochlea with high-resolution scanning electron microscopy. The basal turn is much more susceptible to post-mortem damage than the apical turn. The earliest changes observed just 15 minutes after death consist of separation of the hair bundle stereocilia (with loss of lateral links) and ballooning of the apical surface of the sensory cells. By 2 h after death fusion of stereocilia is common and there is severe disruption of the cuticular surfaces of the hair cells. By 4 h most of the

IHCs at the base have disintegrated. Many of these changes resemble those found after experimental pneumococcal meningitis. Cochleas included in the ultrastructural study were all fixed within two minutes of removal from animals which appeared to be well oxygenated. Thus post-mortem artefact is unlikely to explain the observed lesions. In any case, tearing and distortion of the cuticular surface of the hair cells and disruption of the tight junctions between the cells cannot be ascribed to post-mortem damage as these are late phenomena.

Drug-induced ototoxicity due to aminoglycosides or platinum agents usually affects OHCs more than MCs. Defects range from mild disruption of the stereocilia to complete loss of the sensory cell. First row OHCs appear to be particularly susceptible to kanamycin which in a sufficient dose destroys all the OHCs in the first two turns of the guinea pig cochlea, resulting in a 90% fall in cochlear microphonics (Dallos *et al* 1972). Hair cells and their hair bundles rather than supporting cells bear the brunt of the damage. Whereas in meningitis stereocilia appear to become completely detached from the cuticular plate, after kanamycin treatment the roots remain (Osborne and Comis, 1990). This suggests a difference in the underlying mechanism, which is possibly due to the disruption of actin filaments as a result of raised intracellular calcium. The more severe damage such as formation of fusion/extrusion bodies on the surface of the sensory cells closely resembles the ballooning of the apical surface of the OHCs seen in pneumococcal meningitis. As in other conditions, drug-induced ototoxicity preferentially affects the basal turn of the cochlea before the apex (Osborne and Comis, 1990).

### **5.3. The role of pneumococcal products in causing meningogenic deafness.**

#### **5.3.1. Interpreting data in insertion-duplication mutagenesis studies: a caution.**

Investigating the pathogenesis of infection by omitting key virulence factors would appear to yield much useful data. But in spite of many refinements in the genetic techniques, interpreting such studies is not immediately straightforward. The problem may be illustrated thus: omitting a fuse in a circuit and finding that the power fails does not mean that the missing fuse is the source of the power. In the same way, omitting pneumolysin from the armoury of toxins produced by *S. pneumoniae* and finding a significant reduction in hearing loss does not necessarily mean that pneumolysin itself was responsible for all of the hearing loss. It is possible that pneumolysin could act as a co-factor by its actions on the immune system or by allowing another toxin access to structures it cannot normally reach. For

example, a study with the autolysin-deficient mutant AL-1 showed reduced virulence for mouse bacteraemia. This was not because autolysin itself enhances virulence directly, but because without autolysin pneumococci fail to lyse so preventing the release of pneumolysin (Berry et al 1992).

Then there is the possibility that the genetic manipulation alters the pathogenicity of the organism in some subtle way. One problem is that of a polar effect, where the gene manipulation inadvertently disrupts gene expression at a site downstream from the insertion site. Insertion-duplication mutagenesis causes more of a problem in this respect than the direct introduction of point mutations into the existing chromosomal gene. This so-called “polar effect” is a possible explanation for the poor in vivo growth of the  $\Delta$ HY1 mutant. One way of circumventing this would be to attempt to reconstitute full virulence by inserting a plasmid expressing hyaluronidase. If virulence is restored then it is clear that the absence of hyaluronidase itself is critical, as any downstream genes inadvertently disrupted by the original manipulation will remain inactivated.

The stability of the mutant might be proven in one in vivo system but not be assured under the different, perhaps harsher, pressures of growth in another system. Again this is a problem with insertion-duplication mutagenesis where it might be imagined a large chunk of DNA could be shed from the chromosome with some advantage to the cell. Undetected reversion to wild-type phenotype would result in misleading findings, particularly when there is no apparent difference between the outcome of infection with the wild-type and with the mutant, as in the ANA1 study reported here. Thus in the experiments conducted in this thesis organisms recovered from the CSF were subjected to careful phenotypic analysis. As a further check, Southern blotting would have demonstrated preservation of the insert but this was not performed. Checks for antibiotic sensitivity were less helpful in this regard as there appeared to be some loss of antibiotic resistance with full preservation of the mutant phenotype in recovered organisms. This remains unexplained.

Therefore conclusions from insertion-duplication mutagenesis studies should be consistent with expected biological activities of the products concerned. For PLN-A the findings are entirely consistent with the expected effects of omitting pneumolysin. The findings with  $\Delta$ NA1 and especially  $\Delta$ HY1 need much more cautious interpretation because much less data are available about the in vitro and in vivo effects of neuraminidase and hyaluronidase.

### **5.3.2. Pneumolysin**

Microperfusion of purified recombinant pneumolysin (PLY; 0.5 to 10  $\mu$ g total in 10  $\mu$ l) into scala tympani causes rapid devastation of the organ of Corti in a concentration-dependent

fashion (Comis *et al* 1993). Both the compound action potential and cochlear microphonics are reduced substantially. At lower doses the effect of **PLY** on CAP and CM is reversible. Ultrastructural damage consists of disruption and splaying of the hair bundle stereocilia, cratering of the apical surface of the hair cells and supporting cells and tearing away of the hair cells from the adjacent supporting cells. These changes are qualitatively identical but more severe and less patchy than those occurring after pneumococcal meningitis. The outermost row of OHCs is most susceptible to purified **PLY**, whereas in pneumococcal meningitis it is the innermost rows that sustain the most damage. The difference in the site of maximum damage is likely to be due to different localised concentrations of **PLY** when administered by cochlear perfusion compared to its natural release during meningitis.

It is striking that the very ultrastructural changes induced by **PLY** are those that are abolished by infection with pneumolysin-deficient **PLN-A**. Compared to D39, infection with **PLN-A** caused an identical meningeal inflammatory response (as far as the power of the study allowed detection of these secondary differences), significantly less hearing loss at all frequencies tested (12 dB vs. 50 dB at 12 h at 10 kHz) and a slower rate of hearing loss (1 dB/h vs. 4 dB/h). Damage to the reticular lamina and associated tight junctions, cratering of the apical surfaces of sensory cells and supporting cells, and significant damage to the hair bundles did not occur after **PLN-A** infection.

The effect of pneumolysin expression on the toxicity of *S. pneumoniae* for respiratory mucosa has been studied by inoculating isolated human turbinate tissue maintained in an organ culture with an air interface with  $10^7$  CFU/ml *S. pneumoniae* D39 or **PLN-A** (Rayner *et al* 1995). Wild-type infection causes a progressive fall in ciliary beat frequency over 48 h. Organisms particularly adhere to the mucus layer and damaged areas of mucosa. Damage to the mucosal surface consists of disorganisation of cilia, extrusion of ciliated cells, blebbing and cratering of the apical cell surfaces, and tearing of the tight junctions between unciliated epithelial cells. Organisms bind to the free edges of these cells. This damage very much resembles that seen in the organ of Corti as a result of pneumococcal meningitis, with the exception of bacterial adherence to damaged cells. When inoculated with **PLN-A**, ciliary beat frequency falls less quickly and a smaller area of the mucosa sustains significant damage. Cilia are unaffected and tight junctions between unciliated cells remain intact, so that far fewer organisms bind to normal mucosa. This is entirely consistent with the reduced effects of **PLN-A** on the guinea pig cochlea. Thus pneumolysin expression aids the adherence of *S. pneumoniae* to normal respiratory epithelium and causes additional ultrastructural pathology which is of a similar character to that observed in the organ of Corti after pneumococcal meningitis.

Pneumolysin expression appears not to affect the course of the acute meningeal inflammatory response in experimental pneumococcal meningitis, even though purified pneumolysin is capable of evoking an inflammatory response (see section 1.2.6). In rabbits Friedland *et al* (1995) found that inoculation with mid log-phase *S. pneumoniae* D39 or PLN-A ( $3 \times 10^3$  CFU) yielded identical changes in CSF white cell count, protein and TNF $\alpha$  concentration. The in vivo growth curves were also identical and there was no evidence of a lag phase. In the guinea pig model reported here there was also no difference in the meningeal inflammatory response evoked by *S. pneumoniae* D39 or PLN-A. In spite of this there were striking differences in ultrastructural and electrophysiological damage sustained by the organ of Corti. This data together with the lack of cochlear damage induced by intracisternal injection of pneumococcal cell wall suggest that non-specific meningeal inflammation cannot of itself mediate hearing loss.

Although pneumolysin expression may not influence the development of meningeal inflammation the evidence presented in this thesis and the toxicity shown in cochlear perfusion studies support a major role for pneumolysin in the pathogenesis of hearing loss in pneumococcal meningitis.

### 5.3.3. Neuraminidase

In this study, there were no distinguishable differences between the course of meningeal inflammation, in vivo growth, bacteraemia or cochlear damage induced by intracranial inoculation of wild-type *S. pneumoniae* D39 or its neuraminidase-deficient derivative  $\Delta$ NA1. The data in this thesis are among the first available on the behaviour of a neuraminidase-deficient pneumococcal mutant in vivo. In experimental mouse pneumonia,  $\Delta$ NA1 fails to replicate in the alveoli but can induce a bacteraemia (TJ Mitchell, unpublished observations). Identical strains made in the same laboratory were used in the mouse pneumonia study and the meningitis experiments reported here. The finding of widely different behaviour in vivo in these two different models therefore gives greater confidence to the results: a polar effect is less likely to explain the poor growth in the mouse alveoli given that the organisms grow well in guinea pig CSF and blood, and the  $\Delta$ NA1 strain used in the meningitis study is definitely less virulent in certain settings.

It is possible that *S. pneumoniae* D39 only expresses a small amount of neuraminidase, which is critical for intra-alveolar replication but whose lack does not impair replication in the CSF or blood. In this regard, the neuraminidase production of *S. pneumoniae* D39 in vitro is around 7 mU/mg cell protein whereas in the type III strain GB05 it is about 1000 mU/mg cell protein (TJ Mitchell, personal communication). Only in vivo expression

experiments would ascertain whether neuraminidase production between strains differed within the CSF space during infection.

In conclusion the existing evidence that neuraminidase has an important role in the pathophysiology of pneumococcal meningitis is circumstantial (see section 1.2.7). This study does not support any role in pathogenesis once intracranial pneumococcal infection is established, although neuraminidase may well be important in earlier stages of pneumococcal infection.

#### **5.3.4. Hyaluronidase**

Preliminary data about the course of infection with a hyaluronidase-deficient strain of *S. pneumoniae* ( $\Delta$ HY1) are presented. In spite of the poor survival of  $\Delta$ HY1 in vivo, the cochlea sustains almost as much electrophysiological and ultrastructural damage as in wild-type infection. Presumably, sufficient quantities of pneumococcal cell wall and pneumolysin were present in the initial inoculum to ensure the subsequent pathological effects. In preliminary experiments in the mouse pneumonia model,  $\Delta$ HY1 fails to replicate in the alveoli and animals do not become bacteraemic, results that are consistent with the meningitis data (TJ Mitchell et al unpublished data). It would be attractive to conclude that hyaluronidase has some hitherto unsuspected nutritional or anti-host defence action, but a polar effect of the  $\Delta$ HY1 mutation must first be excluded (see section 5.3.1).

#### **5.3.5. Pneumococcal cell wall**

The purpose of inducing meningitis with pneumococcal cell wall was to see if a sterile meningeal inflammatory response alone would cause cochlear pathology, and to better define the role of PCW (if any) in this process (see section 1.2.5). A small amount (1.6 mg) of PCW from strain **R364** the unencapsulated derivative of D39 used for the wild-type meningitis experiments, was kindly provided by Prof. A Tomasz, Rockefeller University, New York. Estimates in the literature of the amount of PCW per pneumococcus range from  $5 \times 10^7$  to  $5 \times 10^{10}$  organisms per mg cell wall (Tuomanen et al 1985b; Tuomanen et al 1985a; Prof Tomasz, personal communication). The estimate is imprecise because pneumococci tend to clump together so that optical density determinations have a substantial error, and an unknown amount of PCW is lost during purification. Thus a dose of 100  $\mu$ g as used in this study represents somewhere between  $5 \times 10^6$  and  $5 \times 10^9$  organisms, which is broadly similar to the number of viable organisms inoculated ( $3 \times 10^7$  CFU). Once the suspension of PCW had been vigorously sonicated, a moderate meningeal inflammatory response could be evoked, although in only one of the three successful experiments was the CSF protein concentration elevated. Hearing loss was significantly less than after a similar duration of

meningitis induced by viable *S. pneumoniae* D39. Unfortunately, no histological specimens were preserved. This constitutes limited evidence that PCW is not critically involved in meningogenic deafness. It is possible that there is insufficient PCW in  $3 \times 10^7$  organisms to induce significant pathology (Prof Tomasz, personal communication). Challenge with 100  $\mu\text{g}$  of pneumococcal cell wall represents a large but transient pro-inflammatory stimulus which might evoke a different host inflammatory reaction to that induced by pneumococcal cell wall continuously released from organisms replicating in vivo.

## **5.4. Cochlear perfusion.**

In order to model what happens when organisms invade the scala tympani via the cochlear aqueduct a suspension of viable organisms was perfused through the perilymphatic space. The time course of subsequent pathophysiological events was monitored. One key modification to the model previously in use in the laboratory (and used to investigate the effects of purified pneumolysin on the cochlea) was to reduce the CSF flow through the fistulised cochlea by opening the cisterna magna (Salt *et al* 1991). This was intended to prevent the inoculum from being washed away before a chain of pro-inflammatory events was established.

### **5.4.1. Comparison with cochlear lesions in meningitis**

Perfusion of viable pneumococci into the perilymphatic space damaged the organ of Corti of the guinea pig within three hours. By contrast, intracochlear perfusion of comparable inoculum of a relatively apathogenic strain of *E. coli* was well tolerated, at least in this acute setting, suggesting that bacterial growth in the scala tympani *per se* does not affect the organ of Corti. The results further suggest that if and when pneumococci reach the inner ear during meningitis serious and possibly irreversible damage to the organ of Corti may follow rapidly.

The two main ultrastructural lesions detected (damage to stereocilia and cratering of the apical surface of border cells) are broadly similar to those induced by experimental *H. influenzae* type b and *E. coli* meningitis in rabbits and experimental pneumococcal and *E. coli* meningitis in guinea pigs (this thesis). Together, these data constitute good evidence that such lesions are almost certainly due to bacterial invasion of the cochlea. However, the preservation of the CM suggests that bacterial perfusion itself does not acutely impair OHC function or affect the endocochlear potential. In contrast to the findings in experimental meningitis and after cochlear perfusion of purified pneumolysin (Comis *et al* 1993), scanning electron microscopy revealed little damage to the OHCs after direct pneumococcal

perfusion of the cochlea. The ototoxic mechanisms in this hyperacute situation may therefore differ slightly from those acting during the longer time-course of meningitis, particularly in regard to OHC damage.

The preservation of hearing during the first hour after perfusion of pneumococci could be explained in at least two ways. First, it could be due to a lag phase in bacterial growth and/or the delayed release of ototoxic host inflammatory mediators. Second, it is possible that organisms complete a few rounds of replication before autolysis, only then releasing intracellular pneumolysin and cell wall material.

#### **5.4.2. Antibiotic effects**

##### ***Does antibiotic reach the perilymph?***

One study has shown that cefotaxime (100 mg/kg) reliably penetrates the perilymphatic space of healthy (i.e. non-infected) guinea pigs when administered as an intravenous bolus (Sun et al 1996). The concentration of CTX and its metabolite desacetylcefotaxime was measured in the CSF and perilymph by high-performance liquid chromatography. The concentrations in the perilymph exceeded that in the CSF at all times. One hour after injection, the concentration of CTX in the perilymph was 5.5 mg/l compared to 2 mg/l in the CSF. The reported MICs for CTX for penicillin-resistant pneumococci are between 0.04 and 1 mg/l. The data show that in the guinea pig, supra-MIC levels of CTX and its active metabolite are achieved in the perilymph for at least 6 h after a single bolus dose of 100 mg/kg; they would be expected to be even higher during meningeal or perilymphatic inflammation. Filamentous forms, long chain formation and bacterial cell wall distortion characteristic of penicillin activity were observed 75 min after perfusion of viable pneumococci into the scala tympani of amoxicillin-pretreated guinea pigs. This suggests that a concentration of amoxicillin in excess of the MIC was achieved in the perilymphatic space when amoxicillin (100 mg/kg) was injected intraperitoneally 30 min pre-perfusion.

##### ***The pro-inflammatory theory***

According to previous work, antibiotic pretreatment might be expected to exacerbate local inflammation and by implication hearing loss (Tuomanen et al 1987; Pfister et al 1994). But in fact antibiotic pretreatment substantially protected the cochlea from the acute effects of pneumococcal perfusion. This is consistent with a recent study of hearing loss in experimental pneumococcal meningitis in rabbits in which it was found that even without adjuvant dexamethasone, antibiotic treatment both reduced the chance of deafness and aided recovery of hearing if lost (Bhatt et al 1995) (see section 5.2.1). The timing of antibiotic administration is important. In experimental rabbit pneumococcal meningitis, the

magnitude of the antibiotic-induced inflammatory burst is highly dependent on the numbers of bacteria in the CSF. Inflammation is enhanced by administering an intravenous ampicillin bolus at the threshold of log-phase growth *in vivo* but is postponed when a bolus is given early in the course of infection (Pfister et al 1994). Furthermore, in experimental *E. coli* meningitis in the rabbit the mean concentration of free endotoxin in the CSF four hours after an antibiotic bolus is at least ten-fold lower than in untreated animals (Friedland et al 1993). These studies suggest that reducing the cumulative bacterial load outweighs any transient antibiotic-induced inflammatory burst. This would explain the data obtained. By inhibiting the initial period of bacterial replication, antibiotic pretreatment limits the amount of toxin and cell wall material to that contained in the initial inoculum, release of which is still sufficient to cause some hearing loss. With no antibiotic pretreatment, bacterial replication increases the total amount of toxin and cell wall material available for release, so increasing hearing loss.

## **5.5. Mechanisms of cochlear damage and its prevention.**

Evidence has been presented for the role of pneumolysin in causing cochlear damage. It has been assumed (but not experimentally proven) that the pneumolysin-dependent ultrastructural lesions are responsible for the majority of hearing loss in this experimental meningitis model. It does not however follow that measures to block the action of pneumolysin would necessarily prevent deafness occurring. It could be that sufficient pneumolysin is released early in infection to cause profound cochlear damage. Also, other bacterial toxins such as the putative cytotoxic toxin produced by *H. influenzae* might trigger cochlear damage by similar mechanisms (Amaee, 1995; Dover *et al* unpublished findings). It is likely that cochlear damage has already begun by the time some patients present with bacterial meningitis. Therefore it is useful to try and identify the final common pathways of damage, as intervention at this level might be more successful in preventing meningogenic deafness. There are many similarities between the damage induced by pneumococcal meningitis and those which occur post-mortem or follow acoustic trauma or cochlear perfusion with ototoxic drugs or excitotoxic agonists. This suggests that these insults act via a shared final common pathway. Some new potential mechanisms of damage will now be discussed.

### **5.5.1. Dissipation of the endocochlear potential and mixing of cochlear fluids**

Craters in supporting cells and tearing away of hair cells from supporting processes will disrupt the integrity of the reticular lamina. This will lead to mixing of cochlear fluids,

raising the potassium concentration in the perilymph and dissipating the endocochlear potential which is essential for mechano-electrical transduction. A similar process probably occurs after auditory trauma, where hair cells can be ejected from the reticular lamina (Bohne and Rabbitt, 1983; Slepecky, 1986). The stria vascularis is damaged in *H. influenzae* and *E. coli* meningitis in the rabbit (Osborne *et al* 1995) and by perfusion of endotoxin through the scala tympani (Guo *et al* 1994), and such damage will further compromise the endocochlear potential. Holes in the reticular lamina are eventually sealed by phalangeal scarring and it is probable that the stria vascularis can recover, thus hearing loss resulting from dissipation of the endocochlear potential may be reversible. There is as yet no direct experimental evidence to support this theory because it is technically very difficult to measure the endocochlear potential over the prolonged time course of experimental meningitis.

#### **5.5.2. Loss of hair cells and damage to hair bundles: the putative role of nitric oxide.**

Many insults to the cochlea result in loss of sensory cells. Such cells are replaced by scar tissue so damage of this nature is irreversible. Ballooning of the apical surface of outer hair cells and disruption of OHC and IHC hair bundles is common after pneumococcal meningitis, perfusion of pneumolysin into the cochlea, and auditory trauma (Osborne and Comis, 1995; Comis *et al* 1993; Bohne and Rabbitt, 1983). Guinea pig outer hair cells *in vitro* are killed by a 60-minute exposure to endotoxin (10µg/ml) (Dulon *et al* 1990). The relationship between OHC damage and hearing loss is not clear cut (see section 5.2.2). Inner hair cells carry about 95% of the afferent innervation so damage to or loss of IHC hair bundles such as the fusion, uprooting and splaying of stereocilia seen in pneumococcal meningitis will clearly cause a fall in afferent nerve potential. Damage to stereocilia alone can account for a shift in  $N_1$  threshold (Slepecky, 1986).

The action of a common mediator might explain why hair cells and hair bundles sustain similar damage in response to a wide variety of insults. One likely candidate is nitric oxide (NO) which is implicated in many different pathologies including neural damage and microvascular changes in meningitis (Pfister *et al* 1994; Koedel *et al* 1995) (see section 1.4.2). The pathological production of NO by an inducible NO synthase is a non-specific immunological defence. NO reacts with oxygen superoxide to form peroxynitrite anions which decompose to the potent oxidants OH. and NO<sub>2</sub>. (Moncada *et al* 1991). In the CNS, NO is released by microglia in response to pro-inflammatory cytokines (Boje and Arora, 1992) and by neurons in response to glutamergic stimulation of N-methyl-D-aspartate (NMDA) receptors (Garthwaite *et al* 1988). NO synthase has been localised to the spiral ganglion cells of the rat cochlea (Zdanski *et al* 1994). Perfusion of the cochlea with sodium

nitroprusside, a nitric oxide donor, induces damage to OHCs, ballooning of the apical surface of supporting cells and swelling of nerve endings beneath the IHCs which closely resembles damage found in pneumococcal meningitis (Amaee, 1995). The severe damage which follows perfusion of 10  $\mu\text{g}$  pneumolysin into the guinea pig cochlea is almost completely abolished by preperfusion with **N<sup>G</sup>-methyl-L-arginine** (50 mM), an inhibitor of NO synthase (Amaee *et al* 1995). Pneumolysin in the scala tympani probably punches transmembrane pores in hair and supporting cells. Intracellular calcium rises due to voltage-dependent or glutamate-dependent channels, and this induces **Ca<sup>2+</sup>/calmodulin** dependent NO synthase. Pneumolysin is not the only pneumococcal product responsible for NO release since heat-killed pneumococci can induce NO production by cerebral endothelial cells (Haberl *et al* 1994).

Damage may also be mediated by oxygen free radicals which are liberated by polymorphonuclear leukocytes and macrophages during inflammation. Guinea pig outer hair cells are highly susceptible to free-radical induced damage in vitro (Dulon *et al* 1990). Free radical scavengers reduce injury in experimental bacterial meningitis (Pfister *et al* 1992d; Koedel *et al* 1995) but their efficacy in preventing hearing loss has not been assessed.

### **5.5.3. Excitotoxic and physical damage to the neural elements**

One consistent finding in all of the meningitis experiments was pathological damage to nerve endings. This damage was not related to the production or absence of pneumolysin. Because hearing loss in the absence of pneumolysin (and, as far as can be ascertained, in *E. coli* meningitis) was minimal, the importance of the ultrastructural changes observed is uncertain. Damage to nerve endings such as dendritic swelling beneath the IHCs is commonly seen in a wide variety of toxic insults to the cochlea, including acoustic overstimulation (Spoendlin, 1971), ischaemia, hypoxia, post-mortem change and excitotoxic damage induced by perfusion of excitatory amino acid (EAA) agonists kainate, quisqualate or glutamate (Osborne *et al* unpublished findings). There is a great deal of experimental evidence that excessive release of glutamate has a major role in the onset and evolution of various neuropathologies and there is intense interest in the potential role for glutamate receptor antagonists as cytoprotective agents in ischaemic stroke, epilepsy and brain trauma (Meldrum, 1995; Lipton, 1993). Excitotoxic injury is probably mediated by ionic channel gated post-synaptic receptors which promote large cation fluxes and entry of Cl<sup>-</sup> into the cell, causing osmotic swelling. **Ca<sup>2+</sup>-dependent** processes then lead to the generation of NO (see above). Intervention against excitotoxic damage is therefore possible at three stages: prevention of excess glutamate release; blockade of glutamergic receptors and reduction of the post-receptor osmotic and **Ca<sup>2+</sup>** mediated events.

Few studies of the role of EAA antagonists in the pathophysiology of bacterial meningitis have been published, although EAAs are detectable in the brain interstitial fluid during experimental *E. coli* meningitis (Guerra-Romero *et al* 1993; Perry *et al* 1993). Kynurenic acid, a nonselective excitatory amino acid (EAA) receptor antagonist, partially protects cortical and hippocampal neurons against injury in experimental streptococcal meningitis in rats (Leib *et al* 1996). HU-211, a novel non-competitive NMDA antagonist which also blocks  $\text{Ca}^{2+}$  uptake, reduces brain oedema in ceftriaxone-treated experimental pneumococcal meningitis in rats (Bass *et al* 1996). Neurotoxicity in the cochlea itself appears to be mediated by both NMDA and non-NMDA receptors (Eybalin, 1993, p348). NMDA antagonists such as D-2-amino-5-phosphovalerate (AP-5) only affect the CAP at high stimulus intensities (Puel *et al* 1991). AP-5 and another NMDA-receptor antagonist **MK-801** (dizocilpine) possibly block the deleterious actions of pneumolysin (10  $\mu\text{g}$ ) when preperfused into the guinea pig cochlea, but no details of the concentrations used were given (Amaee *et al* 1995).

Spontaneous firing of single nerve units can be induced by raising the perilymph potassium concentration, which depolarises the afferent endings either directly or indirectly by releasing transmitter (probably glutamate) (Leng and Comis, 1979). In this way, breach of the reticular lamina may both reduce the endocochlear potential and cause a depolarisation nerve block. The accumulation of extracellular glutamate generated by spontaneous excitation or neuronal cell death could eventually overwhelm the putative glutamate-glutamine cycle and cause wider pathological effects as above.

Sections proximal to the nerve endings were not examined in this study, but it would be reasonable to assume that inflammation and resulting swelling could compress dendrites where they pass through the narrow *habenula perforata* to leave the modiolus. Damage to the auditory nerve at the level of the internal auditory meatus would reduce brain-stem evoked potentials but would not affect the compound action potential recorded at the round window.

#### **5.5.4. Other factors**

Cochlear damage probably results from a combination of all of the factors above, many of which are interconnected. Other mechanisms that might contribute toward hearing loss in meningitis (septic embolism of the internal auditory artery, disturbance of the brain stem etc.) were discussed in section 1.5.2.

## 5.6. Conclusions

What conclusions can be drawn from these experimental studies that might change clinical management of bacterial meningitis?

Convincing evidence has been presented confirming the crucial role of pneumolysin in causing cochlear damage in pneumococcal meningitis. The electrophysiological data add to the evidence that cochlear damage is the chief cause of deafness in meningitis (see section 1.5.2). In the meningitis model, a substantial hearing deficit developed in just a few hours, and under controlled conditions cochlear function was impaired just 90 minutes after exposure to viable pneumococci. The rapid onset of cochlear damage is consistent with two recent clinical studies showing that if deafness does occur in meningitis, it is usually present at the time of admission (Wald *et al* 1995; Richardson *et al* 1995). This emphasises the importance of immunisation as the chief tool in preventing meningitis and its neurological sequelae, since it may be too late to save hearing once the patient presents.

The data obtained in these studies also emphasise the need to treat bacterial meningitis with appropriate antibiotics as urgently as possible to minimise the cumulative inflammatory stimulus and to reduce the probability of bacterial invasion of the inner ear with the potential ototoxic sequelae demonstrated here.

Further evidence is needed of the importance of excitotoxic and NO-induced damage in the pathophysiology of meningitis. Adjuvant anti-inflammatory therapy to minimise the antibiotic-induced inflammatory burst has been promoted as a way of reducing the long-term neurological sequelae of bacterial meningitis (including deafness) but remains controversial (Schaad *et al* 1995). It would seem more sensible to focus attention on the final common pathways of damage, rather than on the inflammatory cascade. Intervention at this stage has the possibility of reversing damage already triggered by the pro-inflammatory cytokine cascade or the actions of bacterial toxins. Several cytoprotective agents are in clinical trials of efficacy in ischaemic stroke (Meldrum, 1995). It is unlikely that a pharmaceutical company will develop a drug specifically for use to prevent complications in meningitis. Future experimental meningitis studies should therefore evaluate cytoprotective agents that are likely to come on to the market in the near future licensed for other indications.

Further specific experiments extending those presented in this thesis should include:

- Investigating if the haemolytic or complement-activating actions of pneumolysin are important in causing cochlear damage by inducing meningitis with the variants of D39 containing defined point mutations in the **PLY** gene (Rubins *et al* 1996). A better

understanding of how pneumolysin damages the cochlea will help the search for efficacious adjuvant treatments.

- Investigating the efficacy of cytoprotective agents such as NMDA-antagonists in preventing cochlear damage in experimental meningitis. These agents could easily be assessed in the guinea pig model, which offers the great advantage that protection can be evaluated in terms of both hearing loss and ultrastructural damage
- Perfusing the cochlea with suspensions of PLN-A to see if pneumolysin is responsible for cochlear damage in that situation.
- Defining more clearly the putative role of hyaluronidase in pneumococcal replication in vivo.

Finally, this study has demonstrated how a powerful molecular technique such as insertion-duplication mutagenesis can contribute to understanding the pathogenesis of infection when combined with careful physiological and microscopic techniques. It is only by such close co-operation across disciplines that we will better understand the incredible complexity of the interaction between microbe and host. Similar co-operation between the fields of infectious disease, clinical neurology, paediatrics and neuroscience may yet yield an effective adjuvant therapy that will prevent meningogenic deafness.

## Appendix A: Composition of solutions used

<b><i>Phosphate buffer (0.2M) for fixative:</i></b>	<b><i>Final</i></b>
1.35g $\text{KH}_2\text{PO}_4$ in 50 ml dH <sub>2</sub> O+	0.2 M
0.31 g NaOH in 39 ml dH <sub>2</sub> O	pH 7.2

<b><i>Glutaraldehyde fixative:</i></b>	
25 ml 0.2 M phosphate buffer	0.05 M
10 ml 25% glutaraldehyde	2.5 %
1.73 g sucrose	
to 100 ml with dH <sub>2</sub> O	Osmolarity = 350 mmol/kg

<b><i>Osmium tetroxide</i></b>	
2.5 ml 0.2 M phosphate buffer	0.05 M
0.1 g $\text{OsO}_4$	0.1%
0.855 g sucrose	
to 10 ml with dH <sub>2</sub> O	Osmolarity = 350 mmol/kg

<b><i>10% buffered formalin for histological fixation</i></b>
100 ml 10x PBS (Gibco BRL, Ca/Mg free, 042-0400)
100 ml 40% formaldehyde (BDH, Poole, UK)
800 ml dH <sub>2</sub> O

<b><i>Counting fluid (stains white cells in CSF):</i></b>
1 ml Glacial acetic acid
2.5 ml Propan 1,2 diol
1.5 ml Crystal violet 1% in water
to 100 ml with dH <sub>2</sub> O
Kept in the dark at 4°C

### *TEM embedding resin*

After Mollenhaur 1964; all chemicals from Agar Scientific, Essex

<b>2.5 ml</b>	Agar 100
<b>3.3 ml</b>	Araldite Cy212
<b>4.2ml</b>	Dodecenylsuccinic anhydride
<b>0.15 ml</b>	Dibutylphthalate
<b>0.25 ml</b>	<b>2,4,6-tri(dimethylaminomethyl)phenol</b>

### *Artificial perilymph.*

Batches of **APL** (100 ml) were filter-sterilized (0.2  $\mu\text{m}$ ) and aliquots of **5 ml** were stored at 4°C. The composition is thus:

	<b>mM</b>	<b>g/l</b>
NaCl	<b>137</b>	8
KCl	<b>5</b>	<b>0.37</b>
CaCl <sub>2</sub>	2	2 ml of 1mM solution
NaH <sub>2</sub> PO <sub>4</sub> ·2H <sub>2</sub> O	1	0.156
MgCl <sub>2</sub> ·6H <sub>2</sub> O	1	0.202
NaHCO <sub>3</sub>	12	1.01
Glucose	11	1.982
Osmolarity = <b>300 ± 3</b> mmol/kg		

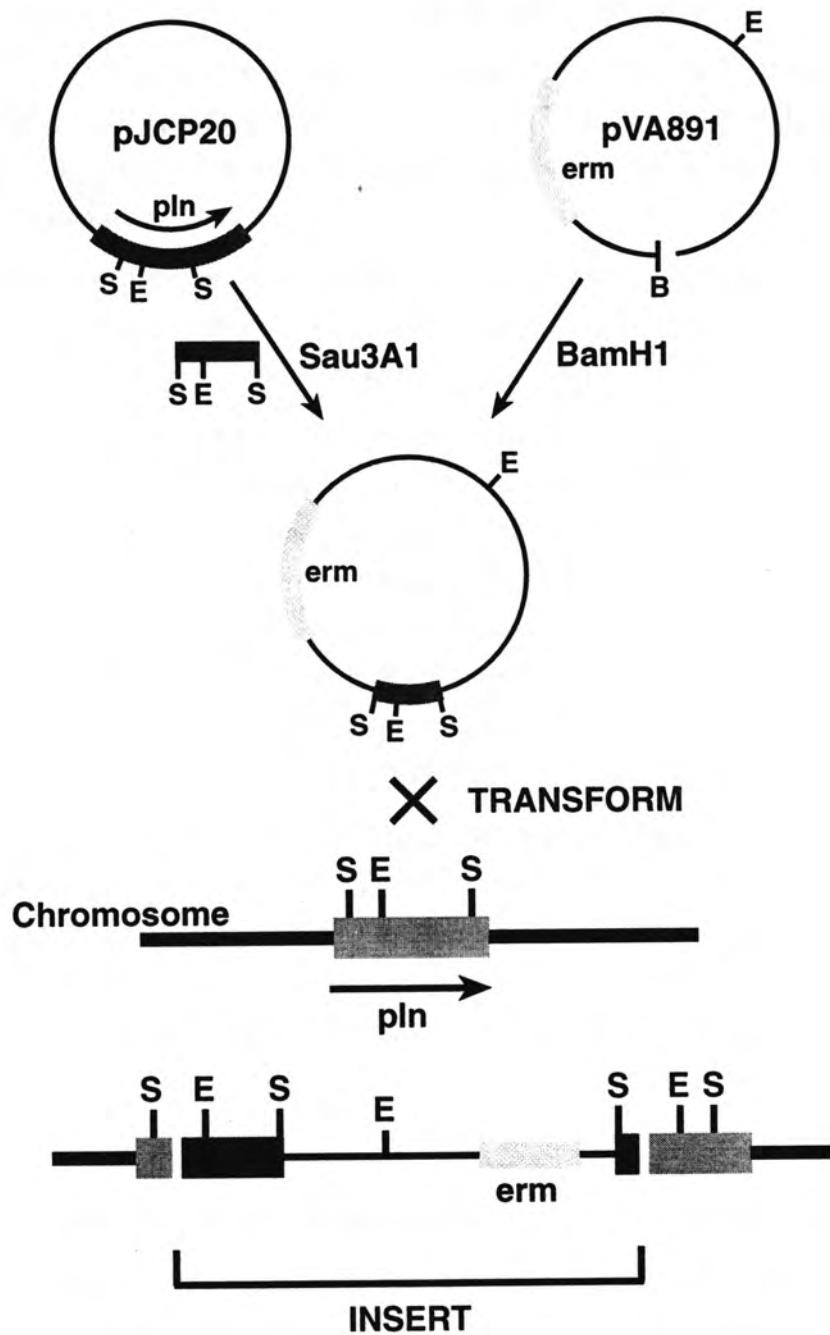
## **Appendix B: Details of the construction of the isogenic mutants of *S.pneumoniae* D39 deficient in pneumolysin, neuraminidase or hyaluronidase.**

All derivatives of D39 were kindly provided by Dr Tim Mitchell, Dept of Microbiology, University of Leicester. A brief description of their manufacture is given below.

**PLN-A:** PLN-A deficient in pneumolysin was made by a two-stage process (see figure) because direct transformation of encapsulated D39 proved impossible. Plasmid pJCP20, a derivative of pBR322, carries the complete *S.pneumoniae* pneumolysin gene (pln) (Paton *et al* 1986). A 690 bp fragment of the pln gene was excised from pJCP20 and ligated into the vector pVA891 which carries a streptococcal gene (erm) encoding erythromycin resistance. pVA891 was transformed into *E. coli* K-12 DH1. The recombinant plasmid was purified and used to transform a non-encapsulated derivative of D39 (Rx1). By homologous recombination between the pneumolysin gene fragment in the plasmid and the *S. pneumoniae* chromosomal DNA the chromosomal coding sequence for pneumolysin was interrupted. This was confirmed with Southern blot hybridisation. DNA from this organism was finally transformed into encapsulated D39 and the failure to make a translated gene product confirmed with immunoblot analysis and a haemolytic assay (Berry *et al* 1989). PLN-A has been used in a number of studies of pneumococcal pathogenesis (Berry *et al* 1989; Rayner *et al* 1995; Benton *et al* 1995; Friedland *et al* 1995; Canvin *et al* 1995).

**$\Delta$ HY1:**  $\Delta$ HY1 deficient in hyaluronidase activity was also made by insertion-duplication mutagenesis, but this time by direct transformation of D39. The sequence of the hyaluronidase gene was established by Berry (1994) (Adelaide) and Hill (1995) (Leicester). A 1.3 kb fragment of the hyaluronidase gene was cloned into pG+host 5, a "suicide vector" which has a temperature-sensitive origin of replication. Transformation of D39 with the shuttle vector pVA838 (including the erythromycin resistance gene) was enhanced by adding competence factor from strain Rx1 and incubating at 22°C. A putative hyaluronidase-negative mutant was isolated and designated  $\Delta$ HY1. This failed to cleave hyaluronic acid in the agarose plate assay. Southern blot hybridisation confirmed incorporation of the inserted DNA into the chromosomal hyaluronidase gene.

**$\Delta$ NA1:**  $\Delta$ NA1 deficient in neuraminidase activity was made by a similar process. The sequence of a neuraminidase gene (nanA) had been previously established (Camara *et al* 1991). A putative neuraminidase mutant ( $\Delta$ NA1) was unable to cleave *MUAN* and Southern blot hybridisation again confirmed interruption of the chromosomal gene for neuraminidase.



**Appendix figure:** Scheme for insertion-duplication mutagenesis of the pneumolysin gene. erm, erythromycin resistance marker; pln, pneumolysin gene; E, *EcoR1*; B, *BamH1*; S, *Sau3A1*.

### **Appendix C: Assays for pneumolysin, neuraminidase and hyaluronidase.**

I am grateful to Andrew Wallis and Dr Val Clarke, Department of Microbiology and Immunology, University of Leicester for performing the assays described below.

Single colonies of either the inoculum under test or organisms recovered from the CSF were inoculated into 10 ml BHI with or without erythromycin (5 µg/ml), incubated overnight at 37°C and then pelleted. Cell lysates were prepared by ultrasonication. Total cell protein was determined by a BioRad microassay.

Pneumolysin activity was detected by a standard haemolytic assay. Twofold serial dilutions of the cell lysates were mixed with an equal volume of 2% sheep erythrocytes and incubated for 30 min at 37°C. Results were reported as either plus or minus.

Neuraminidase activity was assayed fluorometrically by adding 20 µl of cell lysate to 200 µl of 150 µM 2'-(4-methylumbelliferyl)- $\alpha$ -D-N-acetylneuraminic acid (MUAN) in a 100 mM citrate-phosphate buffer at pH 6.5 and incubating for 16 min at 37°C. Neuraminidase cleaves fluorescent 4-methylumbelliferone from MUAN. The reaction was stopped by adding 2 ml of 0.5 M Na<sub>2</sub>CO<sub>3</sub>. Fluorescence was excited at a wavelength of 365 nm with an emission wavelength of 446 nm. The lower limit of detection of the assay was about 0.5-0.6 mU/mg cell protein while the wildtype D39 expressed about 6.4 mU/mg cell protein. Assays were performed in duplicate on two separate occasions.

Hyaluronidase activity was assessed in a qualitative agarose plate assay. Plates were prepared by adding 1 ml hyaluronic acid (2 mg/ml in PBS) and 1 ml bovine serum albumin (8 mg/ml in PBS) to 4 ml of 1.6% (wh) agarose in PBS and allowed to set for 1 h at 37°C. Cell lysate (10 µl) was added to a well and incubated for 16 h at 37°C. The plate was overlaid with a 10% cetylpyridinium solution. Hyaluronidase activity was detected as a clear zone around the well.

### **Appendix D: Raw data from meningitis experiments**

In the following pages the raw data from the comparative meningitis experiments are tabulated. Each column represents an individual cochlea. Figures given are the CAP loss (dB) at each of the eight frequencies measured at 3, 6, 9 and 12 h post inoculation. Blank cells represent failed recordings.

Freq (kHz)	Experiment number																Mean	SD	95% CI	
	D39(14) L	D39(14) R	D39(15) L	D39(15) R	D39(16) L	D39(17) L	D39(17) R	D39(19) L	D39(19) R	PL2 (L)	PL2 (R)	NA+1L	NA+1R	NA+2L	NA+2R					
3h	3	-1	4	1	5	5	1	-3	3	4	8	12	0	1		5	3	3.8	2.2	
	4			0	9	1	-1	-2	0	-5			3	1	9	5	2	4.4	2.9	
	5			1	16	1	1	-2	0	-8			1	2	10	9	3	6.5	4.4	
	6			-1	26	0	1	-1	-1	-10			-5	2	8	7	2	9.3	6.2	
	7			-4	30	3	2	-1	-7	-3			-7	2	17	8	4	11.2	7.5	
	8			-8	28	4	2	-4	-1	5				-3	8	1	3	9.9	7.1	
	9			-7	30	3	5	-3	6	10				-1	9	0	5	10.2	7.3	
	10	3	17	2	32	7	1	-3	6	16	0	11	2	5	23	5	8	9.7	5.3	
	6h	3	5	4	2	36	4	15	6	7	39	26	19	12	16	27	8	15	12	6.6
		4			9	40	-1	12	7	19	28			12	21	10	10	15	11.3	7.6
5				23	49	3	9	7	10	15			10	25	13	18	17	12.7	8.5	
6				30	53	4	5	7	10	14			6	27	12	16	17	14.8	9.9	
7				32	49	5	5	7	16	25			3	31	24	16	19	14.4	9.7	
8				26	42	4	-3	3	19	31			-7	30	13	5	15	15.9	10.7	
9				24	42	2	-5	0	23	33			0	36	15	2	16	16.8	11.3	
10		44	30	34	43	6	1	0	23	38	34	31	18	54	27	3	26	16.9	9.4	
9h		3	19	0	30	70	6	38	33	11	44	25	19	19	26	59	38	29	18.9	10.5
		4			37	71	5	41	36	14	58			19	28	50	49	37	19.7	13.2
	5			43	71	8	38	39	10	50			32	38	62	54	40	19.4	13	
	6			45	75	9	40	38	9	54			36	44	58	52	42	19.6	13.2	
	7			39	75	8	36	35	10	62			36	40	77	50	43	22.6	15.2	
	8			28	72	6	32	33	19	63			32	37	63	28	38	20.2	13.6	
	9			27	71	8	36	36	19	55			32	38	60	32	38	18.2	12.2	
	10	42	30	32	66	14	40	36	18	58	38	32	48	50	70	36	41	15.8	8.7	
	12h	3	54	44	37	70	23	43	34	25	48	31	27	30	33	59	70	42	15.5	8.6
		4			44	71	28	45	38	28	54			40	33	65	75	47	16.7	11.2
5				49	71	36	43	43	22	58			49	43	72	84	52	18	12.1	
6				53	75	40	47	45	22	59			50	49	72	83	54	17.4	11.7	
7				45	75	37	45	55	23	68			42	45	77	83	54	19.1	12.8	
8				34	72	31	40	40	28	57			32	43	63	75	47	17	11.4	
9				31	71	31	42	40	22	63			33	44	60	72	46	17.4	11.7	
10		56	62	34	66	37	45	42	21	65	37	32	49	54	70	75	50	15.9	8.8	

CAP loss data in meningitis due to D39

Freq (kHz)	Experiment number										Mean	SD	95% CI		
	PLN-A(11)L	11R	10L	10R	15L	15R	13L	13R	5L	5R					
3h	3	2	3	0	2	9	14	0	0	7	3	4	4.6	3.3	
	4	-1	0	2	2	3	7	0	-1	9	0	2	3.4	2.4	
	5	1	1	0	1	-1	9	-1	-1	4	3	2	3.1	2.2	
	6	1	1	2	0	2	7	0	0	5	2	2	2.3	1.7	
	7	0	0	1	0	3	10	1	1	8	0	2	3.6	2.6	
	8	4	1	-4	-1	3	7	0	-1	7	3	2	3.6	2.6	
	9	3	0	-2	-1	6	4	3	0	6	2	2	2.8	2.0	
	10	3	2	-1	3	7	5	3	3	8	5	4	2.6	1.8	
	6h	3	3	10	8	0	9	18	6	6	9	6	8	4.8	3.4
		4	5	9	10	3	2	12	6	5	9	6	7	3.2	2.3
5		4	9	8	4	4	21	5	2	7	7	7	5.3	3.8	
6		5	5	9	1	5	20	6	2	7	6	7	5.2	3.7	
7		4	7	9	1	9	20	7	4	10	1	7	5.5	4.0	
8		7	9	9	-2	6	10	10	3	11	1	6	4.4	3.1	
9		7	13	7	-4	2	6	12	7	7	-2	6	5.4	3.9	
10		4	10	11	2	2	5	10	6	8	0	6	3.9	2.8	
9h		3	9	18	10	3	12	15	15	7	18	8	12	5.0	3.6
		4	7	17	9	2	10	17	15	7	18	3	11	5.9	4.2
	5	7	17	8	4	9	24	9	6	14	4	10	6.4	4.5	
	6	5	11	8	1	12	22	11	8	15	3	10	6.1	4.4	
	7	6	12	9	3	15	23	14	8	18	-2	11	7.4	5.3	
	8	6	17	10	3	10	14	16	6	19	-4	10	7.1	5.1	
	9	7	17	10	-1	8	13	19	4	14	-5	9	7.7	5.5	
	10	5	16	15	5	9	14	18	6	14	-2	10	6.4	4.6	
	12h	3	17	18	15	6	15	16	24	26	25	13	18	6.1	4.4
		4	18	19	16	9	7	19	29	32	26	18	19	8.0	5.7
5		15	15	12	10	9	23	33	32	19	20	19	8.5	6.0	
6		14	12	14	10	12	21	35	36	20	22	20	9.3	6.7	
7		14	14	13	7	14	21	30	29	22	13	18	7.5	5.4	
8		13	17	13	1	9	11	29	26	18	10	15	8.2	5.9	
9		11	12	14	-3	7	10	27	24	10	6	12	8.6	6.2	
10		10	10	19	-2	9	12	19	27	11	7	12	7.9	5.7	

CAP loss data in meningitis due to PLN-A

Freq (kHz)	Experiment number										Mean	SD	95% CI		
	NA1 (1L)	1R	2L	2R	3L	3R	5L	5R	6L	6R					
3h	3	0	5	30	16	14	1	7	-3	8	5	<b>8</b>	10	<b>6.9</b>	
	4	4	11	30	24	6	2	8	-8	5	4	<b>9</b>	11	<b>7.8</b>	
	5	3	21	32	25	5	2	15	-2	0	6	<b>11</b>	12	<b>8.4</b>	
	6	8	32	34	20	4	4	18	0	1	5	<b>13</b>	13	<b>9.0</b>	
	7	5	38	37	21	5	6	15	0	6	5	<b>14</b>	14	<b>9.9</b>	
	8	9	42	42	27	10	3	16	4	5	8	<b>17</b>	15	<b>10.8</b>	
	9	7	41	47	38	6	2	2	-5	-3	10	<b>15</b>	20	<b>14.0</b>	
	10	-1	45	48	36	8	6	9	3	-3	13	<b>16</b>	19	<b>13.7</b>	
	6h	3	0	40	60	56	4	24	34	22	8	15	<b>26</b>	21	<b>15.0</b>
		4	9	45	65	53	4	30	47	30	7	13	<b>30</b>	22	<b>15.5</b>
5		13	52	66	62	2	30	67	34	11	13	<b>35</b>	25	<b>17.9</b>	
6		22	52	68	61	0	34	75	46	11	14	<b>38</b>	26	<b>18.6</b>	
7		18	54	70	64	0	25	69	44	8	16	<b>37</b>	27	<b>19.0</b>	
8		22	47	74	70	1	11	59	38	1	21	<b>34</b>	27	<b>19.6</b>	
9		19	45	74	73	-1	6	42	25	-3	26	<b>31</b>	28	<b>19.9</b>	
10		19	48	69	69	0	8	44	18	-1	27	<b>30</b>	26	<b>18.7</b>	
9h		3	20	65	60	56	31	42	31	36	43	5	<b>39</b>	19	<b>13.2</b>
		4	25	67	65	53	40	44	44	47	53	6	<b>44</b>	18	<b>13.0</b>
	5	38	72	66	62	42	45	63	62	59	11	<b>52</b>	18	<b>13.0</b>	
	6	46	74	68	61	40	46	73	81	58	12	<b>56</b>	21	<b>14.7</b>	
	7	43	75	70	64	32	38	67	75	51	11	<b>53</b>	21	<b>15.3</b>	
	8	44	64	74	70	20	24	60	67	39	6	<b>47</b>	24	<b>17.1</b>	
	9	46	63	74	73	15	21	42	54	34	12	<b>43</b>	23	<b>16.3</b>	
	10	41	65	69	69	16	21	45	48	38	18	<b>43</b>	20	<b>14.6</b>	
	12h	3	60	66	60	56	34	58	27	37	42	10	<b>45</b>	18	<b>12.9</b>
		4	65	67	65	53	42	57	31	47	51	14	<b>49</b>	17	<b>12.0</b>
5		72	72	66	62	46	57	61	64	58	22	<b>58</b>	15	<b>10.6</b>	
6		72	74	68	61	45	58	70	82	57	24	<b>61</b>	17	<b>11.9</b>	
7		78	78	70	64	36	55	63	79	48	27	<b>60</b>	18	<b>13.0</b>	
8		64	78	74	70	22	50	54	69	36	28	<b>55</b>	20	<b>14.3</b>	
9		61	75	74	73	15	46	37	56	32	35	<b>50</b>	21	<b>14.8</b>	
10		71	75	69	69	19	43	43	52	37	40	<b>52</b>	19	<b>13.2</b>	

CAP loss data in meningitis due to NA1

Freq (kHz)	Experiment number						Mean	SD	95% CI
	4L	4R	5L	6L	6R	7R			
<b>3h</b>									
3			23	3	-3	4	<b>7</b>	11	<b>17.9</b>
4			28	-2	-5	3	<b>6</b>	15	<b>23.9</b>
5			20	6	-6	1	<b>5</b>	11	<b>17.5</b>
6			15	23	-6	3	<b>9</b>	13	<b>20.4</b>
7			25	24	-7	3	<b>11</b>	16	<b>25.2</b>
8			26	26	-7	5	<b>13</b>	16	<b>26.0</b>
9			29	23	-8	6	<b>13</b>	17	<b>26.7</b>
10			25	23	2	6	<b>14</b>	12	<b>18.6</b>
<b>6h</b>									
3	6	7	3	5	0	6	<b>5</b>	3	<b>2.7</b>
4	22	5	27	0	-2	3	<b>9</b>	12	<b>12.8</b>
5	23	3	25	5	5	2	<b>11</b>	11	<b>11.1</b>
6	31	7	31	16	5	9	<b>17</b>	12	<b>12.4</b>
7	28	8	41	16	4	-1	<b>16</b>	16	<b>16.7</b>
8	25	9	42	16	7	0	<b>17</b>	15	<b>15.9</b>
9	31	15	46	13	7	2	<b>19</b>	16	<b>17.3</b>
10	30	5	46	20	7	2	<b>18</b>	17	<b>18.0</b>
<b>9h</b>									
3	43	21	25	0	12	28	<b>22</b>	15	<b>15.3</b>
4	65	26	41	0	16	35	<b>31</b>	22	<b>23.4</b>
5	71	22	44	6	15	39	<b>33</b>	24	<b>24.7</b>
6	83	21	49	7	13	46	<b>37</b>	29	<b>29.9</b>
7	83	27	54	7	13	47	<b>39</b>	29	<b>29.9</b>
8	83	27	47	6	18	39	<b>37</b>	27	<b>28.3</b>
9	84	27	47	10	24	35	<b>38</b>	26	<b>27.0</b>
10	92	16	43	10	24	30	<b>36</b>	30	<b>31.3</b>
<b>12h</b>									
3	52	36	27	4	1	26	<b>24</b>	19	<b>20.3</b>
4	79	45	41	3	1	33	<b>34</b>	29	<b>30.6</b>
5	81	42	44	12	10	37	<b>38</b>	26	<b>27.2</b>
6	91	43	50	27	9	47	<b>45</b>	27	<b>28.8</b>
7	89	54	56	28	8	46	<b>47</b>	27	<b>28.8</b>
8	88	48	48	27	5	37	<b>42</b>	28	<b>29.0</b>
9	88	46	47	22	-1	33	<b>39</b>	30	<b>31.3</b>
10	94	39	44	25	11	29	<b>40</b>	29	<b>30.1</b>

CAP loss data in meningitis due to HY1

## REFERENCES

- Alexander JE, *et al* (1994) Immunization of mice with pneumolysin toxoid confers a significant degree of protection against at least 9 serotypes of *Streptococcus pneumoniae*. *Infect.Immun.* **62**:5683-5688.
- Allendoerfer R, *et al* (1991) Combined therapy with fluconazole and flucytosine in murine cryptococcal meningitis. *Antimicrob.Agents.Chemother.* **35**:726-729.
- AlonsoDeVelasco E, *et al* (1995) *Streptococcus pneumoniae*: Virulence factors, pathogenesis and vaccines. *Microbiol.Rev.* **59**:591-603.
- Alwmark A, *et al* (1981) Improvement of the splenectomized rat model for overwhelming pneumococcal infection: standardization of the bacterial inoculum. *Eur.Surg.Res.* **13**:339-343.
- Amaee FR. (1995) Deafness in bacterial meningitis: Ototoxic potential of *H. influenzae* type B cell fractions, pneumolysin and nitric oxide. PhD Thesis. University of Birmingham.
- Amaee FR, Comis SD and Osborne MP (1995) N-methyl-L-arginine protects the guinea pig cochlea from the cytotoxic effects of pneumolysin. *Acta.Otolaryngol.* **115**:386-391.
- Andersen NE, *et al* (1989) Brain acidosis in experimental pneumococcal meningitis. *Journal of Cerebral Blood Flow & Metabolism* **9**:381-387.
- Andersson PB, Perry VH and Gordon S (1992) Intracerebral injection of proinflammatory cytokines or leukocyte chemotaxins induces minimal myelomonocytic cell recruitment to the parenchyma of the central nervous system. *Journal of Experimental Medicine* **176**:255-259.
- Angel CS, Ruzek M and Hostetter MK (1994) Degradation of C3 by *Streptococcus pneumoniae*. *J.Infect.Dis.* **170**:600-608.
- Askenasy OM, George RC and Begg NT (1995) Pneumococcal bacteraemia and meningitis in England and Wales 1982-1992. *Communic.Dis.Rep.* **5**:R45-50.
- Austrian R (1981) Pneumococcus: the first one hundred years. *Rev.Infect.Dis* **3**:183-189.
- Austrian R (1986) Some aspects of the pneumococcal carrier state. *Journal of Antimicrobial Chemotherapy* **18**:35-45.
- Avery OT and Dubos R (1931) The protective action of a specific enzyme against type III pneumococcus infection in mice. *Journal of Experimental Medicine* **54**:73-89.
- Baer M, Vuento R and Vesikari T (1995) Increase in bacteraemic pneumococcal infections in children. *Lancet* **345**:661
- Bass R, *et al* (1996) A novel nonpsychotropic cannabinoid, HU-211, in the treatment of experimental pneumococcal meningitis. *J.Infect.Dis.* **173**:735-738.
- Beilke MA (1989) Vascular endothelium in immunology and infectious disease. *Rev.Infect.Dis* **11**:273-283.
- Benton K, A., Everson M and Briles DE (1995) A pneumolysin-negative mutant of *Streptococcus pneumoniae* causes chronic bacteremia rather than acute sepsis in mice. *Infect.Immun.* **63**:448-455.
- Berry AM, *et al* (1988) Cloning and expression of the pneumococcal neuraminidase gene in *Escherichia coli*. *Gene* **71**:299-305.
- Berry AM, *et al* (1989) Reduced virulence of a defined pneumolysin-negative mutant of *Streptococcus pneumoniae*. *Infect.Immun.* **57**:2037-2042.

- Berry AM, Paton JC and Hansman D (1992) Effect of insertional inactivation of the genes encoding pneumolysin and autolysin on the virulence of *Streptococcus pneumoniae* type-3. *Microb.Pathogen.* **12**:87-93.
- Berry AM, *et al* (1994) Cloning and nucleotide-sequence of the *Streptococcus pneumoniae* hyaluronidase gene and purification of the enzyme from recombinant *Escherichia-coli*. *Infect.Immun.* **62**:1101-1108.
- Berry AM, *et al* (1995) Effect of defined point mutations in the pneumolysin gene on the virulence of *Streptococcus pneumoniae*. *Infect.Immun.* **63**:1969-1974.
- Bevilacqua MP, *et al* (1989) Endothelial leucocyte adhesion molecule 1: an inducible regulator of neutrophils related to complement regulatory proteins and lectins. *Science* **243**:1160-1165.
- Bhatt S, *et al* (1991) Hearing loss and pneumococcal meningitis: an animal model. *Laryngoscope* **101**:1285-1292.
- Bhatt SM, *et al* (1993) Progression of hearing loss in experimental pneumococcal meningitis: correlation with cerebrospinal fluid cytochemistry. *J.Infect.Dis.* **167**:675-683.
- Bhatt SM, *et al* (1995) The impact of dexamethasone on hearing loss in experimental pneumococcal meningitis. *Ped.Infect.Dis.J.* **14**:93-96.
- Blank AL, *et al* (1994) Acute *Streptococcus pneumoniae* meningogenic labyrinthitis: an experimental guinea-pig model and literature-review. *Arch.Oto.Laryngol.Head.Neck.Surg.* **120**:1342-1346.
- Bohne BA and Rabbitt KD (1983) Holes in the reticular lamina after noise exposure: implications for continuing damage in the organ of Corti. *Hearing Res* **11**:41-53.
- Boje KM and Arora PK (1992) Microglial-produced nitric oxide and reactive nitrogen oxides mediate neuronal cell death. *Brain.Res.* **587**:250-256.
- Boje KMK (1995) Inhibition of nitric-oxide synthase partially attenuates alterations in the blood cerebrospinal-fluid barrier during experimental meningitis in the rat. *European Journal Of Pharmacology* **272**:297-300.
- Boulnois GJ (1992) Pneumococcal proteins and the pathogenesis of disease caused by *Streptococcus pneumoniae*. *J.Gen.Microbiol* **138**:249-259.
- Bradford MM (1976) A rapid and sensitive method for the quantitation of microgram quantities of protein utilizing the principle of protein-dye binding. *Anal.Biochem.* **72**:248-254.
- British Society for the Study of Infection (1995) Bacterial meningitis: causes for concern. *J.Infect.* **30**:89-94.
- Brown CJ and Abbas PJ (1987) A comparison of AP and ABR tuning curves in the guinea pig. *Hearing Res* **25**:193-204.
- Bryan JP, *et al* (1990) Etiology and mortality of bacterial meningitis in Northeastern Brazil. *Rev.Infect.Dis* **12**:128-135.
- Burroughs M, *et al* (1992) Bacterial components and the pathophysiology of injury to the blood-brain barrier: does cell wall add to the effects of endotoxin in gram-negative meningitis?. *J.Infect.Dis.* **165 Suppl 1**:S82-S85.
- Burroughs MH, *et al* (1995) Effect of thalidomide on the inflammatory response in cerebrospinal- fluid in experimental bacterial-meningitis. *Microb.Pathogen.* **19**:245-255.
- Buser P and Imbert M. (1992) Audition. Cambridge, MA: The MIT Press.
- Cabellos C, *et al* (1992) Differing roles for platelet-activating factor during inflammation of the lung and subarachnoid space. The special case of *Streptococcus pneumoniae*. *J.Clin.Invest.* **90**:612-618.
- Camara M, *et al* (1991) *Streptococcus pneumoniae* produces at least 2 distinct enzymes with neuraminidase activity: cloning and expression of a second neuraminidase gene in *Escherichia coli*. *Infect.Immun.* **59**:2856-2858.

- Camara M, *et al* (1994) A neuraminidase from *Streptococcus pneumoniae* has the features of a surface protein. *Infect.Immun.* **62**:3688-3695.
- Canard B, *et al* (1994) Molecular-genetic analysis of the *nagh* gene encoding a hyaluronidase of clostridium-perfringens. *Molecular & General Genetics* **243**:215-224.
- Canvin JA, *et al* (1995) The role of pneumolysin and autolysin in the pathology of pneumonia and septicemia in mice infected with a type 2 pneumococcus. *J.Infect.Dis.* **172**:119-123.
- Carroll KJ and Carroll C (1994) A prospective investigation of the long-term auditory-neurological sequelae associated with bacterial-meningitis: a study from vanuatu. *J.Trop.Med.Hyg.* **97**:145-150.
- Chao CC, *et al* (1992) Cytokine release from microglia: differential inhibition by pentoxifylline and dexamethasone. *J.Infect.Dis.* **166**:847-853.
- Chao CC, *et al* (1995) Interleukin-1 and tumor-necrosis-factor-alpha synergistically mediate neurotoxicity: involvement of nitric-oxide and of n-methyl-d-aspartate receptors. *Brain Behavior And Immunity* **9**:355-365.
- Cody AR, *et al* (1980) Electrophysiological and morphological changes in the guinea pig cochlea following mechanical trauma to the organ of Corti. *Acta.Otolaryngol.* **89**:440-452.
- Collee JG, *et al* (1989) Mackie & McCartney Practical Medical Microbiology. Edinburgh: Churchill Livingstone.
- Comber KR, Boon RJ and Sutherland R (1977) Comparative effects of amoxycillin and ampicillin on the morphology of *Escherichia coli* in vivo and correlation with activity. *Antimicrob.Agents.Chemother.* **12**:736-744.
- Comis SD, Osborne MP and Tarlow MJ (1991) The effect of bacterial endotoxin upon the morphology of the tectorial membrane and stereocilia in the guinea pig cochlea. *Scanning Microscopy* **5**:1129-1134.
- Comis SD, *et al* (1993) Cytotoxic effects on hair cells of guinea pig cochlea produced by pneumolysin, the thiol activated toxin of *Streptococcus pneumoniae*. *Acta.Otolaryngol.* **113**:152-159.
- Comis SD and Leng G (1979) Action of putative neurotransmitters in the guinea pig cochlea. *Exp.Brain.Res.* **36**:119-128.
- Cross AS, *et al* (1993) Choice of bacteria in animal models of sepsis. *Infect.Immun.* **61**:2741-2747.
- Cundell D, Masure HR and Tuomanen EI (1995) The molecular-basis of pneumococcal infection – a hypothesis. *Clin.Infect.Dis.* **21**:S 204-S 212.
- Dacey RG and Sande MA (1974) Effect of probenecid on cerebrospinal fluid concentrations of penicillin and cephalosporin derivatives. *Antimicrob.Agents.Chemother.* **6**:437-441.
- Dagan R (1996) Bacterial meningitis: not gone with *Haemophilus influenzae* vaccination. 7th International Congress for Infectious Disease, Hong Kong June 1996 [Abstract 92.001]
- Dallos P, *et al* (1972) Cochlear inner and outer hair cells: functional differences. *Science* **177**:356-358.
- Daum RS, *et al* (1978) Ventricular involvement in experimental *Hemophilus influenzae* meningitis. *J.Pediatr.* **93**:927-930.
- Dawson KP, Abbot GD and Mogridge N (1988) Bacterial meningitis in childhood: a 13-year review. *New Zealand Medical Journal* **101**:758-760.
- Delostoyos JR, *et al* (1996) Functional analysis of pneumolysin by use of monoclonal antibodies. *Infect.Immun.* **64**:480-484.
- Devries HE, *et al* (1996) The influence of cytokines on the integrity of the blood-brain-barrier in-vitro. *J.Neuroimmunol* **64**:37-43.

- Dodge PR, *et al* (1984) Prospective evaluation of hearing impairment as a sequela of acute bacterial meningitis. *New.Engl.J.Med.* **311**:869-874.
- Donaldson JA, Duckert LG and Lambert PM. (1992) Anson-Donaldson Surgical Anatomy of the Temporal Bone. New York: Raven.
- Duane PG, *et al* (1993) Identification of hydrogen-peroxide as a *Streptococcus pneumoniae* toxin for rat alveolar epithelial-cells. *Infect.Immun.* **61**:4392-4397.
- Duckert L (1974) The morphology of the cochlear aqueduct and periotic duct of the guinea pig: a light and electron microscope study. *Tr Am Acad Ophth Otol* **78**:21-48.
- Dulon D, Huang M and Schnacht J (1990) Outer hair cells as potential targets of inflammatory mediators. *Ann.Otol.Rhinol.Laryngol.* **99(supp)**:35-38.
- Duvall AJ and Quick CA (1969) Tracers and endogenous debris in delineating cochlear barriers and pathways: an experimental study. *Ann.Otol.Rhinol.Laryngol.* **78**:1041-1057.
- Dwarakanath AD, *et al* (1995) The production of neuraminidase and fucosidase by helicobacter pylori – their possible relationship to pathogenicity. *FEMS.Immunol.Med.Microbiol.* **12**:213-216.
- Eavey RD, *et al* (1985) Otologic features of bacterial meningitis of childhood. *J.Pediatr.* **106**:402-407.
- Edwards JR and Nairn K (1992) Comparative efficacy of meropenem, ceftriaxone and ceftizidime in experimental meningitis [Abstract no 952]. In: Proceedings and Abstracts of the 32nd Interscience Conference on Antimicrobial Agents and Chemotherapy. Washington, DC: American Society for Microbiology.
- Eggermont JJ (1976) Analysis of compound action potential responses to tone bursts in the human and guinea pig cochlea. *Journal of Acoustic Society of America* **60**:1132-1139.
- Ernst JD, Decazes JM and Sande MA (1983) Experimental pneumococcal meningitis: role of leukocytes in pathogenesis. *Infect.Immun.* **41**:275-279.
- Ernst JD, *et al* (1984) Complement (C5)-derived chemotactic activity accounts for accumulation of polymorphonuclear leukocytes in cerebrospinal fluid of rabbits with pneumococcal meningitis. *Infect.Immun.* **46**:81-86.
- Evans E and Harrison R (1975) Correlation between outer hair cell damage and deterioration of cochlear nerve tuning properties. *J.Physiol.(Lond)* **256**:43-44P.
- Eybalin M (1993) Neurotransmitters and neuromodulators of the mammalian cochlea. *Physiol.Rev.* **73**:309-373.
- Feldman C, *et al* (1991) Pneumolysin induces the salient histologic features of pneumococcal infection in the rat lung in vivo. *Am.J.Resp.Cell.Mol.Biol.* **5**:416-423.
- Feldman WE (1976) Concentrations of bacteria in cerebrospinal fluid of patients with bacterial meningitis. *J.Pediatr.* **88**:549-552.
- Ferrante A, Rowan-Kelly B and Paton JC (1984) Inhibition of in vitro human lymphocyte response by the pneumococcal toxin pneumolysin. *Infect.Immun.* **46**:585-589.
- Fine DP (1975) Pneumococcal type-associated variability in alternate complement pathway activation. *Infect.Immun.* **12**:772-778.
- Fortnum HM (1992) Hearing impairment after bacterial meningitis: a review. *Arch.Dis.Child.* **67**:1128-1133.
- Frasch CE (1995) Serogroup and serotype classification of bacterial pathogens. *Methods In Enzymology* **235**:159-172.

- Frei K, *et al* (1993) Immune-mediated injury in bacterial meningitis. *International Review of Experimental Pathology* **34 Pt B**:183-192.
- Freyer D, *et al* (1996) Pneumococcal cell-wall components induce nitric-oxide synthase and TNF-alpha in astroglial-enriched cultures. *Glia* **16**:1-6.
- Friedland IR, *et al* (1993) Comparison of endotoxin release by different antimicrobial agents and the effect on inflammation in experimental *Escherichia coli* meningitis. *J.Infect.Dis.* **168**:657-662.
- Friedland IR, *et al* (1995) The limited role of pneumolysin in the pathogenesis of pneumococcal meningitis. *J.Infect.Dis.* **172**:805-809.
- Gardner MJ and Altman DG. (1989) *Statistics with confidence*. London: BMJ.
- Garthwaite J, Charles SL and Chess-Williams R (1988) Endothelium-derived relaxing factor release on activation of NMDA receptors suggests a role as intracellular messenger in the brain. *Nature* **336**:385-388.
- Geelen S, Bhattacharyya C and Tuomanen E (1993) The cell wall mediates pneumococcal attachment to and cytopathology in human endothelial cells. *Infect.Immun.* **61**:1538-1543.
- George RC. (1995) The epidemiology of pneumococcal disease. In Mayon-White RT (ed): *The clinical impact of pneumococcal disease and strategies for its prevention*. London: Royal Society of Medicine, pp. 1-7.
- Girgis NI, *et al* (1989) Dexamethasone treatment for bacterial meningitis in children and adults. *Ped.Infect.Dis.J.* **8**:848-851.
- Granert C, *et al* (1994) Inhibition of leukocyte rolling with polysaccharide fucoidin prevents pleocytosis in experimental meningitis in rabbits. *J.Clin.Invest.* **93**:929-936.
- Greenwood D. (1982) *Antibiotics of the beta-lactam group*. John Wiley.
- Guerra-Romero L, *et al* (1993) Amino acids in cerebrospinal and brain interstitial fluid in experimental pneumococcal meningitis. *Pediatr.Res.* **33**:510-513.
- Guiscafre H, *et al* (1984) Reversible hearing loss after meningitis. Prospective assessment using auditory evoked responses. *Ann.Otol.Rhinol.Laryngol.* **93**:229-232.
- Guo Y, *et al* (1994) Endotoxic damage to the stria vascularis: the pathogenesis of sensorineural hearing loss secondary to otitis media?. *Journal of Laryngology & Otology* **108**:310-313.
- Haberl RL, *et al* (1994) Is nitric-oxide involved as a mediator of cerebrovascular changes in the early phase of experimental pneumococcal meningitis. *Neurological Research* **16**:108-112.
- Harter DH and Petersdorf RG (1960) A consideration of the pathogenesis of bacterial meningitis: review of the experimental and clinical studies. *Yale J Biol Med* **32**:280-289.
- Heumann D, *et al* (1994) Gram-positive cell walls stimulate synthesis of tumor necrosis factor-lpha and interleukin-6 by human monocytes. *Infect.Immun.* **62**:2715-2721.
- Hill J, Andrew PW and Mitchell TJ (1994) Amino-acids in pneumolysin important for hemolytic-activity identified by random mutagenesis. *Infect.Immun.* **62**:757-758.
- Hill J, *et al* (1996) The role of hyaluronidase in the virulence of serotype II *Streptococcus pneumoniae*. (UnPub)
- Hochwald GM, *et al* (1984) Cerebrospinal fluid glucose and leukocyte responses in experimental meningitis. *Journal of the Neurological Sciences* **63**:381-391.
- Houldsworth S, Andrew PW and Mitchell TJ (1994) Pneumolysin stimulates production of tumor-necrosis-factor-alpha and interleukin-1-beta by human mononuclear phagocytes. *Infect.Immun.* **62**:1501-1503.
- Hudspeth A (1985) The cellular basis of hearing: the biophysics of hair cells. *Science* **230**:742-752.

- Hunter CA, Roberts CW and Alexander J (1992) Kinetics of cytokine mRNA production in the brains of mice with progressive toxoplasmic encephalitis. *Eur.J.Immunol.* **22**:2317-2322.
- Hynes WL, Hancock L and Ferretti JJ (1995) Analysis of a 2nd bacteriophage hyaluronidase gene from streptococcus-pyogenes – evidence for a 3rd hyaluronidase involved in extracellular enzymatic-activity. *Infect.Immun.* **63**:3015-3020.
- Igarishi M, *et al* (1974) Temporal bone findings in pneumococcal meningitis. *Arch.Oto.Laryngol.Head.Neck.Surg.* **99**:79-83.
- Igarishi M and Schucknecht HF (1962) Pneumococcal otitis media, meningitis and labyrinthitis. *Arch.Oto.Laryngol.Head.Neck.Surg.* **76**:126-130.
- Jewett DL and Williston JS (1971) Auditory-evoked far fields averaged from the scalp of humans. *Brain* **94**:681-696.
- Johnson AP, *et al* (1996) Prevalence of antibiotic resistance and serotypes in pneumococci in England and Wales: results of observational surveys in 1990 and 1995. *Br.Med.J.* **312**:1454-1456
- Johnson MH, *et al* (1995) CT of postmeningitic deafness – observations and predictive value for cochlear implants in children. *Am.J.Neuroradiol.* **16**:103-109.
- Johnson MK, *et al* (1992) Confirmation of the role of pneumolysin in ocular infections with *Streptococcus pneumoniae*. *Current Eye Research* **11**:1221-1225.
- Kadurugamuwa JL, *et al* (1989) Inhibition of complement-factor-5a-induced inflammatory reactions by prostaglandin E2 in experimental meningitis. *J.Infect.Dis.* **160**:715-719.
- Kanra GY, *et al* (1995) Beneficial effects of dexamethasone in children with pneumococcal meningitis. *Ped.Infect.Dis.J.* **14**:490-494.
- Kaplan SL, *et al* (1984) Onset of hearing loss in children with bacterial meningitis. *Pediatrics* **73**:575-578.
- Kaplan SL, *et al* (1989) Invasion of the inner ear by *Haemophilus influenzae* type b in experimental meningitis. *J.Infect.Dis.* **159**:923-930.
- Kay R, Palmer AC and Taylor PM (1984) Hearing in the dog as assessed by auditory brainstem evoked potentials. *Veterinary Record* **114**:81-84.
- Kay R (1991) The site of the lesion causing hearing loss in bacterial meningitis: a study of experimental streptococcal meningitis in guinea-pigs. *Neuropath.Appl.Neurobiol.* **17**:485-493.
- Kelly RT, Grieff D and Farmer S (1966) Neuraminidase activity in *Diplococcus pneumoniae*. *J.Bacteriol.* **91**:601-603.
- Kelly RT, Farmer S and Grieff D (1967) Neuraminidase activities of clinical isolates of *Diplococcus pneumoniae*. *J.Bacteriol.* **94**:272-273.
- Kelly RT and Grieff D (1970) Toxicity of pneumococcal neuraminidase. *Infect.Immun.* **2**:115-117.
- Kelly T, Dillard JP and Yother J (1994) Effect of genetic switching of capsular type on virulence of *Streptococcus pneumoniae*. *Infect.Immun.* **62**:1813-1819.
- Kiang N, Moxon E and Kahn A. (1976) The relationship of gross potentials recorded from the cochlea to single unit activity in the auditory nerve. In Ruben R, Elberling C and Salomon G (eds): *Electrocochleography*. Baltimore: University Park Press, pp. 95-115.
- Kim KS, *et al* (1992a) The K1 capsule is the critical determinant in the development of *Escherichia coli* meningitis in the rat. *J.Clin.Invest.* **90**:897-905.

- Kim KS, *et al* (1992b) Modulation of blood-brain barrier permeability by tumor necrosis factor and antibody to tumor necrosis factor in the rat. *Lymphokine & Cytokine Research* **11**:293-298.
- Kim YS, Kennedy S and Tauber MG (1995) Toxicity of *Streptococcus pneumoniae* in neurons, astrocytes, and microglia in-vitro. *J.Infect.Dis.* **171**:1363-1368.
- Kimura RS, Schucknecht HF and Ota C (1974) Blockage of the cochlear aqueduct. *Acta.Otolaryngol.* **77**:1-12.
- Klugman KP (1994a) Pneumococcal resistance to the 3rd-generation cephalosporins -clinical, laboratory and molecular aspects. *Int.J.Antimicrob.Agents.* **4**:63-67.
- Klugman KP (1994b) Management of antibiotic-resistant pneumococcal infections. *Journal of Antimicrobial Chemotherapy* **34**:191-193.
- Koedel U, Pfister HW and Tomasz A (1994) Methylprednisolone attenuates inflammation, increase of brain water-content and intracranial-pressure, but does not influence cerebral blood-flow changes in experimental pneumococcal meningitis. *Brain.Res.* **644**:25-31.
- Koedel U, *et al* (1995) Experimental pneumococcal meningitis – cerebrovascular alterations, brain edema, and meningeal inflammation are linked to the production of nitric-oxide. *Annals of Neurology* **37**:313-323.
- Koller H, Buchholz J and Siebler M (1994) Bacterial endotoxins impair electrophysiological properties of cultured astrocytes but not of cultured neurons. *Journal of the Neurological Sciences* **124**:156-162.
- Konkol RJ, *et al* (1987) *Hemophilus influenzae* meningitis in the rat – behavioral, electrophysiological, and biochemical consequences. *Annals of Neurology* **21**:353-360.
- Korchev YE, Bashford CL and Pasternak CA (1992) Differential sensitivity of pneumolysin-induced channels to gating by divalent-cations. *J.Membr.Biol.* **127**:195-203.
- Kornelisse RF, Degroot R and Neijens HJ (1995) Bacterial-meningitis – mechanisms of disease and therapy. *Eur.J.Pediatr.* **154**:85-96.
- Kornfield SJ and Plaut AG (1981) Secretory immunity and bacterial IgA proteases. *Rev.Infect.Dis* **3**:521-534.
- Kostyukova NN, *et al* (1995) A study of pathogenic factors of *Streptococcus pneumoniae* strains causing meningitis. *FEMS.Immunol.Med.Microbiol.* **10**:133-137.
- Krivan HC, Roberts DD and Ginsberg V (1988) Many pulmonary pathogenic bacteria bind specifically to the carbohydrate sequence GalNAc $\beta$ 1-4Gal found in some glycolipids. *Proc.Nat.Acad.Sci.U.S.A.* **85**:6157-6161.
- Lancet (1985) Acute respiratory infections in under-fives: 15 million deaths a year. *Lancet* **2**:699-701.
- Lebel MH, Freij BJ and Syrogiannopoulos GA (1988) Dexamethasone therapy for bacterial meningitis: results of 2 double-blind placebo controlled studies. *New.Engl.J.Med.* **319**:964-971.
- Lebel MH, Hoyt MJ and McCracken GH, Jr. (1989) Comparative efficacy of ceftriaxone and cefuroxime for treatment of bacterial meningitis [see comments]. *J.Pediatr.* **114**:1049-1054.
- Lee CJ and Wang TR (1994) Pneumococcal infection and immunization in children. *Critical Reviews In Microbiology* **20**:1-12.
- Leib SL, *et al* (1996) Neuroprotective effect of excitatory amino acid antagonist kynurenic acid in experimental bacterial meningitis. *J.Infect.Dis.* **173**:166-171.
- Leichenger H and Abelson SM (1937) Deafness associated with meningococcemia. *Arch.Oto.Laryngol.Head.Neck.Surg.* **26**:306-309.
- Leng G and Comis SD (1979) The effect of potassium on the activity of auditory nerve fibres of the guinea pig cochlea. *Acta.Otolaryngol.* **87**:36-46.

- Levy SL, Sullivan N and Gorbach SL. (1978) Pathogenicity of conventional and debilitated *Escherichia coli* K12. *Nature* **274**:395-396.
- Libman E (1905) A pneumococcus producing a peculiar form of hemolysis (cited by Paton 1993). *Proc.N.Y.Pathol.Sci.* **5**:168
- Liebman EP, *et al* (1969) Hearing improvement following meningitis deafness. *Arch.Oto.Laryngol.Head.Neck.Surg.* **90**:92-95.
- Lim D (1986) Functional structure of the organ of Corti. A review. *Hearing Res* **22**:117-146.
- Lipton S (1993) Prospects for clinically tolerated NMDA antagonists: open channel blockers and alternative redox states of nitric oxide. *Trends.Neurolog.Sci* **12**:527-532.
- Lock RA, Paton JC and Hansman D (1988a) Comparative efficacy of pneumococcal neuraminidase and pneumolysin as immunogens protective against *Streptococcus pneumoniae*. *Microb.Pathogen.* **4**:33-43.
- Lock RA, Paton JC and Hansman D (1988b) Purification and immunological characterization of neuraminidase produced by *Streptococcus pneumoniae*. *Microb.Pathogen.* **4**:33-43.
- Lock RA, Hansman D and Paton JC (1992) Comparative efficacy of autolysin and pneumolysin as immunogens protecting mice against infection by *Streptococcus pneumoniae*. *Microb.Pathogen.* **12**:137-143.
- Lorenzl S, *et al* (1993) Imaging of leukocyte-endothelium interaction using in vivo confocal laser scanning microscopy during the early phase of experimental pneumococcal meningitis. *J.Infect.Dis.* **168**:927-933.
- Marin C, Mosquera J and Rodrigueziturbe B (1995) Neuraminidase promotes neutrophil, lymphocyte and macrophage infiltration in the normal rat kidney. *Kidney.Int.* **47**:88-95.
- McCracken GH, Jr. (1995) Management of meningitis caused by multiple drug resistant *Streptococcus pneumoniae* (Abstract C83). In: Proceedings and abstracts of the 35th Interscience Conference on Antimicrobial Agents and Chemotherapy. (San Francisco, CA). Washington, DC: American Society for Microbiology.
- McCracken GH, Jr. and Sakata Y (1985) Antimicrobial therapy of experimental meningitis caused by *Streptococcus pneumoniae* strains with different susceptibilities to penicillin. *Antimicrob.Agents.Chemother.* **27**:141-145.
- McKnight AA, *et al* (1992) Oxygen free radicals and the cerebral arteriolar response to group B streptococci. *Pediatr.Res.* **31**:640-644.
- Meldrum BS (1995) Cytoprotective therapies in stroke. *Current Opinion In Neurology* **8**:15-23.
- Mertsola J, *et al* (1991) Endotoxin concentrations in cerebrospinal fluid correlate with clinical severity and neurologic outcome of *Haemophilus influenzae* type B meningitis. *Am.J.Dis.Child.* **145**:1099-1103.
- Miles AA and Misra SS (1938) The estimation of the bactericidal power of the blood. *J Hyg Camb* **38**:732
- Mitchell TJ, *et al* (1991) Complement activation and antibody-binding by pneumolysin via a region of the toxin homologous to a human acute-phase protein. *Molecular Microbiology* **5**:1883-1888.
- Mitchell TJ, *et al* (1992) Molecular studies of pneumolysin, the thiol-activated toxin of *Streptococcus pneumoniae*, as an aid to vaccine design. *Zbl.Bakt.Suppl.* **23**:429-438.
- Moncada S, Palmer RMJ and Higgs EA (1991) Nitric oxide: physiology, pathophysiology and pharmacology. *Pharmacol.Rev.* **43**:109-142.
- Morgan PJ, *et al* (1993) Characterization of the solution properties and conformation of pneumolysin, the membrane-damaging toxin of *Streptococcus pneumoniae*. *Biochem.J.* **296**:671-674.
- Morgan PJ, *et al* (1995) Subunit organization and symmetry of pore-forming, oligomeric pneumolysin. *FEBS Lett.* **371**:77-80.

- Moscovitch DH, Gannon RP and Laszlo CA (1973) Perilymph displacement by cerebrospinal fluid in the cochlea. *Ann Otol* **82**:53-61.
- Moxon ER and Ostrow PT (1977) *Haemophilus influenzae* meningitis in infant rats: role of bacteremia in pathogenesis of age-dependent inflammatory responses in cerebrospinal fluid. *J.Infect.Dis.* **135**:303-307.
- Mulder CJ, van Alphen L and Zanen HC (1984) Neonatal meningitis caused by *Escherichia coli* in the Netherlands. *J.Infect.Dis.* **150**:935-940.
- Mustafa MM, *et al* (1989a) Increased endotoxin and interleukin-1 beta concentrations in cerebrospinal fluid of infants with coliform meningitis and ventriculitis associated with intraventricular gentamicin therapy. *J.Infect.Dis.* **160**:891-895.
- Mustafa MM, *et al* (1989b) Modulation of inflammation and cachectin activity in relation to treatment of experimental *Haemophilus influenzae* type b meningitis. *J.Infect.Dis.* **160**:818-825.
- Mustafa MM, *et al* (1990) Cerebrospinal fluid prostaglandins, interleukin 1 beta, and tumor necrosis factor in bacterial meningitis. Clinical and laboratory correlations in placebo-treated and dexamethasone-treated patients. *Am.J.Dis.Child.* **144**:883-887.
- Moller A and Jannetta PJ. (1986) Simultaneous surface and direct brainstem recordings of brainstem auditory evoked potentials (BAEP) in man. In Cracco RQ and Bodis-Wollner IB (eds): Evoked potentials. New York: Alan Liss , pp. 227-234.
- Nakajima Y, *et al* (1991) A comparison of central nervous lesions directly induced by *Escherichia coli* lipopolysaccharide in piglets, calves, rabbits and mice. *J.Comp.Pathol.* **104**:57-64.
- Nanninga N. (1985) Molecular cytology of *Escherichia coli*. Academic Press: London
- Nau, *et al* (1994) Rifampin therapy for experimental pneumococcal meningitis in rabbits. *Antimicrob.Agents.Chemother.* **38**:1186-1189.
- O'Donoghue JM, Schweid A and Beaty HN (1974) Experimental pneumococcal meningitis I: A rabbit model. *Proc.Soc.Exp.Biol.Med.* **146**:571-574.
- O'Toole RD, Goode L and Howe C (1971) Neuraminidase activity in bacterial meningitis. *J.Clin.Invest.* **50**:979-985.
- O'Toole RD and Stahl WC (1975) Experimental pneumococcal meningitis: Effects of neuraminidase and other pneumococcal constituents on cerebrospinal fluid in the intact dog. *J.Neurol.Sci.* **26**:167-178.
- Obaro SK, Monteil MA and Henderson DC (1996) The pneumococcal problem. *Br.Med.J.* **312**:1521-1524
- Odio CM, *et al* (1991) The beneficial effects of early dexamethasone administration in infants and children with bacterial meningitis [see comments]. *New.Engl.J.Med.* **324**:1525-1531.
- Osborne MP, Comis SD and Pickles JO (1984) Morphology and cross-linkage of stereocilia in the guinea-pig labyrinth examined without the use of osmium as a fixative. *Cell Tissue Res* **237**:43-48.
- Osborne MP and Comis SD (1990) High resolution scanning electron microscopy of stereocilia in the cochlea of normal, post-mortem and drug-treated guinea pigs. *J.Electr.Micr.Tech.* **15**:245-260
- Osborne MP, *et al* (1995) The cochlear lesion in experimental bacterial meningitis of the rabbit. *Int.J.Exp.Pathol.* **76**:317-330.
- Owen RHG, *et al* (1994) A role in cell binding for the c-terminus of pneumolysin, the thiol activated toxin of *Streptococcus pneumoniae*. *FEMS.Microbiol.Lett.* **121**:217-221
- Ozdamar O, Kraus N and Stein L (1983) Auditory brainstem responses in infants recovering from bacterial meningitis: audiologic evaluation. *Arch.Oto.Laryngol.Head.Neck.Surg.* **109**:13-18.

- Palva T (1970) Cochlear aqueduct in infants. *Acta.Otolaryngol.* **70**:83-94.
- Paris MM, *et al* (1994) Dexamethasone (dmx) therapy (rx) and CSF sterilization in experimental meningitis produced by penicillin and cephalosporin- resistant *Streptococcus pneumoniae* (pcrp). *Pediatr.Res.* **35**:190
- Paris MM, *et al* (1995) Effect of interleukin-1 receptor antagonist and soluble tumor-necrosis-factor receptor in animal-models of infection. *J.Infect.Dis.* **171**:161-169.
- Paton JC, *et al* (1983) Effect of immunisation with pneumolysin on survival time of mice challenged with *Streptococcus pneumoniae*. *Infect.Immun.* **40**:548-552.
- Paton JC, Rowan-Kelly B and Ferrante A (1984) Activation of human complement by the pneumococcal toxin pneumolysin. *Infect.Immun.* **43**:1085-1087.
- Paton JC, *et al* (1986) Cloning and expression in *Escherichia coli* of the *Streptococcus pneumoniae* gene encoding pneumolysin. *Infect.Immun.* **54**:50-55.
- Paton JC, *et al* (1993a) Molecular analysis of the pathogenicity of *Streptococcus pneumoniae* – the role of pneumococcal proteins. *Annu.Rev.Microbiol.* **47**:89-115.
- Paton JC, *et al* (1993b) Immunization of mice with salmonella-typhimurium c5 aroa expressing a genetically toxoided derivative of the pneumococcal toxin pneumolysin. *Microb.Pathogen.* **14**:95-102
- Paton JC (1996) The contribution of pneumolysin to the pathogenicity of *Streptococcus pneumoniae*. *Trends In Microbiology* **4**:103-106.
- Perlman HB and Lindsay JR (1939) Relation of the internal ear spaces to the meninges. *Arch.Oto.Laryngol.Head.Neck.Surg.* **29**:12-23.
- Perry FE, *et al* (1993) Inhibition of the respiratory burst of neutrophils by *Streptococcus pneumoniae* – role of pneumolysin. *Am.Rev.Resp.Dis.* **147**:461
- Perry FE, *et al* (1994) Characterization of an oxidative response inhibitor produced by *Streptococcus pneumoniae*. *Thorax* **49**:676-683.
- Perry VL, *et al* (1993) Effect of experimental *Escherichia-coli* meningitis on concentrations of excitatory and inhibitory amino-acids in the rabbit brain – in-vivo microdialysis study. *Pediatr.Res.* **34**:187-191.
- Petersdorf RG and Luttrell CN (1962) Studies of the pathogenesis of meningitis. I. Intrathecal infection. *J.Clin.Invest.* **41**:311-319.
- Pfister HW, *et al* (1990) Microvascular changes during the early phase of experimental bacterial meningitis. *Journal of Cerebral Blood Flow & Metabolism* **10**:914-922.
- Pfister HW, *et al* (1992a) Cerebrovascular complications of bacterial meningitis in adults. *Neurology* **42**:1497-1504.
- Pfister HW, *et al* (1992b) Transforming growth factor beta 2 inhibits cerebrovascular changes and brain edema formation in the tumor necrosis factor alpha-independent early phase of experimental pneumococcal meningitis. *J.Exp.Med.* **176**:265-268.
- Pfister HW, *et al* (1992c) Effect of catalase on regional cerebral blood flow and brain edema during the early phase of experimental pneumococcal meningitis. *J.Infect.Dis.* **166**:1442-1445.
- Pfister HW, *et al* (1992d) Antioxidants attenuate microvascular changes in the early phase of experimental pneumococcal meningitis in rats. *Stroke* **23**:1798-1804.
- Pfister HW, *et al* (1994) Mechanisms of brain injury in bacterial meningitis: workshop summary. *Clin.Infect.Dis.* **19**:463-479.

- Puel RL, *et al* (1991) Electrophysiological evidence for the presence of NMDA receptors in the guinea pig cochlea. *Hearing Res* **51**:255-264.
- Quagliariello VJ, Long WJ and Scheld WM (1986) Morphologic alterations of the blood-brain barrier with experimental meningitis in the rat. Temporal sequence and role of encapsulation. *J.Clin.Invest.* **77**:1084-1095.
- Quagliariello VJ, *et al* (1991a) Ultrastructural localization of albumin transport across the cerebral microvasculature during experimental meningitis in the rat. *J.Exp.Med.* **174**:657-672.
- Quagliariello VJ, *et al* (1991b) Recombinant human interleukin-1 induces meningitis and blood-brain barrier injury in the rat. Characterization and comparison with tumor necrosis factor. *J.Clin.Invest.* **87**:1360-1366
- Quagliariello VJ and Scheld WM (1992) Bacterial meningitis: pathogenesis, pathophysiology and progress. *New.Engl.J.Med.* **327**:864-872.
- Ramilo O, *et al* (1990) Tumor necrosis factor alpha/cachectin and interleukin 1 beta initiate meningeal inflammation. *Journal of Experimental Medicine* **172**:497-507.
- Rask-Anderson H, Stahle J and Wilbrand H (1977) Human cochlear aqueduct and its accessory canals. *Ann.Otol.Rhinol.Laryngol.* **86**(S42):1-16.
- Rayner CFJ, *et al* (1995) Interaction of pneumolysin-sufficient and -deficient isogenic variants of *Streptococcus pneumoniae* with human respiratory mucosa. *Infect.Immun.* **63**:442-447.
- Rees DD, *et al* (1990) Dexamethasone prevents the induction by endotoxin of a nitric oxide synthase and the associated effects on vascular tone: An insight into endotoxin shock. *Biochem.Biophys.Res.Comm.* **173**:541-547.
- Reese TS and Karnovsky MJ (1967) Fine structural localization of a blood brain barrier to exogenous peroxidase. *J.Cell.Biol.* **34**:207-217.
- Richardson MP, *et al* (1995) A prospective study of hearing loss in childhood bacterial meningitis. (Abstract K165). In: Proceedings and abstracts of the 35th Interscience Conference on Antimicrobial Agents and Chemotherapy. (San Francisco, CA). Washington, DC: American Society for Microbiology, pp. 317
- Rodriguez AF, *et al* (1991) Hematogenous pneumococcal meningitis in the infant rat: description of a model. *J.Infect.Dis.* **164**:1207-1209.
- Roesor RJ, Cambell JC and Daly DD (1975) Recovery of auditory function following meningitic deafness. *J Speech Hear Dis* **40**:405-411.
- Roodman GD, Johnson RA and Clibon U (1990) Tumor necrosis factor  $\alpha$  and the anemia of chronic disease: Effects of chronic exposure to TNF on erythropoiesis in vivo. *Adv.Exp.Med.Biol* **271**:185-196.
- Rubins JB, *et al* (1992) Toxicity of pneumolysin to pulmonary endothelial-cells invitro. *Infect.Immun.* **60**:1740-1746.
- Rubins JB, *et al* (1993) Toxicity of pneumolysin to pulmonary alveolar epithelial-cells. *Infect.Immun.* **61**:1352-1358.
- Rubins JB, *et al* (1994) Pneumolysin activates phospholipase-a in pulmonary-artery endothelial-cells. *Infect.Immun.* **62**:3829-3836.
- Rubins JB, *et al* (1995) Dual function of pneumolysin in the early pathogenesis of murine pneumococcal pneumonia. *J.Clin.Invest.* **95**:142-150.
- Rubins JB, *et al* (1996) Distinct roles for pneumolysin's cytotoxic and complement activities in the pathogenesis of pneumococcal pneumonia. *Am.J.Resp.Crit.Care.Med.* **153**:1339-1346.

- Saez-Llorens X, *et al* (1990) Pentoxifylline modulates meningeal inflammation in experimental bacterial meningitis. *Antimicrob.Agents.Chemother.* **34**:837-843.
- Saez-Llorens X, *et al* (1991) Enhanced attenuation of meningeal inflammation and brain edema by concomitant administration of anti-CD18 monoclonal antibodies and dexamethasone in experimental *Haemophilus meningitis*. *J.Clin.Invest.* **88**:2003-2011.
- Salih MAM, Khaleefa OH and Bushara M (1991) Long term sequelae of childhood acute bacterial meningitis in a developing country. A study from Sudan. *Scand.J.Infect.Dis.* **23**:175-182.
- Salit IE and Tomalty L (1986) Experimental meningococcal infection in mice: a model for mucosal invasion. *Infect.Immun.* **51**:648-652.
- Salt AN, *et al* (1991) Evaluation of procedures to reduce fluid-flow in the fistulized guinea-pig cochlea. *Acta.Otolaryngol.* **111**:899-907.
- Salt AN and Stopp PE (1979) The effect of cerebrospinal fluid pressure on perilymphatic flow in the opened cochlea. *Acta.Otolaryngol.* **88**:198-202.
- Salt AN and Vora AR (1990) Cochlear threshold assessment using tone-derived action potentials. *Audiology* **29**:135-145.
- Salwen KM, Viskerfors T and Olcen P (1987) Increased incidence of childhood bacterial meningitis. A 25-year study in a defined population in Sweden. *Scand.J.Infect.Dis.* **19**:1-11.
- Sando I, *et al* (1971) Perilymphatic communication routes in guinea pig cochlea. *Ann Otol* **80**:826-834.
- Sato K, *et al* (1996) Roles of autolysin and pneumolysin in middle-ear inflammation caused by a type-3 *Streptococcus pneumoniae* strain in the chinchilla otitis- media model. *Infection And Immunity* **64**:1140-1145.
- Saukkonen KM, *et al* (1990) The role of cytokines in the generation of inflammation and tissue damage in experimental gram-positive meningitis. *Journal of Experimental Medicine* **171**:439-448.
- Saunders FK, *et al* (1989) Pneumolysin, the thiol-activated toxin of *Streptococcus pneumoniae*, does not require a thiol group for in vitro activity. *Infect.Immun.* **57**:2547-2552.
- Savic DJ and Ferretti JJ (1994) Group A Streptococci do not produce neuraminidase. *Med.Microbiol.Lett.* **3**:358-362.
- Schaad UB *et al* (1993) Dexamethasone therapy for bacterial meningitis in children. *Lancet* **342**:457-461
- Schaad UB, Kaplan SL and McCracken GH, Jr. (1995) Steroid therapy for bacterial meningitis. *Clin.Infect.Dis.* **20**:685-690.
- Scheifele DW, *et al* (1980) *Haemophilus influenzae* bacteremia and meningitis in infant primates. *J.Lab.Clin.Med.* **95**:450-462.
- Scheld WM, *et al* (1979) Clearance of bacteria from cerebrospinal fluid to blood in experimental meningitis. *Infect.Immun.* **24**:102-105.
- Scheld WM and Brodeur JP (1983) Effect of methylprednisolone on entry of ampicillin and gentamicin into cerebrospinal fluid in experimental pneumococcal and *Escherichia coli* meningitis. *Antimicrob.Agents.Chemother.* **23**:108-112.
- Schlech WF, *et al* (1985) Bacterial meningitis in the United States, 1978 through 1981. The National Bacterial Meningitis Surveillance Study. *J.Amer.Med.Assoc.* **253**:1749-1754.
- Shieh JH, Peterson RHF and Moore MAS (1993) Cytokines and dexamethasone modulation of IL-1 receptors on human neutrophils in vitro. *J.Immunol.* **150**:3515-3524.
- Shumway CN and Klebanoff SJ (1971) Purification of pneumolysin. *Infect.Immun.* **4**:388-392.

- Simpson SQ, Singh R and Bice DE (1994) Heat-killed pneumococci and pneumococcal capsular polysaccharides stimulate tumor-necrosis-factor-alpha production by murine macrophages. *Am.J.Resp.Cell.Mol.Biol.* **10**:284-289.
- Slepecky N (1986) Overview of mechanical damage to the inner ear: noise as a tool to probe cochlear function. *Hearing Res* **22**:307-321.
- Spangelo BL, Isakson PC and MacLeod RM (1990) Production of interleukin-6 by anterior pituitary cells is stimulated by increased intracellular adenosine 3',5'-monophosphate and vasoactive intestinal peptide. *Endocrinology* **127**:403-409.
- Spellerberg B and Tuomanen EI (1994) The pathophysiology of pneumococcal meningitis. *Annals Of Medicine* **26**:411-418.
- Spoendlin H (1971) Primary structural changes in the organ of Corti after acoustic overstimulation. *Acta.Otolaryngol.* **71**:166-176.
- Spratt BG (1975) Distinct penicillin binding protein involved in the division, elongation and shape of *Escherichia coli* K12. *Proc.Nat.Acad.Sci.U.S.A.* **72**:2999-3003.
- Steinfort C, *et al* (1989) Effect of *Streptococcus pneumoniae* on human respiratory epithelium in vitro. *Infect.Immun.* **57**:2006-2013.
- Sun AH, Parnes LS and Freeman DJ (1996) Comparative perilymph permeability of cephalosporins and its significance in the treatment and prevention of suppurative labyrinthitis. *Ann.Otol.Rhinol.Laryngol.* **105**:54-57.
- Syrogianopoulos GA, *et al* (1987) Dexamethasone in the treatment of experimental *Haemophilus influenzae* type b meningitis [published erratum appears in J Infect Dis 1987 Jun;155(6):1359]. *J.Infect.Dis.* **155**:213-219.
- Syrogianopoulos GA, *et al* (1994) Dexamethasone therapy for bacterial meningitis in children: 2- versus 4-day regimen. *J.Infect.Dis.* **169**:853-858.
- Takeno S, *et al* (1994) Induction of selective inner hair cell damage by carboplatin. *Scanning Microscopy* **8**:97-106.
- Tanaka K, *et al* (1994) Anti-CD18 antibody prevents polymorphonuclear cell (pmn) diapedesis but not margination induced by pneumococcal (pn) cell-wall (cw) in the rabbit model of meningitis. *Lab.Invest* **70**:145
- Tarlow MJ, Comis SD and Osborne MP (1991) Endotoxin induced damage to the cochlea in guinea pigs. *Arch.Dis.Child.* **66**:181-184.
- Tauber MG, *et al* (1984) Antibacterial activity of beta-lactam antibiotics in experimental meningitis due to *Streptococcus pneumoniae*. *J.Infect.Dis.* **149**:568-574.
- Tauber MG, *et al* (1987) Antibiotic therapy, endotoxin concentration in cerebrospinal fluid and brain edema in experimental *Escherichia coli* meningitis in rabbits. *J.Infect.Dis.* **156**:456-462.
- Tauber MG, Borschberg U and Sande MA (1988) Influence of granulocytes on brain edema, intracranial pressure, and cerebrospinal fluid concentrations of lactate and protein in experimental meningitis. *J.Infect.Dis.* **157**:456-464.
- Tauber MG, *et al* (1992a) Experimental pneumococcal meningitis causes central nervous system pathology without inducing the 72-kd heat shock protein. *Am.J.Pathol* **141**:53-60.
- Tauber MG, *et al* (1992b) Toxicity in neuronal cells caused by cerebrospinal fluid from pneumococcal and gram-negative meningitis. *J.Infect.Dis.* **166**:1045-1050.
- Tauber MG, *et al* (1993) Fluid administration, brain edema, and cerebrospinal fluid lactate and glucose concentrations in experimental *Escherichia coli* meningitis. *J.Infect.Dis.* **168**:473-476.

- Tauber MG and Zwahlen A (1994) Animal models for meningitis. *Methods In Enzymology* **235**:93-106.
- Toriya R, *et al* (1991) Ultrastructure of the guinea-pig cochlear aqueduct – an electron-microscopic study of decalcified temporal bones. *Acta.Otolaryngol.* **111**:699-706.
- Townsend GC and Scheld WM (1994) Platelet-activating-factor augments meningeal inflammation elicited by *Haemophilus influenzae* lipooligosaccharide in an animal-model of meningitis. *Infect.Immun.* **62**:3739-3744.
- Trolle E (1950) Defective hearing after meningococcal meningitis. *Acta.Otolaryngol.* **38**:384-402.
- Tunkel AR, Wispelwey B and Scheld WM (1990a) Bacterial meningitis: recent advances in pathophysiology and treatment [see comments]. *Ann.Intern.Med.* **112**:610-623.
- Tunkel AR, Wispelwey B and Scheld WM (1990b) Pathogenesis and pathophysiology of meningitis. *Inf.Dis.Clin.N.Amer.* **4**:555-581.
- Tunkel AR and Scheld WM (1993a) Pathogenesis and pathophysiology of bacterial meningitis. *Clin.Microbiol.Rev.* **6**:118-136.
- Tunkel AR and Scheld WM (1993b) Pathogenesis and pathophysiology of bacterial meningitis. *Annu.Rev.Med.* **44**:103-120.
- Tuomanen E, *et al* (1985a) The induction of meningeal inflammation by components of the pneumococcal cell wall. *J.Infect.Dis.* **151**:859-868.
- Tuomanen E, *et al* (1985b) The relative role of bacterial cell wall and capsule in the induction of inflammation in pneumococcal meningitis. *J.Infect.Dis.* **151**:535-540.
- Tuomanen E, *et al* (1986) The role of complement in inflammation during experimental pneumococcal meningitis. *Microb.Pathogen.* **1**:15-32.
- Tuomanen E, *et al* (1987) Nonsteroidal anti-inflammatory agents in the therapy for experimental pneumococcal meningitis. *J.Infect.Dis.* **155**:985-990.
- Tuomanen E, *et al* (1989) Reduction of inflammation, tissue damage, and mortality in bacterial meningitis in rabbits treated with monoclonal antibodies against adhesion-promoting receptors of leukocytes. *Journal of Experimental Medicine* **170**:959-969.
- Tuomanen E (1994) A spoonful of sugar to control inflammation. *J.Clin.Invest.* **93**:917-918.
- Tuomanen E, Austrian R and Masure HR (1995) Pathogenesis of pneumococcal infection. *New.Engl.J.Med.* **332**:1280-1283.
- Tureen JH, *et al* (1990) Loss of cerebrovascular autoregulation in experimental meningitis in rabbits. *J.Clin.Invest.* **85**:577-581.
- Tureen JH, Tauber MG and Sande MA (1991) Effect of indomethacin on the pathophysiology of experimental meningitis in rabbits. *J.Infect.Dis.* **163**:647-649.
- Ulich TR, Guo K and del Castillo J (1989) Endotoxin-induced cytokine gene expression in vivo. I. Expression of tumor necrosis factor mRNA in visceral organs under physiologic conditions and during endotoxemia. *Am.J.Pathol* **134**:11-14.
- Ulich TR, *et al* (1990) Endotoxin-induced cytokine gene expression in vivo. II. Regulation of tumor necrosis factor and interleukin-1 alpha/beta expression and suppression. *Am.J.Pathol* **137**:1173-1185.
- Ulich TR, *et al* (1992) Endotoxin-induced cytokine gene expression in vivo. IV. Expression of interleukin-1 alpha/beta and interleukin-1 receptor antagonist mRNA during endotoxemia and during endotoxin-initiated local acute inflammation. *Am.J.Pathol* **141**:61-68.

- van Furth AM, *et al* (1994) In vitro effect of dexamethasone, pentoxifylline and anti-endotoxin monoclonal antibody on the release of proinflammatory mediators by human leukocytes stimulated with *Haemophilus influenzae* type B. *Pediatr.Res.* **35**:725-728.
- van Heusden E and Smoorenburg GF (1981) Eighth-nerve action potentials evoked by tone bursts in cats before and after inducement of an acute noise trauma. *Hearing Res* **5**:1-23.
- Vanbenthem PPG, *et al* (1992) Glycocalyx heterogeneity in normal and hydroptic cochleas of the guinea-pig. *Acta.Otolaryngol.* **112**:976-984.
- Velasco S, *et al* (1991) Temperature-dependent modulation of lipopolysaccharide-induced interleukin-1 beta and tumor necrosis factor alpha expression in cultured human astroglial cells by dexamethasone and indomethacin. *J.Clin.Invest.* **87**:1674-1680.
- Vienny H, *et al* (1984) Early diagnosis and evolution of deafness in childhood bacterial meningitis: a study using brainstem auditory evoked potentials. *Pediatrics* **73**:579-586.
- Wald ER, *et al* (1995) Dexamethasone therapy for children with bacterial meningitis. *Pediatrics* **95**:21-28.
- Walker JA, *et al* (1987) Molecular cloning, characterization, and complete nucleotide sequence of the gene for pneumolysin, the sulfhydryl-activated toxin of *Streptococcus pneumoniae*. *Infect.Immun.* **55**:1184-1189.
- Watson DA, *et al* (1993) A brief history of the Pneumococcus in biomedical research: a panoply of scientific discovery. *Clin.Infect.Dis.* **17**:913-924.
- Welkos S and O'Brien A (1994) Determination of median lethal and infectious doses in animal model systems. *Methods In Enzymology* **235**:29-39.
- Wenger JD, *et al* (1990) Bacterial meningitis in the United States, 1986: report of a multistate surveillance study. The Bacterial Meningitis Study Group. *J.Infect.Dis.* **162**:1316-1323.
- Wiedermann BL, *et al* (1986) Pathogenesis of labyrinthitis associated with *Haemophilus-influenzae* type-b meningitis in infant rats. *J.Infect.Dis.* **153**:27-32.
- Wilken B, *et al* (1995) Hearing impairment in children under 16 months after bacterial-meningitis with reference to elastase in cerebrospinal-fluid. *Klinische Padiatrie* **207**:12-16.
- Williams AE and Blakemore WF (1990a) Monocyte-mediated entry of pathogens into the central nervous system. *Neuropath.Appl.Neurobiol.* **16**:377-392.
- Williams AE and Blakemore WF (1990b) Pathogenesis of meningitis caused by *Streptococcus suis* type 2. *J.Infect.Dis.* **162**:474-481.
- Winter AJ, *et al* (1996) Ultrastructural damage to the organ of Corti during experimental *Escherichia coli* and pneumococcal meningitis in guinea pigs. *Acta.Otolaryngol.* **116**:401-407
- Wispelwey B *et al* (1988) *Haemophilus influenzae* lipopolysaccharide-induced blood brain barrier permeability during experimental meningitis in the rat. *J.Clin.Invest.* **82**:1339-1346
- Wood WB, Jr. and Smith MR (1949) The inhibition of surface phagocytosis by the capsular "slime layer" of pneumococcus type III. *Journal of Experimental Medicine* **90**:85-99.
- Yanagita N, *et al* (1984) Defense mechanism of the cochlear aqueduct against infection: a morphological study in the guinea pig. *ORL* **46**:294-301.
- Zdanski CJ, *et al* (1994) Nitric-oxide synthase is an active enzyme in the spiral-ganglion cells of the rat cochlea. *Hearing Res* **79**:37-47.
- Ziegler EJ, *et al* (1991) Treatment of gram-negative bacteremia and septic shock with HA-1A human monoclonal antibody against endotoxin. *New.Engl.J.Med.* **324**:429-436.

Zwahlen A, *et al* (1982) Complement mediated opsonic activity in normal and infected human CSF: early response during bacterial meningitis. *J.Infect.Dis.* **145**:635-646.

Zwislowski J (1984) How OHC lesions can lead to cochlear neural hypersensitivity. *Acta.Otolaryngol.* **97**:529-534.